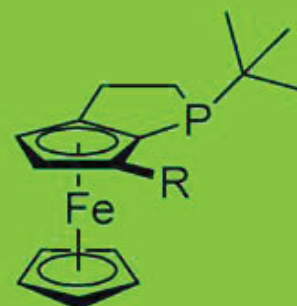


P-Chiral Phosphorus Ligands: Synthesis and Application in Asymmetric Hydrogenation

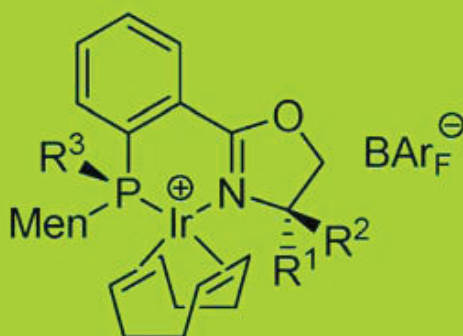
Secondary
Phosphine Oxides



Ferrocenephospholanes



Phosphino-Oxazolines



P-Chiral Phosphorus Ligands: Synthesis and Application in Asymmetric Hydrogenation

Inauguraldissertation

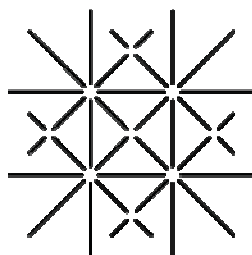
zur
Erlangung der Würde eines Doktors der Philosophie
vorgelegt der
Philosophisch-Naturwissenschaftlichen Fakultät
der Universität Basel

von

Björn Gschwend

aus
Altstätten SG

Basel 2009



**UNI
BASEL**

Bibliografische Information der Deutschen Nationalbibliothek

Die Deutsche Nationalbibliothek verzeichnet diese Publikation in der Deutschen Nationalbibliografie; detaillierte bibliografische Daten sind im Internet über <http://dnb.d-nb.de> abrufbar.

1. Aufl. - Göttingen : Cuvillier, 2009

Zugl.: Basel, Univ., Diss., 2009

978-3-86955-153-1

Genehmigt von der Philosophisch-Naturwissenschaftlichen Fakultät auf Antrag von:

Prof. Dr. Andreas Pfaltz

Prof. Dr. Edwin C. Constable

Basel, den 15.9.2009

Prof. Dr. Eberhard Parlow

Dekan

© CUVILLIER VERLAG, Göttingen 2009

Nonnenstieg 8, 37075 Göttingen

Telefon: 0551-54724-0

Telefax: 0551-54724-21

www.cuvillier.de

Alle Rechte vorbehalten. Ohne ausdrückliche Genehmigung des Verlages ist es nicht gestattet, das Buch oder Teile daraus auf fotomechanischem Weg (Fotokopie, Mikrokopie) zu vervielfältigen.

1. Auflage, 2009

Gedruckt auf säurefreiem Papier

978-3-86955-153-1

Für meine Eltern

This thesis was supervised by Prof. Dr. Andreas Pfaltz from October 2005 to August 2009 at the University of Basel, Department of Chemistry.

Acknowledgements

I would like to thank my supervisor Professor Dr. Andreas Pfaltz for the opportunity to work in his research group, for his support and the freedom in developing my project.

I would like to thank Professor Dr. Edwin C. Constable for co-examination of this thesis and Prof. Dr. Helma Wennemers for chairing the defense.

I thank Dr. Benoît Pugin and Heidi Landert for fruitful discussions and Solvias AG in general for carrying out the hydrogenation experiments.

I thank Jürgen Rotzler and Marc Liniger who contributed to this piece of research by synthetic work during their practical courses.

I thank Dr. Axel Franzke for recording several NMR-spectra. I am grateful to Ivana Fleischer, Dr. Fabiola Barrios-Landeros and Dr. Daniel Häussinger for supporting my own NMR-measurments. I thank Markus Neuburger for collecting X-ray data from almost every sample I gave him. The raw data was then kindly refined by Markus Neuburger, Dr. Silvia Schaffner and Marcus Schrems. Dr. Heinz Nadig measured the EI and FAB mass spectra and Werner Kirsch determined all elemental analyses. I thank Christian Ebner for the numerous ESI-MS measurements in the lonely basement.

I thank Jaroslav Padevet for solving numerous computer problems and countless restarts of the NMR-machine.

I am extremely thankful to Dr. Anthony Weatherwax and Christian Ebner for spending their time proof-reading this manuscript.

I thank the members of the workshop for technical support.

I thank Marina Mambelli-Johnson for her never-ending organisational work, the voluntary jobs for the group and the delicious meals “Chez Mambelli”.

I thank all the past and present members of the Pfaltz group who made my time in Basel enjoyable. The colleagues in lab 208 are especially acknowledged for the good working atmosphere and music.

Schliesslich danke ich meiner Familie, die mich seit Jahren in meinem Studium unterstützt hat, ohne genau zu verstehen, was ich eigentlich mache.

Table of Contents

1	Ferrocenephospholanes as Ligands in the Transition-Metal Catalyzed Asymmetric Hydrogenation	1
1.1	Introduction	3
1.1.1	P-Stereogenic Ligands in Asymmetric Catalysis	3
1.1.1.1	Chirality at Phosphorus Atoms	3
1.1.1.2	Preparation of P-Stereogenic Phosphines	4
1.1.1.3	Transition Metal-Catalyzed Asymmetric Hydrogenation of Functionalized Olefines	5
1.1.2	Cyclic Phosphines	10
1.1.2.1	Synthesis of Cyclic Phosphines	10
1.1.2.2	Phospholanes in Catalysis	12
1.1.3	Ferrocene	13
1.1.3.1	Structural Properties	13
1.1.3.1	Ligands with a Ferrocenyl Backbone	14
1.1.4	Objectives of this Work	16
1.1.5	References	17
1.2	Synthesis of Ferrocenephospholanes	21
1.2.1	<i>Ugi's</i> Amine	21
1.2.2	Formation of a Simple Ferrocenephospholane	21
1.2.3	Approaches to a Secondary Ferrocenephospholane	24
1.2.4	Functionalized Ferrocenephospholanes	33
1.2.5	Attempted Synthesis of a Ferrocene-Based P,N-Ligand with only Planar Chirality	39
1.2.6	Conclusions	42
1.2.7	References	43
1.3	Rhodium-Complexes and their Application in the Asymmetric Hydrogenation of Olefins	45
1.3.1	Coordination Behaviour	45
1.3.2	Hydrogenations	50
1.3.2.1	Substrate Screening	50
1.3.2.2	Ligand Screening	58
1.3.3	Conclusions	66
1.3.4	References	67

1.4	Iridium-Complexes and their Application in the Asymmetric Hydrogenation of Olefins	67
1.4.1	Hydrogenation with <i>in situ</i> Generated Complexes	67
1.4.1.1	Substrate Screening	67
1.4.1.2	Ligand Screening	75
1.4.2	Hydrogenation with Isolated Complexes	82
1.4.3	Hydrogenation of Unfunctionalized Olefins with a Ferrocenephospholane-Pyridine-Iridium Complex	90
1.4.4	Conclusions	92
1.4.5	References	93
1.5	Properties of Ferrocenephospholane-Complexes	95
1.5.1	X-Ray Observations	95
1.5.2	Competition Experiments in Solution	100
1.5.2.1	Competition Experiments in Methanol	100
1.5.2.2	Competition Experiments in Dichloromethane	103
1.5.3	Conclusions	109
1.5.4	References	110
2	Phosphines with Additional Functional Group as Ligands in Catalysis	111
2.1	Introduction	113
2.1.1	Secondary Phosphine Oxides	113
2.1.1.1	Properties of Secondary Phosphine Oxides	113
2.1.1.2	Synthesis of Secondary Phosphine Oxides	115
2.1.1.3	Metal Complexes	117
2.1.1.4	Application in Catalysis	119
2.1.2	Miscellaneous Functionalized Phosphines	121
2.1.3	Objectives of this Work	122
2.1.4	References	123
2.2	Synthesis and Catalysis Experiments	125
2.2.1	Secondary Phosphine Oxides	125
2.2.1.1	SPO-Phosphine Ligands	125
2.2.1.2	Terpene-Derived Secondary Phosphine Oxides	128
2.2.2	Hydroxyethyl-Functionalized Phosphines	138
2.2.3	Conclusions	142
2.2.4	References	144

3	P-Chiral Phosphino-Oxazolines as Ligands in the Iridium-Catalyzed Asymmetric Hydrogenation	145
3.1	Introduction	147
3.1.1	Historical Overview	147
3.1.2	Mechanism	151
3.1.2.1	The Catalytic Cycle	151
3.1.2.2	The Counter-Ion Effect	154
3.1.3	Objectives of this Work	156
3.1.4	References	157
3.2	Synthesis and Hydrogenation Experiments	159
3.2.1	Preparation of P-Chiral Phosphino-Oxazoline-Iridium Complexes	159
3.2.2	Asymmetric Hydrogenation	163
3.2.3	Influence of Temperature in the Reduction of 2-(4-Methoxyphenyl)-1-butene	173
3.2.4	Conclusions	174
3.2.5	References	175
4	Experimental	177
4.1	Working Techniques and Reagents	179
4.2	Analytical Methods	179
4.3	Experimental Procedures	181
4.3.1	Preparation of Ferrocenephospholanes	181
4.3.2	Preparation of Terpene-Derived Phosphorus Compounds	218
4.3.3	Preparation of P-Chiral Iridium-PHOX Complexes	232
4.3.4	Preparation of Single Crystals	244
4.3.5	Procedure for the Competition Experiments	244
4.3.6	Hydrogenation Procedures	245
4.3.6.1	Automated Parallel Hydrogenations (<i>SYMYX</i>)	245
4.3.6.2	Hydrogenations with Iridium-Complexes	246
4.3.6.3	Analytical Data of Hydrogenation Substrates	247
4.4	References	250

5	Appendix	251
5.1	Crystallographic Data	253
5.2	List of Abbreviations	262
5.3	References	265
6	Summary	267

Chapter 1

Ferrocenephospholanes as Ligands in the
Transition-Metal Catalyzed Asymmetric
Hydrogenation

1.1 Introduction

1.1.1 P-Stereogenic Ligands in Asymmetric Catalysis

1.1.1.1 Chirality at Phosphorus Atoms

Identical to a sp^3 hybridized carbon, trivalent and tetravalent phosphorus compounds adopt a tetrahedral geometry. Depending on the substitution pattern this can result in the formation of a stereogenic center. In trivalent phosphorus species the free electron pair is counted as a substituent and, unlike the corresponding nitrogen compounds, their geometry is configurationally stable and does not undergo inversion under ambient conditions. The inversion barrier of phosphines is generally 125-145 kJ/mol.^[1] For example, PH_3 has an inversion barrier of 132 kJ/mol compared to 24 kJ/mol for NH_3 .^[2]

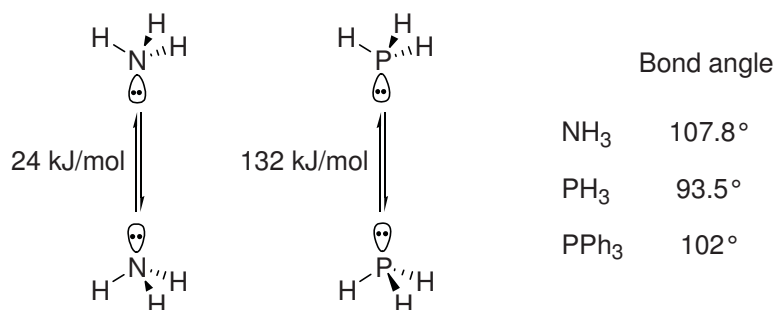


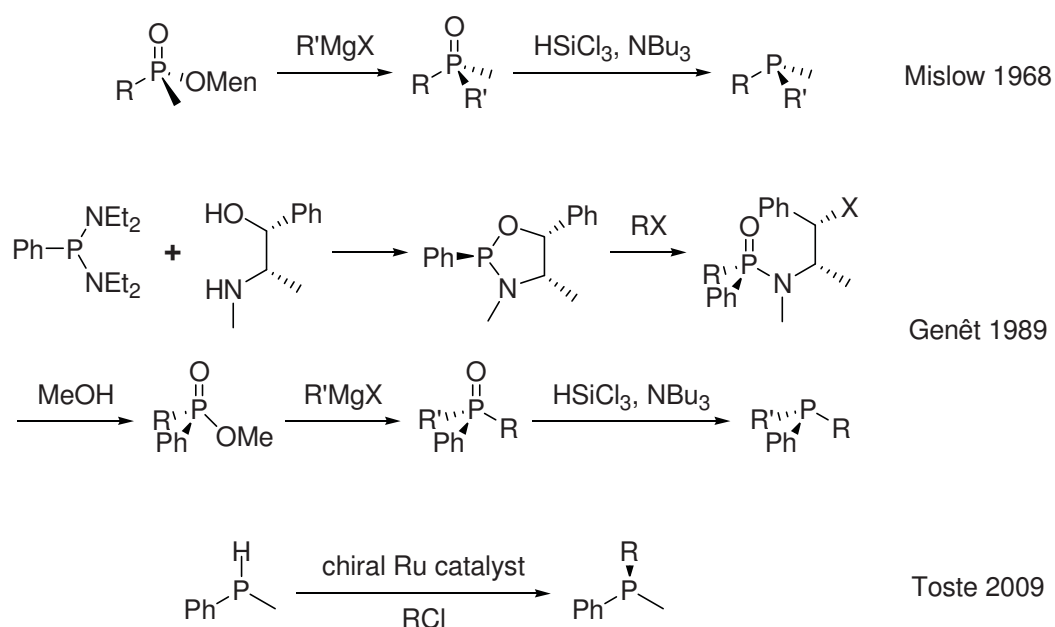
Figure 1.1. Physical properties of phosphines.

The increased energy requirement for the phosphorus inversion follows from the enhanced geometrical distortion necessary to form the trigonal planar transition state. Larger bonding angles need less distortion than smaller bonding angles. The bond angles in trivalent phosphorus compounds are smaller than those of trivalent nitrogen or tetravalent carbon species. This can be explained as a result of endothermic hybridization energy combined with VSEPR-theory.^[3] Whereas the electron distribution favours a geometry with orthogonal orbitals (bonding angle of 90°), VSEPR-theory, based on electron-electron repulsion, predicts an alignment close to the geometry of a tetrahedron. The two effects oppose each other and the outcome is a compromise, as seen in the numbers of Figure 1.1.

1.1.1.2 Preparation of P-Stereogenic Phosphines

Preparation of enantiomerically pure chiral phosphines dates back to the 1960's when the groups of *Horner* and *Mislow* were studying the stereochemistry of substitution reactions on phosphorus compounds. In the beginning, the phosphines were prepared by electrochemical reduction of optically pure phosphonium compounds which had been resolved by fractional crystallization.^[4a] Later, a synthesis was developed consisting of the resolution of menthyl phosphinates followed by addition of a *Grignard*-reagent and reduction of the resulting phosphine oxides (Scheme 1.1).^[4b] Later, *Knowles'* P-stereogenic diphosphine ligand DIPAMP was synthesized by oxidative coupling of two phosphines.^[5]

Twenty years passed before *Jugé* and *Genêt* described a new methodology that avoided chiral resolution. The synthetic route consisted of the diastereoselective formation of chiral oxazaphospholidines and the subsequent displacement by aryl or alkyl halides (Scheme 1.1).^[6a] The group of *Corey* also published a similar procedure using oxathiaphospholidines.^[6b]



Scheme 1.1. Stereoselective syntheses of chiral phosphines.

Despite these advances, the stereoselective preparation of acyclic chiral phosphines has remained a rather undeveloped area. Since they are mostly used as ligands in transition metal catalyzed reactions, the success of ligands with a chiral backbone instead of a chiral

phosphorus did not encourage researchers to develop new synthetic methodologies to overcome the tedious preparation of chiral phosphines. Only recently have new efforts, using catalysis, been seen.^[7] By employing chiral Pd-,^[8a] Pt-^[8b] or Ru-catalysts^[8c,d] enantioselective hydrophosphination and alkylation reactions have been achieved by several research groups.

1.1.1.3 Transition Metal-Catalyzed Asymmetric Hydrogenation of Functionalized Olefines

In 1965 *Wilkinson* found a practical rhodium-catalyst for homogeneous hydrogenation (Figure 1.2).^[9] Based on the finding that chiral trivalent phosphorus compounds can exist as stable, non-interconverting enantiomers by *Mislow* and *Horner*,^[10] *Knowles* was able to demonstrate in 1968 the first asymmetric hydrogenation shortly before *Horner*.^[11] The discovery of bidentate phosphines with chirality on the ligand backbone instead on the phosphorus as effective ligands by *Kagan*^[12] and the development of an industrial scale asymmetric hydrogenation of *L*-DOPA at Monsanto^[13] established this type of reaction in organic chemistry.

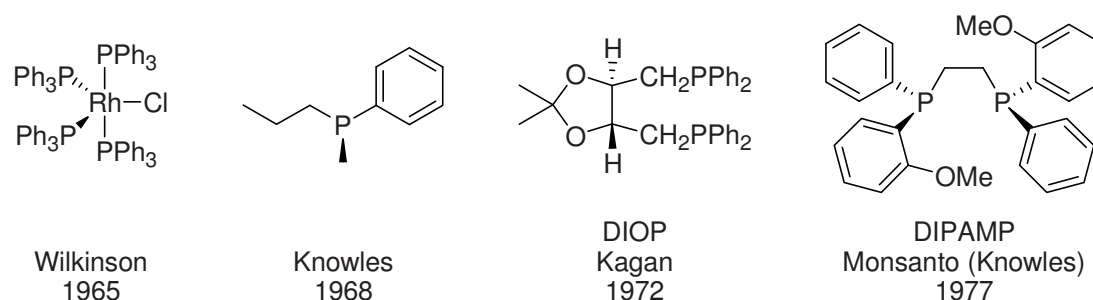
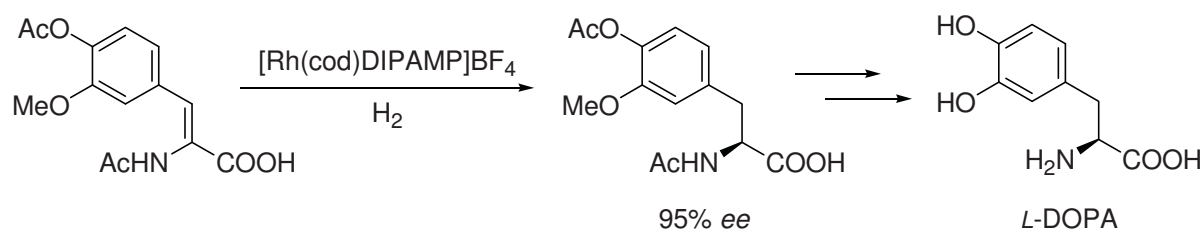
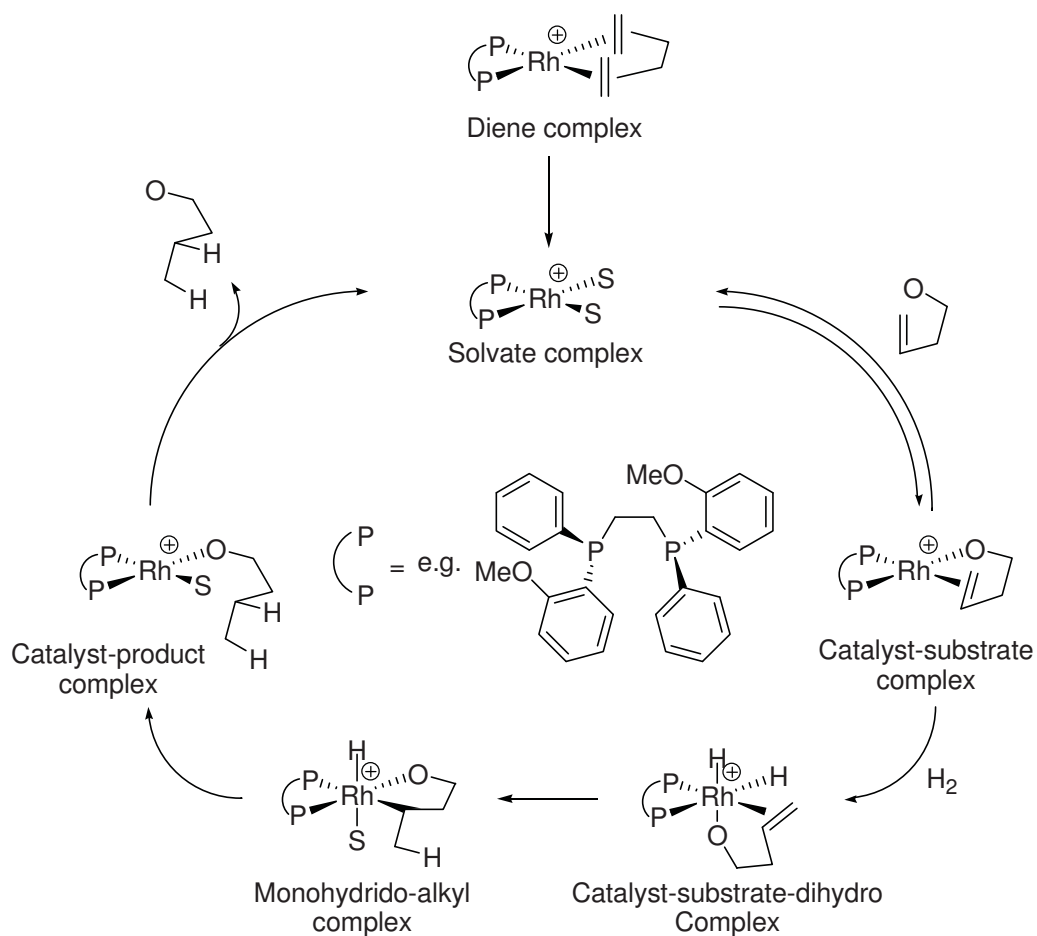


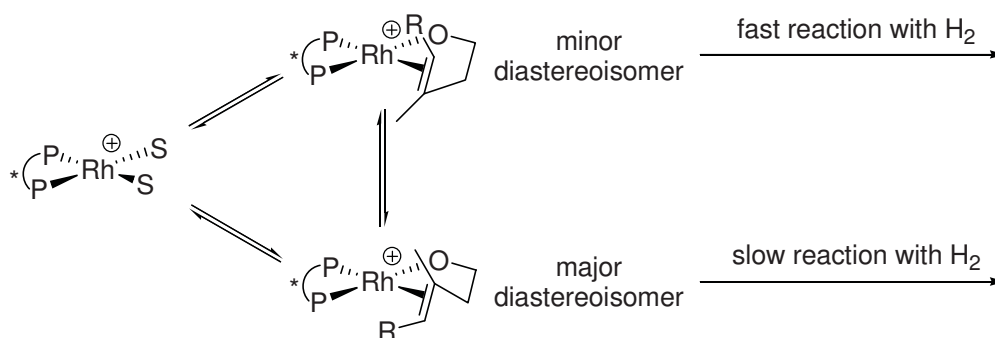
Figure 1.2. Early systems in Rh-catalyzed hydrogenation.



Scheme 1.2. Rh-catalyzed hydrogenation in the *L*-DOPA synthesis at Monsanto.



Scheme 1.3. Unsaturated pathway of the Rh-catalyzed hydrogenation

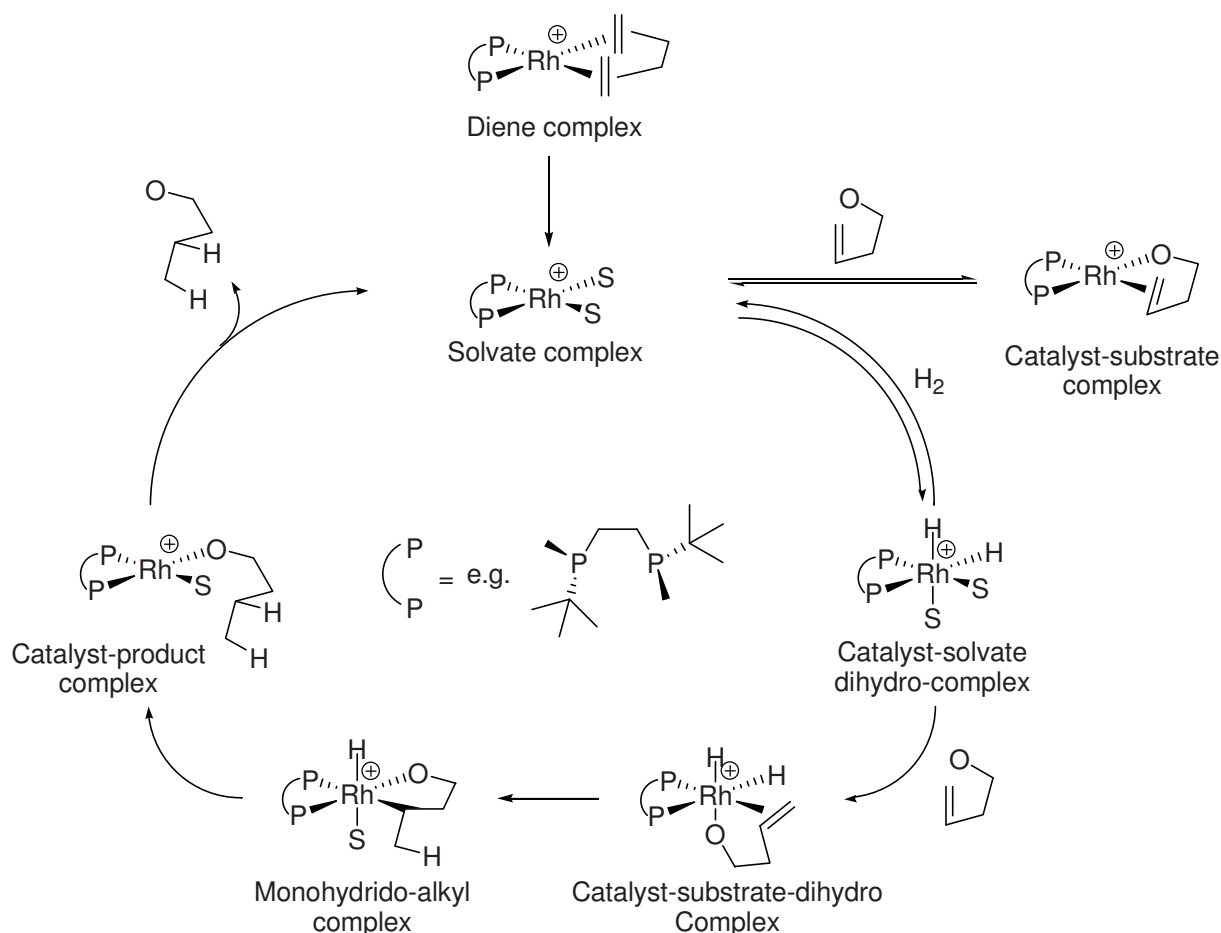


Scheme 1.4. Interconversion of the diastereomeric catalyst-substrate complexes.

The mechanism of Rh-catalyzed asymmetric hydrogenation has been extensively studied.^[14] Analyses of kinetic data^[15] and characterization of reaction intermediates by NMR^[16] or X-ray crystallography^[17] provided insight into the catalytic cycle depicted in Scheme 1.3. The cationic bisphosphine-rhodium complex exists in methanol as a bis-solvate species with a low affinity towards dihydrogen. In the presence of the substrate, bidentate complexation occurs to form the catalyst-substrate complex. Addition of dihydrogen is rate-limiting and the subsequent migratory insertion gives the monohydrido-alkyl complex. The intermediate catalyst-substrate-dihydrido complex is assumed but has never been observed. Reductive elimination and dissociation of the hydrogenation product regenerates the catalyst and closes the cycle (Scheme 1.3).

For C_2 -symmetrical chiral diphosphine ligands the catalyst-substrate complex exists as two interconverting diastereoisomers (Scheme 1.4). The interconversion can take place intramolecularly or via the solvate complex, the latter being less important. Usually one diastereoisomeric catalyst-substrate complex is more abundant in the equilibrium but, at least in the catalytic cycle shown above, this major diastereoisomer does not lead to the preferred hydrogenation product. The minor diastereoisomer reacts faster with dihydrogen to give the monohydrido-alkyl complex and therefore determines the stereochemical outcome of the reaction.

With the development of new bis-phosphine ligands the catalytic cycle was further investigated, and especially for electron rich phosphine donors, a slightly different pathway was found (Scheme 1.5).^[18] Reversible formation of the catalyst-solvate-dihydro complex, whose diastereoisomers exist in equilibrium, is the first step. This dihydride reacts with the substrate to give the monohydrido-alkyl complex as the next detectable intermediate. The product is liberated after reductive elimination.



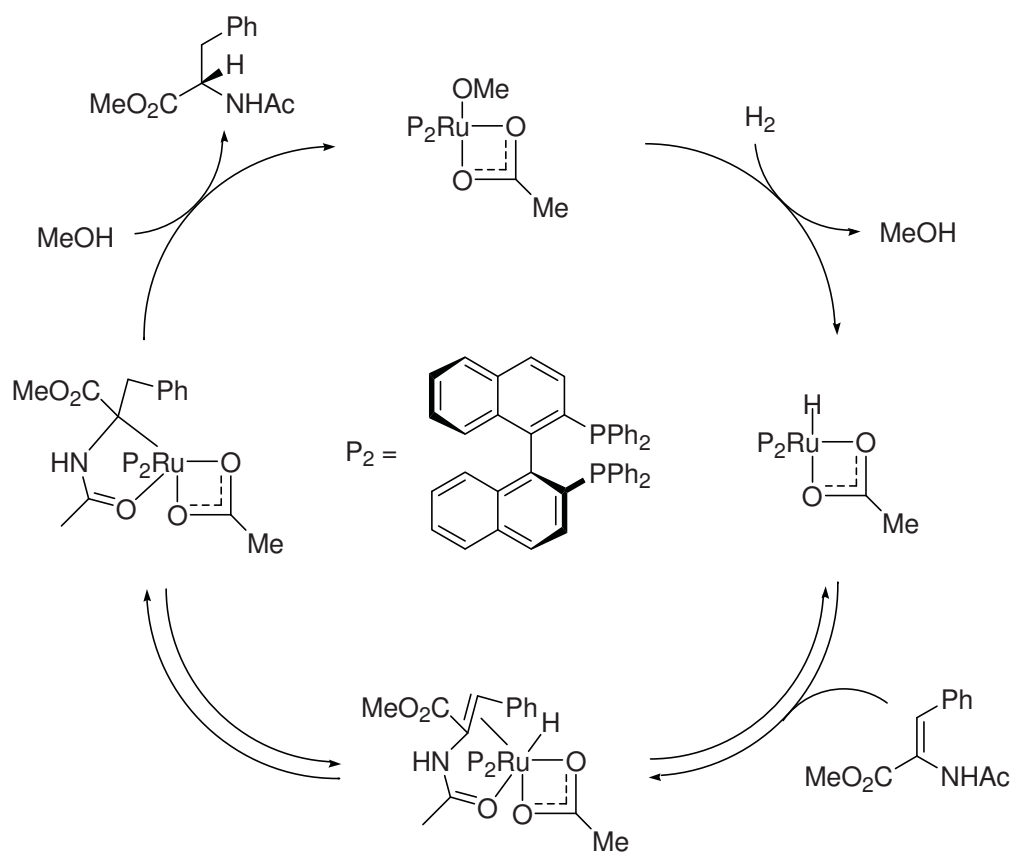
Scheme 1.5. Dihydride pathway for the Rh-catalyzed hydrogenation.

The distinction between the unsaturated and the dihydride pathway is blurred. At least in some cases, both mechanisms are operating, joining in a single pathway, since the catalyst-substrate-dihydro complex is a common intermediate in both cycles.

The catalytic cycle of bisphosphine-iridium-catalyzed hydrogenations of functionalized olefins is less well studied, presumably due to their, in most cases, weaker performance and thus lower synthetic importance. On the other hand, the slower reaction rates were used to study intermediate analogs of the rhodium cycles. In these experiments precatalyst-dihydride, catalyst-substrate and monohydrido-alkyl complexes of iridium-bisphosphine catalysts have been characterized.^[19] Therefore, the mechanism should be similar to the rhodium case but the complete catalytic cycle has not been determined.

Although Ru-catalyzed homogeneous hydrogenation has been known since the 1960's, its asymmetric variant was developed much later than for rhodium. Not until 1980 when *Noyori*

introduced the BINAP ligand, was ruthenium also proved to be able to generate a catalytic species with high activity and selectivity.^[20] Detailed kinetic studies were carried out involving [(BINAP)Ru(OAc)₂] in the reduction of methyl acetamidocinnamate^[21a] and tiglic acid.^[21b] The derived catalytic cycle is shown in Scheme 1.6.^[21a] In contrast to the rhodium mechanism the cleavage of dihydrogen occurs heterolytically, forming a ruthenium-monohydride complex. Coordination of the substrate followed by hydride transfer then gives a ruthenium-alkyl complex. Finally, exchange of the hydrogenation product with methanol closes the catalytic cycle.

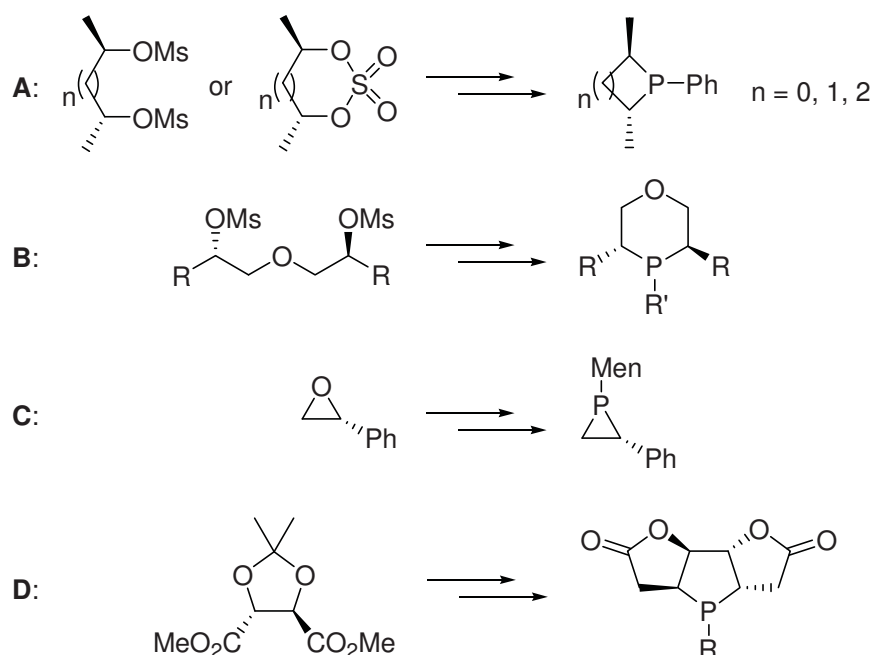


Scheme 1.6. Main pathway of the hydrogenation of methyl acetamidocinnamate catalyzed by [(BINAP)Ru(OAc)₂].

1.1.2 Cyclic Phosphines

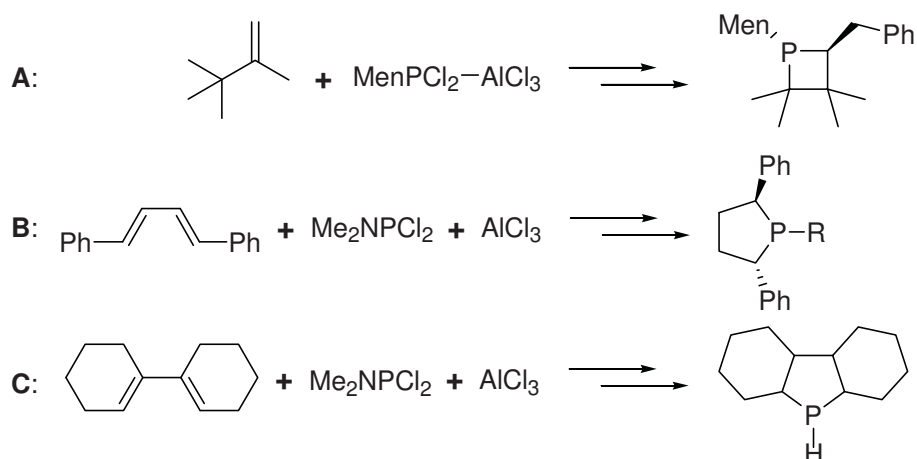
1.1.2.1 Synthesis of Cyclic Phosphines

Several different types of cyclic phosphines have been reported and various synthetic methods were developed for their synthesis.^[22] Cyclic phosphines with ring sizes of 3,^[23a] 4^[23b] and 5^[23c] have been prepared by nucleophilic substitution on mesylated diols or cyclic sulfates (Scheme 1.7 **A**). Following a similar procedure, six-membered cyclic phosphines have been prepared with an additional endocyclic oxygen (**B**).^[24] Enantiomerically pure styrene oxide has been opened with a nucleophilic phosphine species and converted to the corresponding phosphirane (**C**).^[25] Tartaric acid has also been used as starting material for the synthesis of multiply substituted cyclic phosphines employing hydrophosphination as the key step (**D**).^[26]



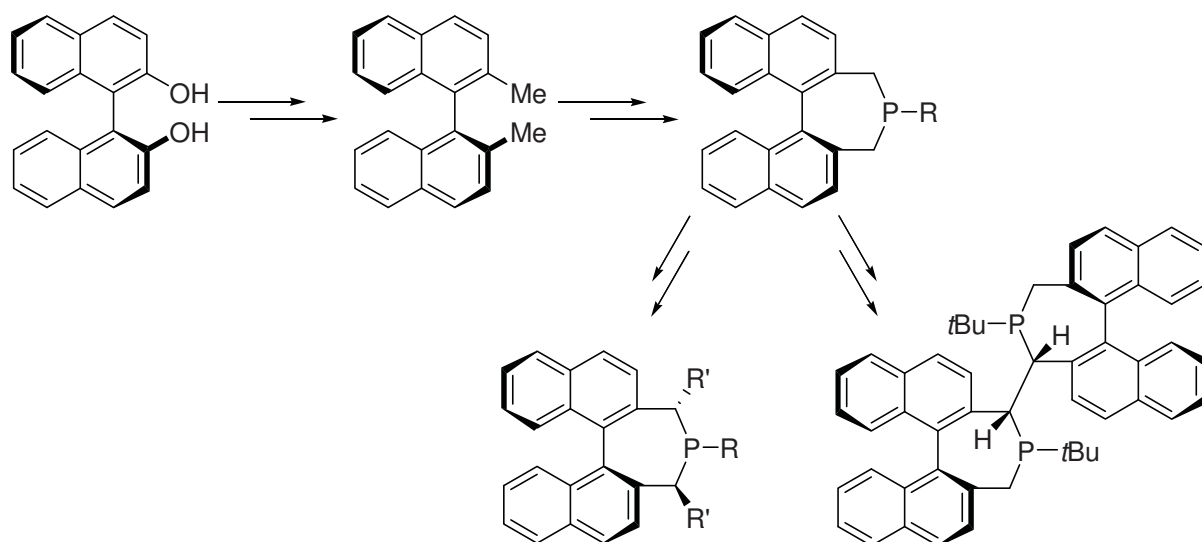
Scheme 1.7. Chiral cyclic phosphines from enantiomerically pure starting materials.

Other possibilities are reactions of electrophilic phosphorus species with alkenes (Scheme 1.8). Additions involving rearrangements^[27] (*McBride* reaction, **A**) and formal cycloadditions^[28] (*McCormack* reaction, **B** and **C**) have been carried out.



Scheme 1.8. Cyclic phosphines by addition of phosphorus to C-C double bonds.

The binaphthyl structure has also been incorporated to synthesize cyclic phosphines by deprotonation of benzylic methyl groups followed by reaction with a suitable phosphorus compound.^[29] Further functionalization^[30] or dimerization^[31] provided more complex structures (Scheme 1.9).



Scheme 1.9. Binaphthyl-derived cyclic phosphines.

1.1.2.2 Phospholanes in Catalysis

Among the cyclic phosphines phospholanes are the most common class in asymmetric catalysis. Phospholanes consist of a five-membered ring with an endocyclic phosphorus. The parent structure is phosphole (Figure 1.3).

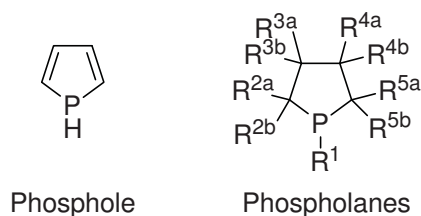


Figure 1.3. Phospholanes.

A variety of structures containing phospholanes have been synthesized and used in asymmetric hydrogenation reactions.^[32] The first successful applications were reported by *Burk* using the bidentate phospholanes DuPhos and BPE (Figure 1.4).^[23c, 33] These ligand types provide very selective catalysts for various substrate classes. Many different analogues have been reported with diverse bridging units or substitution patterns on the five-membered ring.^[32] Later, *Zhang* synthesized phospholane ligands including stereogenic phosphorus atoms, such as TangPhos and DuanPhos, and successfully applied them in asymmetric hydrogenations.^[34]

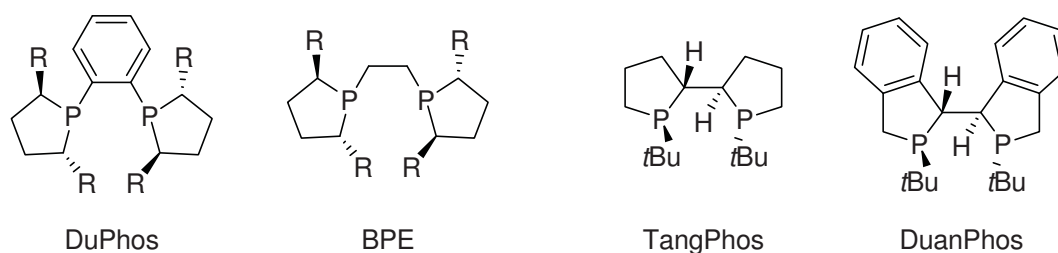


Figure 1.4. Successful phospholane ligands for asymmetric hydrogenations.

Besides asymmetric hydrogenation reactions, phospholanes have also been applied as nucleophilic catalysts in kinetic resolutions by acyl transfer^[35] and carbon-carbon bond forming reactions,^[36] although with only moderate efficiency.

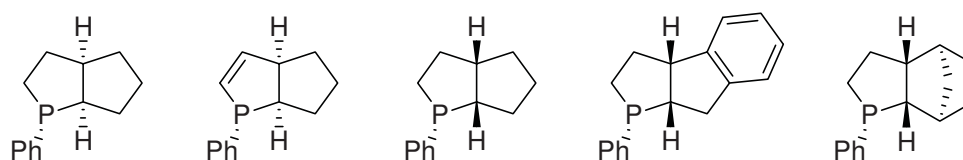


Figure 1.5. Phospholanes used as nucleophilic catalysts.

1.1.3 Ferrocene

1.1.3.1 Structural Properties

Discovered in 1951^[37] ferrocene was first used as a structural moiety for ligand development by *Hayashi* in the 1970's.^[38] The unique geometry and the chemical stability proved to be very fruitful for catalyst design.

The rather rigid structure allowed for the installation of donor atoms at defined distances for the control of ligand geometry. The gap between the two phosphorus atoms is larger in 1,2-disubstituted ferrocenes than in 1,1'-disubstituted ferrocenes and the latter likewise exhibits a greater distance than 1,2-disubstituted benzenes (Figure 1.6).

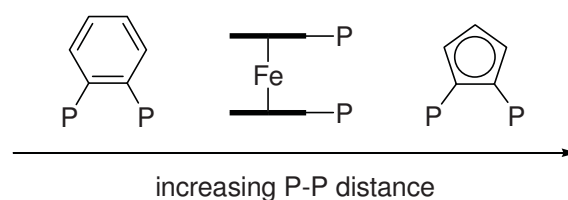


Figure 1.6. P-P distances with different ligand backbones.

This tuning of the bite-angle allowed for the development of ligands for many applications.^[39] Another important property of ferrocene is the generation of chirality upon multiple substitution of the cyclopentadienyl rings. In contrast to benzene, in which under the same circumstances a plane of symmetry still exists, the presence of a second aromatic ring breaks the symmetry in ferrocene giving rise to a plane of chirality. *Schlögl* proposed a nomenclature for ferrocenes having planar chirality (Figure 1.7).^[40]

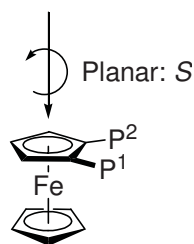


Figure 1.7. *Schlögl*-definition of planar chirality on ferrocenes.

1.1.3.2. Ligands with a Ferrocenyl Backbone

The most common strategy for the synthesis of ferrocenyl ligands is the metallation of ferrocene, or one of its derivatives, and subsequent reaction with an electrophile. This metallation reaction does not generally need harsh conditions. Butyllithium in a suitable solvent is usually sufficient and the use of *ortho*-directing groups allows for the selective establishment of a desired substitution pattern.^[41] *Ortho*-directing groups developed in classic aromatic chemistry can also be easily applied to the ferrocene system and since multiple substitution on a ferrocene ring generates planar chirality, the *ortho*-directed metallation can be carried out in an enantioselective or diastereoselective fashion. A chiral directing group or an achiral functionality in combination with a chiral base can be used to induce selectivity. Although some good results have been achieved with the latter strategy,^[42] the application of chiral *ortho*-directing groups is much more common. For example, amines,^[43] acetals,^[44] sulfoxides^[45] or oxazolines^[46] have all been employed (Figure 1.8).

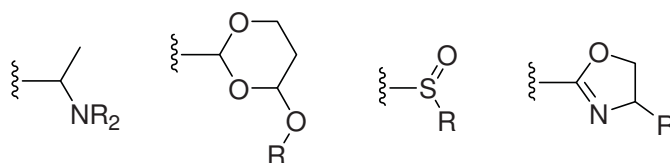


Figure 1.8. Common chiral *ortho*-directing groups.

Through these procedures, numerous phosphine ligands have been developed and successfully applied in asymmetric catalysis.^[39]

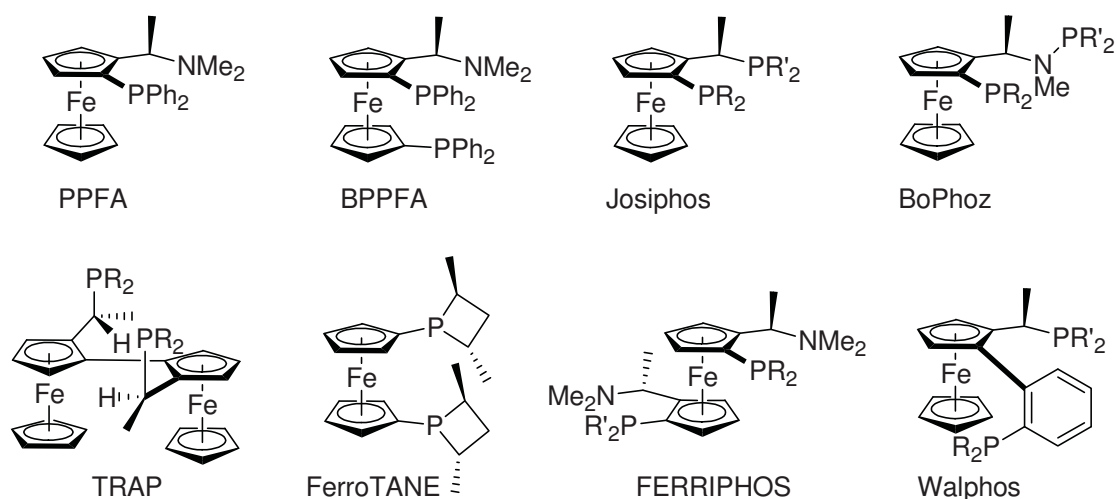
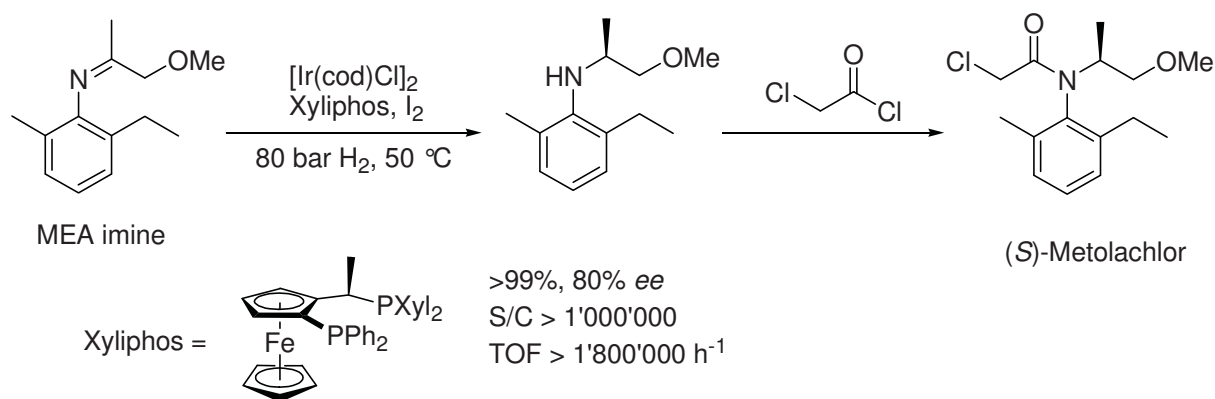


Figure 1.9. Selection of ferrocenyl-phosphine ligands.

The first examples were ppfa and bppfa by *Kumada* and *Hayashi*.^[47] In the following years the structural diversity of ferrocenyl ligands constantly grew, with the ligand families of Josiphos,^[48] FERRIPHOS,^[49] BoPhoz,^[50] Walphos,^[51] TRAP^[52] and FerroTANE^[53] representing only a selection of the diversity available.

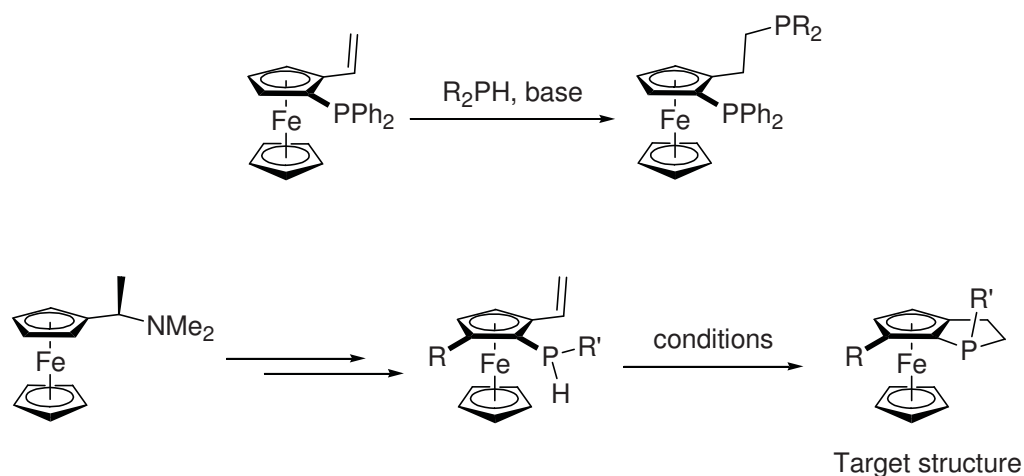
The most successful application of ferrocenyl ligands is the iridium-catalyzed hydrogenation of an imine in the industrial scale synthesis of the herbicide (*S*)-Metolachlor at Syngenta. The catalyst system containing a Josiphos derivative is extremely active and several tons per year are being produced using asymmetric catalysis (Scheme 1.10).^[54]



Scheme 1.10. Industrial scale (*S*)-Metolachlor process. Xyl = 3,5-dimethylphenyl.

1.1.4 Objectives of this Work

The aim of this project was the synthesis of P-stereogenic ferrocenephospholanes. According to a reported intermolecular hydrophosphination^[55] the phospholane ring can be constructed by the intramolecular addition of a secondary phosphine to a vinyl group under basic conditions (Scheme 1.11). For this purpose, functionalized ferrocene derivatives had to be synthesized starting from *Ugi*'s amine and cyclization procedures were to be evaluated.



Scheme 1.11. Proposed synthesis of ferrocenephospholanes.

These synthetic procedures should result in monodentate and bidentate ligands for the complexation of transition metals whereupon their coordination mode was to be examined.

The phosphines obtained were then to be tested in the transition metal catalyzed asymmetric hydrogenation of olefins using rhodium-, ruthenium- and iridium-complexes.

1.1.5 References

- [1] L. D. Quinn, *A Guide to Organophosphorus Chemistry*, Wiley-Interscience, **2000**, 272.
- [2] C. Kölmel, C. Ochsenfeld, R. Ahlrichs, *Theor. Chim. Acta.* **1991**, *82*, 271-284.
- [3] J. Huheey, E. Keiter, R. Keiter, *Anorganische Chemie: Prinzipien von Struktur und Reaktivität*, 2. Auflage, de Gruyter, Berlin, New York, **1995**, 257-262.
- [4] a) L. Horner, H. Winkler, A. Rapp, A. Mentrup, H. Hoffmann, P. Beck, *Tetrahedron Lett.* **1961**, *5*, 161-166; b) O. Korpiun, R. A. Lewis, J. Chickos, K. Mislow, *J. Am. Chem. Soc.* **1968**, *90*, 4842-4846.
- [5] W. S. Knowles, M. J. Sabacky, B. D. Vineyard, D. J. Weinkauff, *J. Am. Chem. Soc.* **1975**, *97*, 2567-2568.
- [6] a) S. Jugé, J.-P. Genêt, *Tetrahedron Lett.* **1989**, *30*, 2783; b) E. J. Corey, Z. Chen, G. J. Tanoury, *J. Am. Chem. Soc.* **1993**, *115*, 11000.
- [7] D. S. Glueck, *Chem. Eur J.* **2008**, *14*, 7108-7117.
- [8] a) B. Join, D. Mimeau, O. Delacroix, A.-C. Gaumont, *Chem. Commun.* **2006**, 3249-3251; b) C. Scriban, D. S. Glueck, *J. Am. Chem. Soc.* **2006**, *128*, 2788-2789; c) V. S. Chan, I. C. Stewart, R. G. Bergman, F. D. Toste, *J. Am. Chem. Soc.* **2006**, *128*, 2786-2787; d) V. S. Chan, M. Chiu, R. G. Bergman, F. D. Toste, *J. Am. Chem. Soc.* **2009**, *131*, 6021-6032.
- [9] J. A. Osborn, F. H. Jardine, G. W. Wilkinson, *J. Chem. Soc. A* **1966**, 1711.
- [10] a) L. Horner, H. Winkler, *Annalen* **1965**, *685*, 1; b) L. Horner, W. D. Balzer, D. J. Peterson, *Tetrahedron Lett.* **1966**, 3315; c) O. Korpiun, K. Mislow, *J. Am. Chem. Soc.* **1967**, *89*, 4784; d) O. Korpiun, R. A. Lewis, J. Chickos, K. Mislow, *J. Am. Chem. Soc.* **1968**, *90*, 4842; e) K. Naumann, G. Zon, K. Mislow, *J. Am. Chem. Soc.* **1969**, *91*, 7012.
- [11] a) W. S. Knowles, M. J. Sabacky, *Chem. Commun.* **1968**, 1445; b) L. Horner, H. Siegel, H. Bueche, *Angew. Chem. Int. Ed.* **1968**, *7*, 942.
- [12] H. B. Kagan, T. P. Kang, *J. Am. Chem. Soc.* **1972**, *94*, 6429.
- [13] B. D. Vineyard, W. S. Knowles, M. J. Sabacky, G. L. Bachmann, D. J. Weinkauff, *J. Am. Chem. Soc.* **1977**, *99*, 5946.
- [14] For an overview see: a) L. A. Oro, D. Carmona in *Handbook of Homogeneous Hydrogenation*, J. G. de Vries, C. J. Elsevier Eds., Wiley-VHC, Weinheim, **2007**, 3-30; b) J. M. Brown in *Handbook of Homogeneous Hydrogenation*, J. G. de Vries, C. J. Elsevier Eds., Wiley-VHC, Weinheim, **2007**, 1073-1103.
- [15] a) J. Halpern, *Science*, **1982**, *217*, 401; b) J. Halpern, A. S. C. Chan, *J. Am. Chem. Soc.* **1980**, *102*, 838; c) A. S. C. Chan, J. J. Pluth, J. Halpern, *J. Am. Chem. Soc.* **1980**, *102*, 5052; d) C. R. Landis, J. Halpern, *J. Am. Chem. Soc.* **1987**, *109*, 1746; e) Y. K. Sun, R. N. Landau, J. Wang, C. Leblond, D. G. Blackmond, *J. Am. Chem. Soc.* **1996**, *118*, 1348.
- [16] a) J. M. Brown, P.A. Chaloner, P. N. Nicholson, *J. Chem. Soc., Chem. Commun.* **1978**, 646; b) J. M. Brown, P.A. Chaloner, *Tetrahedron Lett.* **1978**, 1877; c) J. M. Brown, P.A. Chaloner, *J. Chem. Soc., Chem. Commun.* **1978**, 321; d) J. M. Brown, P.A. Chaloner, G. Descotes, R. Glaser, D. Lafont, D. Sinou, *J. Chem. Soc., Chem. Commun.* **1979**, 611; e) J. M. Brown, P.A. Chaloner, *J. Chem. Soc., Chem. Commun.* **1979**, 613; f) J. M. Brown, P.A. Chaloner, *J. Chem. Soc., Chem. Commun.* **1980**, 344; g) J. M. Brown, P.A. Chaloner, R. Glaser, S. Geresh, *Tetrahedron* **1980**, 815; h) G. Descotes, D. Lafont, D. Sinou, J. M. Brown, P. A. Chaloner, D. Parker, *New J. Chem.* **1981**, *5*, 167.

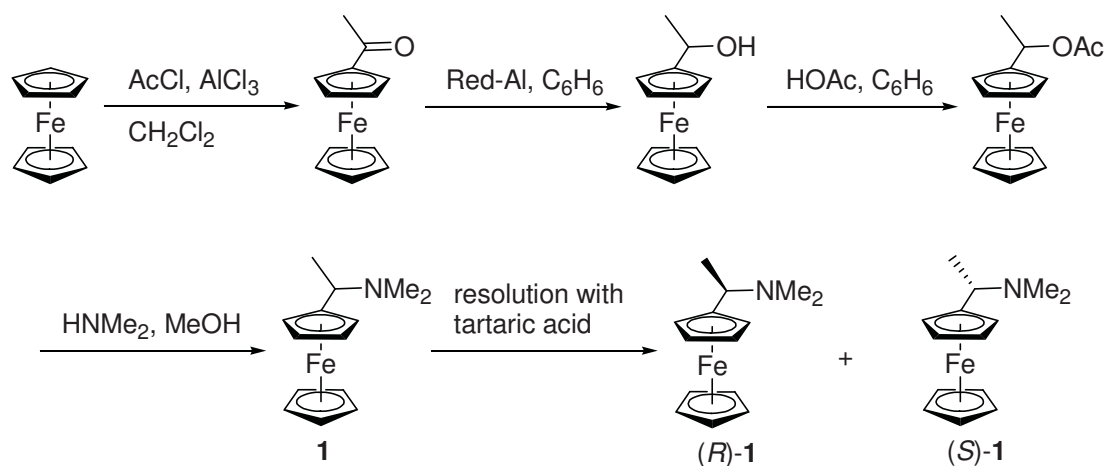
- [17] J. Halpern, A. S. C. Chan, J. J. Pluth, *J. Am. Chem. Soc.* **1980**, *102*, 5952.
- [18] a) c) I. D. Gridnev, N. Higashi, K. Asakura, T. Imamoto, *J. Am. Chem. Soc.* **2000**, *122*, 7183; b) I. D. Gridnev, Y. Yamanoi, N. Higashi, M. Yasutake, T. Imamoto, *Adv. Synth. Catal.* **2001**, *343*, 118; c) K. V. L. Crépy, T. Imamoto, *Adv. Synth. Catal.* **2003**, *345*, 79; d) I. D. Gridnev, T. Imamoto, *Acc. Chem. Res.* **2004**, *37*, 633.
- [19] a) N. W. Alcock, J. M. Brown, A. E. Derome, A. R. Lucy, *J. Chem. Soc., Chem. Commun.* **1985**, 575-578; b) S. K. Armstrong, J. M. Brown, M. J. Burk, *Tetrahedron Lett.* **1993**, *34*, 879-882; c) B. F. M. Kimmich, E. Somsook, C. L. Landis, *J. Am. Chem. Soc.* **1998**, *120*, 10115-10125.
- [20] A. Miyashita, A. Yasuda, H. Takaya, K. Toriumi, T. Ito, T. Souchi, R. Noyori, *J. Am. Chem. Soc.* **1980**, *102*, 7932.
- [21] a) M. Kitamura, M. Tsukamoto, Y. Bessho, M. Yoshimura, U. Kobs, M. Widhalm, R. Noyori, *J. Am. Chem. Soc.* **2002**, *124*, 6649; b) M. T. Ashby, J. Halpern, *J. Am. Chem. Soc.* **1991**, *113*, 589-594.
- [22] G. Erre, S. Enthaler, K. Junge, S. Gladiali, M. Beller, *Coordination Chemistry Reviews* **2008**, *252*, 471-491.
- [23] a) X. Li, K. D. Robinson, P. P. Gaspar, *J. Org. Chem.* **1996**, *61*, 7702; b) A. Marinetti, V. Kruger, F.-X. Buzin, *Tetrahedron Lett.* **1997**, *38*, 2947; c) M. J. Burk, J. E. Feaster, W. A. Nugent, R. L. Harlow, *Tetrahedron: Asymmetry* **1991**, *2*, 569.
- [24] M. Ostermeier, J. Prieß, G. Helmchen, *Angew. Chem.* **2002**, *114*, 625.
- [25] A. Marinetti, F. Mathey, L. Ricard, *Organometallics* **1993**, *12*, 1207.
- [26] V. Bilenko, A. Spannenberg, W. Baumann, I. Komarov, A. Börner, *Tetrahedron: Asymmetry* **2006**, *17*, 2082.
- [27] a) A. Marinetti, L. Ricard, *Tetrahedron* **1993**, *49*, 10291; b) A. Marinetti, L. Ricard, *Organometallics* **1994**, *13*, 3956.
- [28] a) F. Guillen, J.-C. Fiaud, *Tetrahedron Lett.* **1999**, *40*, 2939; b) F. Guillen, M. Rivard, M. Toffano, J.-Y. Legros, J. C. Daran, J.-C. Fiaud, *Tetrahedron* **2002**, *58*, 5895; c) N. V. Dubrovina, H. Jiao, V. I. Tararov, A. Spannenberg, R. Kadyrov, A. Monsees, A. Christiansen, A. Börner, *Eur. J. Org. Chem.* **2006**, *15*, 3412.
- [29] a) K. Tani, L. D. Brown, J. Ahmed, J. A. Ibers, M. Yokota, A. Nakamura, S. Otsuka, *J. Am. Chem. Soc.* **1977**, *99*, 7876; b) A. Cope, E. C. Friedrich, *J. Am. Chem. Soc.* **1968**, *90*, 909; c) D. Xiao, Z. Zhang, X. Zhang, *Org. Lett.* **1999**, *1*, 1679-1681; d) K. Junge, G. Oehme, A. Monsees, T. Riermeier, U. Dingerdissen, M. Beller, *Tetrahedron Lett.* **2002**, *43*, 4977-4980.
- [30] P. Kasák, K. Mereiter, M. Widhalm, *Tetrahedron: Asymmetry* **2005**, *16*, 3416.
- [31] W. Tang, W. Wang, Y. Chi, X. Zhang, *Angew. Chem., Int. Ed.* **2003**, *42*, 3509-3511.
- [32] a) M. J. Burk, *Acc. Chem. Res.* **2000**, *33*, 363-372; H.-U. Blaser, C. Malan, B. Pugin, F. Spindler, H. Steiner, M. Studer, *Adv. Synth. Catal.* **2003**, *245*, 103; c) W. Tang, X. Zhang, *Chem. Rev.* **2003**, *103*, 3029; d) T. P. Clark, C. R. Landis, *Tetrahedron: Asymmetry* **2004**, *15*, 2123; e) C. J. Cobley, P. H. Moran in *Handbook of Homogeneous Hydrogenation*, J. G. de Vries, C. J. Elsevier Eds., Wiley-VHC, Weinheim, **2007**, 773-831.
- [33] a) M. J. Burk, J. E. Feaster, R. L. Harlow, *Organometallics* **1990**, *9*, 2653; b) M. J. Burk, R. L. Harlow, *Angew. Chem. Int. Ed.* **1990**, *29*, 1462; c) M. J. Burk, *J. Am. Chem. Soc.* **1991**, *113*, 8518.
- [34] a) W. Tang, X. Zhang, *Angew. Chem. Int. Ed.* **2002**, *41*, 1612; b) D. Liu, X. Zhang, *Eur. J. Org. Chem.* **2005**, 646-649.
- [35] J. A. MacKay, E. Vedejs, *J. Org. Chem.* **2006**, *71*, 498-503.
- [36] Z. Pakulski, O. M. Demchuck, J. Frelek, R. Luboradzki, K. M. Pietrusiewicz, *Eur. J. Org. Chem.* **2004**, 3913-3918.
- [37] T. J. Kealy, P. L. Pauson, *Nature* **1951**, *168*, 1039.

- [38] T. Hayashi, M. Tajika, K. Tamao, M. Kumada, *J. Am. Chem. Soc.* **1976**, *98*, 3718.
- [39] T. J. Colacot, *Chem. Rev.* **2003**, *103*, 3101-3118.
- [40] a) K. Schlögl, *Topics Stereochem.* **1967**, *1*, 39; b) K. Schlögl, *J. Organomet. Chem.* **1986**, *300*, 219.
- [41] a) P. Beak, V. Snieckus, *Acc. Chem. Res.* **1982**, *15*, 306-312; b) V. Snieckus, *Chem. Rev.* **1990**, *90*, 879-933.
- [42] a) D. Price, N. S. Simpkins, *Tetrahedron Lett.* **1995**, *36*, 6135; b) M. Tsukazaki, M. Tinkl, A. Roglans, B. J. Chapell, N. J. Taylor, V. Snieckus, *J. Am. Chem. Soc.* **1996**, *118*, 685; c) Y. Nishibayashi, Y. Arikawa, K. Ohe, S. Uemura, *J. Org. Chem.* **1996**, *61*, 1172.
- [43] a) D. Marquarding, H. Klusaceck, G. Gokel, P. Hoffmann, I. Ugi, *J. Am. Chem. Soc.* **1970**, *92*, 5389; b) L. E. Batelle, R. Bau, G. Gokel, I. Ugi, *J. Am. Chem. Soc.* **1973**, *95*, 482; c) C. Ganter, T. Wagner, *Chem. Ber.* **1995**, *128*, 1157.
- [44] a) O. Riant, O. Samuel, H. B. Kagan, *J. Am. Chem. Soc.* **1993**, *115*, 5836; b) O. Riant, O. Samuel, T. Flessner, S. Taudien, H. B. Kagan, *J. Org. Chem.* **1997**, *62*, 6733.
- [45] a) F. Rebière, O. Riant, L. Ricard, H. B. Kagan, *Angew. Chem. Int. Ed. Engl.* **1993**, *32*, 568; b) D. H. Hua, N. M. Lagneau, Y. Chen, P. M. Robben, G. Clapham, P. D. Robinson, *J. Org. Chem.* **1996**, *61*, 4508.
- [46] a) T. Sammakia, H. A. Latham, D. R. Schaad, *J. Org. Chem.* **1995**, *60*, 10; b) Y. Nishibayashi, S. Uemura, *Synlett* **1995**, *79*; c) C. J. Richards, T. Damalidis, D. E. Hibbs, M. B. Hursthouse, *Synlett* **1995**, *74*; d) T. Sammakia, H. A. Latham, *J. Org. Chem.* **1995**, *60*, 6002; e) T. Sammakia, H. A. Latham, *J. Org. Chem.* **1996**, *61*, 1629.
- [47] a) T. Hayashi, K. Yamamoto, M. Kumada, *Tetrahedron Lett.* **1974**, 4405; b) T. Hayashi in *Ferrocenes*; A. Togni, T. Hayashi. Eds.; Wiley-VCH, Weinheim, **1995**, 105-142.
- [48] A. Togni, C. Breutel, A. Schnyder, F. Spindler, H. Landert, A. Tijiani, *J. Am. Chem. Soc.* **1994**, *116*, 4062.
- [49] a) J. J. Almena Perea, A. Börner, P. Knochel, *Tetrahedron Lett.* **1998**, *39*, 8073-8076; b) M. Lotz, T. Ireland, J. J. Almena Perea, P. Knochel, *Tetrahedron: Asymmetry* **1999**, *10*, 1839-1842.
- [50] N. W. Boaz, S. D. Debenham, E. B. Mackenzie, S. E. Large, *Org. Lett.* **2002**, *4*, 2421.
- [51] T. Sturm, W. Weissensteiner, F. Spindler, *Adv. Synth. Catal.* **2003**, *345*, 160-164.
- [52] Y. Ito, M. Sawamura, *Chem. Rev.* **1992**, *92*, 857.
- [53] U. Berens, M. J. Burk, A. Gerlach, W. Hems, *Angew. Chem., Int. Ed.* **2000**, *39*, 1981.
- [54] a) H.-U. Blaser, H.-P. Buser, K. Coers, R. Hanreich, H.-P. Jalett, E. Jelsch, B. Pugin, H.-D. Schneider, F. Spindler, A. Wegmann, *Chimia* **1999**, *53*, 275-280; b) B. Pugin, H. Landert, F. Spindler, H.-U. Blaser, *Advanced Synthesis & Catalysis* **2002**, *344*, 974-979; c) H.-U. Blaser, *Advanced Synthesis & Catalysis* **2002**, *344*, 17-31.
- [55] B. Gschwend, B. Pugin, A. Bertogg, A. Pfaltz, *Chem. Eur. J.* **2009**, DOI: 10.1002/chem.200902418.

1.2. Synthesis of Ferrocenephospholanes

1.2.1 *Ugi*'s Amine

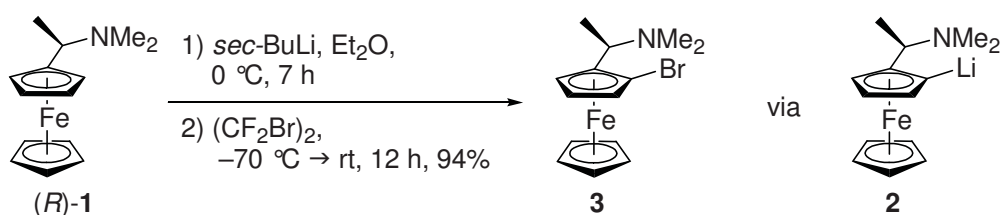
The first step to establish an optically active ferrocene derivative by multiple stereoselective substitutions of one cyclopentadienyl ring was the introduction of a *ortho*-directing group which is able to differentiate between diastereotopic *ortho*-positions. Among a number of possible solutions 1-(*N,N*-dimethylamino)ethylferrocene, *Ugi*'s amine (**1**), was chosen as the starting point of the synthesis. **1** is readily available from ferrocene within a few steps by literature methods (Scheme 1.12). The obtained racemate is then resolved by fractional crystallization as the corresponding tartrate.^[1]



Scheme 1.12. Synthesis and resolution of *Ugi*'s amine.

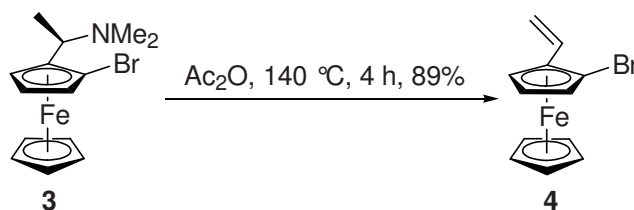
1.2.2 Formation of a Simple Ferrocenephospholane

Although the structure of *Ugi*'s amine is rather simple, the diastereoselectivities in metallation reactions with a suitable alkyllithium reagent are generally above 95:5.^[2] Lithiation of (*R*)-**1** with *sec*-butyllithium in diethyl ether at 0 °C afforded the intermediate lithioferrocene **2** which then was reacted with 1,2-dibromo-1,1,2,2-tetrafluoroethane to give the bromide **3** as a single diastereoisomer in good yield after crystallization (Scheme 1.13).^[3]



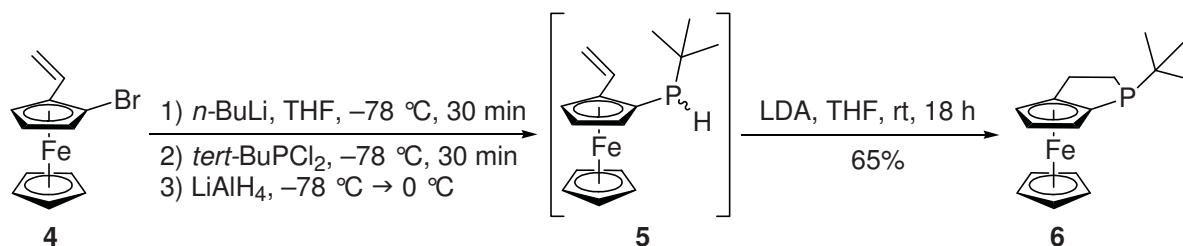
Scheme 1.13. *ortho*-Bromination of Ugi's amine.

After the introduction of planar chirality by 1,2-substitution, the *ortho*-directing group could be manipulated without loss of enantiomeric purity. The dimethylaminoethyl group was converted to an ethenyl group by reaction with acetic anhydride at elevated temperature. The resulting bromo-vinyl-ferrocene **4** was isolated as a dark red liquid in good yield. Interestingly, although the formation of **4** took place at 140 °C, this compound was found to be sensitive to heat after work up and purification, and could only be stored at –20 °C for a few weeks (Scheme 1.14).



Scheme 1.14. Elimination of the dimethylamino group.

The bromide **4** could be lithiated with *n*-butyllithium in THF at –78 °C. The reaction of this metallated ferrocene with *tert*-butylphosphine dichloride followed by reduction with lithium aluminium hydride gave the secondary phosphine **5** as shown in Scheme 1.15. The reaction selectively gave the monoaddition product regardless of the order of addition. Despite a certain stability towards oxygen, **5** was generally not purified but quickly filtered through a plug of silica gel to remove any remaining salts and used directly in the next step. The raw material was analyzed by ¹H- and ³¹P-NMR, and selective formation of **5** as the only ferrocene containing phosphine could be confirmed. **5** was obtained as a 1:1 diastereomeric mixture. This could be clearly observed in the NMR-spectra of **5**, with the ¹H-NMR showing two sets of signals for the phosphine protons at 4.19 ppm (d, ¹J_{HP} = 206 Hz) and 3.84 ppm (d, ¹J_{HP} = 210 Hz). In the ³¹P-spectrum the resonances appear at –36.4 ppm and –46.6 ppm with the expected proton couplings.



Scheme 1.15. Lithiation-chlorophosphinylation-reduction-hydrophosphination sequence.

The hydrophosphination reaction of vinylferrocenes under basic conditions was known for intermolecular examples.^[4] The intramolecular reaction did not proceed under these conditions. Organic bases such as DBU or TBD were not strong enough to induce the hydrophosphination at ambient or elevated temperature. Deprotonation with *n*-butyllithium in toluene, diethyl ether or THF with or without additives such as DBU, TBD or TMEDA gave either no conversion or a mixture of products. Finally, a solution of freshly prepared LDA in THF was found to convert the secondary phosphine **5** into the phospholane **6**. In this stereospecific reaction **6** was formed as a single diastereoisomer and its structure was confirmed by X-ray crystallography (Figure 1.10).

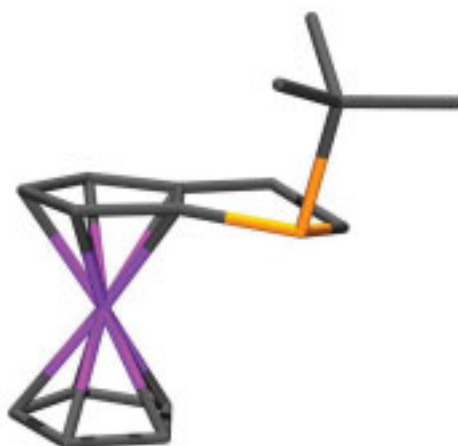
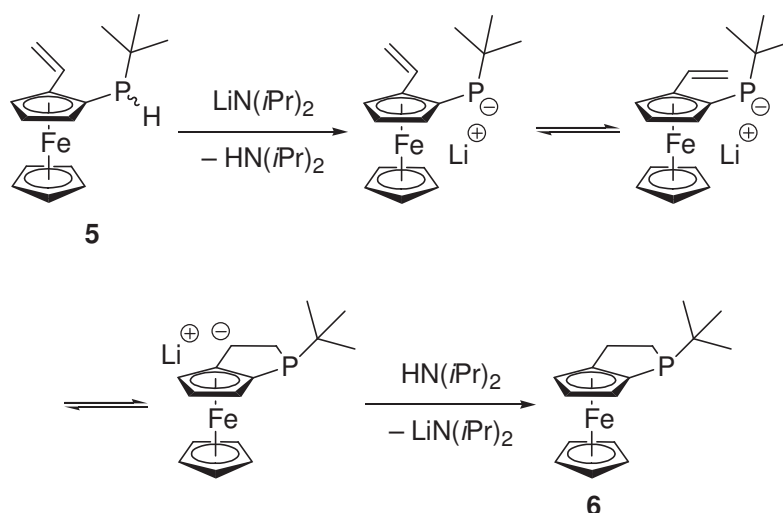


Figure 1.10. Solid state structure of **6**.

Insights into the pathway of this cyclization reaction can be gained from different observations. The base has to be strong enough to completely deprotonate the secondary phosphine but this deprotonation must not be irreversible. The type of substituent on the phosphorus atom is important. When *tert*-butyl was exchanged for phenyl the cyclization failed regardless of the conditions.

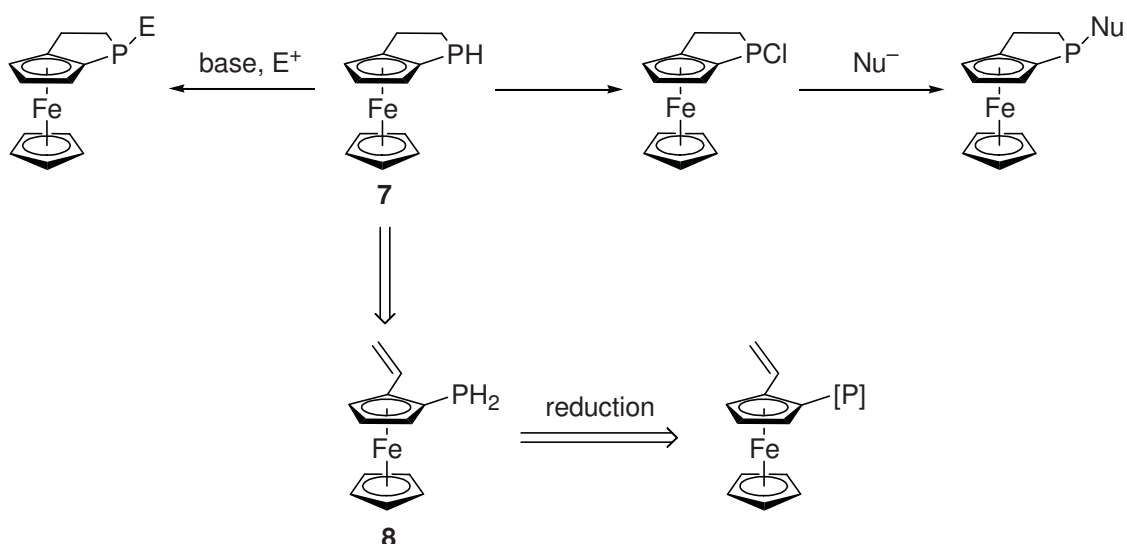


Scheme 1.16. Possible mechanism for the base induced hydrophosphination.

With this in mind, a mechanism for the cyclization reaction can be proposed (Scheme 1.16). When the secondary phosphine **5** is deprotonated the stereogenic center at the phosphorus atom is lost. The bulky *tert*-butyl group then adopts a conformation that minimizes steric interactions and therefore at the same time positions the lone pairs to favor the cyclization. Presumably, substituents smaller than the *tert*-butyl group cannot enforce the desired conformation needed for the attack at the double bond. Keeping in mind that the vinyl group itself is rotating and its favored position is most likely not pointing towards the phosphorus atom, this preorientation of the lone pairs is expected to be crucial. The cyclization reaction may also be reversible with the final protonation driving the reaction towards the product. This would explain the failure of the reaction when using *n*-butyllithium as base. Apparently, the presence of one equivalent of di-*iso*-propylamine is sufficient to complete the reaction.

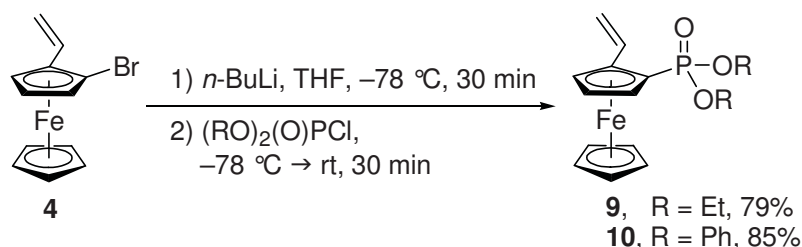
1.2.3 Approaches to a Secondary Ferrocenephospholane

The unique behaviour of the *tert*-butyl group was also demonstrated in the attempted synthesis of structures like **6** without alkyl substituted phosphorus atom. This secondary phospholane **7** would be an interesting phosphine building block as one could expect stereoselective functionalization reactions at the phosphorus atom. Either nucleophilic or electrophilic substitution reactions could be used to give a variety of new structural combinations (Scheme 1.17).



Scheme 1.17. Reactions involving a secondary phospholane.

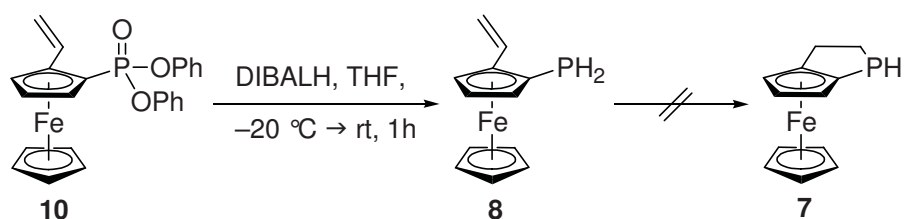
The substrate for the cyclization was the primary phosphine **8** which was synthesized by the reduction of a suitable precursor. A logical route would be the reduction of a phosphine dichloride with lithium aluminium hydride. This phosphine dichloride could be introduced by lithiation of **4** and reaction with phosphorus trichloride. However, this reagent would form highly toxic PH_3 upon treatment with a hydride source and complete removal before the reduction would be crucial. To avoid the danger of generating PH_3 the substrate for the reduction had to be purified before use. Therefore more stable phosphorus compounds than phosphine dichlorides were examined. The functional group of choice turned out to be a phosphonate. The syntheses of the ethyl and phenyl phosphonates were straightforward (Scheme 1.18). Lithiation of **4** and reaction with diethyl or diphenyl chlorophosphate gave the phosphonic acid esters **9** and **10** in good yields. These compounds could easily be purified by chromatography, excluding formation of PH_3 . **10** was used preferentially in the next step as it was isolated as a solid, in contrast to **9** which was found to be an oil.



Scheme 1.18. Introduction of a phosphonate ester.

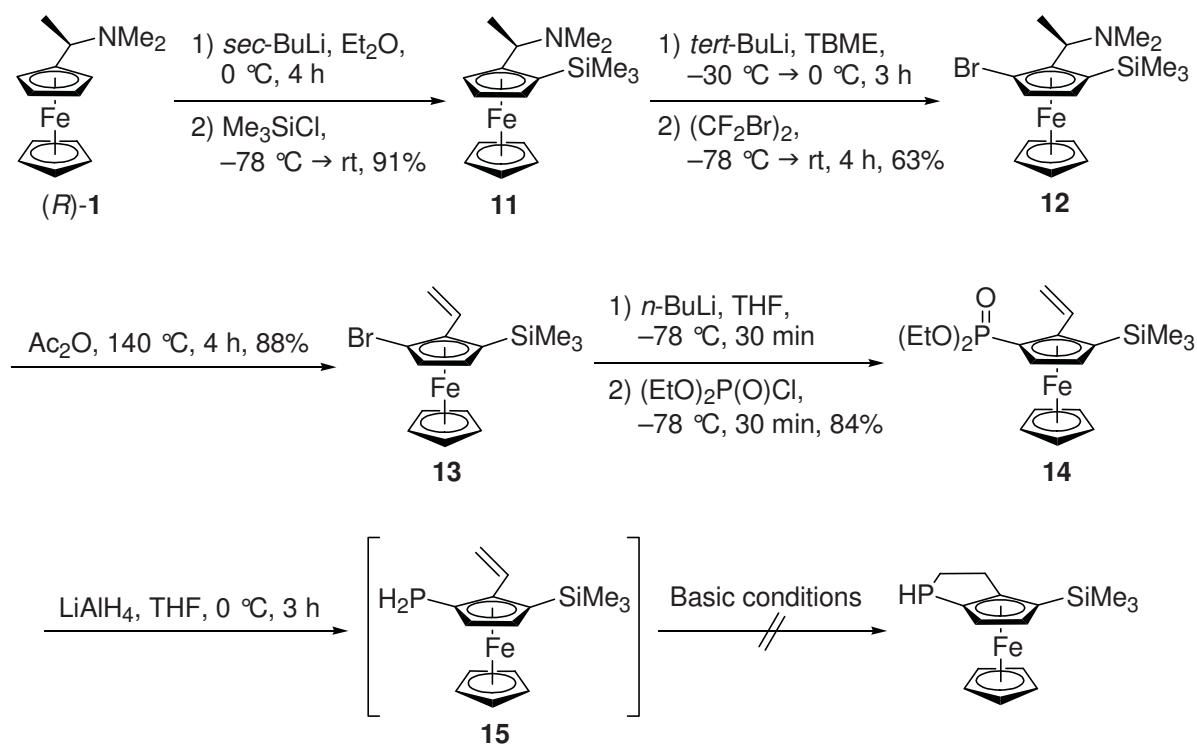
The reduction of **10** with lithium aluminium hydride turned out to not be perfectly selective. The formation of a second primary phosphine was observed in low amounts, possibly due to a

side reaction involving partial reduction of the vinyl group. This problem could be overcome by changing to di-*iso*-butylaluminum hydride as reducing agent. The reaction at $-20\text{ }^{\circ}\text{C}$ followed by work up with aqueous sodium hydroxide and filtration of the solids formed, selectively gave the primary phosphine **8**. Unfortunately, **8** was slightly less stable than the secondary phosphine **5**, therefore further purification was not possible and the crude product was used in the next step. Phosphine **8** showed a resonance in the ^{31}P -NMR spectrum at -157 ppm with triplet splitting of 201 Hz. The characteristic phosphine protons appear at 3.66 ppm and 3.76 ppm as a doublet of doublets with a proton coupling of 12.4 Hz. However, all attempts at cyclization of **8** failed, with only decomposition observed when the primary phosphine was subjected to basic conditions (Scheme 1.19).



Scheme 1.19. Reductive formation of a primary phosphine and attempted cyclization.

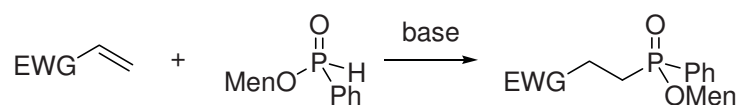
This finding supported the picture of the necessity of preorganization of the substituents to be connected. With this in mind another approach was considered. If the vinyl group were to have less rotational freedom, the lack of preorientation of the phosphine group might be overcome. A straightforward way to constrain the possible conformations was to functionalize the position adjacent to the vinyl group with a bulky substituent. Trimethylsilyl was chosen and installed via the synthetic route outlined in Scheme 1.20. Lithiation of (*R*)-**1** with *sec*-butyllithium at $0\text{ }^{\circ}\text{C}$ followed by addition of trimethylsilyl chloride gave the TMS-substituted diethylaminoethylferrocene **11**. In a second application of butyllithium, the dimethylamino group again directs the deprotonation to the *ortho*-position. However, this deprotonation occurs against the inherent selectivity of the (*N,N*-dimethylamino)ethyl group and therefore requires harsher conditions.



Scheme 1.20. Synthetic pathway to a sterically restricted secondary phospholane.

Lithiation of the second *ortho*-position took place upon treatment of **11** with *tert*-butyllithium in *tert*-butyl methyl ether at 0°C and subsequent reaction with 1,2-dibromo-1,1,2,2-tetrafluoroethane gave the trisubstituted ferrocene **12**. Elimination of the amino group was again achieved in acetic anhydride at elevated temperature giving the vinylferrocene **13**. Halogen lithium exchange with *n*-butyllithium in THF followed by addition of diethyl chlorophosphate resulted in the trisubstituted ferrocene **14**. In contrast to the reduction of **10**, reaction of this species with di-*iso*-butylaluminium hydride required elevated temperature. However, this time even di-*iso*-butylaluminium hydride was not perfectly selective and about 10% of another primary phosphine compound was formed. The desired primary phosphine **15** showed characteristic resonances at -150 ppm with a triplet splitting of 199 Hz in the ^{31}P -NMR and the two phosphine signals in the proton NMR at 3.88 ppm and 3.74 ppm as doublet of doublets with a proton-proton coupling constant of 12.4 Hz. Unfortunately, **15** was found to be comparable to **8** in terms of reactivity and only decomposition was observed when treated under basic conditions.

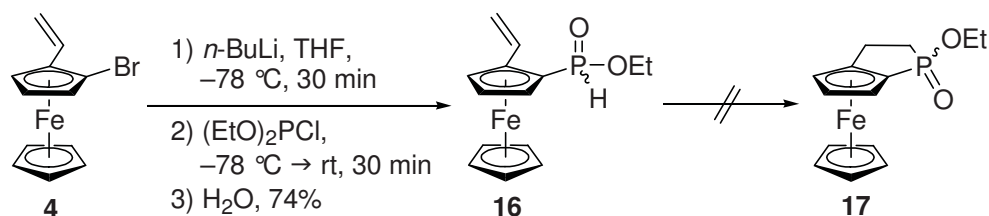
A related addition of phosphorus to double bonds is depicted in Scheme 1.21. Under basic conditions phosphorus carbon bond formation has been reported for phosphinites and electron poor alkenes.^[5]



Scheme 1.21. Reported addition of phosphinites to alkenes.

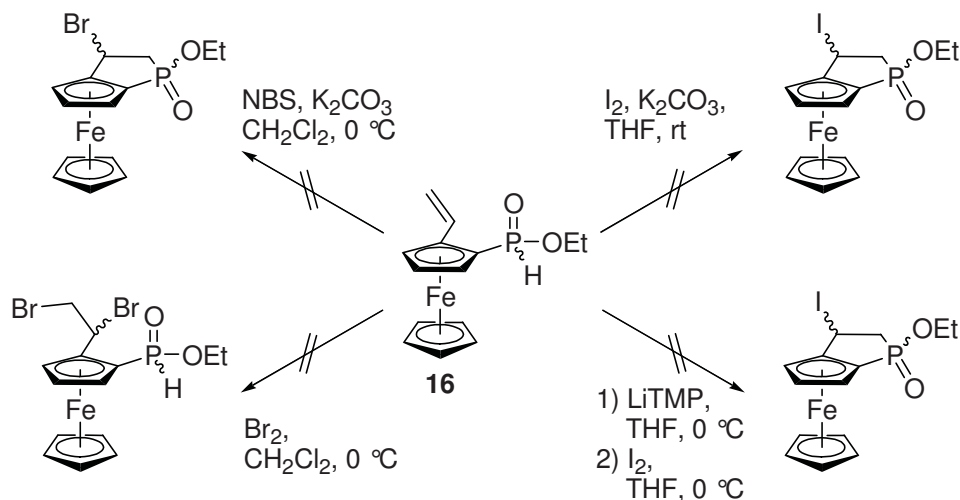
Compared to the primary phosphine **8**, the corresponding phosphinite should be more stable and the product would not be susceptible to oxidation. The resulting phosphonic acid ester could then be reduced to the secondary phosphine **7** using silanes^[6a] or lithium aluminium hydride.^[6b]

The synthesis of the ferrocene phosphinite **16** was straightforward. Lithiation of **4** under the aforementioned conditions followed by addition of diethyl chlorophosphite and hydrolysis gave **16** as a mixture of diastereoisomers. But **16**, like the primary phosphine **8**, did not form the phospholane **17** under basic conditions (Scheme 1.22).



Scheme 1.22. Synthesis of a ferrocenylphosphinite and attempted cyclization.

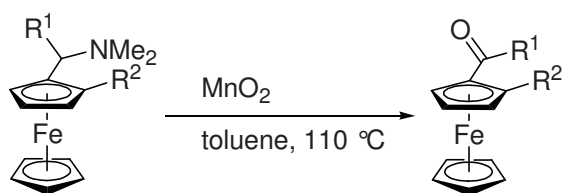
Since it was possible that the vinyl group was not reactive enough, different halogen sources for activation of the double bond were examined as shown in Scheme 1.23. In this reaction, related to iodolactonisation, preliminary formation of a halonium ion would facilitate the addition of the phosphinite.



Scheme 1.23. Cyclization attempts by halogen assistance.

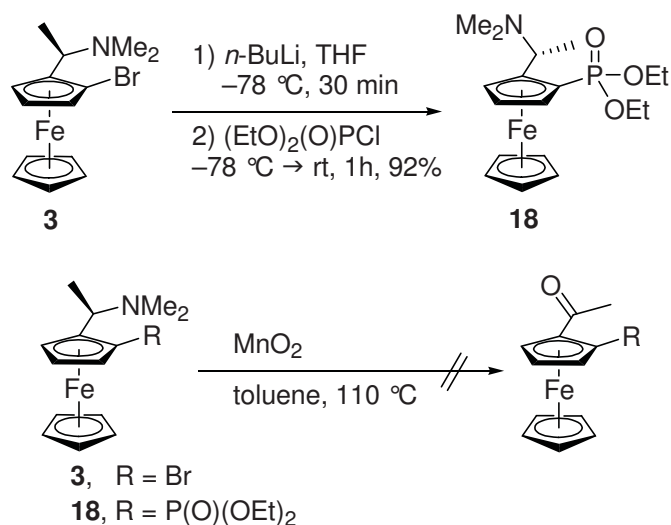
General conditions for iodolactonisations – iodine and potassium carbonate – led to oxidation of the phosphinic acid. Preliminary deprotonation with LiTMP and subsequent treatment with iodine gave the same result. *N*-bromo-succinimide as a halonium source resulted in the formation of multiple unidentifiable products. A possible two-step process by bromination of the vinyl group and a later nucleophilic substitution was also attempted, but the reaction gave again a mixture of products.

These reaction outcomes reflect a general property of ferrocene chemistry. Reductive conditions are generally well tolerated whereas reactions involving oxidations have to be carefully tuned. Strong oxidizing reagents can convert the iron(II)-center to iron(III) leading to a variety of side reactions. An oxidizing agent reported to tolerate the ferrocene system is manganese dioxide. It has been demonstrated by *Malfait et al.* to convert the diethylaminoethyl group to an acetyl group (Scheme 1.24).^[7]



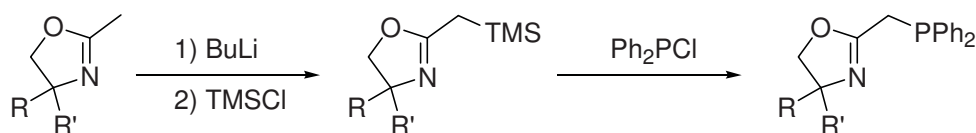
Scheme 1.24. Reported oxidation of the dimethylamino group.

Once the acetyl group is installed, an intramolecular addition of the corresponding enolate to a phosphonic acid would form a five-membered phosphacycle. The synthesis of the phosphonate substituted diethylaminoethylferrocene **18** was accomplished in one step from **3** by lithiation and addition of diethyl chlorophosphate. Unfortunately, the acetyl group was not formed under the reported conditions.^[7] To exclude interference by the phosphonate substituent the same conditions were applied to the brominated ferrocene **3** yet the diethylaminoethyl group was not transformed either (Scheme 1.25).



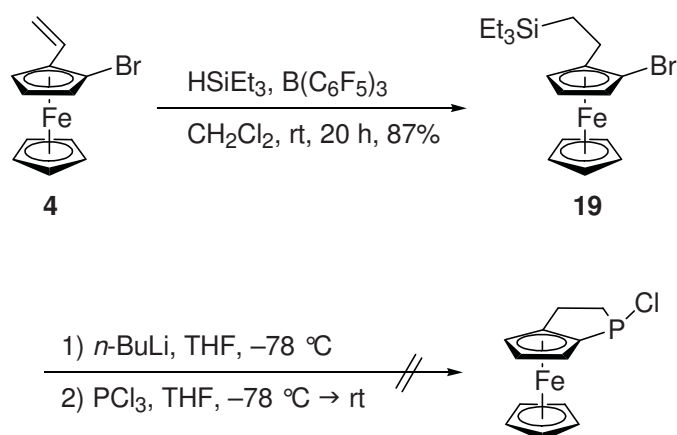
Scheme 1.25. Oxidation reactions with manganese dioxide.

A different approach for the formation of a carbon-phosphorus bond has been reported with the use of silanes. The introduction of silyl groups and the subsequent exchange to phosphines, while avoiding undesired by-products, was successfully applied in the synthesis of phosphino-oxazolines (Scheme 1.26).^[8]



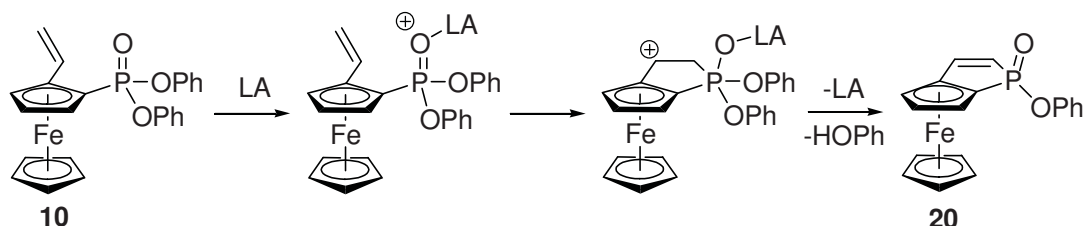
Scheme 1.26. Introduction of phosphines via silyl-exchange.

To apply this methodology to the synthesis of a ferrocenephospholane, the silyl group and the phosphine chloride have to react intramolecularly. In the first step the silane was introduced by using a combination of triethylsilane and tri(pentafluorophenyl)borane to hydrosilate **4**,^[9] the reaction proceeded nicely and in good yield to give **19** (Scheme 1.27). However, the intramolecular cyclization reaction after the introduction of the dichlorophosphine group did not take place.



Scheme 1.27. Hydrosilylation of **4**.

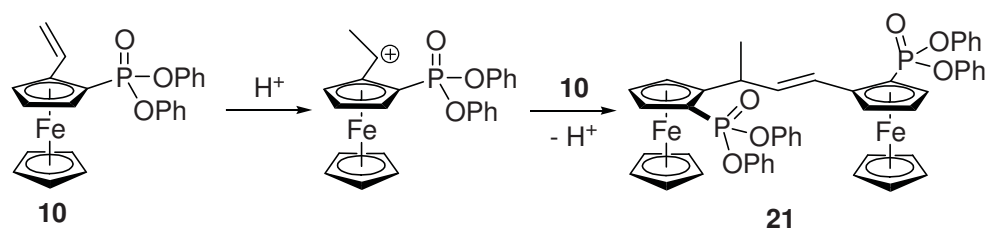
An alternative method would involve activation of the phosphate group towards a nucleophilic attack from the vinylic double bond by a Lewis acid (LA). This reaction would lead to a stabilized carbocation. Related carbocations have already been reported as intermediates in the synthesis of the Josiphos ligands.^[10] After elimination of phenol the bicyclic ferrocene **20** would result (Scheme 1.28).



Scheme 1.28. Proposed Lewis acid catalyzed cyclization of phosphonates.

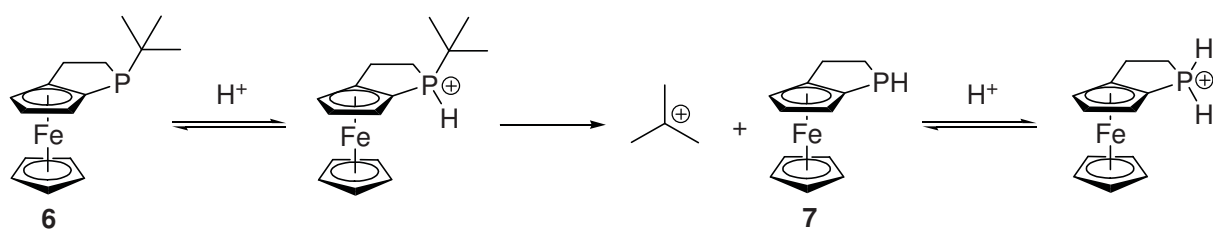
Treatment of **10** with three equivalents of trifluoroborane etherate showed no reaction and when more reagent was used only decomposition of the starting material was observed. Similarly, aluminium trichloride gave a mixture of products. When titanium tetrachloride was added to the starting material an immediate colour change to dark green could be observed which turned back to orange upon hydrolysis. In addition, the TLC showed essentially one product, but the NMR spectra did not support the structure of **20**. After additional NMR experiments the dimeric structure **21** was assigned to the product (Scheme 1.29). This structural assignment was supported by mass spectrometry. The outcome of this reaction can be rationalized by an activation of the double bond instead of the phosphonate by a proton or a titanium species. The electron deficient double bond is then attacked by the double bond of a second ferrocene, a proton is lost and, in the case of a titanium species, hydrolysis gives the dimer **21**. Most likely the dimerization proceeds via protonation - by hydrogen chloride

formed from titanium tetrachloride and moisture - because no reaction occurred when titanium tetra(*iso*-propanolate) was used as a Lewis acid.



Scheme 1.29. Dimerization product under acidic conditions.

Finally, the reactivity of the phospholane **6** towards strong acids was investigated. The removal of the *tert*-butyl group under acidic conditions is known for the deprotection of *tert*-butyl esters or *tert*-butoxycarbamates (boc) groups.^[11] The same methodology should apply to phosphines. The free electron pair can be protonated by a strong base to form a phosphonium ion. The loss of the stable *tert*-butyl cation should be irreversible as the resulting secondary phosphine should be again protonated under the reaction conditions (Scheme 1.30).

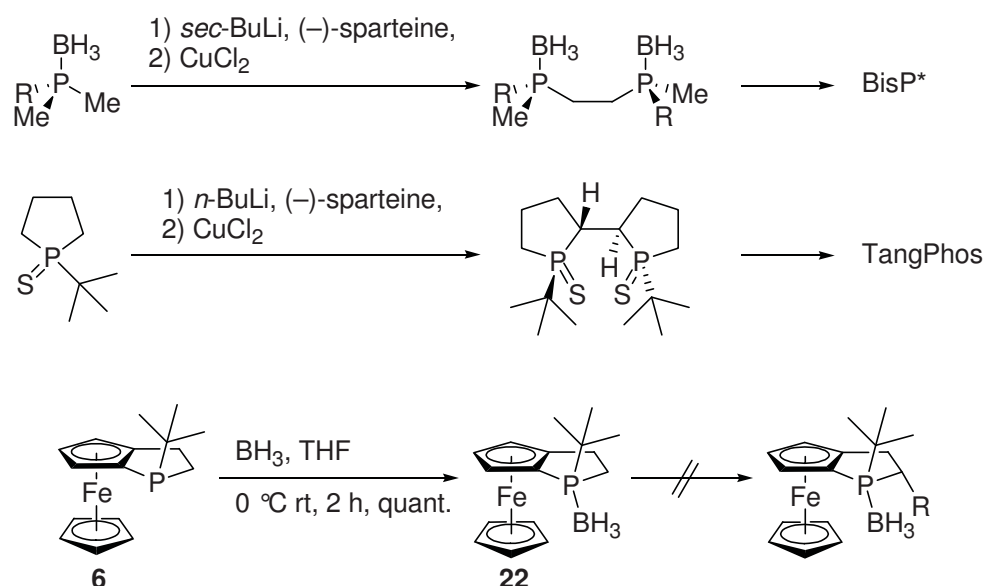


Scheme 1.30. Deprotection strategy.

When the experiment was carried out with hydrogen chloride in *iso*-propanol/THF or trifluoroacetic acid only starting material could be isolated. Using tetrafluoroboric acid in diethyl ether protonation seemed to occur, judged by the observation of a formed precipitate, but after work up only starting material was present. Dissolving **6** in concentrated sulphuric acid did not result in the formation of product **7** either, but rather gave some sulfonated ferrocene derivatives.

1.2.4 Functionalized Ferrocenephospholanes

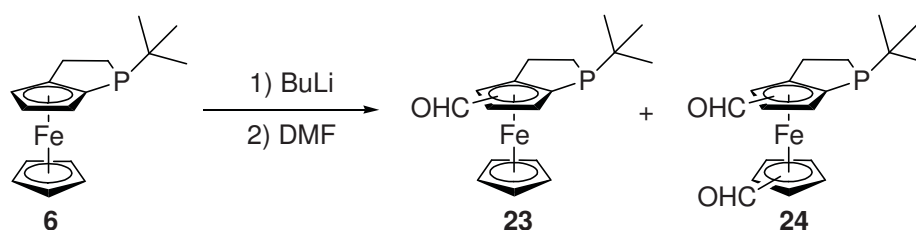
Having been unsuccessful in generating an unsubstituted phospholane, further possibilities for the functionalization of phospholane **6** were investigated. Reactions at the alpha carbon of borane-protected phosphines (BisP*)^[12] and sulphur-protected phospholanes (TangPhos)^[13] have been reported, leading to successful ligands for catalysis (Scheme 1.31). Usually, the combination of butyllithium and a diamine is able to produce the carbanion, which can then undergo subsequent reactions. In the case of phospholane **6**, deprotonation should proceed diastereoselectively even without a chiral diamine, as the *tert*-butyl group is expected to direct the stereoselectivity. However, when the reported conditions were applied, no reaction was observed regardless of the base or electrophile used.



Scheme 1.31. Deprotonation in the α -position to phosphorus.

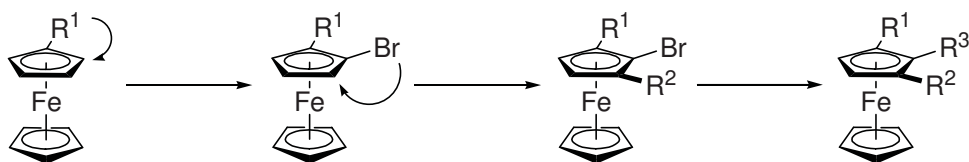
In looking at deprotonation reactions employing unprotected **6** the question arose whether there is a preferential position for proton abstraction. When **6** was added to a solution of *tert*-butyllithium and *N,N,N',N'*-tetramethylethylenediamine (TMEDA) in *tert*-butyl methyl ether (TBME) at -78 °C and warmed to room temperature before reaction with Ph₂PCL, formation of new species with an incorporated phosphine group was observed. This finding was followed by experiments to evaluate the selectivity of this reaction. For this purpose, **6** was treated with different bases and reacted with DMF to identify the sites of deprotonation. Scheme 1.32 shows the outcome of this investigation. Deprotonation occurred when a

combination of butyllithium and TMEDA in TBME was applied. Neither phenyllithium and TMEDA in TBME nor LiTMP in THF were able to deprotonate **6**. A mixture of *tert*-butyllithium and potassium *tert*-butoxide in THF gave a complex mixture of products. There was a difference in selectivity among the different organolithium compounds. *sec*-Butyllithium gave three species of structure **23** in the ratio 100:44:30 as judged by $^1\text{H-NMR}$. The selectivities with *n*-butyllithium (100:18:13) and *tert*-butyllithium (100:10:16) were better but with *tert*-butyllithium double lithiation products (**24**) were also observed. It seemed deprotonation occurred preferentially at the substituted cyclopentadienyl ring but with only low to moderate regioselectivity. Reaction at the unsubstituted cyclopentadienyl ring only took place with *tert*-butyllithium and then not exclusively. While the selectivities would be acceptable for a synthetic procedure, separation of the different regioisomers was not possible.



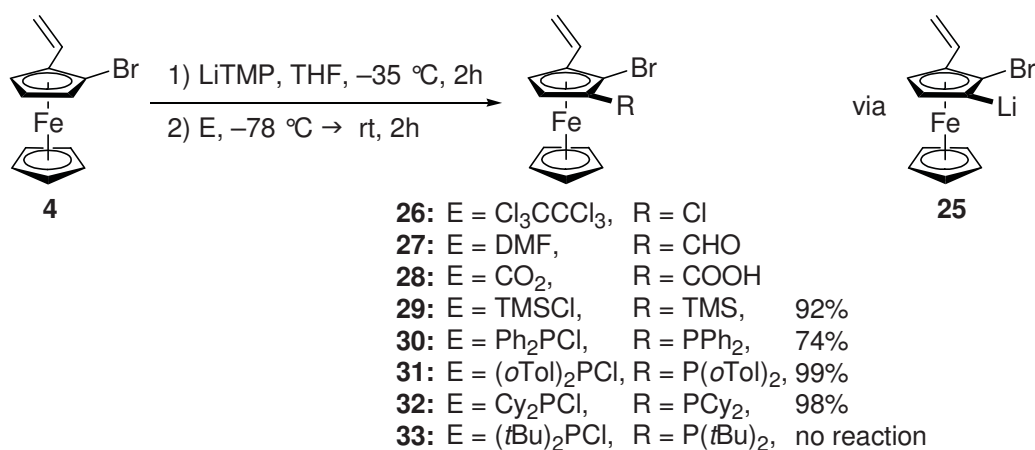
Scheme 1.32. Deprotonation products.

To achieve selective structural variations of the ferrocenephospholane **6** without being able to change the substituent at the phosphorus atom, the cyclopentadienyl ring had to be further functionalized. A convenient method for the selective formation of multiple substituted ferrocenes was introduced by the group of *Weissensteiner* (Scheme 1.33).^[14] Their approach also takes advantage of *ortho*-directing groups. In addition to the common functional groups such as amines, amides, acetals, ethers, esters or oxazolines which, in combination with alkylolithium reagents, allow for regioselective deprotonation, they found that a bromide substituent influences the acidity of the neighbouring hydrogen, enabling a lithium amide base to deprotonate. Lithium 2,2,6,6-tetramethylpiperidide was the base of choice and the resulting bromo-lithio-ferrocene was stable at $-30\text{ }^\circ\text{C}$ and could be reacted with suitable electrophiles. In the next step, the bromide was removed or converted into a desired functional group by lithiation and addition of the corresponding electrophile.



Scheme 1.33. *ortho*-Functionalization strategy by Weissensteiner.

Following this idea, bromoferrocene **4** was subjected to the reaction conditions. An excess of freshly prepared lithium base in THF gave, after 3 h between -40 and -30 °C, the lithiated ferrocene **25**. This species was stable under these conditions; at higher temperatures lithium bromide can be eliminated and the resulting very reactive arine-type product decomposes. This sensitivity towards temperature makes necessary the use of electrophiles reactive enough to undergo substitutions at low temperature. Different reagents were tested to examine the scope of this reaction and the possibilities of further manipulations (Scheme 1.34).



Scheme 1.34. Synthesis of trisubstituted ferrocenes.

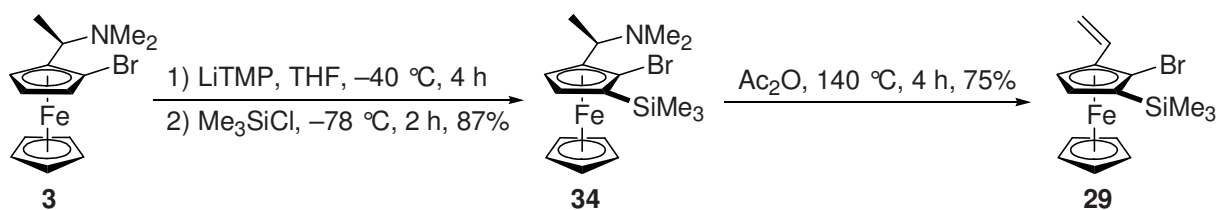
This study contained reagents that would lead to products in which the introduced substituent either could be further manipulated (**26-28**), would install a sterical change in the system (**29**) or would give a second phosphine group for the formation of bidentate bisphosphine ligands (**30-33**).

Generally, the introduction of electron withdrawing substituents destabilized the ferrocene system and gave labile products. Bromo-chloroferrocene **26** was synthesized from the reaction of **25** with hexachloroethane but decomposed during the purification. In the case of bromo-formylferrocene **27**, accessed from **25** and dimethyl formamide, purification was possible with some loss of material but the product decomposed even at -20 °C. When **25** was reacted with carbon dioxide the ferrocenic acid **28** was formed. This molecule was stable when handled under basic conditions and could be isolated in low yield as its 2,2,6,6-

tetramethylpiperidinium salt. Attempts to exchange the piperidinium counterion failed. The dependence of stability upon the presence of a protonated or deprotonated carboxylate again shows the sensitivity of this ferrocene system towards electronic effects.

After changing to substituents without electron withdrawing properties the reaction worked cleanly. The introduction of steric bulk by a tetramethylsilyl group was achieved in good yield by the reaction of **25** with tetramethylsilyl chloride. Ferrocene **29** was more stable than its unsubstituted counterpart **4** and could be stored at $-20\text{ }^{\circ}\text{C}$ without decomposition. Reactions of the bromo-lithioferrocene **25** with different phosphine chlorides again gave products in good yields. The phosphines **30-32** were stable towards oxygen and showed no decomposition upon longer storage at $4\text{ }^{\circ}\text{C}$. An exception was di(*tert*-butyl)phosphine chloride; the formation of **33** did not take place, probably for steric reasons, and only starting material was isolated.

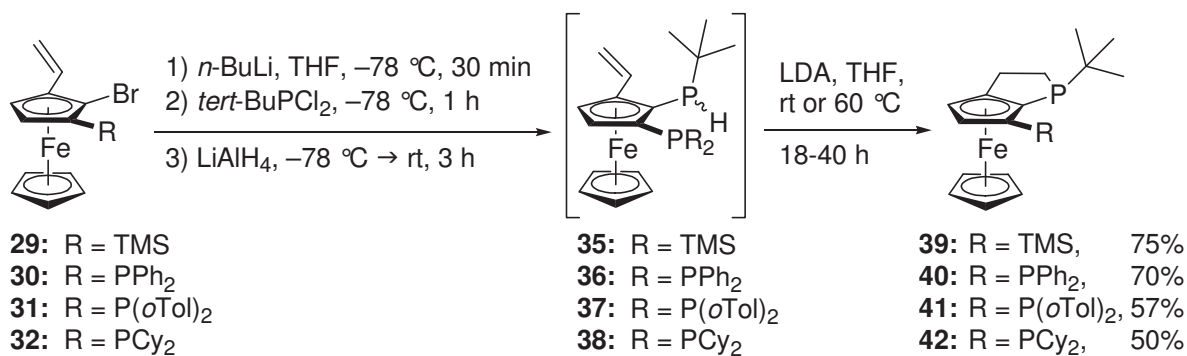
This *ortho*-functionalization was also possible starting from **3** and the trisubstituted ferrocene **34** was isolated in good yield (Scheme 1.35).



Scheme 1.35. *ortho*-Functionalization-elimination sequence.

Although the elimination of the dimethylamino group to give **29** proceeded nicely, this synthetic pathway was not followed further. The elimination reaction was conveniently carried out as an early step avoiding possible side reactions due to the presence of functional groups such as phosphines.

The trisubstituted ferrocenes (**29-32**) were metallated with *n*-butyllithium and after reaction with *tert*-butylphosphine dichloride, reduction with lithium aluminium hydride and filtration through a plug of silica the corresponding secondary phosphines were obtained (Scheme 1.36).



Scheme 1.36. Cyclization of trisubstituted ferrocenes.

In the case of diphenylphosphine substituted ferrocene **36** cyclization to the phospholane **40** took place under the conditions applied to **5** (see Scheme 1.15 on page 23). For the tetramethylsilyl substituted ferrocene **35** and the phosphines **37** and **38** the cyclization had to be carried out at elevated temperature. Under these conditions the phospholanes **39**, **41** and **42** were formed after 14 h. The yields varied from 50% to 75%. Introduction of the phosphine chloride and the reduction were found to be quantitative as judged by ³¹P-NMR but the cyclization step was accompanied by a loss of material.

Single crystals could be grown for compounds **40** and **42**, the structures are shown in Figures 1.11 and 1.12.

The first attempt to synthesize phospholane **39** was performed at room temperature for 4 days with the addition of a second equivalent of LDA after 2 days. Under these unoptimized conditions, a mixture of products was obtained. After purification of the crude material the dimeric phospholane **43** was isolated in low yield. Its structure could be verified by X-ray analysis of a single crystal (Figure 1.13). The formation of this side-product was not observed in the later syntheses at higher temperature.

How the dimerization took place is unknown. A possible pathway is the formation of a stabilized radical either from the anion or from the neutral compound. Recombination of two radicals would give the dimeric phospholane.



Figure 1.11. Crystal structure of **40**. The second molecule in the unit cell is omitted for clarity.

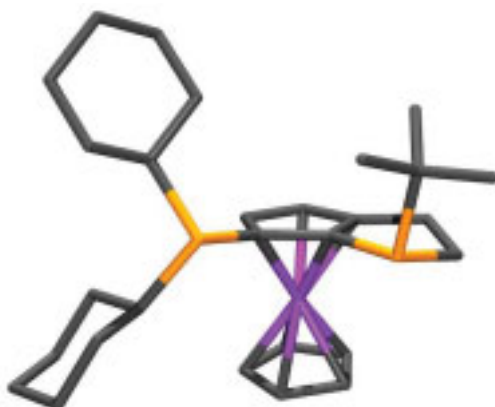


Figure 1.12. Crystal structure of **42**.

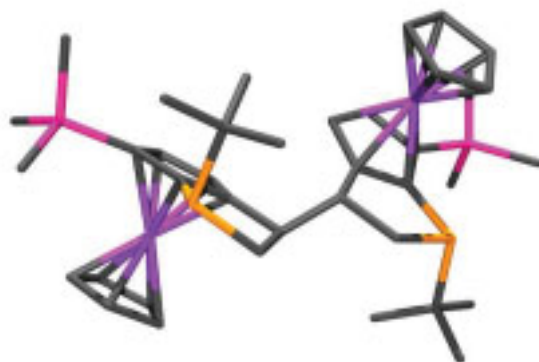


Figure 1.13. Crystal structure of **43**.

1.2.5 Attempted Synthesis of a Ferrocene-Based P,N-Ligand with only Planar Chirality

Recently, *Knochel* reported the synthesis of a pyridyl-phosphine ligand with a ferrocene backbone.^[15] The corresponding iridium-complexes gave selective catalysts for the hydrogenation of imines (Figure 1.14).

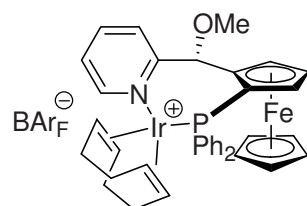
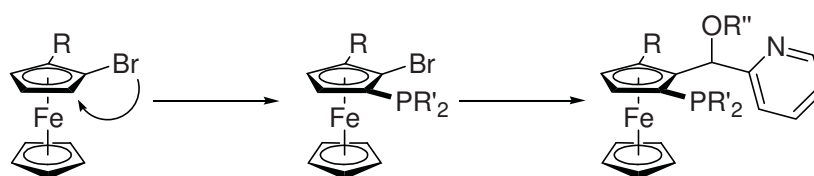


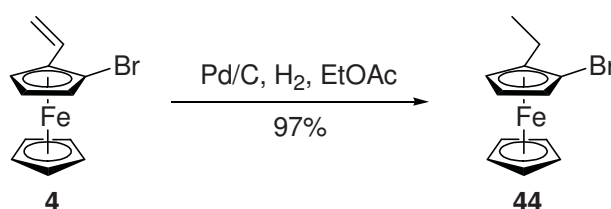
Figure 1.14. Ferrocenyl P,N-ligand reported by *Knochel*.

The synthesis of the ligand in Figure 1.14 included a diastereoselective *ortho*-lithiation directed by a chiral sulfoxide substituent to introduce the planar chirality. Starting from **4**, the *ortho*-lithiation strategy shown in Scheme 1.37 would allow the construction of the same scaffold with an additional substituent on the cyclopentadienyl ring. Since significant influences on selectivity by additional ferrocene substitution has been reported,^[16] the performance of the trisubstituted ferrocene scaffold was examined.



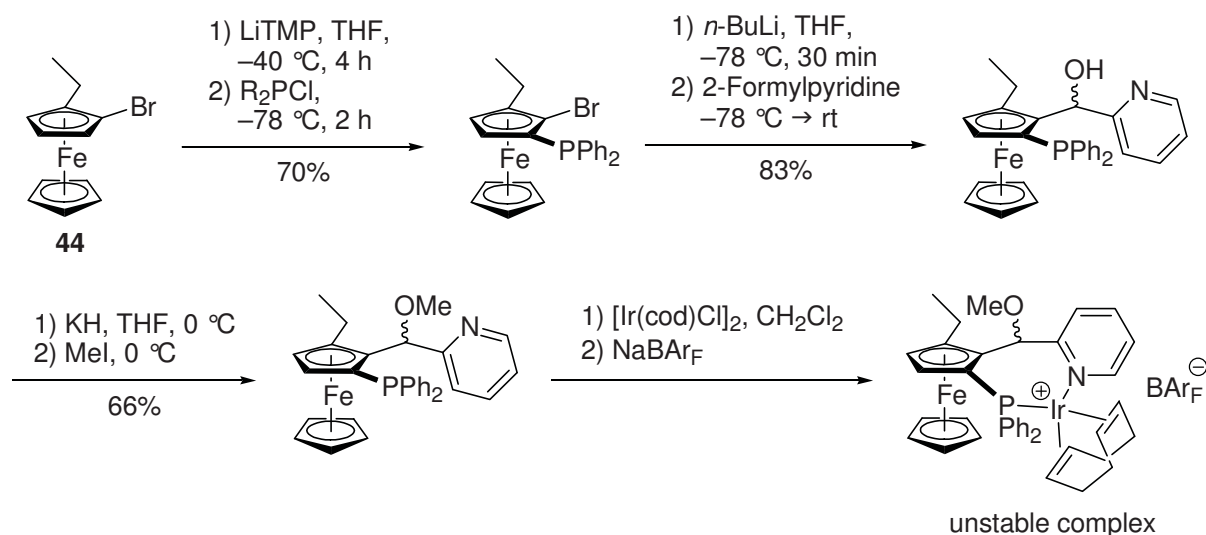
Scheme 1.37. *ortho*-Lithiation strategy for the formation of ferrocenyl P,N-ligands.

To avoid functional group interference, the double bond in **4** was hydrogenated with palladium on charcoal to give bromoferrocene **44** (Scheme 1.38).



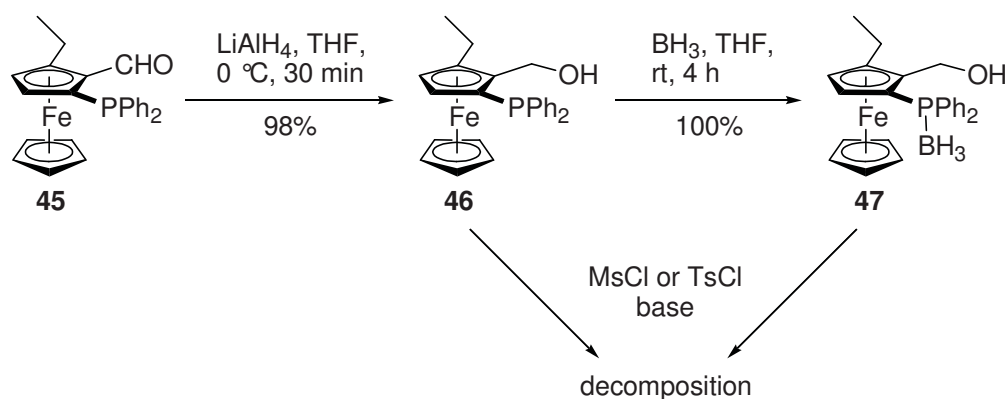
Scheme 1.38. Hydrogenation of the vinylic double bond.

ortho-Phosphination and the introduction of a pyridine moiety gave two isomeric alcohols. Neither the alcohols nor the corresponding methyl ethers were separable by chromatography. Moreover, the iridium complex was unstable and decomposed during purification (Scheme 1.39).



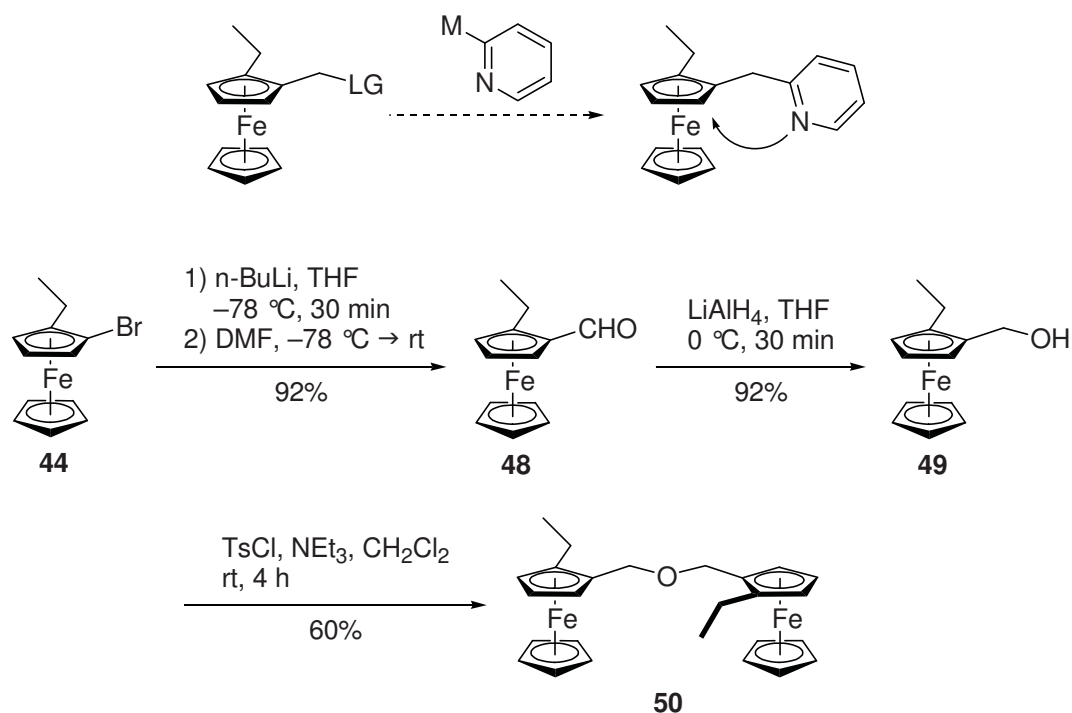
Scheme 1.39. Synthesis of a ferrocenyl P,N-iridium complex.

Apparently, the ethyl group has a tremendous influence on the complex stability. To exclude this destabilizing steric interaction between the ethyl and the methoxy groups, the removal of the ether functionality was envisaged. The first synthesis started from the ferrocenyl aldehyde **45**. The reduction to give the alcohol **46** proceeded smoothly, but the introduction of a leaving group, allowing displacement by an *ortho*-metallated pyridine, led exclusively to decomposition products. To avoid interference by the phosphine, protection with borane was carried out (**47**), but this did not change the outcome of the reaction (Scheme 1.40).



Scheme 1.40. Attempted introduction of leaving groups.

The second idea was to install the pyridine first and then use it as an *ortho*-directing group for the introduction of the phosphine (Scheme 1.41). Functional group transformation from the bromide **44** to the aldehyde **48** by lithiation and reaction with DMF as well as the subsequent reduction to the primary alcohol **49** worked nicely. Unfortunately, the next step, transformation of the alcohol into a leaving group, once again failed to proceed as desired. Reaction of **49** with tosyl chloride did not give the desired sulfonate but instead dimerization to the ether **50** was observed.



Scheme 1.41. Dimerization of ferrocenyl alcohols.

It seems that the reactivity of the tosylate is high enough to undergo reaction spontaneously after its formation with the alcohol starting material. Due to the efficient stabilization of the intermediate benzylic cation, a S_N1-type displacement is favoured in this system.

1.2.6 Conclusions

The synthesis of ferrocenephospholane **6** has been developed. The key step, a stereoconvergent hydrophosphination, took place under basic conditions. This addition of a phosphide nucleophile to the vinylic double bond is in opposition to the general reported reactivity of these species. Usually, the benzylic position of ferrocene derivatives is supposed to stabilize positive charges, as in the final phosphination reaction during the synthesis of the josiphos ligands^[10] or in the acid catalyzed dimerization of **10** (Scheme 2.16). Only *tert*-butyl-substituted secondary phosphines underwent this intramolecular addition to the double bond. Attempts to cyclize with a phenyl-substituted secondary phosphine or a primary phosphine failed.

Following an *ortho*-lithiation strategy, several substituents were introduced prior to cyclization. In particular, phosphine chlorides were proven to react very efficiently to give bidentate phosphine ligands (**40**, **41**, **42**) after formation of the phospholane in acceptable yields.

Functionalization of the parent phospholane **6** after its formation was problematic and proceeded unselectively, if at all.

1.2.7 References

- [1] G. W. Gokel, I. K. Ugi, *J. Chem. Edu.* **1972**, *49*, 294-296.
- [2] D. Marquarding, H. Klusacek, G. Gokel, P. Hoffmann, I. Ugi, *J. Am. Chem. Soc.* **1970**, *92*, 5389-5393.
- [3] J. W. Han, N. Tokunaga, T. Hayashi, *Helv. Chim. Acta* **2002**, *85*, 3848-3854.
- [4] B. Gschwend, B. Pugin, A. Bertogg, A Pfaltz, *Chem. Eur. J.* **2009**, DOI: 10.1002/chem.200902418
- [5] L.-B. Han, C.-Q. Zhao, *J. Org. Chem.* **2005**, *70*, 10121-10123.
- [6] a) J.-M. Denis, H. Forintos, H. Szelke, G. Keglevich, *Tetrahedron Letters* **2002**, *43*, 5569-5571; b) T. Imamoto, T. Oshiki, T. Onozawa, T. Kusumoto, K. Sato, *J. Am. Chem. Soc.* **1990**, *112*, 5244-5252.
- [7] S. Malfait, L. Pélineski, L. Maciejewski, J. Brocard, *Synlett* **1997**, 830-832.
- [8] a) F. Speiser, P. Braunstein, L. Saussine, R. Welter, *Organometallics* **2004**, *23*, 2613-2624; b) P. Braunstein, M. D. Fryzuk, M. Le Dall, F. Naud, S. J. Rettig, F. Speiser, *J. Chem. Soc., Dalton Trans.* **2000**, 1067-1074; c) J. Sprinz, G. Helmchen, *Tetrahedron Letters* **1993**, *34*, 1769-1772.
- [9] M. Rubin, T. Schwier, V. Gevorgyan, *J. Org. Chem.* **2002**, *67*, 1936-1940.
- [10] A. Togni, C. Breutel, A. Schnyder, F. Spindler, H. Landert, A. Tijani, *J. Am. Chem. Soc.* **1994**, *116*, 4062-4066.
- [11] T. W. Greene, P. G. M. Wuts, *Protective Groups in Organic Synthesis*, Wiley-Interscience, **1999**, 404-408, 518-525.
- [12] I. D. Gridnev, Y. Yamanoi, N. Higashi, H. Tsuruta, M. Yasutake, T. Imamoto, *Adv. Synth. Catal.* **2001**, *343*, 118-136.
- [13] W. Tang, W. Wang, X. Zhang, *Angew. Chem. Int. Ed.* **2003**, *42*, 943-946; W. Tang, X. Zhang, *Angew. Chem. Int. Ed.* **2002**, *41*, 1612-1614.
- [14] M. Streuer, K. Tiedl, Y. Wang, W. Weissensteiner, *Chem. Commun.* **2005**, 4929-4931.
- [15] M. N. Cheemala, P. Knochel, *Org. Lett.* **2007**, *9*, 3089-3092.
- [16] X. Feng, B. Pugin, B. Gschwend, F. Spindler, M. Paas, H.-U. Blaser, *ChemCatChem* **2009**, *1*, 85-88.

1.3 Rhodium Complexes and their Application in the Asymmetric Hydrogenation of Olefins

1.3.1 Coordination Behaviour

In advance of the first hydrogenation experiments the coordination mode of the ferrocenephospholanes was examined. For this purpose phospholanes **6**, **39** and **40** were combined in an appropriate solvent with the two different rhodium sources used in the hydrogenation reactions, namely $[\text{Rh}(\text{nbd})_2]\text{BF}_4$ and $[\text{Rh}(\text{nbd})\text{Cl}]_2$, and *cis*- $[\text{Pd}(\text{MeCN})_2\text{Cl}_2]$. The solid state structures of the complexes **51**, prepared from $[\text{Rh}(\text{nbd})\text{Cl}]_2$ and one equivalent of **6** in dichloromethane, as well as **52** and **53**, prepared from *cis*- $[\text{Pd}(\text{MeCN})_2\text{Cl}_2]$ and two equivalents of **6** or **39** in dichloromethane, are shown in Figures 1.14, 1.15 and 1.16. **51** exhibited the expected connectivity with a distorted, square planar rhodium center and one coordinated phospholane.

Complexes **52** and **53** showed a *trans*-arrangement of the two phospholane ligands. The question arose whether this geometry simply reflects the thermodynamically favoured product or whether the *cis* compound cannot exist for steric reasons. In the case of $[\text{Rh}(\text{nbd})_2]\text{BF}_4$ this would mean that **6** is not able to form a precatalyst consisting of two phospholanes ligands and one norbornadiene ligand at one rhodium center. NMR-experiments were performed to look at the formation of the precatalyst. With slightly more than a two fold excess of **6** combined with $[\text{Rh}(\text{nbd})_2]\text{BF}_4$ in deuterated methanol the resulting ^{31}P -NMR spectrum showed two resonances at 38.1 ppm and -1.4 ppm. At 38.1 ppm a doublet splitting with 154 Hz was observed, corresponding to a rhodium-bound phosphorus atom. The appearance of only one signal for the rhodium complex (apart from the signal of remaining ligand at -1.4 ppm) indicated the formation of a bis-phospholane rhodium complex. Later, the crystal structure of this complex (**54**) was solved, confirming that a *cis*-arrangement of the phosphines in the rhodium precatalyst is possible (Figure 1.17).

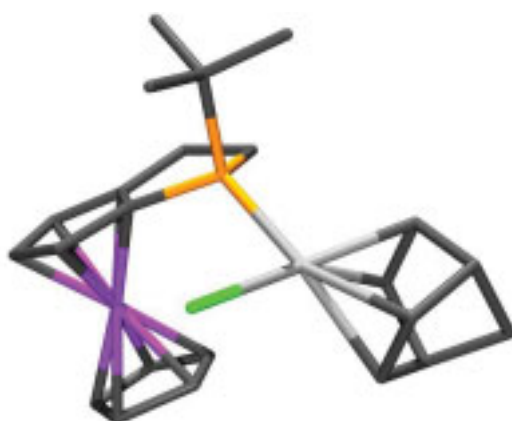


Figure 1.14. Crystal structure of **51**. The second molecule in the unit cell is omitted for clarity.

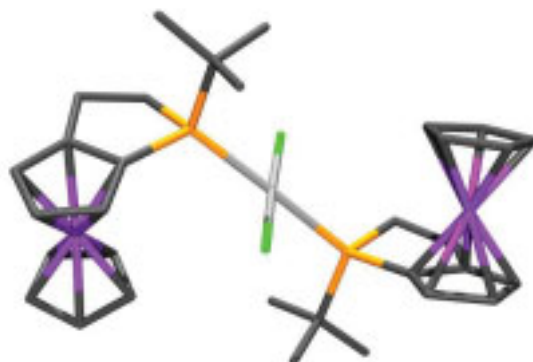


Figure 1.15. Crystal structure of **52**.

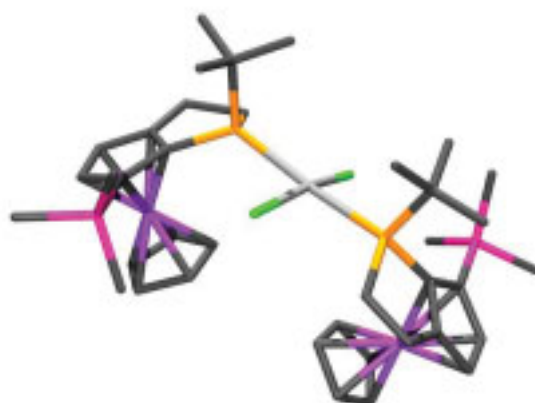


Figure 1.16. Crystal structure of **53**. The second molecule in the unit cell is omitted for clarity.

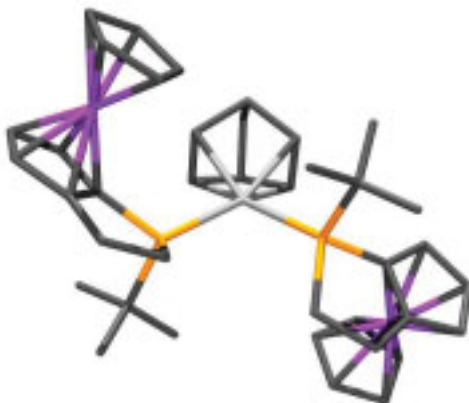


Figure 1.17. Crystal structure of **54**. The second molecule in the unit cell, the BF_4 -counterions and co-crystallized dichloromethane are omitted for clarity.

When **40** was complexed with one equivalent of $[\text{Rh}(\text{nbd})\text{Cl}]_2$ or *cis*- $[\text{Pd}(\text{MeCN})_2\text{Cl}_2]$ in dichloromethane, the corresponding rhodium (**55**) and palladium complexes (**56**) were formed. Their crystal structures are depicted in Figure 1.18 and Figure 1.19.



Figure 1.18. Crystal structure of **55**. Co-crystallized hexane is omitted for clarity.

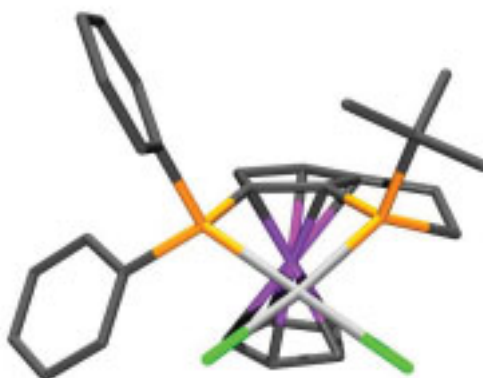


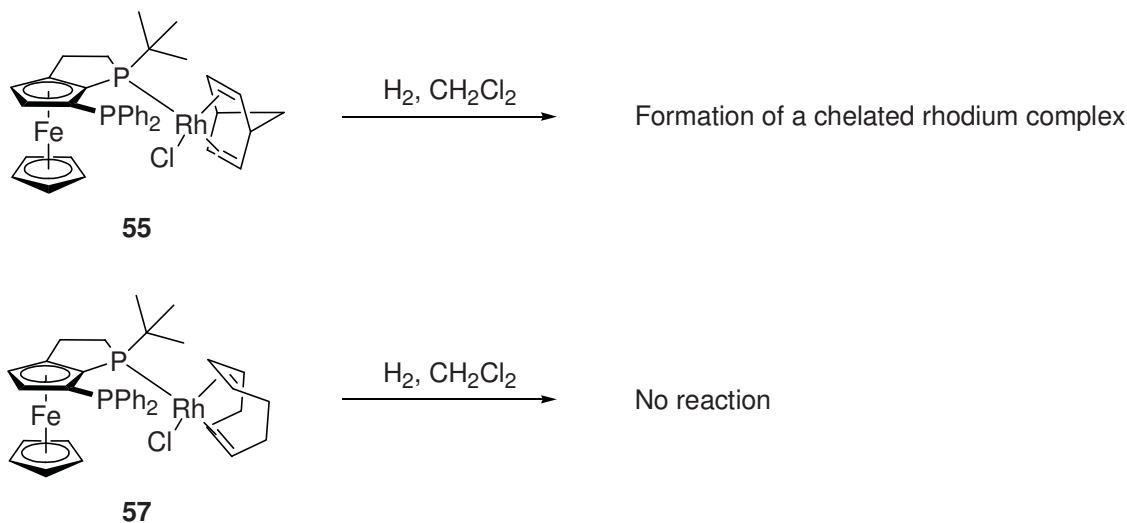
Figure 1.19. Crystal structure of **56**. The second molecule in the unit cell is omitted for clarity.

Complex **55** incorporated, despite of its bidentate ligand, only one phosphorus atom in the coordination sphere of the rhodium atom. This is also the case in solution. The ^{31}P -NMR showed a signal at 47.3 ppm as a doublet of doublets with a phosphorus-rhodium coupling constant of 172 Hz and a phosphorus-phosphorus coupling constant of 4.2 Hz in addition to a resonance at -21.7 ppm as a doublet with a phosphorus-phosphorus coupling constant of 4.2 Hz. The ability of the ligand to act in a bidentate fashion was demonstrated by the structure of the palladium complex **56**. The formation of **55** instead of a bidentate complex might be explained by the strongly coordinating chloride. Presumably, the distortion of the ligand upon chelation and the formation of an ion pair in dichloromethane are too energetically unfavored.¹ Without an available crystal structure of the complex formed from $[\text{Rh}(\text{nbd})_2]\text{BF}_4$ and **55** in methanol, the existence of a chelated rhodium atom had to be confirmed by NMR. Indeed, the ^{31}P -NMR experiments showed two resonances at 30.4 ppm and 16.9 ppm, both as doublets of doublets with a phosphorus-phosphorus coupling constant of 15.5 Hz and a rhodium-phosphorus coupling constant of 157 Hz and 150 Hz respectively.

As observed before, the second phosphine group in **55** was not able to displace the chloride or one of the coordinating double bonds at the rhodium center. However, upon addition of dihydrogen one double bond of norbornadiene should be hydrogenated to create a free coordination site. This position could then be occupied by the available phosphine resulting in a catalytically active species in form of a chelated rhodium atom related to the species observed with the combination of $[\text{Rh}(\text{nbd})_2]\text{BF}_4$ and **40** in methanol. To verify this assumption, complex **55** was stirred under dihydrogen atmosphere to remove the norbornadiene (Scheme 1.42). The reaction was monitored by NMR and aside from hydride signals - the strongest were a doublet of triplets at -20.2 ppm ($J_{\text{HRh}} = 26.9$ Hz, $J_{\text{HP}} = 15.8$ Hz) and a broad signal between -21.0 and -21.3 ppm - the appearance of ^{31}P -resonances with the expected coupling pattern showed again the formation of chelated complexes. First, new resonances appeared at 62.8 ppm and 29.3 ppm with phosphorus-rhodium coupling constants of 116 Hz and 169 Hz. Upon longer reaction time two weaker signal pairs at 40.0 ppm / 8.3 ppm and 37.4 ppm / 10.9 ppm could be seen. After 6 h the spectrum consisted of at least 5 sets of ligand signals. The nature of these hydride species is unknown. The observed phosphorus-proton coupling of 20 Hz indicates that all the observed hydrides are located *cis* to the phosphines, whereas roughly 190 Hz would be expected for a *trans*-arrangement.^[1]

¹ In methanol this is not the case, see Section 1.5.2 for the discussion.

A noteworthy observation was made when the same conditions were applied to the related complex **57** formed from **40** and $[\text{Rh}(\text{cod})\text{Cl}]_2$. In this case, the 1,5-cyclooctadiene ligand impeded the activation of the precatalyst and the complex was inert towards dihydrogen. This finding emphasizes the generally neglected influence of the diene ligand on catalysis results. The inexistence of reactivity of a diene-diphosphine-rhodium complex under the reaction conditions does not necessarily mean that the actual diphosphine-rhodium catalyst is inactive. Similar observations of the influence of the diene ligand on precatalyst activation have already been reported in the literature, although complete inactivity was not found.^[2] Presumably, this is due to the fact that these experiments were carried out with a precatalyst having a non-coordinating counter ion.



Scheme 1.42. Differences in precatalyst activation.

The complexation experiments proved that there is formation of a chelated complex when the phospholane **40** is treated with the corresponding rhodium source. In the case of the chloride counterion, chelation occurred upon removal of the diene ligand, whereas the tetrafluoroborate salt showed a chelated structure even for the precatalyst. The monodentate ligand **6** was also found to form a complex with two coordinating phosphines, in this case from two discrete ligands coordinated to the rhodium center. Based on these findings, the ligands **39**, **40** and **41** were assumed to behave in a similar manner, forming active catalysts bearing two coordinating phosphorus atoms. To avoid problems removing the cyclooctadiene ligand, norbornadiene-bound metal sources were chosen for formation of the precatalyst employed in the hydrogenation reactions.

1.3.2 Hydrogenations

1.3.2.1 Substrate Screening

To evaluate the potential of the phospholane-rhodium complexes in the asymmetric hydrogenation, several types of substrates were tested (Figure 1.43).

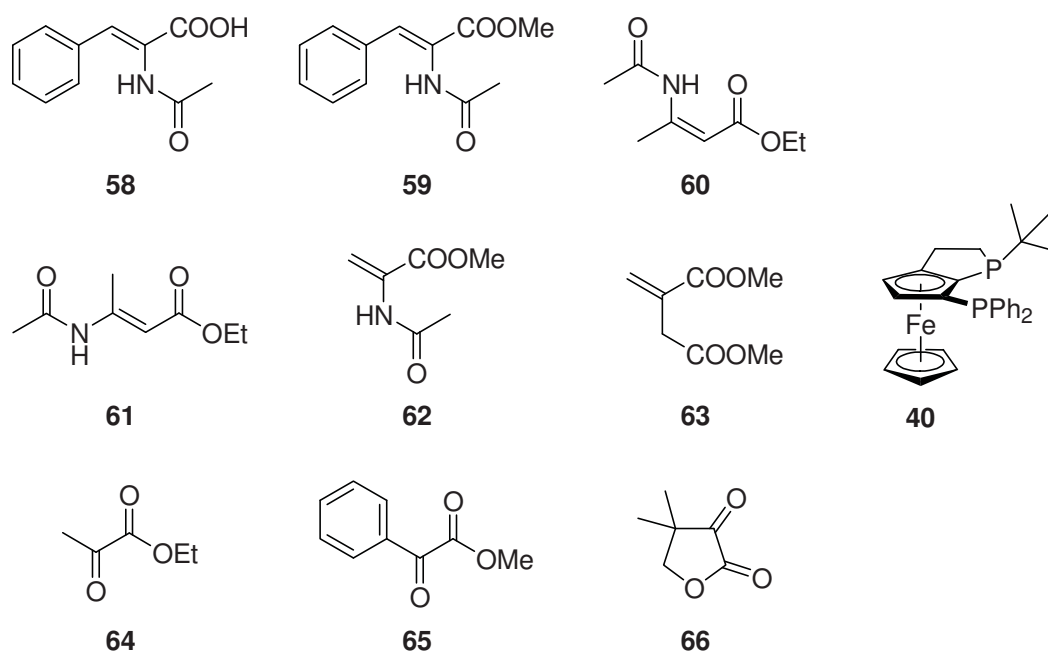


Figure 1.43. Substrates and the ligand used in the screening.

The substrate set included several dehydroamino acid derivatives, such as the cinnamates **58** and **59**, the isomeric crotonates **60** and **61** and the acrylate **62**. Furthermore, the unsaturated ester **63** and the α -ketoesters **64**, **65** and **66** were examined.

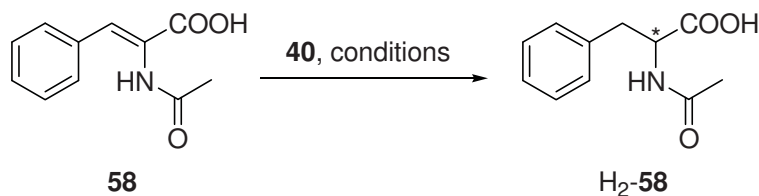
40 was chosen as the ligand for the initial screening with different metal sources. Several solvents, different catalyst loadings and various substrate concentrations as well as addition of base were tested. Reaction time, reaction temperature and hydrogen pressure for performance efficiency with the given substrates had been identified in preliminary experiments. The results of the hydrogenation reactions are shown in the following tables.

After a few selected hydrogenation experiments to determine the general reactivity, the screening was carried out on an automated system. This allowed the simultaneous hydrogenation of 96 combinations of substrate, catalyst and solvent. The precatalysts were generated *in situ* by combining a solution of the metal source in ethanol and a solution of the ligand in DCE. The solutions were stirred for 10 minutes then the solvent was removed under reduced pressure. Dissolving the precatalyst in the appropriate solvent and addition of the substrate was followed by shaking the reaction mixture under hydrogen atmosphere.

The amount of results generated in a single run demand for an automated analytical system. Therefore the conversion and enantiomeric excess were determined by automatic integration which, especially at low conversion, could lead to relatively large errors. Therefore the best results were manually checked for their accuracy and these verifications generally supported the automated screening results.

Not every possible combination was tested because of the substantial costs of a single run of 96 parallel experiments. Therefore the run was optimized for the most promising experiments and most information output.

Table 1.1. Hydrogenation of acetamido cinnamic acid (**58**).



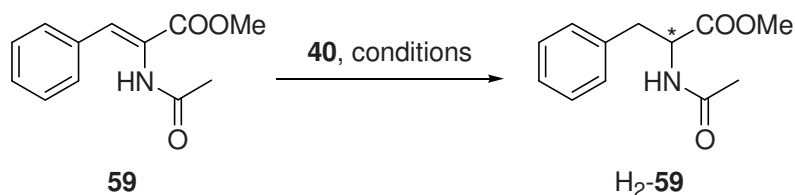
Entry ^a	Metal source	Solvent	s/c	conc. [mol/l]	conv. [%] ^b	ee [%] ^b
1	[Rh(nbd) ₂]BF ₄	EtOH	25	0.083	40	12 (<i>S</i>)
2 ^c	[Rh(nbd) ₂]BF ₄	EtOH	100	0.333	20	rac.
3	[Rh(nbd) ₂]BF ₄	THF	25	0.083	100	26 (<i>R</i>)
4 ^c	[Rh(nbd) ₂]BF ₄	THF/EtOH	100	0.333	100	rac.
5 ^d	[Rh(nbd)Cl] ₂	DCE	25	0.083	30	86 (<i>R</i>)
6 ^{c,d}	[Rh(nbd)Cl] ₂	DCE/EtOH	100	0.333	20	37 (<i>R</i>)

^aReaction was carried out with a metal source to ligand ratio of 1:1 under 1 bar H₂ and 25 °C for 2 h.

^bDetermined by chiral GC. ^cWith dabco as additive. ^dMetal source to ligand ratio of 1:2.

Full conversion in the hydrogenation of the cinnamic acid **58** was achieved with $[\text{Rh}(\text{nbd})_2]\text{BF}_4$ (Table 1.1 entries 3 and 4). In THF the corresponding enantioselectivity was only moderate and in ethanol/THF with additional base only racemic product was obtained. The best selectivity of 86% *ee* gave $[\text{Rh}(\text{nbd})\text{Cl}]_2$ albeit with only 30% conversion (entry 5).

Table 1.2. Hydrogenation of methyl acetamidocinnamate (**59**).

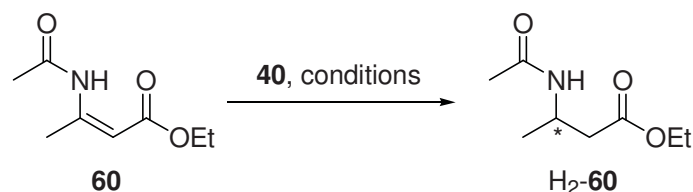


Entry ^a	Metal source	Solvent	s/c	conc. [mol/l]	conv. [%] ^b	<i>ee</i> [%] ^b
1	$[\text{Rh}(\text{nbd})_2]\text{BF}_4$	EtOH	25	0.083	60	51 (<i>R</i>)
2	$[\text{Rh}(\text{nbd})_2]\text{BF}_4$	EtOH	100	0.333	20	46 (<i>R</i>)
3	$[\text{Rh}(\text{nbd})_2]\text{BF}_4$	THF	25	0.083	>99	77 (<i>R</i>)
4	$[\text{Rh}(\text{nbd})_2]\text{BF}_4$	THF	100	0.333	40	87 (<i>R</i>)
5 ^c	$[\text{Rh}(\text{nbd})\text{Cl}]_2$	DCE	25	0.083	>99	90 (<i>R</i>)
6 ^c	$[\text{Rh}(\text{nbd})\text{Cl}]_2$	DCE	100	0.333	40	85 (<i>R</i>)

^aReaction was carried out with a metal source to ligand ratio of 1:1 under 1 bar H_2 and 25 °C for 2 h.

^bDetermined by chiral GC. ^cMetal source to ligand ratio of 1:2.

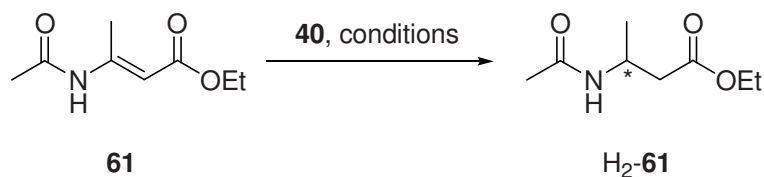
Compared to the free acid **58**, the methyl cinnamic ester **59** showed generally higher conversions and enantioselectivities (Table 1.2). Full conversion was generated with $[\text{Rh}(\text{nbd})_2]\text{BF}_4$ and $[\text{Rh}(\text{nbd})\text{Cl}]_2$ but only with 4 mol% catalyst loading in aprotic solvents (entries 3 and 5). The products were obtained with 77% *ee* and 90% *ee* respectively. A higher substrate concentration increased the selectivity in the case of $[\text{Rh}(\text{nbd})_2]\text{BF}_4$ in THF (entry 4), the opposite trend was observed in ethanol (entry 2) and with $[\text{Rh}(\text{nbd})\text{Cl}]_2$ (entry 6).

Table 1.3. Hydrogenation of ethyl *Z*-acetamidocrotonate (**60**).

Entry ^a	Metal source	Solvent	s/c	conc. [mol/l]	conv. [%] ^b	ee [%] ^b
1	[Rh(nbd) ₂]BF ₄	EtOH	25	0.083	>99	26 (<i>R</i>)
2	[Rh(nbd) ₂]BF ₄	EtOH	100	0.333	30	22 (<i>R</i>)
3	[Rh(nbd) ₂]BF ₄	THF	25	0.083	>99	12 (<i>R</i>)
4	[Rh(nbd) ₂]BF ₄	THF	100	0.333	20	rac.
5 ^c	[Rh(nbd)Cl] ₂	DCE	25	0.083	40	58 (<i>R</i>)
6 ^c	[Rh(nbd)Cl] ₂	DCE	100	0.333	5	64 (<i>R</i>)

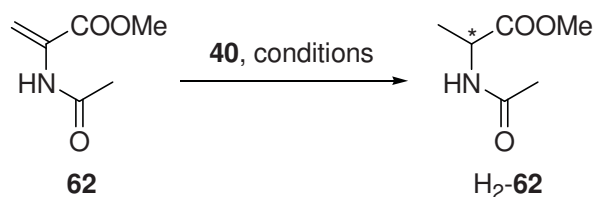
^aReaction was carried out with a metal source to ligand ratio of 1:1 under 1 bar H₂ at 25 °C for 14 h with 2,2,2-trifluoroethanol as additive. ^bDetermined by chiral GC. ^cMetal source to ligand ratio of 1:2.

Hydrogenation of the isomeric crotonates **60** and **61** revealed generally higher activities for the *E*-configured enamide **61** independent of the conditions. Full conversion was observed with 4 mol% catalyst loading for both substrates in ethanol and THF with [Rh(nbd)₂]BF₄ as the metal source (Table 1.3 entries 1 and 3, Table 1.4 entries 1 and 3). In the case of **61** the combination of [Rh(nbd)Cl]₂ in DCE gave almost full conversion (Table 1.4 entry 5) whereas **60** was reduced much slower (Table 1.3 entry 5). The conversions dropped significantly when the catalyst loading was reduced to 1 mol%. The selectivities were almost independent of catalyst and substrate concentration. The best results were obtained with [Rh(nbd)Cl]₂ in DCE. The *E*-isomer **61** was reduced with an *ee* of 72% and 95% conversion (Table 1.4 entry 5). The *Z*-isomer **60** gave 58% *ee* accompanied by lower conversion (Table 1.3 entry 5). The reduction is stereospecific as illustrated by the opposite enantiomers predominantly generated when comparing the hydrogenation products of the two isomeric enamides.

Table 1.4. Hydrogenation of ethyl *E*-acetamidocrotonate (**61**).

Entry ^a	Metal source	Solvent	s/c	conc. [mol/l]	conv. [%] ^b	ee [%] ^b
1	[Rh(nbd) ₂]BF ₄	EtOH	25	0.083	>99	15 (<i>S</i>)
2	[Rh(nbd) ₂]BF ₄	EtOH	100	0.333	50	14 (<i>S</i>)
3	[Rh(nbd) ₂]BF ₄	THF	25	0.083	>99	12 (<i>S</i>)
4	[Rh(nbd) ₂]BF ₄	THF	100	0.333	40	9 (<i>S</i>)
5 ^c	[Rh(nbd)Cl] ₂	DCE	25	0.083	95	72 (<i>S</i>)
6 ^c	[Rh(nbd)Cl] ₂	DCE	100	0.333	40	60 (<i>S</i>)

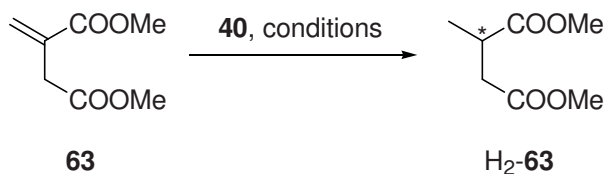
^aReaction was carried out with a metal source to ligand ratio of 1:1 under 1 bar H₂ at 25 °C for 14 h. ^bDetermined by chiral GC. ^cMetal source to ligand ratio of 1:2.

Table 1.5. Hydrogenation of methyl acetamidoacrylate (**62**).

Entry ^a	Metal source	Solvent	s/c	conc. [mol/l]	conv. [%] ^b	ee [%] ^b
1	[Rh(nbd) ₂]BF ₄	EtOH	25	0.083	>99	65 (<i>S</i>)
2	[Rh(nbd) ₂]BF ₄	EtOH	100	0.333	>99	56 (<i>S</i>)
3	[Rh(nbd) ₂]BF ₄	THF	25	0.083	>99	34 (<i>S</i>)
4	[Rh(nbd) ₂]BF ₄	THF	100	0.333	>99	42 (<i>S</i>)
5 ^c	[Rh(nbd)Cl] ₂	DCE	25	0.083	>99	10 (<i>S</i>)
6 ^c	[Rh(nbd)Cl] ₂	DCE	100	0.333	70	10 (<i>R</i>)

^aReaction was carried out with a metal source to ligand ratio of 1:1 under 1 bar H₂ at 25 °C for 2 h. ^bDetermined by chiral GC. ^cMetal source to ligand ratio of 1:2.

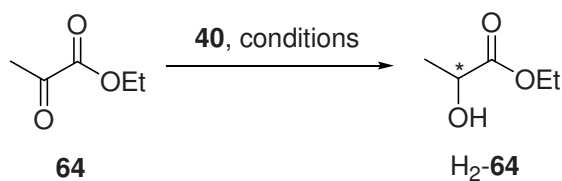
The acrylate **62** showed high activity with both metal sources in all solvents even at 1 mol% catalyst loading (Table 1.5). The concentration of the solution did not have a consistent influence. Whereas in ethanol the selectivity dropped at higher concentration (entry 1 vs. entry 2), the opposite result was observed in THF (entry 3 vs. entry 4). With [Rh(nbd)Cl]₂ in DCE a inversion of selectivity was observed, although on a low level (entry 5 vs. entry 6). The best enantioselectivity was obtained with [Rh(nbd)₂]BF₄ in ethanol with an *ee* of 65% (entry 1).

Table 1.6. Hydrogenation of dimethyl itaconate (**63**).


Entry ^a	Metal source	Solvent	s/c	conc. [mol/l]	conv. [%] ^b	ee [%] ^b
1	[Rh(nbd) ₂]BF ₄	EtOH	25	0.083	>99	44 (<i>R</i>)
2	[Rh(nbd) ₂]BF ₄	EtOH	100	0.333	60	58 (<i>R</i>)
3	[Rh(nbd) ₂]BF ₄	THF	25	0.083	>99	30 (<i>R</i>)
4	[Rh(nbd) ₂]BF ₄	THF	100	0.333	40	57 (<i>R</i>)
5 ^c	[Rh(nbd)Cl] ₂	DCE	25	0.083	95	10 (<i>S</i>)
6 ^c	[Rh(nbd)Cl] ₂	DCE	100	0.333	20	11 (<i>S</i>)

^aReaction was carried out with a metal source to ligand ratio of 1:1 under 1 bar H₂ at 25 °C for 14 h. ^bDetermined by chiral GC. ^cMetal source to ligand ratio of 1:2.

The itaconate **63** was hydrogenated with full conversion at a catalyst loading of 4 mol%. At a higher substrate to catalyst ratio incomplete reduction was observed (Table 1.6). [Rh(nbd)Cl]₂ in DCE showed very low selectivity compared to [Rh(nbd)₂]BF₄ in ethanol or THF. Additionally, the two different metal sources did not generate the same product configuration. The enantioselectivities were slightly higher when a more concentrated solution was used, with 58% *ee* being the best result (entry 2).

Table 1.7. Hydrogenation of ethyl pyruvate (**64**).


Entry ^a	Metal source	Solvent	s/c	conc. [mol/l]	conv. [%] ^b	ee [%] ^{b,c}
1	[Rh(nbd)Cl] ₂	Tol	25	0.083	5	28
2 ^d	[Rh(nbd)Cl] ₂	Tol/THF	25	0.083	50	rac.
3	[Rh(nbd)Cl] ₂	THF	25	0.083	5	11
4 ^d	[Rh(nbd)Cl] ₂	THF	25	0.083	30	6
5	[Rh(nbd)(TFA)] ₂	Tol	25	0.083	50	-11
6 ^d	[Rh(nbd)(TFA)] ₂	Tol/THF	25	0.083	90	-20
7 ^e	[Rh(nbd) ₂]BF ₄	EtOH	25	0.083	70	rac.
8 ^{d,e}	[Rh(nbd) ₂]BF ₄	EtOH/THF	25	0.083	>99	-29

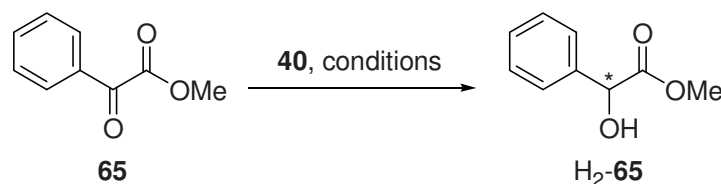
^aReaction was carried out with a metal source to ligand ratio of 1:2 under 20 bar H₂ at 25 °C for 14 h.

^bDetermined by chiral GC. ^cFirst eluting enantiomer minus second eluting enantiomer. ^dWith dabco as additive.

^eMetal source to ligand ratio of 1:1.

In the reduction of pyruvate **64**, [Rh(nbd)TFA]₂ and [Rh(nbd)₂]BF₄ showed acceptable reactivities whereas [Rh(nbd)Cl]₂ performed poorly (Table 1.7). The addition of dabco enhanced conversion in all cases. Enantioselectivities were generally low and did not exceed 30% *ee*. The best result was with [Rh(nbd)₂]BF₄ and dabco in ethanol/THF, which gave full conversion and 29% *ee* (entry 8).

Table 1.8. Hydrogenation of methyl phenylglyoxylate (**65**).



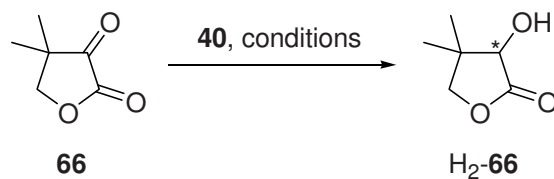
Entry ^a	Metal source	Solvent	s/c	conc. [mol/l]	conv. [%] ^b	<i>ee</i> [%] ^{b,c}
1	[Rh(nbd)Cl] ₂	Tol	25	0.083	0	-
2 ^d	[Rh(nbd)Cl] ₂	Tol/THF	25	0.083	20	5
3	[Rh(nbd)Cl] ₂	THF	25	0.083	5	rac.
4 ^d	[Rh(nbd)Cl] ₂	THF	25	0.083	10	7
5	[Rh(nbd)(TFA)] ₂	Tol	25	0.083	40	rac.
6 ^d	[Rh(nbd)(TFA)] ₂	Tol/THF	25	0.083	>99	-17
7 ^e	[Rh(nbd) ₂]BF ₄	EtOH	25	0.083	>99	rac.
8 ^{d,e}	[Rh(nbd) ₂]BF ₄	EtOH/THF	25	0.083	80	rac.

^aReaction was carried out with a metal source to ligand ratio of 1:2 under 20 bar H₂ at 25 °C for 14 h.

^bDetermined by chiral GC. ^cFirst eluting enantiomer minus second eluting enantiomer. ^dWith dabco as additive.

^eMetal source to ligand ratio of 1:1.

Glyoxylate **65** showed the same reactivity towards the catalysts from different metal sources as pyruvate **64**. Only the metal sources [Rh(nbd)TFA]₂ and [Rh(nbd)₂]BF₄ led to reduction of the ketone in reasonable amounts. In the case of the trifluoroacetate, additional dabco was needed to achieve full conversion (Table 1.8, entry 6). In most cases racemic product was obtained, only [Rh(nbd)TFA]₂ in toluene/THF with dabco showed a low selectivity of 17% *ee*.

Table 1.9. Hydrogenation of ketopantolactone (**66**).

Entry ^a	Metal source	Solvent	s/c	conc. [mol/l]	conv. [%] ^b	ee [%] ^{b,c}
1	[Rh(nbd)Cl] ₂	Tol	25	0.083	10	37
2 ^d	[Rh(nbd)Cl] ₂	THF/Tol	25	0.083	70	-6
3	[Rh(nbd)Cl] ₂	THF	25	0.083	5	12
4 ^d	[Rh(nbd)Cl] ₂	THF	25	0.083	10	rac.
5	[Rh(nbd)(TFA)] ₂	Tol	25	0.083	90	-29
6 ^d	[Rh(nbd)(TFA)] ₂	THF/Tol	25	0.083	>99	-6
7 ^e	[Rh(nbd) ₂]BF ₄	EtOH	25	0.083	40	-11
8 ^{d,e}	[Rh(nbd) ₂]BF ₄	EtOH/THF	25	0.083	90	12

^aReaction was carried out with a metal source to ligand ratio of 1:2 under 20 bar H₂ at 25 °C for 14 h.

^bDetermined by chiral GC. ^cFirst eluting enantiomer minus second eluting enantiomer. ^dWith dabco as additive.

^eMetal source to ligand ratio of 1:1.

Lactone **66** showed the same trends as the previous ketones in which [Rh(nbd)(TFA)]₂ and [Rh(nbd)₂]BF₄ proved to be superior to [Rh(nbd)Cl]₂ in terms of reactivity. Again, addition of dabco increased the conversion, albeit with erosion of the already low selectivities. The best combination was [Rh(nbd)TFA]₂ as metal source in toluene with 90% conversion and 29% *ee* (Table 1.9 entry 5).

1.3.2.2 Ligand Screening

Based on the initial hydrogenation experiments, it was decided to focus further screening on the reduction of olefins. The substrates and the ligands used, shown in Figure 1.44, include the bidentate ferrocenephospholanes **40-42**, the dehydroamino acid derivatives **58-62** and the unsaturated diester **63**. The results are reported in the following tables.

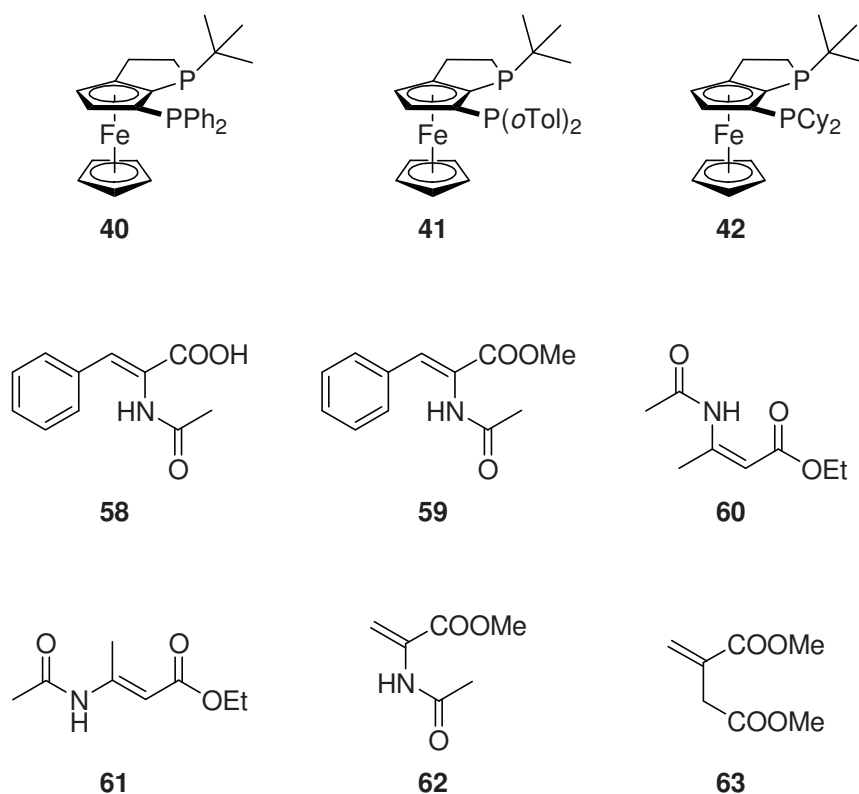
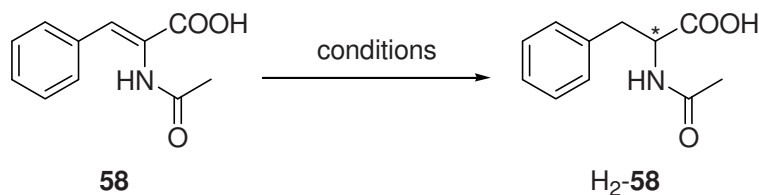


Figure 1.44. Substrates and ligands used in the screening.

Table 1.10. Hydrogenation of acetamido cinnamic acid (**58**).


Entry ^a	Ligand	Solvent	s/c	conc. [mol/l]	conv. [%] ^b	ee [%] ^b
1		EtOH	25	0.083	40	12 (<i>S</i>)
2 ^c		EtOH	100	0.333	20	rac.
3		THF	25	0.083	>99	26 (<i>R</i>)
4 ^c		THF/EtOH	100	0.333	>99	rac.
5 ^d	40	DCE	25	0.083	30	86 (<i>R</i>)
6 ^{c,d}		DCE/EtOH	100	0.333	20	37 (<i>R</i>)
7		EtOH	25	0.083	81	26 (<i>R</i>)
8 ^c		EtOH	100	0.333	30	44 (<i>R</i>)
9		THF	25	0.083	92	21 (<i>R</i>)
10 ^c		THF/EtOH	100	0.333	44	17 (<i>R</i>)
11 ^{d,e}		DCE	25	0.083	n.a.	n.a.
12 ^{c,d}	41	DCE/EtOH	100	0.333	28	35 (<i>R</i>)
13		EtOH	25	0.083	39	22 (<i>S</i>)
14 ^c		EtOH	100	0.333	25	44 (<i>S</i>)
15		THF	25	0.083	41	4 (<i>S</i>)
16 ^c		THF/EtOH	100	0.333	32	38 (<i>S</i>)
17 ^d		DCE	25	0.083	87	89 (<i>R</i>)
18 ^{c,d}		42	DCE/EtOH	100	0.333	23

^aReaction was carried out with [Rh(nbd)₂]BF₄ as metal source with a metal source to ligand ratio of 1:1 under 1 bar H₂ at 25 °C for 2 h. ^bDetermined by chiral GC. ^cWith dabco as additive. ^d[Rh(nbd)Cl]₂ was used as metal source, metal source to ligand ratio of 1:2. ^eAnalysis failed.

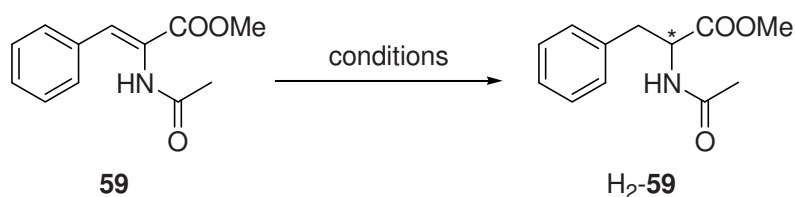
All ligands gave better conversions in the hydrogenation of acid **58** in aprotic solvents. The highest activities with phospholanes **40** and **41** were measured in THF; **42** in combination with DCE was also applicable. Enantioselectivities of 86% *ee* and 89% *ee* could be achieved in DCE with **40** (Table 1.10, entry 5) and **42** (entry 17) although only **42** gave good conversion.

The methyl ester **59** showed higher activities and selectivities compared to the free acid **58** but at a catalyst loading of 1 mol% the conversions dropped in all cases. THF and DCE were superior for the activities with ligands **40** and **42** whereas ethanol was better in combination with **41**. Enantioselectivities were usually lower in ethanol, with ligands **40** and **42** generally

outperforming **41**. The enantioselectivity showed a dependence on substrate concentration in THF and DCE. While a more concentrated solution raised the selectivity in THF, a more dilute reaction mixture was optimal in DCE. The best results were obtained with **40** and **42** in DCE, giving enantiomeric excesses of 90% (Table 1.11, entry 5) and 93% (entry 17).

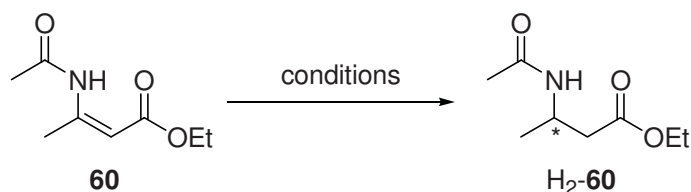
The monodentate ligands **6** and **39** showed no conversion in DCE, and in ethanol or THF the selectivities were rather poor.

Table 1.11. Hydrogenation of methyl acetamidocinnamate (**59**).



Entry ^a	Ligand	Solvent	s/c	conc. [mol/l]	conv. [%] ^b	ee [%] ^b
1		EtOH	25	0.083	60	51 (<i>R</i>)
2		EtOH	100	0.333	20	46 (<i>R</i>)
3		THF	25	0.083	>99	77 (<i>R</i>)
4		THF	100	0.333	40	87 (<i>R</i>)
5 ^c	40	DCE	25	0.083	>99	90 (<i>R</i>)
6 ^c		DCE	100	0.333	40	85 (<i>R</i>)
7		EtOH	25	0.083	99	11 (<i>R</i>)
8		EtOH	100	0.333	43	31 (<i>R</i>)
9		THF	25	0.083	34	26 (<i>R</i>)
10		THF	100	0.333	19	55 (<i>R</i>)
11 ^c	41	DCE	25	0.083	85	38 (<i>R</i>)
12 ^c		DCE	100	0.333	40	38 (<i>R</i>)
13		EtOH	25	0.083	16	17 (<i>R</i>)
14		EtOH	100	0.333	5	rac.
15		THF	25	0.083	98	78 (<i>R</i>)
16		THF	100	0.333	40	87 (<i>R</i>)
17 ^c	42	DCE	25	0.083	>99	93 (<i>R</i>)
18 ^c		DCE	100	0.333	10	72 (<i>R</i>)

^aReaction was carried out with [Rh(nbd)₂]BF₄ as metal source with a metal source to ligand ratio of 1:1 under 1 bar H₂ at 25 °C for 2 h. ^bDetermined by chiral GC. ^c[Rh(nbd)Cl]₂ was used as metal source, metal source to ligand ratio of 1:2.

Table 1.12. Hydrogenation of ethyl Z-acetamidocrotonate (**60**).

Entry ^a	Ligand	Solvent	s/c	conc. [mol/l]	conv. [%] ^b	ee [%] ^b
1		EtOH	25	0.083	>99	26 (<i>R</i>)
2		EtOH	100	0.333	30	22 (<i>R</i>)
3		THF	25	0.083	>99	12 (<i>R</i>)
4		THF	100	0.333	20	rac.
5 ^c	40	DCE	25	0.083	40	58 (<i>R</i>)
6 ^c	40	DCE	100	0.333	5	64 (<i>R</i>)
7		EtOH	25	0.083	>99	15 (<i>R</i>)
8 ^c		EtOH	100	0.333	>99	18 (<i>R</i>)
9		THF	25	0.083	>99	6 (<i>S</i>)
10 ^c		THF	100	0.333	62	13 (<i>S</i>)
11 ^c	41	DCE	25	0.083	52	53 (<i>R</i>)
12 ^c	41	DCE	100	0.333	43	63 (<i>R</i>)
13		EtOH	25	0.083	>99	16 (<i>R</i>)
14		EtOH	100	0.333	28	29 (<i>R</i>)
15		THF	25	0.083	>99	7 (<i>R</i>)
16		THF	100	0.333	30	18 (<i>R</i>)
17 ^c	42	DCE	25	0.083	>99	44 (<i>R</i>)
18 ^c	42	DCE	100	0.333	>99	n.d. ^d

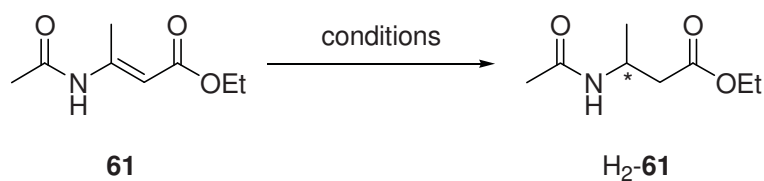
^aReaction was carried out with [Rh(nbd)₂]BF₄ as metal source with a metal source to ligand ratio of 1:1 under 1 bar H₂ at 25 °C for 2 h with 2,2,2-trifluoroethanol as additive. ^bDetermined by chiral GC. ^c[Rh(nbd)Cl]₂ was used as metal source, metal source to ligand ratio of 1:2. ^dSide products were observed.

Hydrogenation of enamide **60** was achieved with full conversion with 4 mol% catalyst loading except for the experiments performed with **40** and **41** in DCE (Table 1.12). At a higher substrate to catalyst ratio only **41** in ethanol showed good activity (entry 8). In the case of **42** in DCE complete consumption of the starting material was observed but the reaction produced a mixture of products (entry 18). The enantioselectivities decreased going from DCE to ethanol to THF. The best result was obtained in DCE with **41** giving 63% *ee* and 43% conversion, at higher conversions the best enantiomeric excess (44%) was generated with **42** in the same solvent (entry 17).

The isomeric enamide **61** showed formation of side products in several experiments (Table 1.13), presumably due to a systematical error during the screening. Looking at the evaluable

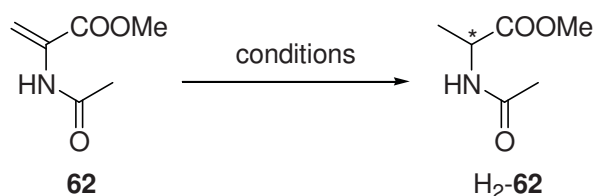
results, the activities were comparable to the *Z*-isomer **60** and the enantioselectivities appeared to be slightly higher. The *E*- and *Z*-isomer produced products of the opposite configuration. 72% *ee* was obtained with **40** in DCE (entry 5). Employing **42** in DCE, full conversion was achieved even at 1 mol% catalyst loading with a slightly lower enantiomeric excess (entry 18).

Table 1.13. Hydrogenation of ethyl *E*-acetamidocrotonate (**61**).



Entry ^a	Ligand	Solvent	s/c	conc. [mol/l]	conv. [%] ^b	<i>ee</i> [%] ^b
1		EtOH	25	0.083	>99	15 (<i>S</i>)
2		EtOH	100	0.333	50	14 (<i>S</i>)
3		THF	25	0.083	>99	12 (<i>S</i>)
4		THF	100	0.333	40	9 (<i>S</i>)
5 ^c		DCE	25	0.083	95	72 (<i>S</i>)
6 ^c	40	DCE	100	0.333	40	60 (<i>S</i>)
7		EtOH	25	0.083	>99	29 (<i>S</i>)
8 ^c		EtOH	100	0.333	96	n.d. ^d
9		THF	25	0.083	>99	36 (<i>S</i>)
10 ^c		THF	100	0.333	94	n.d. ^d
11 ^c		DCE	25	0.083	>99	n.d. ^d
12 ^c	41	DCE	100	0.333	>99	n.d. ^d
13		EtOH	25	0.083	>99	20 (<i>S</i>)
14		EtOH	100	0.333	95	n.d. ^d
15		THF	25	0.083	>99	33 (<i>S</i>)
16		THF	100	0.333	95	n.d. ^d
17 ^c		DCE	25	0.083	>99	65 (<i>S</i>)
18 ^c	42	DCE	100	0.333	>99	62 (<i>S</i>)

^aReaction was carried out with [Rh(nbd)₂]BF₄ as metal source with a metal source to ligand ratio of 1:1 under 1 bar H₂ at 25 °C for 2 h. ^bDetermined by chiral GC. ^c[Rh(nbd)Cl]₂ was used as metal source, metal source to ligand ratio of 1:2. ^dSide products were observed.

Table 1.14. Hydrogenation of methyl acetamidoacrylate (**62**).


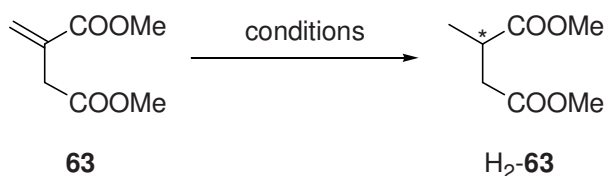
Entry ^a	Ligand	Solvent	s/c	conc. [mol/l]	conv. [%] ^b	ee [%] ^b
1		EtOH	25	0.083	>99	65 (<i>S</i>)
2		EtOH	100	0.333	>99	56 (<i>S</i>)
3		THF	25	0.083	>99	34 (<i>S</i>)
4		THF	100	0.333	>99	42 (<i>S</i>)
5 ^c		DCE	25	0.083	>99	10 (<i>S</i>)
6 ^c		DCE	100	0.333	70	10 (<i>R</i>)
7		EtOH	25	0.083	98	4 (<i>R</i>)
8		EtOH	100	0.333	54	10 (<i>R</i>)
9		THF	25	0.083	98	rac.
10		THF	100	0.333	35	30 (<i>R</i>)
11 ^c		DCE	25	0.083	53	29 (<i>R</i>)
12 ^c		DCE	100	0.333	21	59 (<i>R</i>)
13		EtOH	25	0.083	95	23 (<i>S</i>)
14		EtOH	100	0.333	91	21 (<i>S</i>)
15		THF	25	0.083	97	37 (<i>S</i>)
16		THF	100	0.333	77	37 (<i>S</i>)
17 ^c		DCE	25	0.083	>99	17 (<i>R</i>)
18 ^c		DCE	100	0.333	78	21 (<i>R</i>)

^aReaction was carried out with [Rh(nbd)₂]BF₄ as metal source with a metal source to ligand ratio of 1:1 under 1 bar H₂ at 25 °C for 2 h. ^bDetermined by chiral GC. ^c[Rh(nbd)Cl]₂ was used as metal source, metal source to ligand ratio of 1:2.

The best result in the hydrogenation of acrylate **62** was achieved with the diphenylphosphino substituted phospholane **40** giving full conversion and 65% *ee* (Table 1.14 entry 1). The complexes formed from **40** or **42** and [Rh(nbd)₂]BF₄ showed good activities in ethanol and THF, even at 1 mol% catalyst loading; the conversions in DCE were slightly lower. In ethanol or THF **40** and **42** gave similar selectivities, generally higher than those obtained with **41**. Moreover, in these cases **41** showed the opposite enantioselectivity to the other diphosphines. In DCE the enantioselectivity was better with the *ortho*-tolyl substituted ligand **41** albeit with reduced activity. In some cases an influence of the substrate concentration on the selectivity

was observed. The largest effect was observed with **41** and $[\text{Rh}(\text{nbd})\text{Cl}]_2$ in DCE where an improvement in the enantiomeric excess from 29% to 59% was noted (entries 11 and 12).

Table 1.15. Hydrogenation of dimethyl itaconate (**63**).



Entry ^a	Ligand	Solvent	s/c	conc. [mol/l]	conv. [%] ^b	ee [%] ^b
1		EtOH	25	0.083	>99	44 (<i>R</i>)
2		EtOH	100	0.333	60	58 (<i>R</i>)
3		THF	25	0.083	>99	30 (<i>R</i>)
4		THF	100	0.333	40	57 (<i>R</i>)
5 ^c		DCE	25	0.083	95	10 (<i>S</i>)
6 ^c	40	DCE	100	0.333	20	11 (<i>S</i>)
7		EtOH	25	0.083	>99	15 (<i>R</i>)
8		EtOH	100	0.333	>99	18 (<i>R</i>)
9		THF	25	0.083	>99	14 (<i>R</i>)
10		THF	100	0.333	93	21 (<i>S</i>)
11 ^c	41	DCE	25	0.083	>99	6 (<i>R</i>)
12 ^c		DCE	100	0.333	50	rac.
13		EtOH	25	0.083	>99	rac.
14		EtOH	100	0.333	>99	38 (<i>R</i>)
15		THF	25	0.083	>99	11 (<i>S</i>)
16		THF	100	0.333	>99	rac.
17 ^c	42	DCE	25	0.083	>99	21 (<i>S</i>)
18 ^c		DCE	100	0.333	>99	21 (<i>S</i>)
19 ^d		EtOH	100	0.333	>99	79 (<i>S</i>)
20 ^d		THF	50	0.333	52	59 (<i>S</i>)
21 ^d		EtOH	100	0.333	>99	rac.

^aReaction was carried out with $[\text{Rh}(\text{nbd})_2]\text{BF}_4$ as metal source with a metal source to ligand ratio of 1:1 under 1 bar H_2 at 25 °C for 2 h. ^bDetermined by chiral GC. ^c $[\text{Rh}(\text{nbd})\text{Cl}]_2$ was used as metal source, metal source to ligand ratio of 1:2. ^dWith a metal source to ligand ratio of 1:2.

In ethanol or THF, itaconate **63** was hydrogenated with full conversion even at 1 mol% catalyst loading when ligands **41** and **42** were applied (Table 1.15). Phospholane **40** showed less activity under these conditions but outperformed the other diphosphines in terms of selectivity. Reactions in DCE with $[\text{Rh}(\text{nbd})\text{Cl}]_2$ gave the lowest selectivities and the activity was reduced compared to the other experiments. The best result for the diphosphine ligands was obtained with **40** in ethanol with 58% *ee* but incomplete conversion (entry 2). Again, a dependence on the substrate concentration was noted in some cases where the enantioselectivities increased from 44% *ee* to 58% *ee* (entry 1 vs. entry 2), from 30% *ee* to 57% *ee* (entry 2 vs. entry 4) and from racemic product to 38% *ee* (entry 13 vs. entry 14). Experiments with the monodentate ligands **6** and **39** resulted, in the case of the trimethylsilyl substituted phospholane **39**, in full conversion but racemic product. However, the unsubstituted phospholane **6** gave the best performance among the ligands tested. In ethanol the hydrogenation product was generated with 79% *ee* and full conversion.

1.3.3 Conclusions

The hydrogenation catalysts generated from ferrocenephospholanes and different rhodium sources showed good activity with several functionalized olefins. The selectivities were only moderate with few examples reaching enantiomeric excesses around or above 90%. There did not seem to be a general favoured metal source or bidentate ligand in these reactions. The preferred conditions were dependent on the substrate. For the cinammic acid derivatives **58** and **59** the combination of ligand **42** with $[\text{Rh}(\text{nbd})\text{Cl}]_2$ was superior (Tables 3.10 and 3.11), while in the case of the β -dehydroaminoacid esters **60** and **61** ligand **40** and $[\text{Rh}(\text{nbd})\text{Cl}]_2$ gave the best results (Tables 3.12 and 3.13). The terminal olefins **62** and **63**, on the other hand, performed better with $[\text{Rh}(\text{nbd})_2]\text{BF}_4$ complexed with **40** (Tables 3.14 and 3.15). Interestingly, ligand **41**, having a bis-(*ortho*-tolyl)phosphine group, usually resulted in the formation of less selective catalysts.

The results showed that the ferrocenephospholane-rhodium system is generally inferior to established catalysts. Although selectivities up to 93% *ee* were observed in the reduction of **59** with the tested phospholane system, these results cannot compete with literature values for the ester or the free acid. Different phospholanes,^[3] C_2 -symmetric^[4] and nonsymmetric^[5] bisphosphine ligands as well as phosphine-phosphoramidite structures^[6] are able to generate enantiomeric excesses above 99%.

Several reports have been published in which substrates **60** and **61** were hydrogenated with enantioselectivities up to 99% *ee*. P-stereogenic bisphosphines^[5b] and phospholanes^[7] as well as DuPHOS analogues^[8] proved to be useful systems.

The overall performance of the ligands in the hydrogenation of **62** was only satisfying in terms of reactivity. The enantioselectivities up to 65% *ee* are outperformed by established diphosphine systems. For example, diphosphine ligands with a cyclophane backbone^[9] or a small bite angle^[10] as well as mannitol-derived ferrocenyl phospholanes^[3e] have been reported to generate enantioselectivities above 99% *ee*.

The enantioselectivities for the reduction of **63** with the ferrocenephospholanes tested are also far below the standard. With C_2 -symmetric bisphosphinoethanes,^[11] DuPhos derivatives,^[12] BoPhoz analogues^[6] or mandyphos ligands^[13] enantiomeric excesses above 99% have been achieved.

1.3.4 References

- [1] I. D. Gridnev, N. Higashi, K. Asakura, T. Immoto, *J. Am. Chem. Soc.* **2000**, *122*, 7183.
- [2] a) D. Heller, K. Kortus, R. Selke, *Liebigs Ann.* **1995**, 575-581; b) A. Preetz, H.-J. Drexler, C. Fischer, Z. Dai, A. Börner, W. Baumann, A. Spannenberg, R. Thede, D. Heller, *Chem. Eur. J.* **2008**, *14*, 1445-1451.
- [3] a) W. Li, Z. Zhang, D. Xiao, X. Zhang, *Tetrahedron Lett.* **1999**, *40*, 6701-6704; b) W. Li, Z. Zhang, D. Xiao, X. Zhang, *J. Org. Chem.*, **2000**, *65*, 3489-3496; c) A. Bayer, P. Murszat, U. Thewalt, B. Rieger, *Eur. J. Inorg. Chem.* **2002**, 2614-2624; d) W. Tang, X. Zhang, *Angew. Chem. Int. Ed.* **2002**, *41*, 1612-1614; e) D. Liu, W. Li, X. Zhang, *Org. Lett.*, **2002**, *4*, 4471-4474.
- [4] T. Imamoto, J. Watanabe, Y. Wada, H. Masuda, H. Yamada, H. Tsuruta, S. Matsukawa, K. Yamaguchi, *J. Am. Chem. Soc.* **1998**, *120*, 1635-1636.
- [5] a) A. Ohashi, T. Imamoto, *Org. Lett.*, **2001**, *3*, 373-375; b) H.-P. Wu, and G. Hoge, *Org. Lett.*, **2004**, *6*, 3645-3647.
- [6] X.-P. Hu, Z. Zheng, *Org. Lett.*, **2004**, *6*, 3585-3588.
- [7] D. Lui, X. Zhang, *Eur. J. Org. Chem.* **2005**, 646-649.
- [8] a) G. Zhu, Z. Chen, X. Zhang, *J. Org. Chem.*, **1999**, *64*, 6907-6910; b) T. Jerphagnon, J.-L. Renaud, P. Demonchaux, A. Ferreira, C. Bruneau, *Tetrahedron: Asymmetry* **2003**, *14*, 1973-1977.
- [9] P. J. Pye, K. Rossen, R. A. Reamer, N. N. Tsou, R. P. Volante, P. J. Reider, *J. Am. Chem. Soc.* **1997**, *119*, 6207-6208.
- [10] Y. Yamanoi, T. Imamoto, *J. Org. Chem.* **1999**, *64*, 2988-2989.
- [11] I. D. Gridnev, Y. Yamanoi, N. Higashi, H. Tsuruta, M. Yasutake, T. Imamoto, *Adv. Synth. Catal.* **2001**, *343*, 118-136.
- [12] T. Benincori, T. Pilati, S. Rizzo, F. Sannicolò, M. J. Burk, L. de Ferra, E. Ullucci, O. Piccolo, *J. Org. Chem.* **2005**, *70*, 5436-5441.
- [13] F. Spindler, C. Malan, M. Lotz, M. Kesselgruber, U. Pittelkow, A. Rivas-Nass, O. Briel, H.-U. Blaser, *Tetrahedron: Asymmetry* **2004**, *15*, 2299-2306.

1.4 Iridium Complexes and their Application in the Asymmetric Hydrogenation of Olefines

1.4.1 Hydrogenation with *in situ* Generated Complexes

1.4.1.1 Substrate Screening

Analogously to their rhodium counterparts, iridium complexes of the ferrocenephospholanes were tested in the hydrogenation of various substrates. The coordination behaviour of the iridium complexes was assumed to mirror the observed coordination behaviour of the rhodium compounds (see section 1.3.1). Therefore catalysis was performed without preliminary investigations of precatalyst formation.

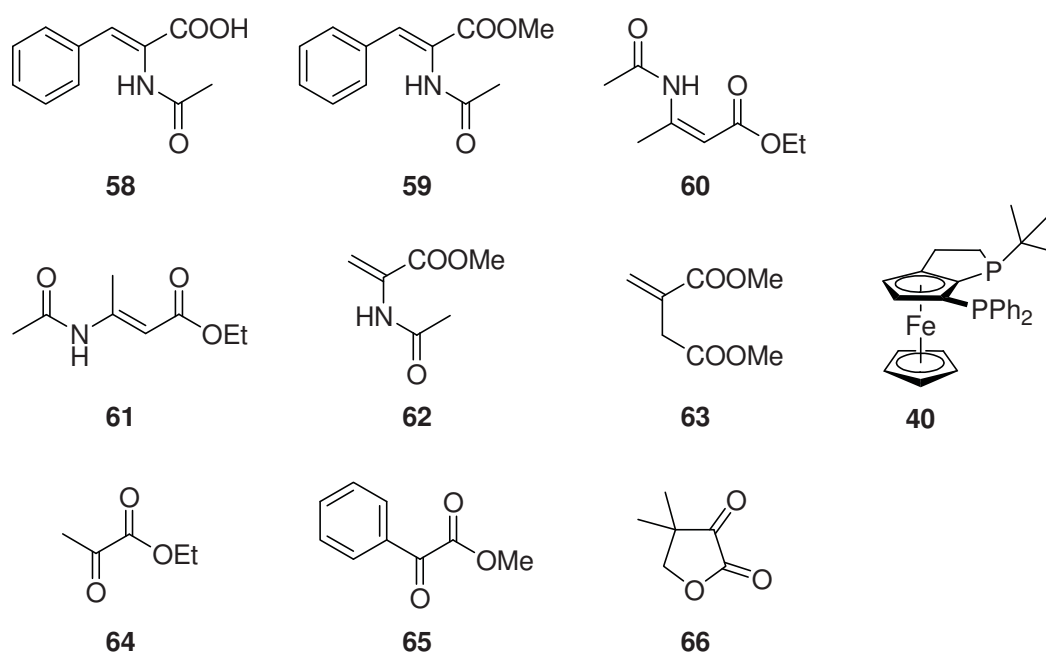
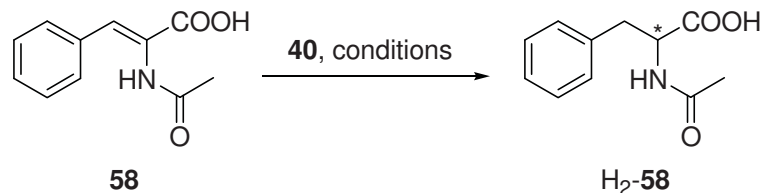


Figure 1.45. Ligand and substrates used in the initial screening.

Again, the dehydroamino acid derivatives **58** and **59**, the isomeric crotonates **60** and **61**, the acrylate **62**, the unsaturated ester **63** and α -ketoesters **64**, **65** and **66** were used as substrates. Ligand **40** in combination with $[\text{Ir}(\text{cod})(\text{bzn})_2]\text{BF}_4$ or $[\text{Ir}(\text{cod})\text{Cl}]_2$ in ethanol, DCE or THF was applied to evaluate the activities and selectivities in the hydrogenation reactions.

The screening was carried out on an automated system and the experimental procedures were identical with those applied for the rhodium catalyzed reactions (see Section 1.3.2.1).

Table 1.16. Hydrogenation of acetamido cinnamic acid (**58**).



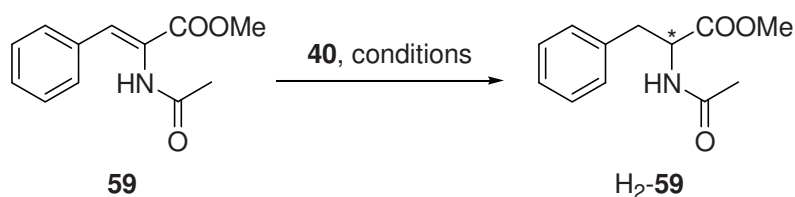
Entry ^a	Metal source	Solvent	s/c	conc. [mol/l]	conv. [%] ^b	ee [%] ^b
1	[Ir(cod)(bzn) ₂] ₂ BF ₄	EtOH	25	0.083	>99	21
2 ^c	[Ir(cod)(bzn) ₂] ₂ BF ₄	EtOH	100	0.333	5	61
3	[Ir(cod)(bzn) ₂] ₂ BF ₄	DCE	25	0.083	20	25
4	[Ir(cod)(bzn) ₂] ₂ BF ₄	DCE	100	0.333	20	24
5 ^d	[Ir(cod)Cl] ₂	THF	25	0.083	0	-
6 ^d	[Ir(cod)Cl] ₂	THF	100	0.333	0	-

^aReaction was carried out with a metal source to ligand ratio of 1:1 under 1 bar H₂ and 25 °C for 2 h.

^bDetermined by chiral GC ^cWith dabco as additive. ^dMetal source to ligand ratio of 1:2.

Acid **58** was reduced with full conversion in ethanol with 4 mol% of [Ir(cod)(bzn)₂]₂BF₄ (Table 1.16, entry 1). All other tested combinations resulted in low consumption of starting material. The selectivities were around 25% *ee*. The enantiomeric excess of 61% in entry 2 has to be taken with some caution as a conversion of only 5% was measured.

Table 1.17. Hydrogenation of methyl acetamidocinnamate (**59**).



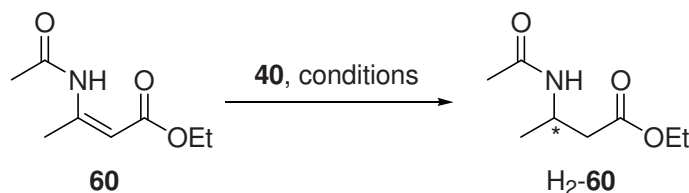
Entry ^a	Metal source	Solvent	s/c	conc. [mol/l]	conv. [%] ^b	ee [%] ^b
1	[Ir(cod)(bzn) ₂] ₂ BF ₄	EtOH	25	0.083	90	44
2	[Ir(cod)(bzn) ₂] ₂ BF ₄	EtOH	100	0.333	5	20
3	[Ir(cod)(bzn) ₂] ₂ BF ₄	DCE	25	0.083	80	27
4	[Ir(cod)(bzn) ₂] ₂ BF ₄	DCE	100	0.333	0	-
5 ^c	[Ir(cod)Cl] ₂	THF	25	0.083	0	-
6 ^c	[Ir(cod)Cl] ₂	THF	100	0.333	0	-

^aReaction was carried out with a metal source to ligand ratio of 1:1 under 1 bar H₂ and 25 °C for 2 h.

^bDetermined by chiral GC ^cMetal source to ligand ratio of 1:2.

The methyl ester **59** showed a similar behaviour (Table 1.17). Only [Ir(cod)(bzn)₂]₂BF₄ at 4 mol% catalyst loading gave acceptable conversions (entries 1 and 3). The enantioselectivity was slightly higher compared to the free acid, which was 44% *ee* in ethanol.

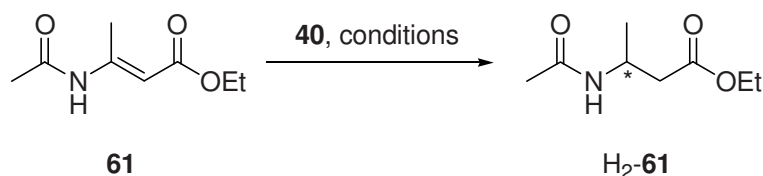
Table 1.18. Hydrogenation of ethyl *Z*-acetamidocrotonate (**60**).



Entry ^a	Metal source	Solvent	s/c	conc. [mol/l]	conv. [%] ^b	<i>ee</i> [%] ^{b,c}
1	[Ir(cod)(bzn) ₂] ₂ BF ₄	EtOH	25	0.083	5	8
2	[Ir(cod)(bzn) ₂] ₂ BF ₄	EtOH	100	0.333	0	-
3	[Ir(cod)(bzn) ₂] ₂ BF ₄	DCE	25	0.083	5	-15
4	[Ir(cod)(bzn) ₂] ₂ BF ₄	DCE	100	0.333	0	-
5 ^d	[Ir(cod)Cl] ₂	THF	25	0.083	5	37
6 ^d	[Ir(cod)Cl] ₂	THF	100	0.333	0	-

^aReaction was carried out with a metal source to ligand ratio of 1:1 under 1 bar H₂ at 25 °C for 14 h with 2,2,2-trifluoroethanol as additive. ^bDetermined by chiral GC. ^cFirst eluting enantiomer minus second eluting enantiomer. ^dMetal source to ligand ratio of 1:2.

Table 1.19. Hydrogenation of ethyl *E*-acetamidocrotonate (**61**).



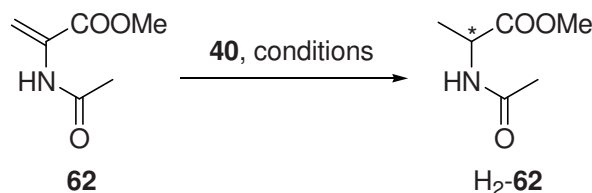
Entry ^a	Metal source	Solvent	s/c	conc. [mol/l]	conv. [%] ^b	<i>ee</i> [%] ^{b,c}
1	[Ir(cod)(bzn) ₂] ₂ BF ₄	EtOH	25	0.083	20	n.d.
2	[Ir(cod)(bzn) ₂] ₂ BF ₄	EtOH	100	0.333	10	-40
3	[Ir(cod)(bzn) ₂] ₂ BF ₄	DCE	25	0.083	30	5
4	[Ir(cod)(bzn) ₂] ₂ BF ₄	DCE	100	0.333	10	-13
5 ^d	[Ir(cod)Cl] ₂	THF	25	0.083	20	-75
6 ^d	[Ir(cod)Cl] ₂	THF	100	0.333	5	-34

^aReaction was carried out with a metal source to ligand ratio of 1:1 under 1 bar H₂ at 25 °C for 14 h. ^bDetermined by chiral GC. ^cFirst eluting enantiomer minus second eluting enantiomer. ^dMetal source to ligand ratio of 1:2.

The dehydro-β-aminoacid derivatives **60** and **61** exhibited generally low activities regardless of the conditions applied. The *Z*-isomer was basically inactive and the conversions in the reaction of the *E*-isomer were only slightly better. The combination of [Ir(cod)Cl]₂ in THF gave the reduced product in 75% *ee* with low conversion (20%) (Table 1.19, entry 5).

The results of the hydrogenation of acrylate **62** followed the trends already observed (Table 1.20). 4 mol% [Ir(cod)(bzn)₂]BF₄ in ethanol were needed to convert the starting material in substantial amounts. The enantiomeric excess of the products formed did not exceed 20%.

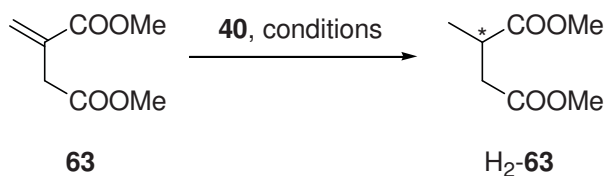
Table 1.20. Hydrogenation of methyl acetamidoacrylate (**62**).



Entry ^a	Metal source	Solvent	s/c	conc. [mol/l]	conv. [%] ^b	ee [%] ^b
1	[Ir(cod)(bzn) ₂]BF ₄	EtOH	25	0.083	90	20 (<i>R</i>)
2	[Ir(cod)(bzn) ₂]BF ₄	EtOH	100	0.333	10	34 (<i>R</i>)
3	[Ir(cod)(bzn) ₂]BF ₄	DCE	25	0.083	>99	12 (<i>S</i>)
4	[Ir(cod)(bzn) ₂]BF ₄	DCE	100	0.333	30	rac.
5 ^c	[Ir(cod)Cl] ₂	THF	25	0.083	0	-
6 ^c	[Ir(cod)Cl] ₂	THF	100	0.333	0	-

^aReaction was carried out with a metal source to ligand ratio of 1:1 under 1 bar H₂ at 25 °C for 2 h. ^bDetermined by chiral GC. ^cMetal source to ligand ratio of 1:2.

Table 1.21. Hydrogenation of dimethyl itaconate (**63**).



Entry ^a	Metal source	Solvent	s/c	conc. [mol/l]	conv. [%] ^b	ee [%] ^b
1	[Ir(cod)(bzn) ₂]BF ₄	EtOH	25	0.083	80	5 (<i>R</i>)
2	[Ir(cod)(bzn) ₂]BF ₄	EtOH	100	0.333	20	rac.
3	[Ir(cod)(bzn) ₂]BF ₄	DCE	25	0.083	>99	14 (<i>R</i>)
4	[Ir(cod)(bzn) ₂]BF ₄	DCE	100	0.333	70	19 (<i>R</i>)
5 ^c	[Ir(cod)Cl] ₂	THF	25	0.083	5	9 (<i>S</i>)
6 ^c	[Ir(cod)Cl] ₂	THF	100	0.333	5	11 (<i>S</i>)

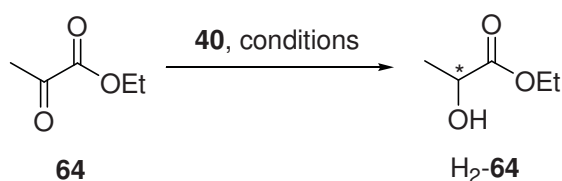
^aReaction was carried out with a metal source to ligand ratio of 1:1 under 1 bar H₂ at 25 °C for 14 h. ^bDetermined by chiral GC. ^cMetal source to ligand ratio of 1:2.

The unsaturated ester **63** was hydrogenated with higher conversions than the previously described substrates (Table 1.21). Even at 1 mol% catalyst loading, 70% product formation was observed (entry 4). Again, [Ir(cod)Cl]₂ did not give an active catalyst. Although

acceptable conversions with $[\text{Ir}(\text{cod})(\text{bzn})_2]\text{BF}_4$ as metal source were obtained the selectivity was very low.

The hydrogenation of ketone **64** was achieved with the best selectivity using $[\text{Ir}(\text{cod})\text{Cl}]_2$ in ethanol (Table 1.22). At 4 mol% catalyst loading the product was obtained with 60% *ee* but low conversion (entry 2). Addition of dabco in THF resulted in complete consumption of the starting material accompanied by erosion and, interestingly, inversion of enantioselectivity (entry 4).

Table 1.22. Hydrogenation of ethyl pyruvate (**64**).



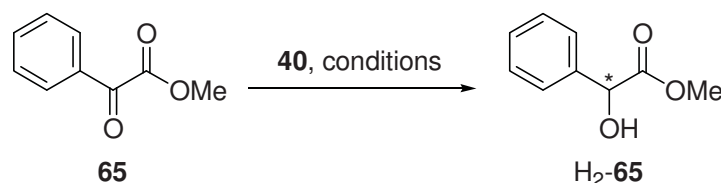
Entry ^a	Metal source	Solvent	s/c	conc. [mol/l]	conv. [%] ^b	<i>ee</i> [%] ^{b,c}
1	$[\text{Ir}(\text{cod})\text{Cl}]_2$	DCE	25	0.083	60	45
2	$[\text{Ir}(\text{cod})\text{Cl}]_2$	EtOH	25	0.083	30	60
3 ^d	$[\text{Ir}(\text{cod})\text{Cl}]_2$	DCE/THF	25	0.083	50	27
4 ^d	$[\text{Ir}(\text{cod})\text{Cl}]_2$	EtOH/THF	25	0.083	>99	-39

^aReaction was carried out with a metal source to ligand ratio of 1:2 under 20 bar H_2 at 25 °C for 14 h.

^bDetermined by chiral GC. ^cFirst eluting enantiomer minus second eluting enantiomer. ^dWith dabco as additive.

Glyoxylate **65** gave generally low to moderate conversions combined with low enantioselectivities (Table 1.23). Similar to the hydrogenation of **64**, the addition of dabco and THF reversed the selectivity of the reduction in ethanol, although on a low level (entry 4).

Table 1.23. Hydrogenation of methyl phenylglyoxylate (**65**).



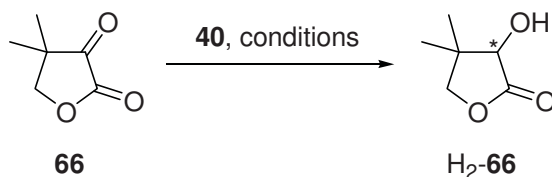
Entry ^a	Metal source	Solvent	s/c	conc. [mol/l]	conv. [%] ^b	<i>ee</i> [%] ^{b,c}
1	$[\text{Ir}(\text{cod})\text{Cl}]_2$	DCE	25	0.083	20	15
2	$[\text{Ir}(\text{cod})\text{Cl}]_2$	EtOH	25	0.083	30	6
3 ^d	$[\text{Ir}(\text{cod})\text{Cl}]_2$	DCE/THF	25	0.083	60	12
4 ^d	$[\text{Ir}(\text{cod})\text{Cl}]_2$	EtOH/THF	25	0.083	50	-10

^aReaction was carried out with a metal source to ligand ratio of 1:2 under 20 bar H_2 at 25 °C for 14 h.

^bDetermined by chiral GC. ^cFirst eluting enantiomer minus second eluting enantiomer. ^dWith dabco as additive.

Reduction of lactone **66** proceeded in DCE to give the product with 40% conversion and 71% *ee* (Table 1.24 entry 1). Addition of dabco and THF resulted in an increase of activity in ethanol and DCE, but also in loss of selectivity. At full conversion, the product was formed with 26% *ee* (entry 3).

Table 1.24. Hydrogenation of ketopantolactone (**66**).



Entry ^a	Metal source	Solvent	s/c	conc. [mol/l]	conv. [%] ^b	<i>ee</i> [%] ^{b,c}
1	[Ir(cod)Cl] ₂	DCE	25	0.083	40	71
2	[Ir(cod)Cl] ₂	EtOH	25	0.083	5	12
3 ^d	[Ir(cod)Cl] ₂	DCE/THF	25	0.083	>99	26
4 ^d	[Ir(cod)Cl] ₂	EtOH/THF	25	0.083	70	31

^aReaction was carried out with a metal source to ligand ratio of 1:2 under 20 bar H₂ at 25 °C for 14 h.

^bDetermined by chiral GC. ^cFirst eluting enantiomer minus second eluting enantiomer. ^dWith dabco as additive.

1.4.1.2 Ligand Screening

After the initial screening the evaluation of ligands **41** and **42** was focused on hydrogenation reactions involving olefins analogous to the experiments described in Chapter 3.2.2 (Figure 1.46). In contrast to the initial screening, $[\text{Ir}(\text{cod})_2]\text{BAR}_\text{F}$ was used instead of $[\text{Ir}(\text{cod})(\text{bzn})_2]\text{BF}_4$ as a metal source with a non-coordinating counterion. The results showed that the effect of the counterion was only marginal.²

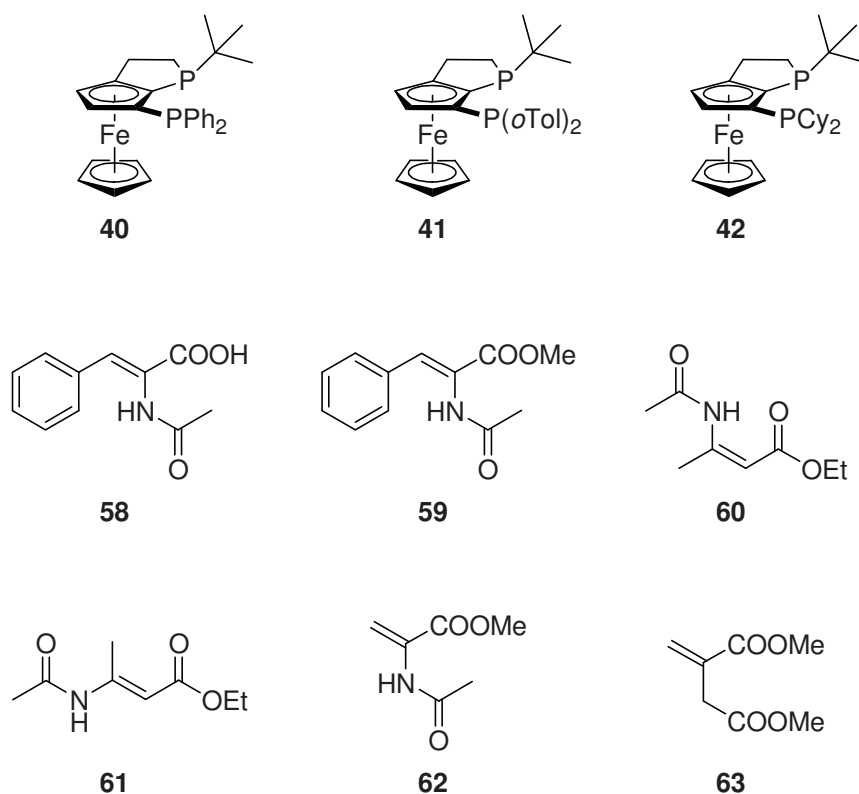


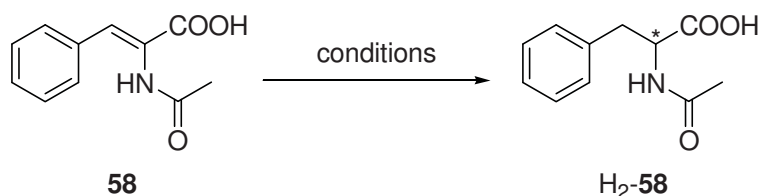
Figure 1.46. Ligands and Substrates used in the screening.

Full conversion in the hydrogenation of acid **58** was only achieved with ligands **40** and **42** in ethanol (Table 1.25 entries 1 and 13). The reactions in DCE applying **41** or **42** showed less activity but, on the other hand, the difference in conversion between 4 mol% and 1 mol% catalyst loading was much smaller. Enantioselectivities did not vary strongly, except in a few cases, where an increase in the enantiomeric excess was noted when a more concentrated solution or dabco as additive was used. The highest selectivity was observed when employing

² For the effect of the counterion on the Ir-catalyzed hydrogenation of unfunctionalized olefines see Section 3.1.2.2.

41 in combination with $[\text{Ir}(\text{cod})_2]\text{BAR}_F$ and dabco in ethanol, giving 48% *ee* but with only 19% conversion (entry 8). The enantiomeric excess of 61% in entry 2 has to be taken with caution due to the low conversion.

Table 1.25. Hydrogenation of acetamido cinnamic acid (**58**).



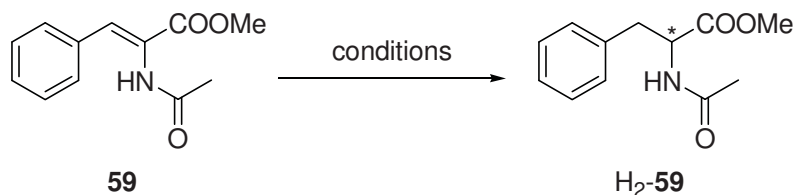
Entry ^a	Ligand	Solvent	s/c	conc. [mol/l]	conv. [%] ^b	<i>ee</i> [%] ^b
1 ^c		EtOH	25	0.083	>99	21 (<i>R</i>)
2 ^{c,d}		EtOH	100	0.333	5	61 (<i>R</i>)
3 ^c		DCE	25	0.083	20	25 (<i>R</i>)
4 ^c		DCE	100	0.333	20	24 (<i>R</i>)
5 ^e		THF	25	0.083	0	–
6 ^e		THF	100	0.333	0	–
7		EtOH	25	0.083	34	rac.
8 ^d		EtOH	100	0.333	19	48 (<i>S</i>)
9		DCE	25	0.083	71	36 (<i>R</i>)
10		DCE	100	0.333	56	26 (<i>R</i>)
11 ^e		THF	25	0.083	42	rac.
12 ^e		THF	100	0.333	38	16 (<i>S</i>)
13		EtOH	25	0.083	99	15 (<i>R</i>)
14 ^d		EtOH	100	0.333	19	23 (<i>R</i>)
15		DCE	25	0.083	81	21 (<i>R</i>)
16		DCE	100	0.333	67	28 (<i>R</i>)
17 ^e		THF	25	0.083	29	8 (<i>R</i>)
18 ^e		THF	100	0.333	41	28 (<i>S</i>)

^aReaction was carried out with $[\text{Ir}(\text{cod})_2]\text{BAR}_F$ as metal source with a metal source to ligand ratio of 1:1 under 1 bar H_2 at 25 °C for 2 h. ^bDetermined by chiral GC. ^c $[\text{Ir}(\text{cod})(\text{bzn})_2]\text{BF}_4$ as metal source. ^dWith dabco as additive. ^e $[\text{Ir}(\text{cod})\text{Cl}]_2$ was used as metal source, metal source to ligand ratio of 1:2.

The methyl ester **59** showed similar reactivities compared to the free acid **58** (Table 1.26). The ligands **40** and **42** were again superior regarding conversion compared to **41**. The best solvent was ethanol followed by DCE. The influence of the catalyst loading was pronounced. With $[\text{Ir}(\text{cod})\text{Cl}]_2$ in THF only ligand **41** showed activity although accompanied by formation of racemic product (entry 11). The selectivities were only moderate and the best results were

obtained in ethanol, with ligand **40** giving 44% *ee* at 90% conversion (entry 1) and ligand **41** giving 55% *ee* at 32% conversion (entry 7).

Table 1.26. Hydrogenation of methyl acetamidocinnamate (**59**).



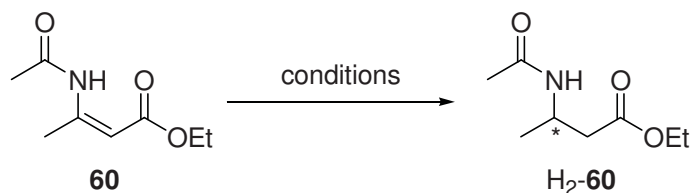
Entry ^a	Ligand	Solvent	s/c	conc. [mol/l]	conv. [%] ^b	<i>ee</i> [%] ^b
1 ^c		EtOH	25	0.083	90	44 (<i>R</i>)
2 ^c		EtOH	100	0.333	5	20 (<i>R</i>)
3 ^c		DCE	25	0.083	80	27 (<i>R</i>)
4 ^c		DCE	100	0.333	0	-
5 ^d		THF	25	0.083	0	-
6 ^d		THF	100	0.333	0	-
7		EtOH	25	0.083	32	55 (<i>R</i>)
8		EtOH	100	0.333	13	46 (<i>R</i>)
9		DCE	25	0.083	31	24 (<i>R</i>)
10		DCE	100	0.333	14	27 (<i>R</i>)
11 ^d		THF	25	0.083	36	rac.
12 ^d		THF	100	0.333	26	rac.
13		EtOH	25	0.083	>99	12 (<i>R</i>)
14		EtOH	100	0.333	11	27 (<i>R</i>)
15		DCE	25	0.083	62	12 (<i>R</i>)
16		DCE	100	0.333	11	55 (<i>R</i>)
17 ^d		THF	25	0.083	5	24 (<i>R</i>)
18 ^d		THF	100	0.333	4	n.d.

^aReaction was carried out with [Ir(cod)₂]BAR_F as metal source with a metal source to ligand ratio of 1:1 under 1 bar H₂ at 25 °C for 2 h. ^bDetermined by chiral GC. ^c[Ir(cod)(bzn)₂]BF₄ as metal source. ^d[Ir(cod)Cl]₂ was used as metal source, metal source to ligand ratio of 1:2.

The reduction of the crotonates **60** and **61** was rather ineffective. The *Z*-isomer generally showed almost no conversion under the conditions applied (Table 1.27) and the *E*-isomer gave a mixture of products in most cases (Table 1.28). The sluggish reactions with ligands **41** and **42** might be caused by the catalyst structure originating from the ligands themselves or by a systematic error during the reaction or analysis. An influence of the BAR_F counterion could be excluded since the reactions with [Ir(cod)Cl]₂ were also affected. **61** was hydrogenated

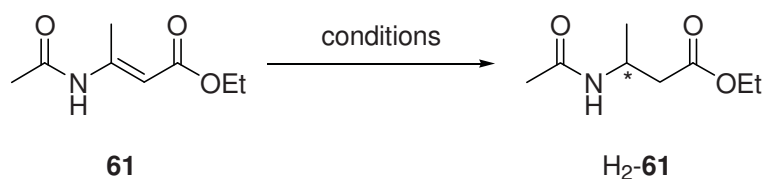
with low conversions using ligand **40** and a maximum enantiomeric excess of 75% in combination with $[\text{Ir}(\text{cod})\text{Cl}]_2$ in THF (entry 5).

Table 1.27. Hydrogenation of ethyl Z-acetamidocrotonate (**60**).



Entry ^a	Ligand	Solvent	s/c	conc. [mol/l]	conv. [%] ^b	ee [%] ^{b,c}
1 ^d		EtOH	25	0.083	5	8
2 ^d		EtOH	100	0.333	0	-
3 ^d		DCE	25	0.083	5	-15
4 ^d		DCE	100	0.333	0	-
5 ^e	40	THF	25	0.083	5	37
6 ^e	40	THF	100	0.333	0	-
7		EtOH	25	0.083	3	n.d.
8		EtOH	100	0.333	2	n.d.
9		DCE	25	0.083	2	n.d.
10		DCE	100	0.333	1	n.d.
11 ^e	41	THF	25	0.083	4	n.d.
12 ^e		THF	100	0.333	1	n.d.
13		EtOH	25	0.083	4	n.d.
14		EtOH	100	0.333	1	n.d.
15		DCE	25	0.083	9	10
16		DCE	100	0.333	4	n.d.
17 ^e	42	THF	25	0.083	5	rac.
18 ^e		THF	100	0.333	3	n.d.

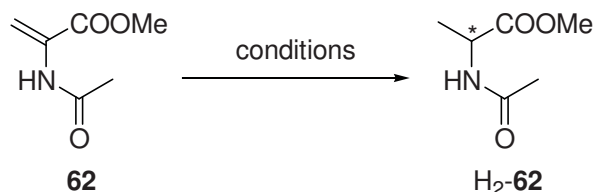
^aReaction was carried out with $[\text{Ir}(\text{cod})_2]\text{BAr}_F$ as metal source with a metal source to ligand ratio of 1:1 under 1 bar H_2 at 25 °C for 2 h with 2,2,2-trifluoroethanol as additive. ^bDetermined by chiral GC. ^cFirst eluting enantiomer minus second eluting enantiomer. ^d $[\text{Ir}(\text{cod})(\text{bzn})_2]\text{BF}_4$ was used as metal source. ^e $[\text{Ir}(\text{cod})\text{Cl}]_2$ was used as metal source, metal source to ligand ratio of 1:2.

Table 1.28. Hydrogenation of ethyl *E*-acetamidocrotonate (**61**).


Entry ^a	Ligand	Solvent	s/c	conc. [mol/l]	conv. [%] ^b	ee [%] ^{b,c}
1 ^d		EtOH	25	0.083	20	n.d.
2 ^d		EtOH	100	0.333	10	-40
3 ^d		DCE	25	0.083	30	5
4 ^d		DCE	100	0.333	10	-13
5 ^e	40	THF	25	0.083	20	-75
6 ^e	40	THF	100	0.333	5	-34
7		EtOH	25	0.083	97	n.d. ^f
8		EtOH	100	0.333	94	n.d. ^f
9		DCE	25	0.083	95	n.d. ^f
10		DCE	100	0.333	93	n.d. ^f
11 ^e	41	THF	25	0.083	96	n.d. ^f
12 ^e	41	THF	100	0.333	94	n.d. ^f
13		EtOH	25	0.083	95	n.d. ^f
14		EtOH	100	0.333	92	n.d. ^f
15		DCE	25	0.083	95	n.d. ^f
16		DCE	100	0.333	93	n.d. ^f
17 ^e	42	THF	25	0.083	96	n.d. ^f
18 ^e	42	THF	100	0.333	92	n.d. ^f

^aReaction was carried out with [Ir(cod)₂]BAR_F as metal source with a metal source to ligand ratio of 1:1 under 1 bar H₂ at 25 °C for 2 h. ^bDetermined by chiral GC. ^cFirst eluting enantiomer minus second eluting enantiomer. ^d[Ir(cod)(bzn)₂]BF₄ was used as metal source. ^e[Ir(cod)Cl]₂ was used as metal source, metal source to ligand ratio of 1:2. ^fSide products were observed.

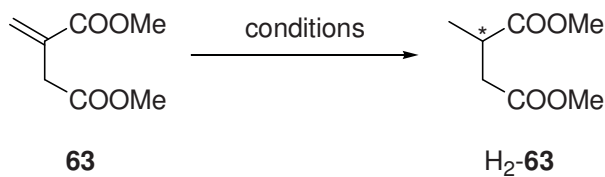
Acrylate **62** was hydrogenated with good conversions using phospholanes **40** and **42** in ethanol or DCE at 4 mol% catalyst loading (Table 1.29). The activity dropped with a higher substrate to catalyst ratio, with [Ir(cod)Cl]₂ as metal source or when ligand **41** was tested. Among the active systems only **40** exhibits some stereoselectivity, resulting in 20% *ee* with almost full conversion (entry 1).

Table 1.29. Hydrogenation of methyl acetamidoacrylate (**62**).

Entry ^a	Ligand	Solvent	s/c	conc. [mol/l]	conv. [%] ^b	ee [%] ^b
1 ^c		EtOH	25	0.083	90	20 (<i>R</i>)
2 ^c		EtOH	100	0.333	10	34 (<i>R</i>)
3 ^c		DCE	25	0.083	>99	12 (<i>S</i>)
4 ^c		DCE	100	0.333	30	rac.
5 ^d	40	THF	25	0.083	0	-
6 ^d		THF	100	0.333	0	-
7		EtOH	25	0.083	13	38 (<i>R</i>)
8		EtOH	100	0.333	6	14 (<i>R</i>)
9		DCE	25	0.083	12	25 (<i>R</i>)
10		DCE	100	0.333	3	n.d.
11 ^d		THF	25	0.083	19	36 (<i>R</i>)
12 ^d		THF	100	0.333	6	55 (<i>R</i>)
13		EtOH	25	0.083	85	6 (<i>R</i>)
14		EtOH	100	0.333	21	5 (<i>R</i>)
15		DCE	25	0.083	>99	rac.
16		DCE	100	0.333	38	rac.
17 ^d		THF	25	0.083	2	n.d.
18 ^d		THF	100	0.333	1	n.d.

^aReaction was carried out with [Ir(cod)₂]BAR_F as metal source with a metal source to ligand ratio of 1:1 under 1 bar H₂ at 25 °C for 2 h. ^bDetermined by chiral GC. ^c[Ir(cod)(bzn)₂]BF₄ was used as metal source. ^d[Ir(cod)Cl]₂ was used as metal source, metal source to ligand ratio of 1:2.

The reduction of dimethyl itaconate (**63**) proceeded in most cases with full conversion. The combinations in ethanol or DCE generally showed good activity (Table 1.30). Even at 1 mol% catalyst loading the substrate was completely consumed, except for the examples with ligand **40**. This variation could be caused by the different counterion influencing the reactivity. [Ir(cod)Cl]₂ in combination with **41** and **42** in THF was found to be a active catalyst at 4 mol% catalyst loading. The selectivities were generally low and the best result was observed with ligand **41** in DCE, which gave 23% *ee* with full conversion (entry 10).

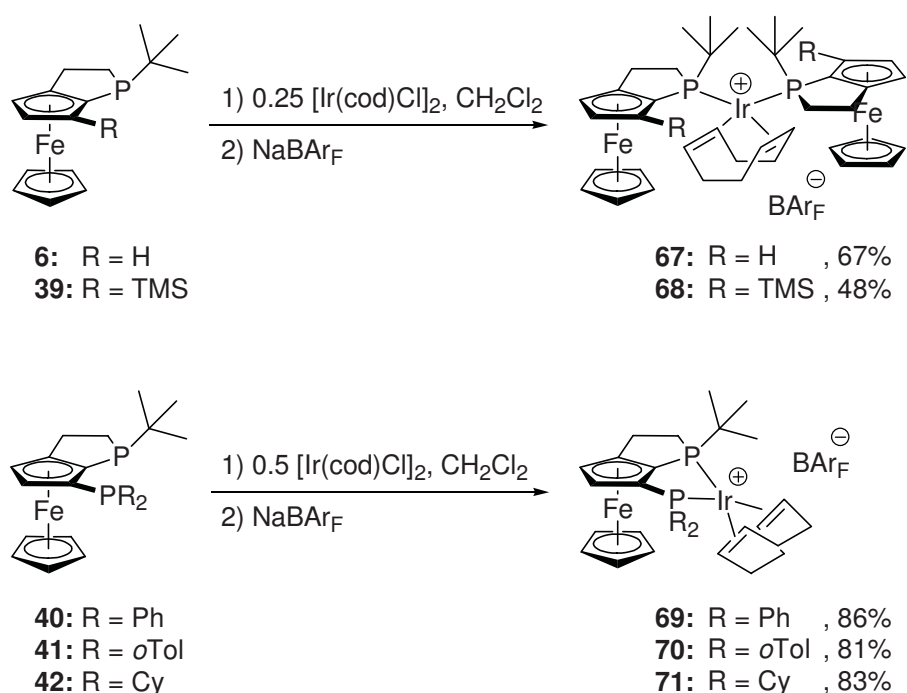
Table 1.30. Hydrogenation of dimethyl itaconate (**63**).


Entry ^a	Ligand	Solvent	s/c	conc. [mol/l]	conv. [%] ^b	ee [%] ^b
1 ^c		EtOH	25	0.083	80	5 (<i>R</i>)
2 ^c		EtOH	100	0.333	20	rac.
3 ^c		DCE	25	0.083	>99	14 (<i>R</i>)
4 ^c		DCE	100	0.333	70	19 (<i>R</i>)
5 ^d		THF	25	0.083	5	9 (<i>S</i>)
6 ^d	40	THF	100	0.333	5	11 (<i>S</i>)
7		EtOH	25	0.083	>99	rac.
8		EtOH	100	0.333	68	rac.
9		DCE	25	0.083	>99	10 (<i>R</i>)
10		DCE	100	0.333	>99	23 (<i>R</i>)
11 ^d		THF	25	0.083	>99	rac.
12 ^d		41	THF	100	0.333	14
13		EtOH	25	0.083	>99	22 (<i>S</i>)
14		EtOH	100	0.333	>99	8 (<i>S</i>)
15		DCE	25	0.083	>99	10 (<i>S</i>)
16		DCE	100	0.333	>99	6 (<i>S</i>)
17 ^d		THF	25	0.083	87	rac.
18 ^d		42	THF	100	0.333	7

^aReaction was carried out with [Ir(cod)₂]BAr_F as metal source with a metal source to ligand ratio of 1:1 under 1 bar H₂ at 25 °C for 2 h. ^bDetermined by chiral GC. ^c[Ir(cod)(bzn)₂]BF₄ as metal source. ^d[Ir(cod)Cl]₂ was used as metal source, metal source to ligand ratio of 1:2. ^eSide products were observed.

1.4.2 Hydrogenation with Isolated Complexes

The use of isolated complexes instead of *in situ* formed precatalysts is sometimes preferred due to the more exact dosage or the precisely defined ligand to metal ratio. To investigate the application and the behaviour of isolated precatalysts the iridium BAR_F complexes of the ferrocenephospholanes were prepared. Reaction of the ligands with $[\text{Ir}(\text{cod})\text{Cl}]_2$ in dichloromethane followed by anion exchange with NaBAR_F gave the complexes **67-71** after chromatography in moderate to good yields (Scheme 1.43).



Scheme 1.43. Preparation of ferrocenephospholane-iridium complexes.

The ^{31}P -NMR spectrum of both **67** and **68** showed only a single resonance, revealing the equivalence of the two coordinating phospholanes (at least in the NMR timescale) and therefore the C_2 -symmetry of these complexes in solution. The crystal structures of the nonsymmetric complexes are depicted in Figures 1.47, 1.48 and 1.49.³

³ For the discussion of the solid state structures see Section 1.5.1.

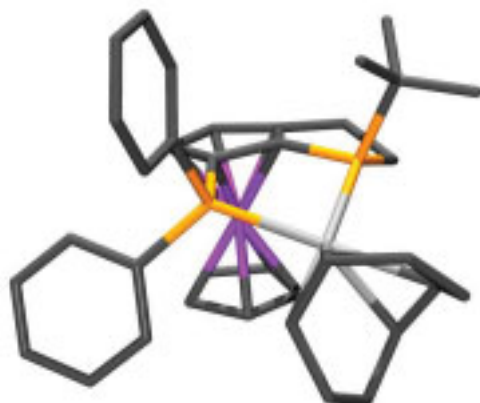


Figure 1.47. Crystal structure of **69**. The BAr_F counterion and co-crystallized dichloromethane are omitted for clarity.

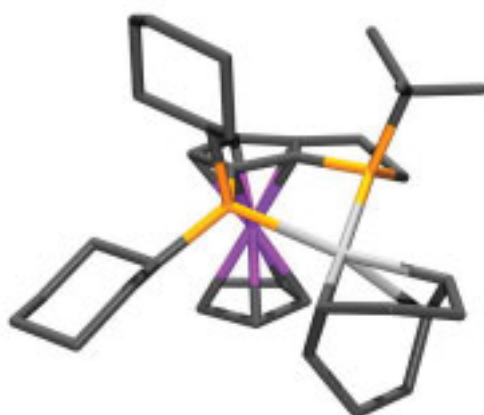


Figure 1.48. Crystal structure of **70**. The BAr_F counterion is omitted for clarity.

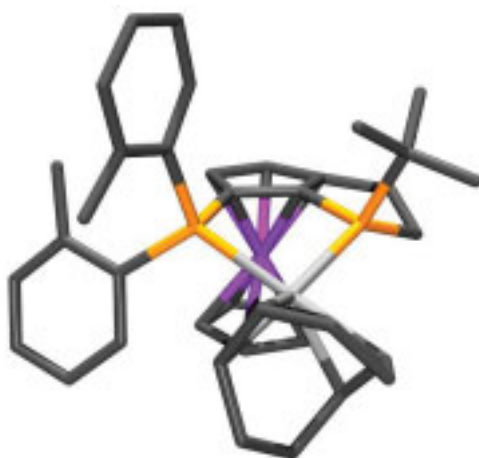
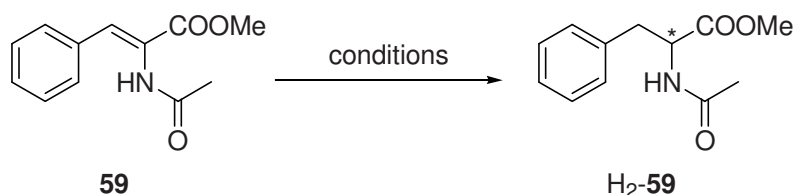


Figure 1.49. Crystal structure of **71**. The BAr_F counterion and co-crystallized hexane are omitted for clarity.

Preliminary experiments showed that the iridium complexes were not active catalysts for the hydrogenation of unfunctionalized olefins such as *trans*- α -methylstilbene. Although the successful hydrogenation of imines with bisphosphino iridium complexes has been reported,^[1] the complexes formed from the ferrocenephospholanes did not convert this class of substrates

In the reduction of acid **58** the use of isolated complexes did not improve the results of the ligand screening (Table 1.31). Generally, low conversions were obtained and in the case of **70** the enantioselectivity was comparable with the reaction employing the *in situ* generated complex (entry 4 vs. entry 5)

Table 1.32. Hydrogenation of methyl acetamidocinnamate (**59**).



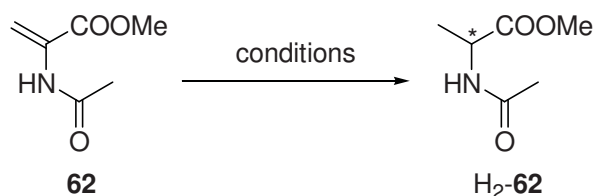
Entry ^a	Complex	conv. [%] ^b	ee [%] ^c
1	67	>99	71 (<i>S</i>)
2 ^d	67	29	77 (<i>S</i>)
3	68	>99	rac.
4	69	53	15 (<i>R</i>)
5 ^e	40 + [Ir(cod)(bzn) ₂]BF ₄	0	-
6	70	>99	7 (<i>R</i>)
7 ^e	41 + [Ir(cod) ₂]BAr _F	14	27 (<i>R</i>)
8	71	25	18 (<i>R</i>)
9 ^e	42 + [Ir(cod) ₂]BAr _F	11	55 (<i>R</i>)

^aReaction was carried out in CH₂Cl₂ at 0.1 M substrate concentration with 0.5 mol% complex under 50 bar H₂ at rt for 2 h. ^bDetermined by GC ^cDetermined by chiral HPLC. ^dReaction at 0 °C for 4 h. ^eReference taken from Table 4.11: Reaction in DCE at 0.333 M substrate concentration and 1 mol% complex under 1 bar H₂ at rt for 2h.

With the isolated iridium complexes the hydrogenation of methyl ester **59** proceeded with generally much higher conversions (Table 1.32). The best result, measured with complex **67** incorporating the previously untested monodentate ligand **6**, was 71% *ee* with full conversion (entry 1). Lowering the temperature resulted in a slightly increased selectivity accompanied by lower conversion (entry 2). The TMS-substituted phospholane **39** derived complex **68** was also active but completely unselective. Interestingly, the C₂-symmetric complex **67** favors the

formation of the opposite product enantiomer as compared to the nonsymmetric complexes **69-71**.

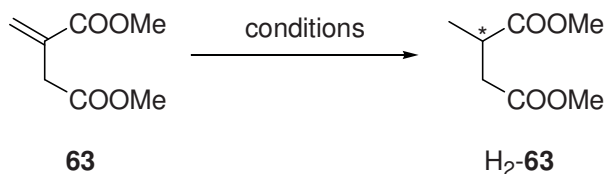
Table 1.33. Hydrogenation of methyl acetamidoacrylate (**62**).



Entry ^a	Complex	conv. [%] ^b	ee [%] ^b
1	67	55	63 (<i>R</i>)
2	68	>99	35 (<i>R</i>)
3 ^c	68	>99	44 (<i>R</i>)
4	69	24	rac.
5 ^d	40 + [Ir(cod)(bzn) ₂]BF ₄	30	rac.
6	70	79	5 (<i>S</i>)
7 ^d	41 + [Ir(cod) ₂]BAr _F	3	n.d
8	71	9	13 (<i>R</i>)
9 ^d	42 + [Ir(cod) ₂]BAr _F	38	rac.

^aReaction was carried out in CH₂Cl₂ at 0.1 M substrate concentration with 0.5 mol% complex under 50 bar H₂ at rt for 2 h. ^bDetermined by chiral GC. ^cReaction at 0 °C for 4 h. ^dReference taken from Table 4.14: Reaction in DCE at 0.333 M substrate concentration and 1 mol% complex under 1 bar H₂ at rt for 2h.

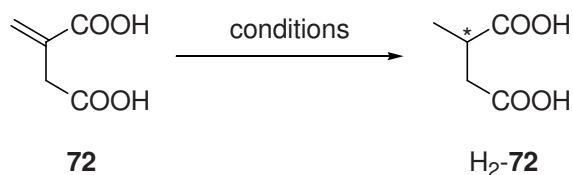
Acrylate **62** was reduced with maximum conversions when the purified iridium complexes were subjected to catalysis (Table 1.33). Complex **70** gave 79% conversion but almost racemic product (entry 6). Employing the C₂-symmetric complexes, the selectivity increased and with **67** 63% *ee* was achieved, albeit with lower activity (entry 1). Complex **68** was more active and gave full conversion even at 0 °C but the selectivities did not exceed 44% *ee* (entry 3).

Table 1.34. Hydrogenation of dimethyl itaconate (**63**).


Entry ^a	Complex	conv. [%] ^b	ee [%] ^b
1	67	8	73 (<i>R</i>)
2 ^c	67	11	48 (<i>R</i>)
3	68	>99	16 (<i>S</i>)
4	69	>99	6 (<i>S</i>)
5 ^d	40 + [Ir(cod)(bzn) ₂]BF ₄	70	19 (<i>S</i>)
6	70	>99	12 (<i>S</i>)
7 ^d	41 + [Ir(cod) ₂]BAr _F	>99	23 (<i>S</i>)
8	71	81	3 (<i>S</i>)
9 ^d	42 + [Ir(cod) ₂]BAr _F	>99	6 (<i>S</i>)

^aReaction was carried out in CH₂Cl₂ at 0.1 M substrate concentration with 0.5 mol% complex under 5 bar H₂ at rt for 2 h. ^bDetermined by chiral GC. ^cReaction under 50 bar H₂. ^dReference taken from Table 4.15: Reaction in DCE at 0.333 M substrate concentration and 1 mol% complex under 1 bar H₂ at rt for 2h.

The reduction of dimethyl itaconate (**63**) was only weakly affected by changing the complex formation strategy (Table 1.34). Notably, complex **67** once again formed the most selective catalyst, but unfortunately the conversion was very low (entry 1) even at 50 bar hydrogen pressure (entry 2). Complexes **69**, **70** and **71** were as active as the *in situ* prepared catalysts but the selectivities were slightly lower.

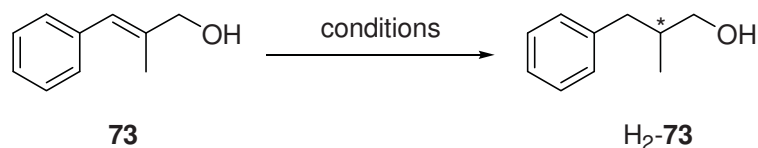
Table 1.35. Hydrogenation of itaconic acid (**72**).


Entry ^a	Complex	conv. [%] ^b	ee [%] ^b
1	67	>99	46 (<i>R</i>)
2 ^c	67	42	37 (<i>R</i>)
3	69	20	5 (<i>S</i>)
4	70	84	7 (<i>S</i>)
5	71	34	5 (<i>S</i>)

^aReaction was carried out in MeOH at 0.1 M substrate concentration with 0.5 mol% complex under 50 bar H₂ at rt for 2 h. ^bDetermined by chiral GC after derivatization with TMS-diazomethane. ^cReaction at 0 °C for 4 h.

Compared to its dimethyl ester, itaconic acid (**72**) showed higher activity with complex **67** but lower conversions with complexes **69-71** (Table 1.35). The selectivities were generally lower with, 46% *ee* being the best result (entry 1).

Table 1.36. Hydrogenation of *E*-2-methyl-3-phenyl-2-propenol (**73**).

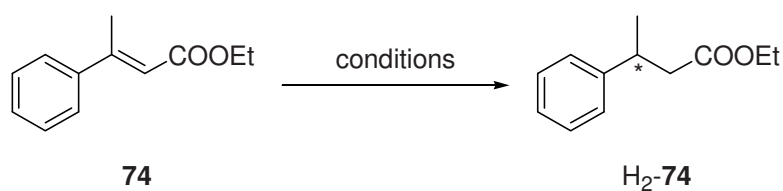


Entry ^a	Complex	conv. [%] ^b	<i>ee</i> [%] ^c
1	67	65 ^d	26 (-)
2	69	>99	27 (-)
3 ^e	69	69	32 (-)
4	70	>99	20 (-)
5	71	>99	11 (-)

^aReaction was carried out in CH₂Cl₂ at 0.1 M substrate concentration with 0.5 mol% complex under 50 bar H₂ at rt for 2 h. ^bDetermined by GC. ^cDetermined by chiral GC and HPLC. ^d50% side products were observed. ^eReaction under 5 bar H₂.

The allylic alcohol **73** was hydrogenated with good conversion under 50 bar hydrogen pressure with the complexes **69-71**, whereas **67** gave a lot of side products (Table 1.36). Low selectivities were obtained with the best enantiomeric excess being 32% under 5 bar hydrogen pressure (entry 3).

Table 1.37. Hydrogenation of ethyl *E*-2-methylcinnamate (**74**).



Entry ^a	Complex	conv. [%] ^b	<i>ee</i> [%] ^b
1	67	8	19 (<i>R</i>)
2	69	93	15 (<i>R</i>)
3 ^c	69	7	13 (<i>R</i>)
4	70	>99	7 (<i>R</i>)
5	71	>99	8 (<i>R</i>)

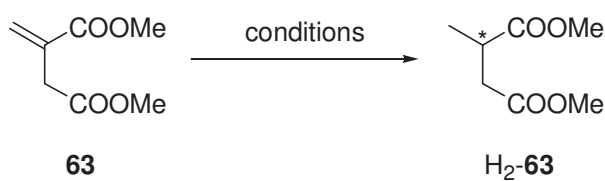
^aReaction was carried out in CH₂Cl₂ at 0.1 M substrate concentration with 0.5 mol% complex under 50 bar H₂ at rt for 2 h. ^bDetermined by chiral GC. ^cReaction under 5 bar H₂.

Only the complexes **69-71** at 50 bar hydrogen pressure were able to reduce the unsaturated ester **74** with high conversions (Table 1.37). The selectivities were generally low, independent of the complex applied.

The experiments showed that the isolated complexes of the bidentate phospholane ligands lead to higher activity than the *in situ* formed precatalysts. In terms of enantioselectivity the two different procedures had no significant influence. Interestingly, the C₂-symmetric complexes usually gave higher enantiomeric excesses than their asymmetric counterparts.

Because of the high activity of the complexes, their deactivation behaviour was briefly investigated. To this end the hydrogenation of dimethyl itaconate with complex **69** was performed with different catalyst loadings and modes of substrate addition (Table 1.38).

Table 1.38. Catalyst stability in the hydrogenation of dimethyl itaconate.



Entry ^a	s/c	After 3 h	After 6 h	conv. [%] ^b	ee [%] ^b
1	100	Work up	–	69	5 (<i>S</i>)
2	100	Addition of a second equivalent 63	Work up	66	5 (<i>S</i>)
3	50	Work up	–	100	5 (<i>S</i>)
4	50	Addition of a second equivalent 63	Work up	52	6 (<i>S</i>)

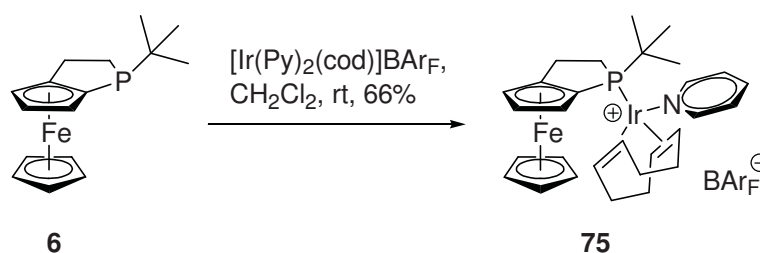
^aReaction was carried out in CH₂Cl₂ with complex **69** at 0.1 M substrate concentration under 1 bar H₂ at rt.

^bDetermined by chiral GC.

Entries 1 and 2 indicate that the active catalyst showed almost no deactivation during the hydrogenation reaction as long substrate was present. The ratio of substrate to hydrogenation product after 3 h reaction time remained the same after a second equivalent of substrate was added and the reaction was continued for another 3 h. When the substrate was consumed deactivation of the catalyst was observed. The second equivalent of substrate was not converted when added after complete consumption of the olefin (entry 4).

1.4.3 Hydrogenation of Unfunctionalized Olefins with a Ferrocenephospholane-Pyridine-Iridium Complex

In an analogy to *Crabtree's* catalyst $[\text{Ir}(\text{PCy}_3)\text{Py}(\text{cod})]\text{PF}_6$, which has been described to efficiently hydrogenate unfunctionalized olefins,^[2] the corresponding iridium phospholane complex **75** was prepared (Scheme 1.44). BAr_F was chosen as the counterion since it has been proven to increase the stability of *Crabtree's* catalyst.^[3]



Scheme 1.44. Preparation of a P,N-iridium complex.

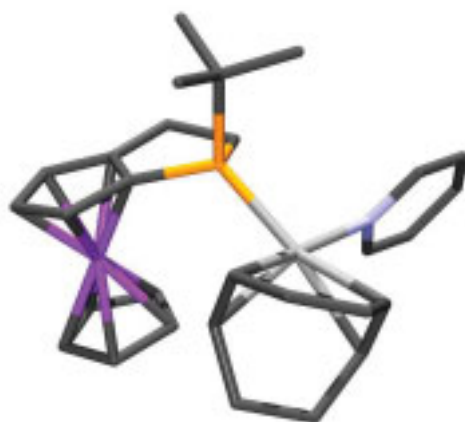


Figure 1.51. Crystal structure of **75**. A second molecule in the unit cell and the BAr_F counterions are omitted for clarity.

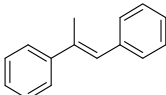
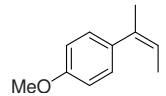
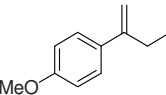
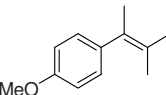
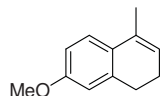
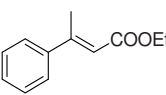
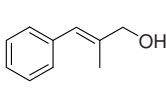
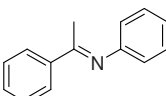
Addition of one equivalent **6** to $[\text{Ir}(\text{Py})_2(\text{cod})]\text{BAr}_\text{F}$ ^[3] gave the complex **75** in 66% yield. In analyzing the complex by NMR-spectroscopy it was not possible to detect all of the expected signals. The phosphorus absorption was hardly visible, in the ^{13}C -NMR-spectrum several signals were missing, and in the proton spectrum the intensities did not fit. Carrying out the measurement at higher temperature improved the spectra. The phosphorus signal was still broad but clearly visible and the ^1H -NMR-spectrum could be properly interpreted. However,

there were still peaks missing in the carbon spectrum. Despite these problems, all other analytical data supported the expected product and the structure was finally confirmed by X-ray analysis (Figure 1.51).

Attempts to synthesize derivatives with different aromatic nitrogen donors or with phospholane **39** failed.

Complex **75** was then tested in the hydrogenation of olefins and the results are shown in Table 1.39.

Table 1.39. Hydrogenation of olefins using complex **75**.

Entry ^a	Substrate	conv. [%] ^b	ee [%] ^c
1		>99	12 (<i>R</i>)
2		90	5 (<i>R</i>)
3		>99	rac.
4		0	n.d.
5		>99	11 (<i>S</i>)
6		95	15 (<i>R</i>)
7		>99	10 (–)
8		>99	25 (<i>S</i>)

^aThe reactions were carried out in CH₂Cl₂ with 1 mol% **75** under 50 bar H₂ at rt for 2 h. ^bDetermined by GC. ^cDetermined by chiral GC or chiral HPLC.

Complex **75** showed good activity in the catalytic hydrogenation of trisubstituted double bonds, with or without an additional functional group. The selectivities were generally low and the tetrasubstituted olefin tested was not hydrogenated under these conditions (entry 4).

1.4.4 Conclusions

The hydrogenation of various substrates with iridium complexes derived from the ferrocenephospholanes **6** and **39-42** proceeded efficiently with usually at least one combination of different metal sources and solvents. The isolated complexes **67-71** were superior to the *in situ* formed precatalysts in terms of activity. The enantioselectivities were generally low to moderate with 71% *ee* being the best result achieved in the reduction of methyl acetamidocinnamate with the isolated iridium complex **67**.

The results in the Ir-catalyzed hydrogenation of functionalized olefins were inferior to the selectivities achieved with rhodium as reported in Chapter 3. These findings are in agreement with the general trend reported in the literature where for the hydrogenation of the functionalized olefins tested herein, complexes derived from rhodium or ruthenium are usually the catalysts of choice. Therefore only a few reports have been published dealing with the iridium-catalyzed hydrogenation of these substrates and the basis for comparison of the results obtained is narrow. For example, with sugar-derived diphosphite ligands the hydrogenation of methyl acetamidoacrylate proceeded with 78% *ee*,^[4] methyl acetamidocinnamate was reduced with 35% *ee* and itaconic acid gave a hydrogenation product of 54% *ee*.^[5] Compared to these results, the iridium-ferrocenephospholane catalysts were of comparable activity and selectivity and actually superior in the case of methyl acetamidocinnamate (77% *ee*).

The phospholane-pyridine-iridium complex **75**, a chiral analogue of *Crabtree's* catalyst, was synthesized and found to form an active but unselective catalyst for the hydrogenation of unfunctionalized trisubstituted olefins.

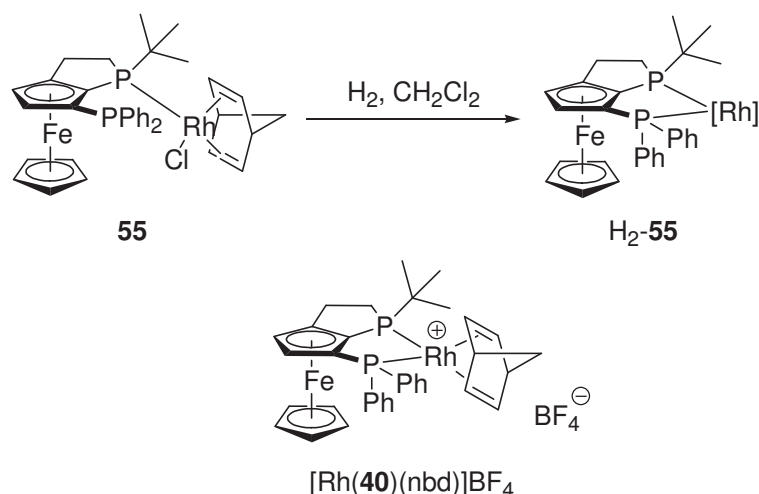
1.4.5 References

- [1] For example see: a) T. Imamoto, N. Iwadate, K. Yoshida, *Org. Lett.* **2006**, *8*, 2289-2292; b) H.-U. Blaser, W. Brieden, B. Pugin, F. Spindler, M. Studer, A. Togni, *Topics in Catalysis* **2002**, *19*, 3-16.
- [2] R. H. Crabtree, H. Felkin, G. E. Morris, *J. Organomet. Chem.* **1977**, *141*, 205-215.
- [3] B. Wüstenberg, A. Pfaltz, *Adv. Synth. & Catal.* **2008**, *350*, 174-178.
- [4] E. Guimet, M. Diéguez, A. Ruiz, C. Claver, *Tetrahedron: Asymmetry* **2004**, *15*, 2247-2251.
- [5] O. Pàmies, G. Net, A. Ruiz, C. Claver, *Eur. J. Inorg. Chem.* **2000**, 1287-1294.

1.5 Properties of Ferrocenephospholane-Complexes

1.5.1 X-Ray Observations

As described in Chapter 3.1, a chelated Rh-complex was formed when **55** was exposed to a hydrogen atmosphere (Scheme 1.44). Additionally, the complex formed of **40** and $[\text{Rh}(\text{nbd})_2]\text{BF}_4$ was also shown to have both phosphorus atoms coordinated to the metal center.



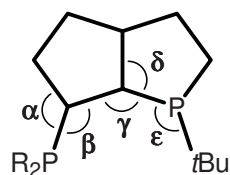
Scheme 1.44. Formation of chelate complexes with ligand **40**.

Looking at the crystal structure of **55** it is apparent that, in order to chelate the rhodium atom, the ligand has to undergo conformational change. Assuming that the picture in Figure 1.52 represents the lowest energy arrangement, the binding vector of the phospholane lone pair does not directly allow the second phosphine to coordinate. Comparing **55** and the free ligand **40**, the conformation of the ferrocene moiety is essentially the same. The chelated complexes in Scheme 1.44 must therefore contain a certain conformational strain to bring both phosphorus atoms into binding distance with the metal center.



Figure 1.52. Crystal structure of **55**. A second molecule in the unit cell is omitted for clarity.

This conformational strain can qualitatively be seen in the solid state structures of the phospholane Ir-complexes introduced in Chapter 4.2. Comparing the bond angles of the free ligand and its iridium complex the geometrical change is apparent (Table 1.40 and Figure 1.53).

Table 1.40. Selected bond angles and differences (Δ) in ferrocenephospholanes and their Ir-complexes.^[a]


	α [°]	β [°]	γ [°]	δ [°]	ϵ [°]
	128.59(18)	124.79(16)	137.51(17)	113.54(16)	104.22(10)
	140.11(18)	112.92(15)	129.46(15)	117.31(17)	110.18(11)
Δ	+11.52(36)	-11.87(31)	-8.05(32)	+3.77(33)	+5.95(21)
	128.32(12)	124.82(13)	138.23(13)	113.28(12)	103.82(8)
	143.93(12)	111.29(10)	130.08(10)	116.81(13)	110.67(7)
Δ	+15.61(24)	-13.53(23)	-8.15(23)	+3.53(25)	+6.85(15)

^aExperimental error in parentheses.

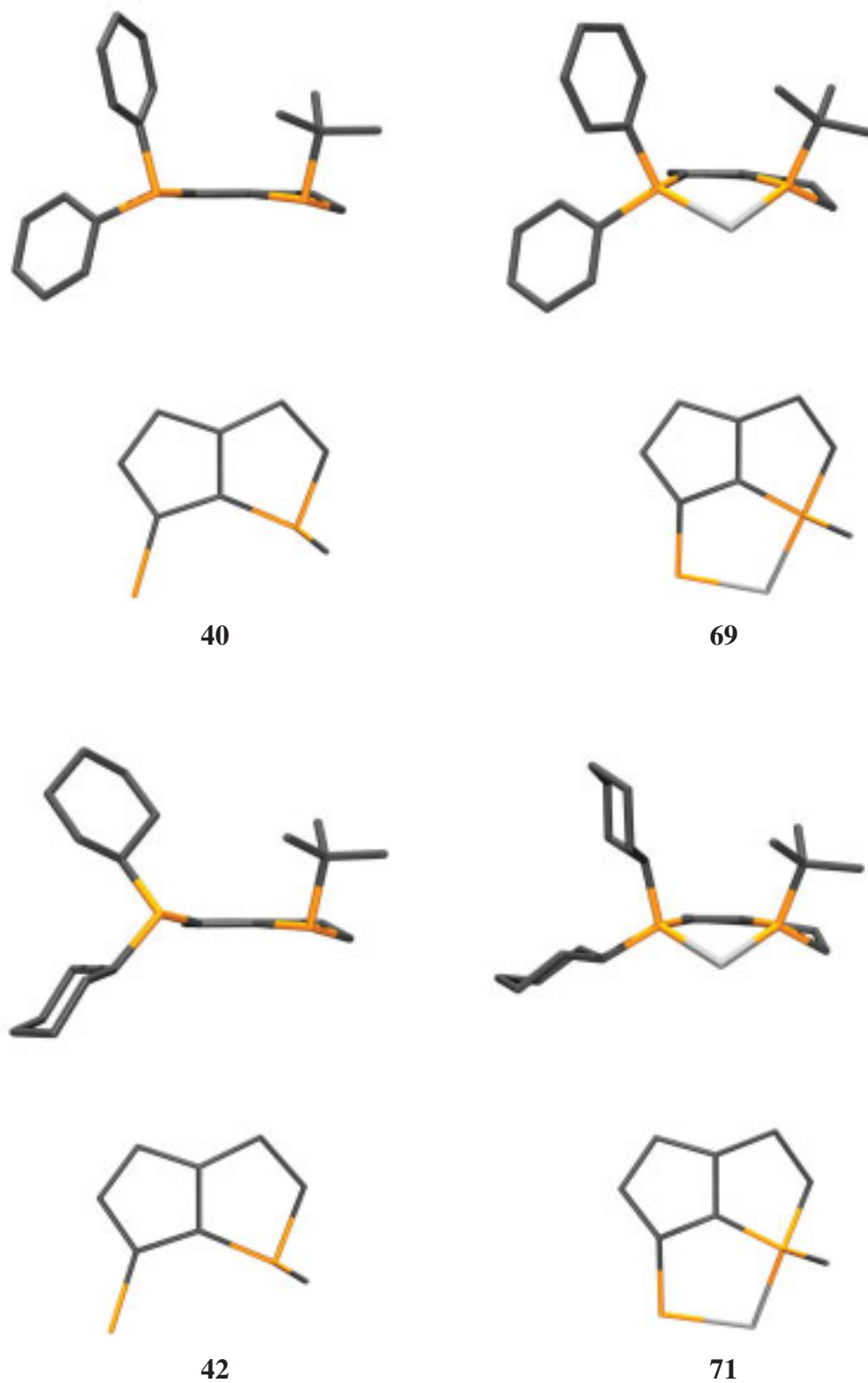


Figure 1.53. Representations of the substituted cyclopentadienyl ring of selected ferrocenephospholanes (left) and their complexes (right).

Upon complexation, several angles change. The greatest difference was observed by looking at the geometry of the bond between the cyclopentadienyl ring and the R₂P-substituent (angles α and β). The introduction of the metal distorted the bond angles by 12-15 degrees. This also influenced the conformation of the aromatic five-membered ring, as seen in the bonding angle between the cyclopentadienyl-plane and the connected groups. In the iridium complexes, all substituents exhibit a bending in direction of the the second cyclopentadienyl ring. The free ligands show distinct differences, such as in **40** which has an almost perfect planarity and in **42** the dicyclohexylphosphino group was even tilted above the aromatic plane.

The conformational change on the phospholane is less strong but still significant. The phosphorus atom shows a shift towards the R₂P-substituent of 8 degrees in both systems (γ). The equal value of γ and the smaller contribution to the overall distortion derive most likely from the rather rigid phospholane ring. The *tert*-butyl substituent is displaced towards the metal center (ϵ) and the phospholane ring is generally less planar than in the free ligand. The bond lengths remain mostly unchanged within experimental error, except for the bond between the phosphorus substituted carbon atoms on the cyclopentadienyl ring which shortens about 3% after coordination of the metal. All these observations showed that the ligand has to reduce its bite angle in order to chelate.

Although the chelate complexes have been identified in the solid state by X-ray crystallography and in solution by NMR, the high degree of ligand distortion in the Ir-complexes despite their rigidity has raised the question whether these complexes are labile regarding the binding mode.

1.5.2 Competition Experiments in Solution

The stability of the phospholane iridium complexes was briefly evaluated by a low level single point DFT calculation (B3LYP/6-311++g(d,p), Gaussian G03) in which the conformation of the free phospholane ligand was compared with its Ir-complex. The energy difference turned out to be 178 kJ/mol for the phenyl derivative and 185 kJ/mol for the cyclohexyl analogue. If this energy difference is comparable with the dissociation energy of a phosphine-iridium bond the chelate complex might open under certain conditions. References for such energy values are very rare. Calculated phosphine ligand dissociation energies for [CpM(L)(PH₃)]-type complexes add up to 121 kJ/mol (M = Rh, L = CO), 132 kJ/mol (M = Rh, L = PH₃), 134 kJ/mol (M = Ir, L = CO) and 138 kJ/mol (M = Ir, L = PH₃).^[1] Although these values correspond to a completely different system, they are situated in the vicinity of the calculated energy differences.

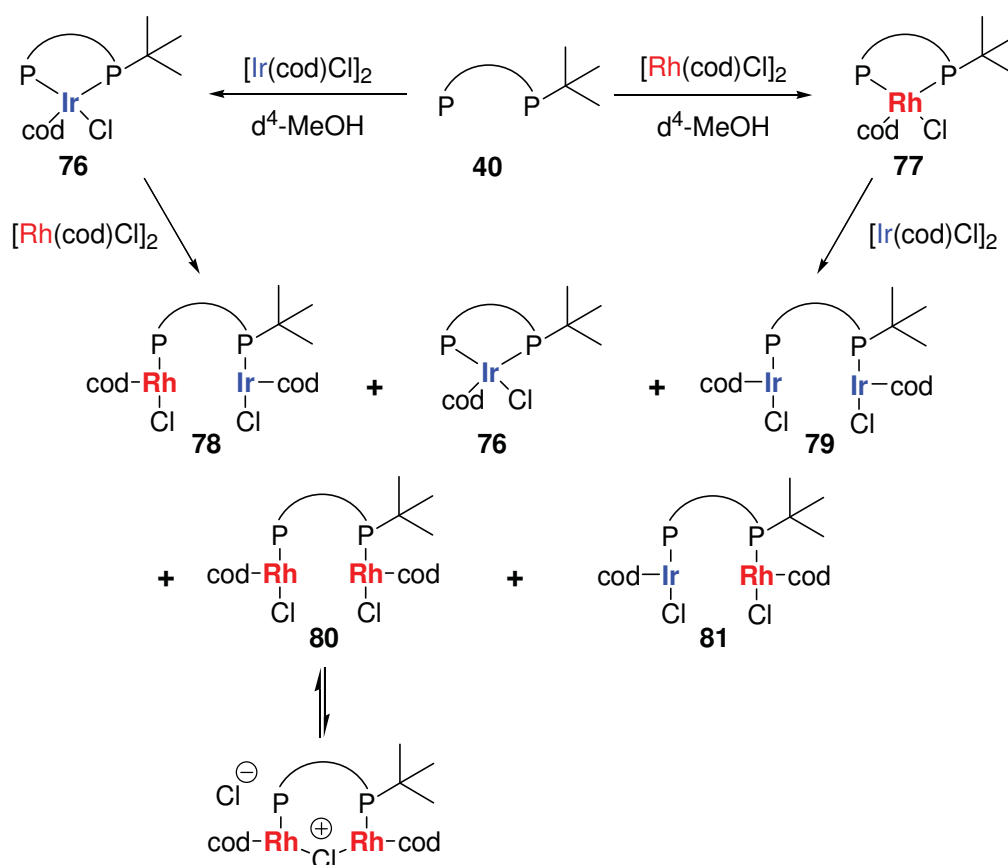
1.5.2.1 Competition Experiments in Methanol

To confirm the potential lability of the complexes formed, phospholane **40** was allowed to react consecutively with suitable rhodium and iridium compounds. The identification of the resulting complexes was performed by ³¹P-NMR spectroscopy. Upon complexation, the chemical shift of the coordinated phosphorus atom is displaced 40-50 ppm downfield and the two metals can be distinguished by the metal-phosphorus coupling constant, which is 150-170 Hz for rhodium and non-existent for iridium.

Initial experiments showed the formation of chelate complexes with [M(cod)₂]BAR_F in dichloromethane and [M(diene)Cl]₂ in methanol (M = Rh, Ir). Due to the commercial availability of the chlorodimers the reactions were carried out in detail with these metal sources.

The results of these experiments are summarized in Scheme 1.45 and Table 1.41. When either [Ir(cod)Cl]₂ or [Rh(cod)Cl]₂ were reacted with **40** in methanol the chelated complexes **76** or **77** were formed. These individual solutions were then treated with one equivalent of the other metal source. Independent of the addition sequence the final reaction mixture consisted of five species. In addition to complex **76** all double-metallated ligand combinations were observed.

Notably, complex **77** was not observed in this mixture. According to the integrals in the phosphorus spectrum, complex **78** was present in about 50%, followed by **76** in roughly 20%. Finally, compounds **79**, **80** and **81** showed almost equal intensities (~10% each). The proposed metal ligand combinations were also observed by ESI-MS. The recorded masses corresponded to the depicted complexes without chloride. Notably, all signals except for that of **80** were of weak and variable intensity. Due to the fact that in ESI-MS only charged species can be observed, complexes **76**, **78**, **79** and **81** are assumed to be neutral in solution and therefore difficult to detect. Complex **80** could exist as a charged species with a dissociated chloride.



Scheme 1.45. Observed complexes from $[\text{Ir}(\text{cod})\text{Cl}]_2$ and $[\text{Rh}(\text{cod})\text{Cl}]_2$ with **40** in methanol.

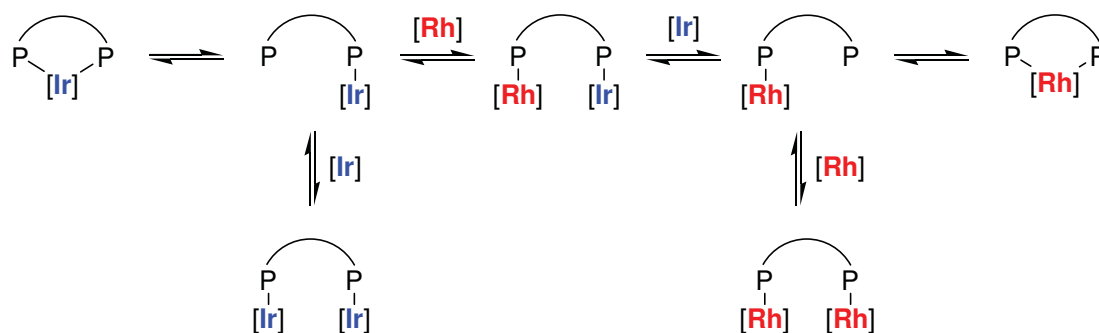
Table 1.41. ^{31}P -NMR resonances of the compounds in Scheme 5.2.

Compound	δ/ppm	Coupling constants		δ/ppm	Coupling constants	
		J_{PRh}	J_{PP}		J_{PRh}	J_{PP}
76	10.7		10 Hz	28.9		10 Hz
77	14.8	138 Hz	8 Hz	30.3	143 Hz	8 Hz
78	23.2	144 Hz	5 Hz	39.7		5 Hz
79	14.8		4 Hz	40.4		4 Hz
80	22.9	140 Hz	5 Hz	48.4	141 Hz	5 Hz
81	14.7		5 Hz	49.3	147 Hz	5 Hz
40	-22.6		15 Hz	-0.8		15 Hz

The exchange reactions took place very rapidly within a few minutes and the spectrum did not change significantly after a longer reaction time, except for a lowering in the quality due to general decomposition.

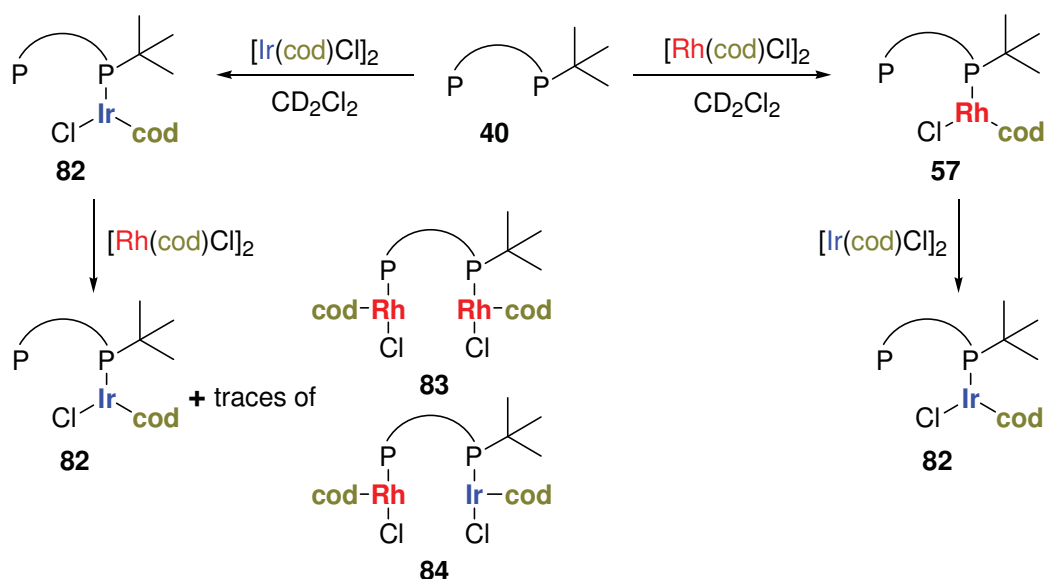
As a reference reaction, the same complexation experiments were carried out with 1,2-bis(diphenylphosphino)ethane (dppe), a flexible diphosphine ligand. In contrast to the rigid ferrocenephospholane, the chelate complexes formed from dppe were stable in solution and did not undergo metal exchange reactions.

The formation of the various metal combinations in Scheme 1.45 could be explained by reversible chelation and reversible binding of a second metal center (Scheme 1.46). The existence of several equilibria in the solution is an indication of the lability of the complexes.

**Scheme 1.46.** Assumed equilibria in methanol.

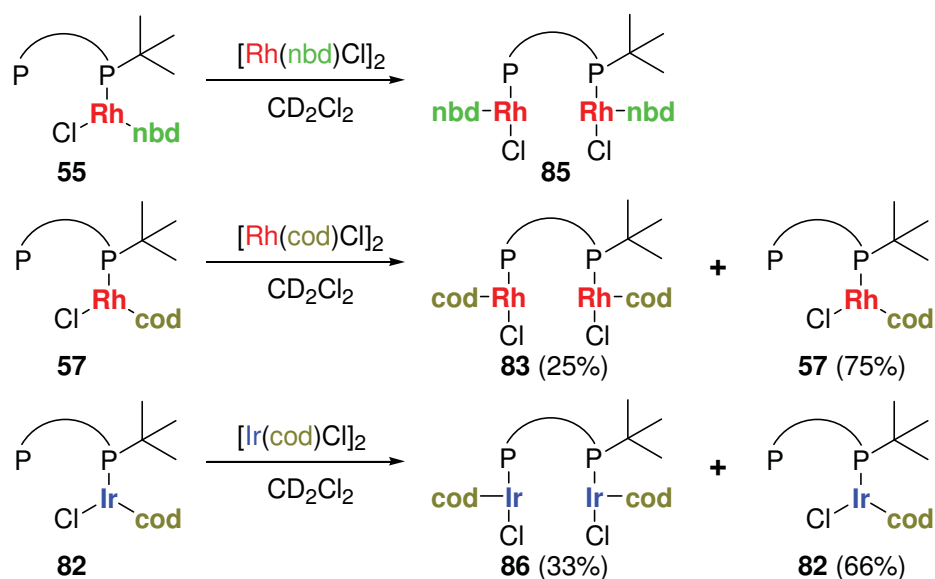
1.5.2.2 Competition Experiments in Dichloromethane

When ligand **40** was combined with the dimeric metal sources in dichloromethane the corresponding monocoordinated complexes **82** and **57** were obtained. However, after addition of the second metal source they showed a distinctly different behaviour to the reactions in methanol. Whereas the solution of **82** remained mostly unchanged upon addition of $[\text{Rh}(\text{cod})\text{Cl}]_2$ (traces of **83** and **84** were detected) the opposite reaction path led to an almost complete exchange of the metal center with only traces of starting Rh-complex **57** left (Scheme 1.47). It seemed that complexation of the phospholane with iridium is thermodynamically favoured over rhodium.



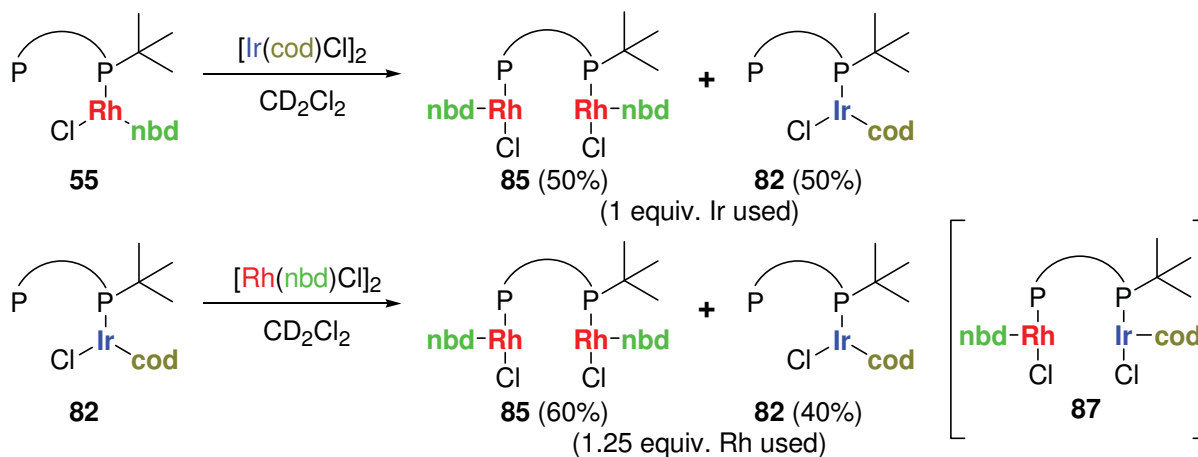
Scheme 1.47. Exchange experiment with cod-complexes in dichloromethane.

Only minor amounts of bimetallic species were detected in these experiments. However, since compounds with two different metal centers might have interesting properties, the selective formation of double metallated species in dichloromethane was investigated. The compounds were identified by ^{31}P -NMR spectroscopy and again the choice of the diene ligand in the metal precursor proved to have a crucial influence on the results (Scheme 1.48).



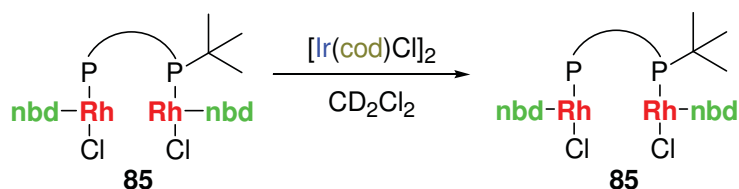
Scheme 1.48. Formation of homobimetallic species in dichloromethane. 1 equivalent of metal was added.

The reaction with the rhodium norbornadiene precursor **55** gave the bimetallic species **85** quickly and quantitatively. In the case of the 1,5-cyclooctadiene-containing metal complexes the formation of the desired products **83** and **86** was incomplete. The ratio between the two species was established within minutes and remained unchanged after several hours. The ratios of 1:3 (**83**:**57**) and 1:2 (**86**:**82**) seemed to reflect the thermodynamic equilibrium distributions, which would imply the complexation to be reversible at least in the case of the 1,5-cyclooctadiene complexes. The difference in complexation behaviour between norbornadiene and 1,5-cyclooctadiene was presumably due to sterics.



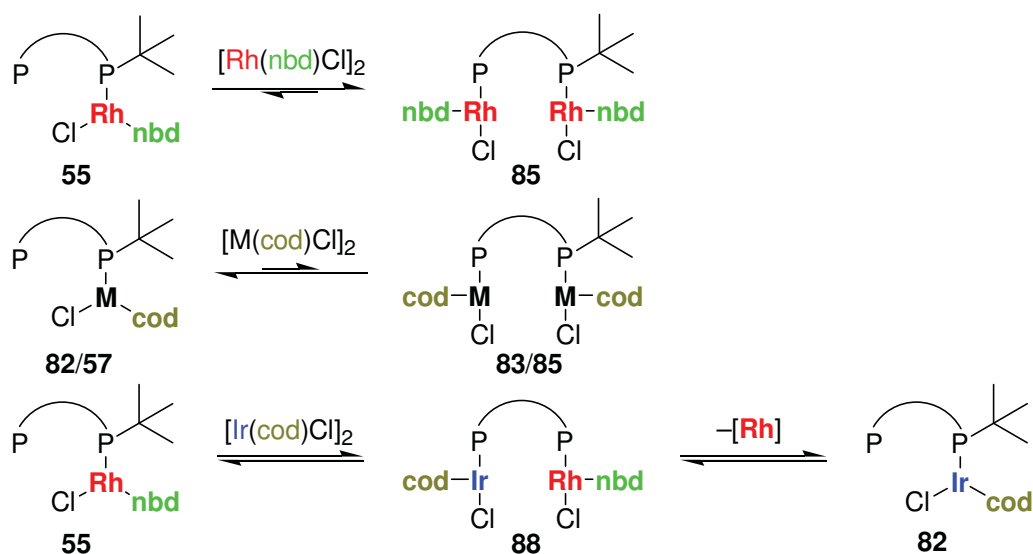
Scheme 1.49. Exchange experiments with cod- and nbd-complexes.

The most interesting experiments proved to be the combination of rhodium-norbornadiene and iridium-1,5-cyclooctadiene complexes (Scheme 1.49). In contrast to the reaction in Scheme 1.47, where a complete metal exchange was observed, the reaction of the monocoordinated Rh-norbornadiene complex **55** with $[\text{Ir}(\text{cod})\text{Cl}]_2$ gave **82** and **85** in equal amounts. The inverse reaction was carried out with a small excess of $[\text{Rh}(\text{nb})\text{Cl}]_2$ to force the heterobimetallic species to form. But instead of the expected mixed complex, again the bis-rhodium complex **85** was formed. Besides the two complexes shown, the heterobimetallic species could be detected in minor amounts but disappeared upon longer reaction time. Presumably, this Rh-Ir-phospholane complex **87** was just an intermediate in the formation of the bis-rhodium compound **85**. The final ratio of 3:2 was roughly consistent with the theoretically maximal possible amount of bis-rhodium complex to be formed. Complex **85** generally seemed to be a favoured species since it was also observed in the maximal possible amount after addition of $[\text{Ir}(\text{cod})\text{Cl}]_2$. Additionally, **85** was almost inert towards the addition of $[\text{Ir}(\text{cod})\text{Cl}]_2$ (Scheme 1.50). Also like complex **80** in Scheme 1.45, it could exist as a bimetallic cation with a dissociated chloride. This overall positive charge would impede the association of any electrophilic metal species and explains its stability in solution.



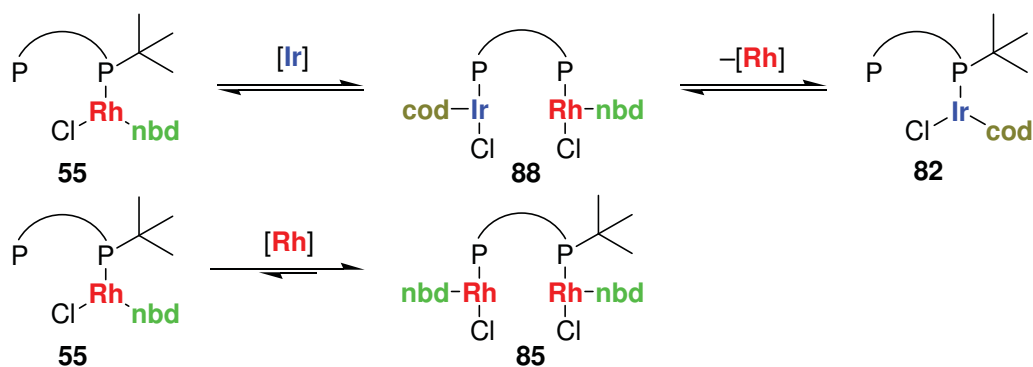
Scheme 1.50. Stability of the bimetallic rhodium-nbd complex.

Again, the reference experiment with dppe as ligand was carried out and did not show metal exchange or the formation of bimetallic complexes. Moreover, this ligand even formed a chelate complex in dichloromethane.



Scheme 1.51. Proposed equilibria in dichloromethane.

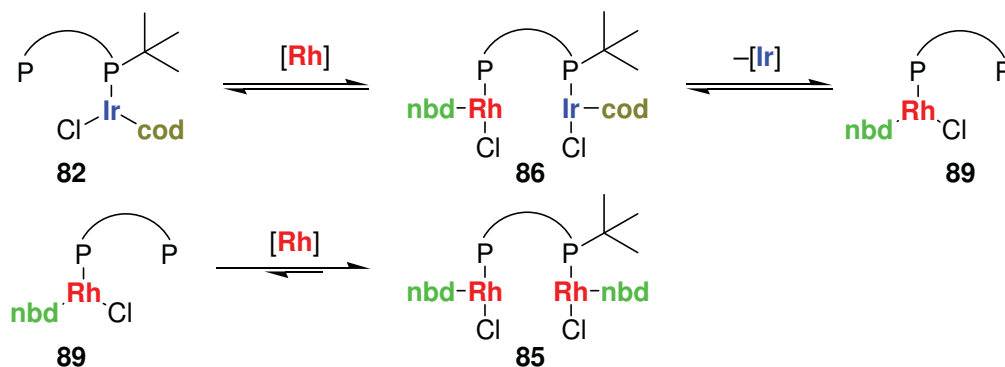
The products formed in the metal exchange experiments can be explained by two assumptions (Scheme 1.51). First, the complexation of a second metal center is favourable with the Rh-norbornadiene complex **55** but unfavourable with 1,5-cyclooctadiene complexes **82** and **57**. Second, the combination of rhodium-norbornadiene and iridium-1,5-cyclooctadiene forms a heterobimetallic species **88** from which either iridium or rhodium can dissociate to form the monocoordinated complex. With these assumptions, the formation of the products in Scheme 1.49 was rationalized as follows.



Scheme 1.52. Addition of $[\text{Ir}(\text{cod})\text{Cl}]_2$ to **55**. **88** was not detected.

When $[\text{Ir}(\text{cod})\text{Cl}]_2$ is added to the monometallic rhodium complex **55** the heterobimetallic compound **88** forms, from which dissociation of rhodium or iridium is possible (Scheme

1.52). In the case of the dissociation of a rhodium center, the observed iridium complex **82** is formed and the expelled rhodium species itself reacts quickly with the starting material to form the stable homobimetallic complex **85**. This reaction pathway is in accordance with the observed product ratio, since every rhodium atom would end up in the bimetallic complex **85**, only half of the starting material can be converted to the iridium compound.



Scheme 1.53. Addition of $[\text{Rh}(\text{nbd})\text{Cl}]_2$ to **82**. **89** was not detected.

In Scheme 1.53 the reaction sequence for the addition of $[\text{Rh}(\text{nbd})\text{Cl}]_2$ to the monocoordinated iridium complex is shown. The formation of the heterobimetallic compound **86** again is the first step, followed by metal dissociation. The resulting monocoordinated rhodium complex **89** is trapped by another Rh-norbornadiene compound until all rhodium has been consumed. With equal amounts of rhodium and iridium a 1:1 mixture of both products would be expected. With the 1.25 equivalents of rhodium applied, the maximum possible ratio is calculated to be 62.5% of bimetallic complex **85** and 37.5% of starting material **82**, which is in good agreement with the observed data (60:40).

The spectroscopical data for the complexes observed in dichloromethane are summarized in Table 1.42. The individual compounds can be distinguished by the chemical shifts and the coupling constants.

Table 1.42. ^{31}P -NMR resonances of the observed complexes in dichloromethane.

Compound	δ/ppm	Coupling constants		δ/ppm	Coupling constants	
		J_{PRh}	J_{PP}		J_{PRh}	J_{PP}
55	-18.1		4 Hz	50.9	172 Hz	4 Hz
82	-16.3		5 Hz	39.7		5 Hz
57	-16.9		5 Hz	48.6	152 Hz	5 Hz
83	26.4	145 Hz	5 Hz	52.0	143 Hz	5 Hz
84	26.7	141 Hz	5 Hz	43.2		5 Hz
85	28.3	167 Hz		50.9	167 Hz	
86	18.4			43.9		
87	29.4	160 Hz	4 Hz	41.9		4 Hz

Reactions shown in Scheme 1.47 and 1.49 involve the liberation of rhodium- or iridium-species which do not end up in the final ferrocenephospholane products. The final nature of these species is unknown. Regeneration of $[\text{Rh}(\text{nbd})\text{Cl}]_2$ or $[\text{Ir}(\text{cod})\text{Cl}]_2$ is possible, as well as non-selective decomposition.

1.5.3 Conclusions

The structure of the ferrocenephospholanes and their iridium complexes were compared and discussed. A structural distortion of the ligand upon complexation was identified and roughly quantified by a DFT calculation.

The suspected lability of the chelate complexes was confirmed by metal exchange experiments. In methanol, chelation occurred with $[\text{Rh}(\text{cod})\text{Cl}]_2$ and $[\text{Ir}(\text{cod})\text{Cl}]_2$ which has not been seen in dichloromethane. The existence of several equilibria and the presence of bimetallic species could be observed in methanol. The formation of bimetallic ferrocenephospholane complexes in dichloromethane was dependent on the metal source employed. $[\text{Rh}(\text{nbd})\text{Cl}]_2$ was able to form the homobimetallic complex quantitatively, whereas with $[\text{Rh}(\text{cod})\text{Cl}]_2$ and $[\text{Ir}(\text{cod})\text{Cl}]_2$ the corresponding compounds were only partially generated. This might originate from the larger steric demand of the 1,5-cyclooctadiene ligand as compared to norbornadiene. Interestingly, this effect seemed only to be significant in dichloromethane, whereas in methanol the formation of bimetallic species is not impeded by the size of the 1,5-cyclooctadiene ligand. Heterobimetallic compounds could not be selectively synthesized, since the presence of the cod-containing iridium center disfavoured the coordination of an additional nbd-rhodium unit. Instead, the involved equilibria drove the reaction towards the formation of the homobimetallic compound consisting of two rhodium centers.

The lability seen in the exchange experiments could influence the performance of these complexes as catalysts in hydrogenation reactions. With the possible dissociation of one phosphorus atom from the metal center during the catalytic cycle, the involvement of several catalytically active species cannot be excluded.

1.5.4 References

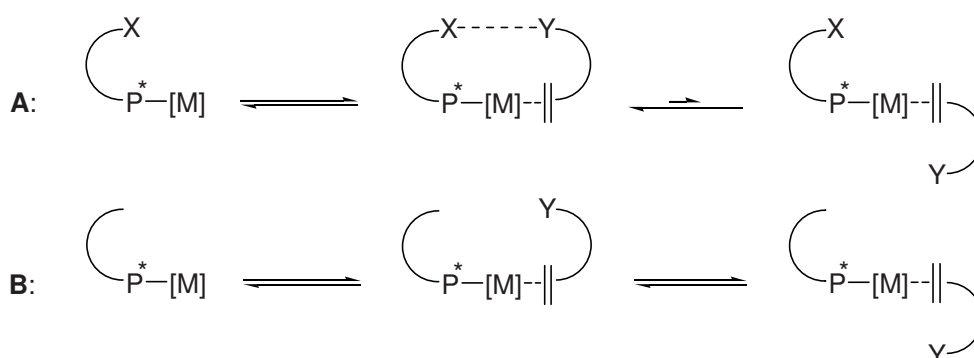
- [1] T. Ziegler, V. Tschinke, L. Fan, A. D. Becke, *J. Am. Chem. Soc.* **1989**, *111*, 9177-9185.

Chapter 2

Phosphines with Additional Functional Group as Ligands in Catalysis

2.1 Introduction

Functionalizations of phosphine ligands are mainly pursued to change solubility properties^[1] or to tune the reactivity of the corresponding catalytically active metal complexes. In the latter case, the additional functional groups generally have two ways to influence the performance of the catalyst. They can either change the conformation of the complex or interact with the substrate.^[2] The concept of secondary interactions in catalysis is depicted in Scheme 2.1. A substrate, for example an olefin, with a functional group should be able to interact with a suitable substituent on the ligand of the complex. Besides the steric stereodifferentiation coming from the chirality of the ligand, this would allow for a second means of directing the coordination of the substrate (equation A).

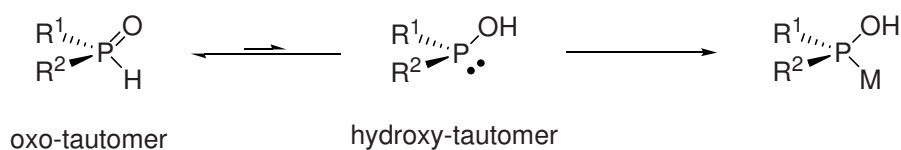


Scheme 2.1. Catalyst-substrate complexes with (A) and without (B) secondary interactions.

2.1.1 Secondary Phosphine Oxides

2.1.1.1 Properties of Secondary Phosphine Oxides

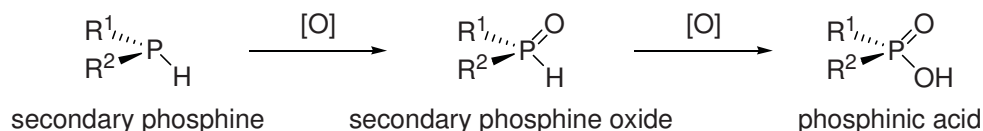
In solution, secondary phosphine oxides (SPO) exist in equilibrium with their tautomeric hydroxy-forms, also called phosphinous acids (Scheme 2.2).^[3] At room temperature the oxo-tautomer predominates, but the equilibrium can be shifted towards the trivalent hydroxy-tautomer by either the presence of electronegative substituents^[4] or coordination of a transition metal.^[5]



Scheme 2.2. Tautomeric forms of secondary phosphine oxides.

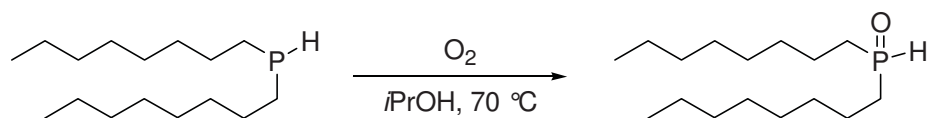
Having two different substituents (R^1 and R^2), the phosphorus atom in the secondary phosphine oxide becomes a stereogenic center. The individual enantiomers are configurationally stable in solution,^[6] and moreover they retain the chiral information upon coordination to a metal center.^[7]

Secondary phosphine oxides stand, in terms of oxidation state, in between the secondary phosphines and the phosphinic acids (Scheme 2.3).



Scheme 2.3. Oxidation products from secondary phosphines.

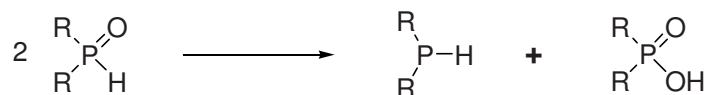
The oxidation of secondary phosphines proceeds with a variety of oxidants, including molecular oxygen; the cause of their notorious air-sensitivity. Secondary phosphine oxides can also undergo oxidation with many oxidation reagents to give phosphinic acids. However, the reaction with dioxygen is rather slow, making these compounds quite air stable. This property is also apparent in an early preparation of secondary phosphine oxides (Scheme 2.4).



Scheme 2.4. Early preparation of secondary phosphine oxides.

The reaction of dioctylphosphine with oxygen gives the secondary phosphine oxide without the formation of the phosphinic acid.^[8]

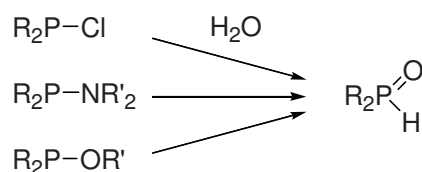
When secondary phosphine oxides are heated above 180 °C they decompose within a few minutes to the corresponding phosphinic acids and phosphines, even under inert atmosphere (Scheme 2.5). This reaction is rather slow at room temperature but might also depend on the substituents at the phosphorus atom.^[9]



Scheme 2.5. Self-disproportionation of secondary phosphine oxides.

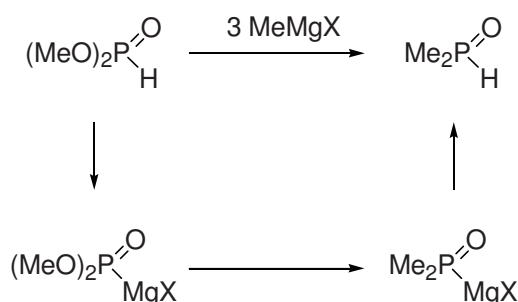
2.1.1.2 Synthesis of Secondary Phosphine Oxides

Besides the direct oxidation of secondary phosphines, which usually has the disadvantage of possible over-oxidation (Scheme 2.3), several methods for the selective synthesis of secondary phosphines have been developed. The hydrolysis of phosphine chlorides, aminophosphines or phosphinites is a general procedure for the formation of secondary phosphine oxides (Scheme 2.6).^[6]



Scheme 2.6. Synthesis of secondary phosphines by hydrolysis of suitable precursors.

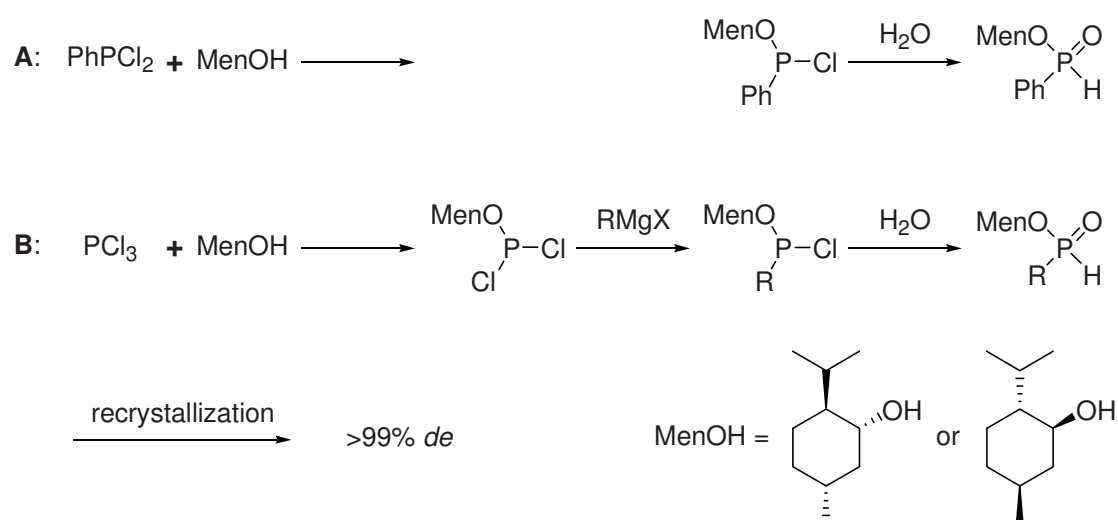
The addition of organometallic compounds to phosphite esters represents a further method for the formation of secondary phosphine oxides. The application of this reaction was used for the first synthesis of dimethylphosphine oxide (Scheme 2.7).^[10]



Scheme 2.7. Nucleophilic addition of a methyl *Grignard* reagent to dimethyl phosphite.

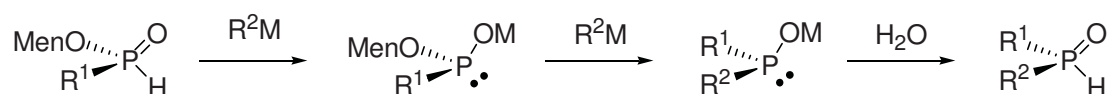
The transformation requires three equivalents of methylmagnesium reagent, where one equivalent first reacts with the weakly acidic proton. Replacement of both alkoxy groups then leads to the secondary phosphine oxide.

As mentioned above, secondary phosphine oxides can occur as chiral molecules, therefore the isolation of the enantiomerically pure compounds has been a topic of research.^[11] Aside from the separation of racemic material by HPLC on a chiral stationary phase,^[12] the resolution into the enantiomers has also been achieved by crystallization.^[13] Only recently have stereoselective syntheses been described.^[14] In most cases, these synthetic methods involve the addition of nucleophiles to enantiomerically pure phosphinates.^[14b-d] These phosphinates are commonly obtained in pure form by fractional crystallization of the diastereoisomeric menthyl derivatives. Two variations of this procedure are shown in Scheme 2.8.



Scheme 2.8. Preparation of enantiomerically pure menthyl phosphinates.

The synthesis of menthyl phenylphosphinate (method A) starts from phenylphosphine dichloride.^[15] Addition of enantiomerically pure menthol followed by hydrolysis gives the diastereomeric phosphinates which are separated by crystallization. A more general approach begins with the synthesis of menthyl phosphordichloridite (method B). Addition of one equivalent of organomagnesium reagent and subsequent hydrolysis again gives the phosphinates as a diastereoisomeric mixture, which are then separated by crystallization.^[16] The diastereoisomerically pure phosphinates can then undergo diastereoselective reactions with organometallic compounds (Scheme 2.9).^[14b-d]

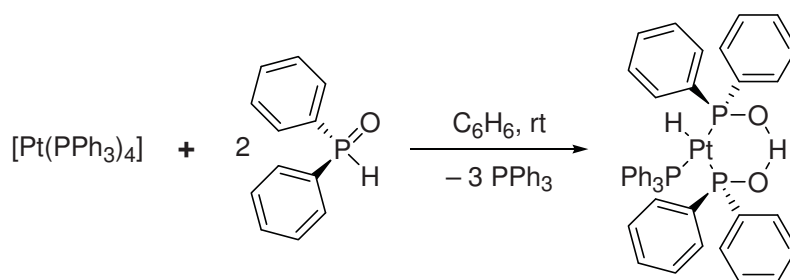


Scheme 2.9. Stereoselective addition of organometallic compounds to menthyl phosphinates.

The addition of an organometallic reagent to menthyl phosphinates generates the alkylation or arylation product with inversion of configuration. In general, two equivalents of the organometallic species are needed, although the transformation employing one equivalent has been reported under certain conditions.^[14d] The first equivalent deprotonates the weakly acidic proton leading to a metalated phosphinate which then undergoes the substitution reaction with the second equivalent of nucleophile expelling the menthol substituent. Tautomerization through hydrolysis gives the secondary phosphine oxide. The diastereoselectivities depend on the organometallic reagent employed but usually the products are obtained in 80-99% *ee* starting from diastereoisomerically pure phosphinates.^[14b-d] In the cases of reduced selectivity, the loss of optical purity was attributed to partial isomerization of the phosphinate starting material under the reaction conditions. Traces of metal alkoxides, even the expelled mentholate, are able to isomerize the phosphinate by transesterification under unoptimized reaction conditions.^[14c]

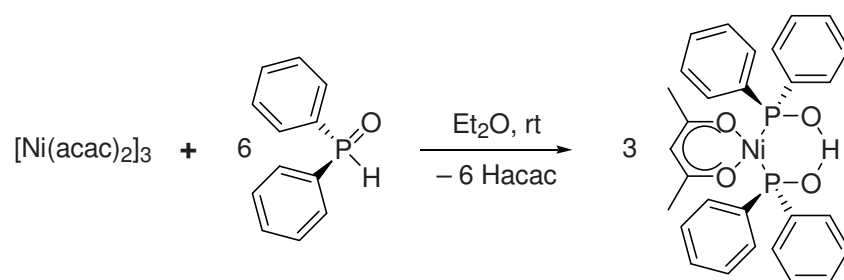
2.1.1.3 Metal Complexes

Secondary phosphine oxides readily undergo reactions with transition metals forming the corresponding coordination compound. Tetrakis(triphenylphosphine)platinum reacts with diphenylphosphine oxide to form a platinum hydride complex (Scheme 2.10).^[17]



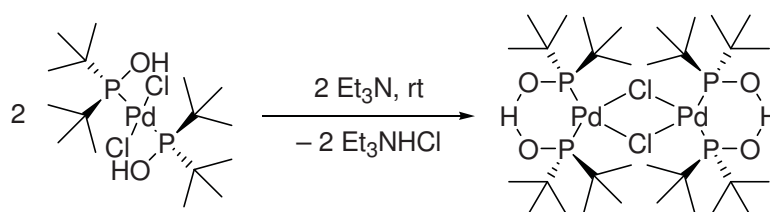
Scheme 2.10. Synthesis of a platinum complex.

A similar reaction was reported with tris(bisacteylacetate)nickel leading to a 2:1 complex (Scheme 2.11).^[18]



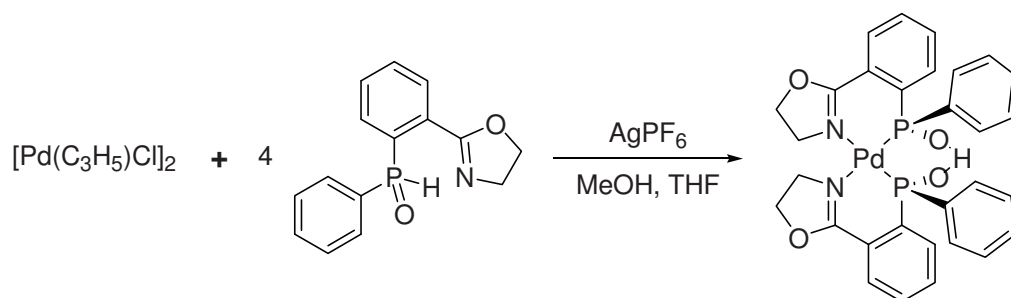
Scheme 2.11. Synthesis of a nickel complex.

A dimeric palladium complex with di(*tert*-butyl)phosphine oxide ligands has been prepared by deprotonation of the monomeric palladium complex synthesized from the secondary phosphine oxide and cyclooctadienedichloropalladium (Scheme 2.12).^[19]



Scheme 2.12. Synthesis of a dimeric palladium complex.

A complex with a bidentate ligand has also been described. Complexation of allylpalladium chloride dimer with an oxazoline-containing secondary phosphine oxide, followed by anion exchange with silver hexafluorophosphate gave the palladium complex shown in Scheme 2.13.^[20] Notably, the complex crystallizes as a neutral species, since the deprotonation of one secondary phosphine oxide balances out the positive charge on palladium.



Scheme 2.13. Synthesis of a bis-P,N-palladium complex.

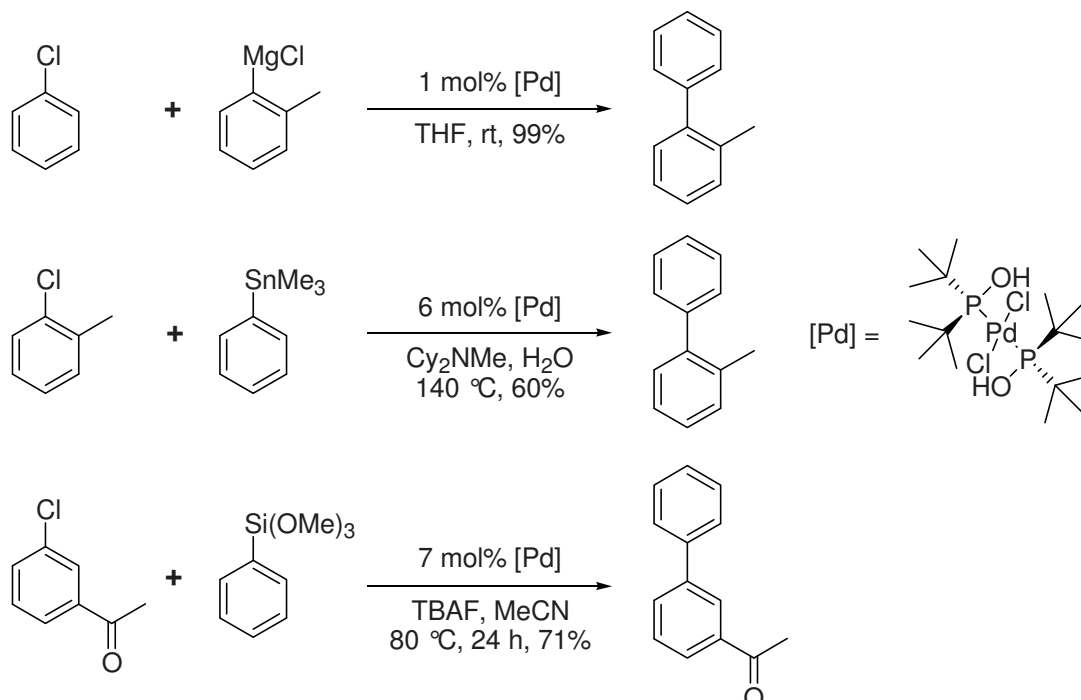
As general observations it can be noted that the secondary phosphine oxides bind to transition metals via the phosphorus center rather than via the oxygen atom. Moreover, they have the tendency to associate through hydrogen bonding, forming a chelate-like complex.

2.1.1.4 Application in Catalysis

Due to their simple preparation, at least in the case of racemic or achiral compounds, and their stability towards moisture and air, secondary phosphine oxides have found applications in catalysis.^[21]

The first example was a platinum-catalyzed hydroformylation reported by *van Leeuwen*.^[22] Complexes of secondary phosphine oxides with platinum have also been used to catalyze nitrile hydrolysis.^[23]

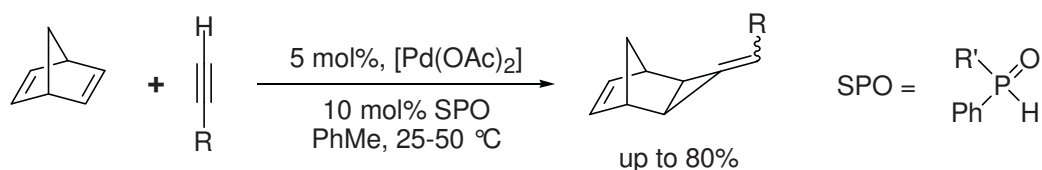
Secondary phosphine oxides in combination with palladium have been widely applied to cross-coupling reactions. Besides *Suzuki*-couplings with aryl chlorides,^[19] *Kumada*,^[24] *Negishi*,^[19b] *Stille*^[25] and *Hiyama*^[26] cross-coupling reactions have been performed. In some cases the use of secondary phosphine oxide palladium complexes allowed the reactions to be carried out in water.^[26b, 27] Moreover, *Sonogashira*^[28] and *Heck*^[25, 29] reactions as well as *Buchwald-Hartwig* aminations^[29] were performed with catalysts consisting of secondary phosphine oxides.



Scheme 2.14. Examples of cross-coupling reactions employing SPO-Pd-complexes.

Palladium complexes have also been reported to induce a formal [2+1] cycloaddition between alkenes and terminal alkynes (Scheme 2.15). With an enantiomerically pure secondary

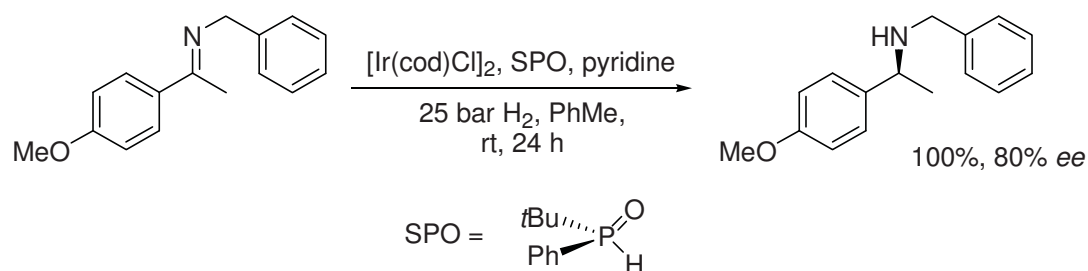
phosphine oxide an asymmetric transformation was also possible, although only with selectivities up to 60% *ee*.^[30]



Scheme 2.15. [2+1]-Cycloaddition reaction between norbornadiene and a terminal alkyne.

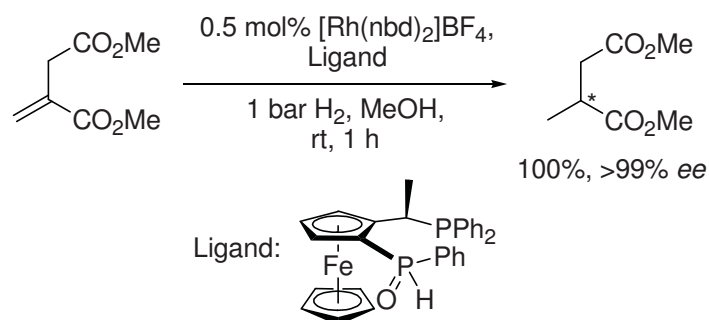
Asymmetric catalysis with chiral palladium-SPO complexes has also been achieved in allylic substitution reactions with moderate enantiomeric excess.^[7]

The asymmetric hydrogenation of imines was described using an iridium-SPO catalyst.^[9, 31] Up to 80% *ee* was achieved with enantiopure *tert*-butylphenylphosphine oxide as ligand (Scheme 2.16). However, the reaction needed 5 mol% catalyst loading and long reaction times to go to completion.



Scheme 2.16. SPO-Ir-catalyzed asymmetric hydrogenation of a ketimine.

Rhodium-SPO-complexes have been successfully applied in the hydrogenation of various substrates. Ferrocene-derived bidentate ligands with a phosphine and a SPO moiety give very selective catalysts for the reduction of, for example, dimethyl itaconate (Scheme 2.17).^[32]



Scheme 2.17. SPO-Rh-catalyzed asymmetric hydrogenation of dimethyl itaconate.

2.1.2 Miscellaneous Functionalized Phosphines

The investigation of functionalized phosphine ligands has been pursued by many research groups and a number of substituents were introduced to study their influence by different secondary interactions.

Landis and *Ito* reported the synthesis of crown-ether functionalized diphosphine ligands (Figure 2.1).^[33] The crown-ethers were supposed to form electrostatic interactions with the substrate. *Landis* examined the complexation chemistry with rhodium and found similar behaviour to the unfunctionalized system.^[33a,b] However, he did not report applications in asymmetric catalysis. *Ito* studied the application of his ligand in palladium-catalyzed allylation reactions but obtained only moderate results.^[33c]

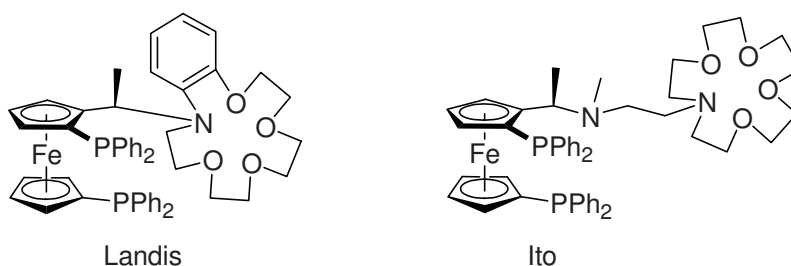


Figure 2.1. Crown-ether functionalized diphosphine ligands.

The effect of incorporated Lewis-acids has also been investigated (Figure 2.2). *Kagan* and *Jacobsen* described the synthesis of a boron analogue of DIOP^[34] but did not find an increase in enantioselectivity in the hydrogenation of dehydroamino acid derivatives.^[34a]

Landis also published the synthesis of a boron-containing diphosphine, but did not report application in catalysis.^[35]

Incorporation of titanium as a Lewis-acid in a diphosphine ligand was achieved by *Börner*, although the corresponding rhodium complex gave only poor results in the examined asymmetric hydroformylation of functionalized olefins.^[36]

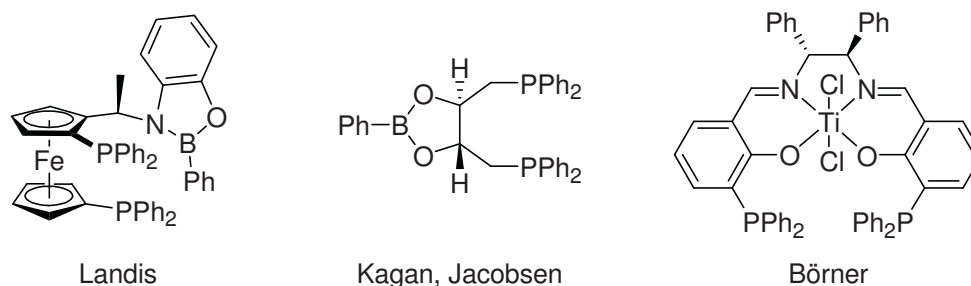


Figure 2.2. Lewis-acid functionalized diphosphine ligands.

Functionalization with hydroxyl groups, thus allowing for hydrogen bonding, was more successful in terms of catalyst performance (Figure 2.3).^[2b] *Hayashi* employed a hydroxyethyl-substituted BPPFA ligand in the palladium-catalyzed asymmetric allylation and obtained better results than with the unfunctionalized analog.^[37]

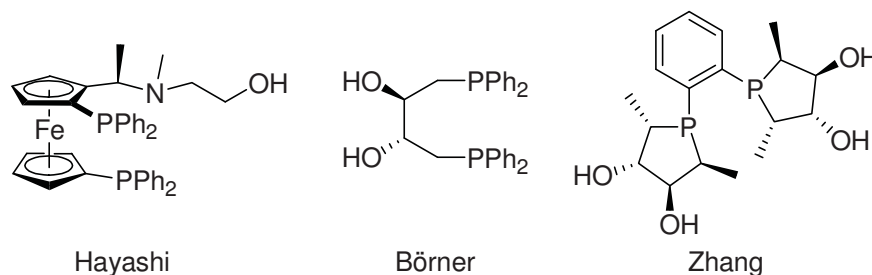


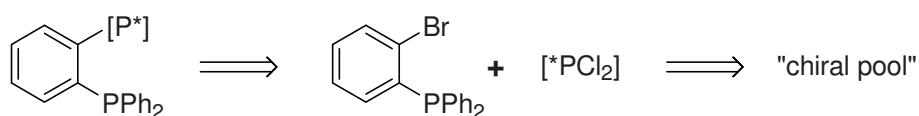
Figure 2.3. Hydroxy functionalized diphosphine ligands.

The investigation of a DIOP ligand with unprotected alcohol groups in the rhodium-catalyzed asymmetric hydrogenation of unsaturated phosphonates by *Börner* showed a substantial increase in reactivity and selectivity as compared to the methyl ether derivative.^[38]

Finally, the tetrahydroxy-RoPHOS ligand of *Zhang* was successfully applied in the hydrogenation of cinnamic acid derivatives.^[39] While the enhancement compared to the corresponding ligands with ether groups^[2b,40] is not large, enantioselectivities of up to 99% *ee* were achieved.

2.1.3 Objectives of this Work

The aim of this project was the stereoselective synthesis of diphosphine ligands with one asymmetric phosphine unit (Scheme 2.18). The introduction of the stereogenic phosphorus atom should occur via a diastereoselective addition of an organometallic species to a chiral dichlorophosphine. This reaction forms a P-chiral chlorophosphine which is then converted to a phosphine by addition of a second organometallic reagent or to a secondary phosphine oxide by hydrolysis.



Scheme 2.18. Retrosynthetic analysis of P-chiral diphosphine ligands.

It was planned to evaluate different chiral chlorophosphines for their selectivity in this addition reaction. Therefore, synthetic procedures had to be developed to convert commercially available and enantiopure starting materials into chiral phosphine dichlorides without loss of optical purity. The performance of these ligands in the rhodium-catalyzed asymmetric hydrogenation of olefins were then to be evaluated.

2.1.4 References

- [1] For example see: a) D. Sinou, *Adv. Synth. Catal.* **2002**, *334*, 221-237; b) T. Dwars, G. Oehme, *Adv. Synth. Catal.* **2002**, *334*, 239-260.
- [2] a) M. Sawamura, Y. Ito, *Chem. Rev.* **1992**, *92*, 857; b) A. Börner, *Eur. J. Inorg. Chem.* **2001**, 327-337.
- [3] J. Chatt, B. T. Heaton, *J. Chem. Soc. A* **1968**, 2745.
- [4] J. E. Griffiths, A. B. Burg, *J. Am. Chem. Soc.* **1960**, *82*, 1507.
- [5] For reviews on the coordination chemistry see: a) D. M. Roundhill, R. P. Sperline, W. B. Beaulieu, *Coord. Chem. Rev.* **1978**, *26*, 263; b) B. Walther, *Coord. Chem. Rev.* **1984**, *60*, 67; c) T. Appleby, J. D. Woolins, *Coord. Chem. Rev.* **2002**, *235*, 121.
- [6] L. D. Quin, *A Guide to Organophosphorus Chemistry*, Wiley-Interscience, New York, **2000**.
- [7] W.-M. Dai, K. K. Y. Yeung, W. H. Leung, R. K. Haynes, *Tetrahedron: Asymmetry* **2003**, *14*, 2821-2826.
- [8] M. M. Rauhut, I. Hechenbleikner, H. A. Currier, V. P. Wystrach, *J. Am. Chem. Soc.* **1958**, *80*, 6690.
- [9] X.-B. Jiang, PhD-Thesis, *Monodentate secondary phosphine oxides (SPO's), Synthesis and application in asymmetric catalysis*, **2004**, University of Groningen.
- [10] H. R. Hayes, *J. Org. Chem.* **1968**, *33*, 3690.
- [11] K. M. Pietrusiewicz, M. Zablocka, *Chem. Rev.* **1994**, *94*, 1375.
- [12] X.-B. Jiang, A. J. Minnaard, B. Hessen, B. L. Feringa, A. L. L. Duchateau, J. G. O. Andrien, J. A. F. Boogers, J. G. de Vries, *Org. Lett.* **2003**, *5*, 1503-1506.
- [13] a) R. K. Haynes, R. N. Free Man, C. R. Mitchell, S. C. Vonwiller, *J. Org. Chem.* **1994**, *59*, 2919; b) J. Drabowicz, P. Lyzwa, J. Omelanczuk, K. M. Pietrusiewicz, M. Mikolajczyk, *Tetrahedron: Asymmetry* **1999**, *10*, 2757; c) R. K. Haynes, T.-L. Au-Yeung, W.-K. Chan, W.-L. Lam, Z.-Y. Li, L.-Y. Yeung, A. S. C. Chan, P. Li, M. Koen, C. R. Mitchell, S. C. Vonwiller, *Eur. J. Org. Chem.* **2000**, 3205; d) F. Wang, P. L. Polavarapu, J. Drabowicz, M. Mikolajczyk, *J. Org. Chem.* **2000**, *65*, 7561; e) J. Holt, A. M. Maj, E. P. Schudde, K. M. Pietrusiewicz, L. Sieron, W. Wieczorek, T. Jerphagnon, I. W. C. E. Arends, U. Hanefeld, A. J. Minnaard, *Synthesis* **2009**, 2061-2065.
- [14] a) A. Leyris, D. Nuel, L. Giordano, M. Achard, G. Buono, *Tetrahedron Lett.* **2005**, *46*, 8677; b) A. Leyris, J. Bigeault, D. Nuel, L. Giordano, G. Buono, *Tetrahedron Lett.* **2007**, *48*, 5247-5250; c) D. Moraleda, D. Gatineau, D. Martin, L. Giordano, G. Buono, *Chem. Commun.* **2008**, 3031-3033; d) Q. Xu, C.-Q. Zhao, L.-B. Han, *J. Am. Chem. Soc.* **2008**, *130*, 12648-12655.
- [15] W. B. Farnham, R. K. Murray, K. Mislow, *J. Am. Chem. Soc.* **1970**, *92*, 5809.

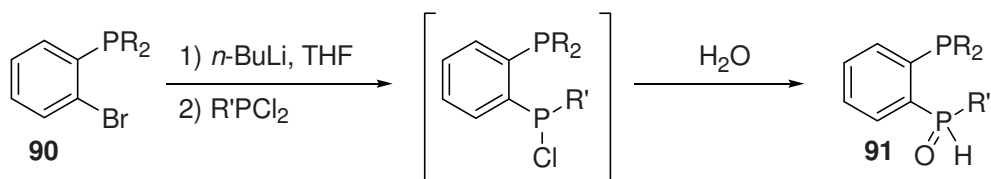
- [16] Q. Xu, C.-Q. Zhao, L.-B. Han, *J. Am. Chem. Soc.* **2008**, *130*, 12648-12655.
- [17] W. B. Beaulieu, T. B. Rauchfuss, D. M. Roundhill, *Inorg. Chem.* **1975**, *14*, 1732.
- [18] B. Walther, H. Hartung, M. Maschmeier, U. Baumeister, B. Messbauer, *Z. Anorg. Allg. Chem.* **1988**, *566*, 121.
- [19] a) G. Li, *Angew. Chem. Int. Ed.* **2001**, *40*, 1513; b) G. Li, *J. Org. Chem.* **2002**, *67*, 3643.
- [20] Christian Ebner, Master-Thesis, *Synthese und Screening racemischer Katalysatoren für die asymmetrische allylische Substitution*, **2008**, University of Basel.
- [21] L. Ackermann, *Synthesis* **2005**, 1557-1571.
- [22] P. W. N. M. van Leeuwen, C. F. Roobeek, R. L. Wife, J. H. G. Frins, *J. Chem. Soc. Chem. Commun.* **1986**, 31.
- [23] a) T. Ghaffar, A. W. Parkins, *Tetrahedron Lett.* **1995**, *36*, 8657; b) J. Akisanya, A. W. Parkins, J. W. Steed, *Org. Process Res. Dev.* **1998**, *2*, 274; c) C. J. Cobley, M. van den Heuvel, A. Abbadi, J. G. de Vries, *Tetrahedron Lett.* **2000**, *41*, 2467; d) X.-B. Jiang, A. J. Minnaard, B. L. Feringa, J. G. de Vries, *J. Org. Chem.* **2004**, *69*, 2327.
- [24] G. Y. Li, *J. Organomet. Chem.* **2002**, *653*, 63.
- [25] C. Wolf, R. Lerebours, *J. Org. Chem.* **2003**, *68*, 7077.
- [26] a) C. Wolf, R. Lerebours, *Org. Lett.* **2004**, *6*, 1147; b) R. Lerebours, C. Wolf, *Synthesis* **2005**, 2287.
- [27] C. Wolf, R. Lerebours, *J. Org. Chem.* **2003**, *68*, 7551.
- [28] a) D. Gelman, S. L. Buchwald, *Angew. Chem. Int. Ed.* **2003**, *42*, 5993; b) C. Wolf, R. Lerebours, *Org. Biomol. Chem.* **2004**, *2*, 2162.
- [29] G. Y. Li, G. Zheng, A. F. Noonan, *J. Org. Chem.* **2001**, *66*, 8677.
- [30] J. Bigeault, L. Giordano, G. Buono, *Angew. Chem. Int. Ed.* **2005**, *44*, 4753.
- [31] X.-B. Jiang, A. J. Minnaard, B. Hessen, B. L. Feringa, A. L. L. Duchateau, J. G. O. Andrien, J. A. F. Boogers, J. G. de Vries, *Org. Lett.* **2003**, *5*, 1503-1506.
- [32] A. Pfaltz, Y. Ribourdouille, X. Feng, B. Ramalingam, B. Pugin, F. Spindler, PCT Int., Application WO 2007135179 (A1), **2007**.
- [33] a) D. K. MacFarland, C. R. Landis, *Organometallics* **1996**, *15*, 483-485; b) C. L. Landis, R. A. Sawyer, E. Somsook, *Organometallics* **2000**, *19*, 994-1002; c) M. Sawamura, Y. Nakayama, W.-M. Tang, Y. Ito, *J. Org. Chem.* **1996**, *61*, 9090-9096.
- [34] a) A. Börner, W. K. Kortus, H. B. Kagan, *Tetrahedron: Asymmetry* **1993**, *4*, 2219-2228; b) L. B. Fields, E. N. Jacobsen, *Tetrahedron: Asymmetry* **1993**, *4*, 2229-2240.
- [35] B. F. M. Kimmich, C. R. Landis, D. R. Powell, *Organometallics* **1996**, *15*, 4141-4146.
- [36] M. Quirnbach, A. Kless, J. Holz, V. Tarachov, A. Börner, *Tetrahedron: Asymmetry* **1999**, *10*, 1803-1811.
- [37] T. Hayashi, K. Kanehira, T. Hagihara, M. Kumada, *J. Org. Chem.* **1988**, *53*, 113-120.
- [38] a) S. Borns, R. Kadyrov, D. Heller, W. Baumann, A. Spannenberg, R. Kempe, J. Holz, A. Börner, *Eur. J. Inorg. Chem.* **1998**, 1291-1295; b) S. Borns, R. Kadyrov, D. Heller, W. Baumann, J. Holz, A. Börner, *Tetrahedron: Asymmetry* **1999**, *10*, 1425-1431; c) J. Holz, R. Kadyrov, S. Borns, D. Heller, A. Börner, *J. Organomet. Chem.* **2000**, *603*, 61-68.
- [39] a) W. Li, Z. Zhang, D. Xiao, X. Zhang, *Tetrahedron Lett.* **1999**, *40*, 6701-6704; b) W. Li, Z. Zhang, D. Xiao, X. Zhang, *J. Org. Chem.* **2000**, *65*, 3489-3496.
- [40] Holz, M. Quirnbach, U. Schmidt, D. Heller, R. Stürmer, A. Börner, *J. Org. Chem.* **1998**, *63*, 8031-8034.

2.2 Synthesis and Catalysis Experiments

2.2.1 Secondary Phosphine Oxides

2.2.1.1 SPO-Phosphine Ligands

The synthesis of bidentate ligands containing a phosphine and a secondary phosphine oxide was recently achieved at Solvias AG. The original synthetic procedure is outlined in Scheme 2.19. Lithiation of an *ortho*-brominated phosphinobenzene (**90**) and reaction with a suitable dichlorophosphine followed by hydrolysis gave the desired compounds **91**.



Scheme 2.19. Synthesis of SPO-phosphine ligands.

According to this procedure, several derivatives were prepared and the corresponding enantiomers separated by semipreparative chiral HPLC. Hydrogenation experiments using the enantiomerically pure ligands showed very high selectivities in the reduction of various substrates.^[1]

The above mentioned ligands form a five-membered chelate upon complexation of a metal center. Following the established synthetic route, ligands with an additional carbon atom were to be synthesized to examine the catalytic properties of the corresponding metal complexes with a six-membered chelate ring (Figure 2.4).

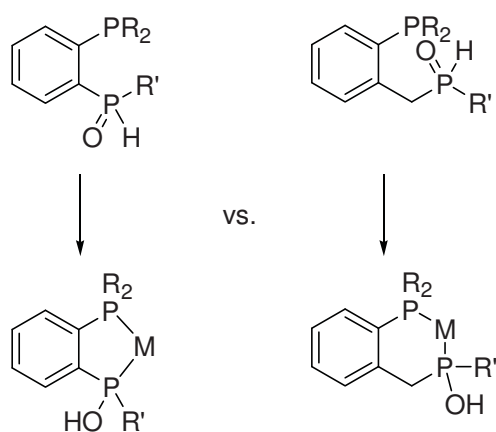
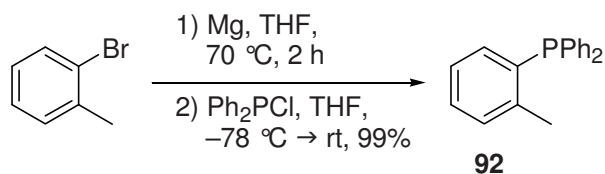


Figure 2.4. Five-membered versus six-membered chelate.

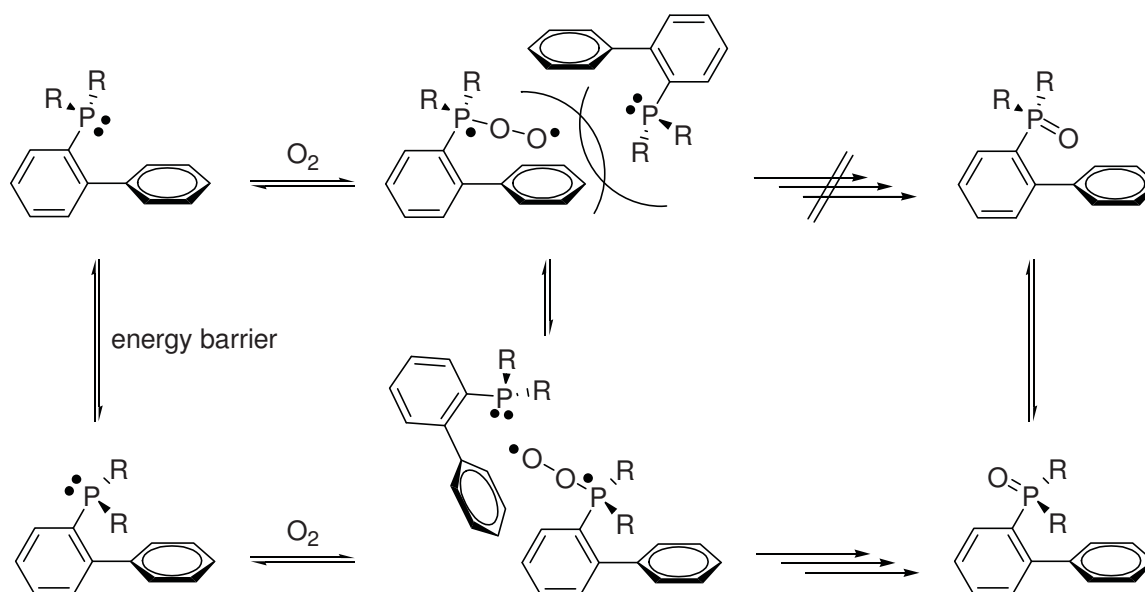
The starting material, diphenyl-(*ortho*-tolyl)phosphine **92**, was commercially available as well as easily synthesized by addition of 2-methylphenylmagnesium bromide to diphenylchlorophosphine (Scheme 2.20).



Scheme 2.20. Synthesis of (*ortho*-tolyl)diphenylphosphine.

Metalation at the benzylic position of **92** was achieved following a literature procedure.^[2] When *n*-butyllithium was added to a solution containing **92** and potassium *tert*-butoxide in pentane at $-10\text{ }^{\circ}\text{C}$ the formation of a red solid was observed upon warming up to room temperature (Scheme 2.21). Addition of phenyl dichlorophosphine at $-78\text{ }^{\circ}\text{C}$ followed by hydrolysis installed the SPO group. Unlike its counterpart, shown in Scheme 2.19, the phosphine-SPO **93** was not stable towards oxidation and was only isolated as the bis-oxide **94**.

according to the proposed mechanism,^[4] cannot be completed by reaction with a second phosphine (Scheme 2.24).



Scheme 2.24. Proposed oxidation mechanism for dialkylbiarylphosphines by *Buchwald*.^[3]

Ligands **91** might profit from the same effect. The phosphine-SPO **93** has, due to the additional methylene group, more conformational freedom, possibly allowing for an easier rotation. According to the mechanism shown in Scheme 2.24, this should facilitate the reaction with oxygen and the approach of a second phosphine. The involvement of the SPO-functional group in the oxidation mechanism is also possible.

2.2.1.2 Terpene-Derived Secondary Phosphine Oxides

Since the ligands derived from diphenyl-(*ortho*-tolyl)phosphine were found to be sensitive to oxidation, the focus turned back on structures giving a five-membered chelate. The initial synthesis gave access to racemic secondary phosphine oxides which had to be separated by chiral HPLC. The use of a phosphine dichloride with a chiral substituent would allow for a diastereoselective formation of the intermediate phosphine chloride.^[5] Indeed, the reaction of menthylphosphine dichloride with **90** proved to be very selective, and under optimized conditions the secondary phosphine oxide **96** was isolated with a diastereoisomeric ratio of about 10:1 (Scheme 2.25). Further purification could be achieved by recrystallization.^[1]

The successful application of menthylphosphine dichloride in the synthesis of secondary phosphine oxides led to the examination of further alcohols from the chiral pool. Many terpenes are commercially available in enantiomerically pure form and the alcohols fenchol (**100**), borneol (**101**) and isopinocampheol (**102**) were synthetically evaluated (Figure 2.5).

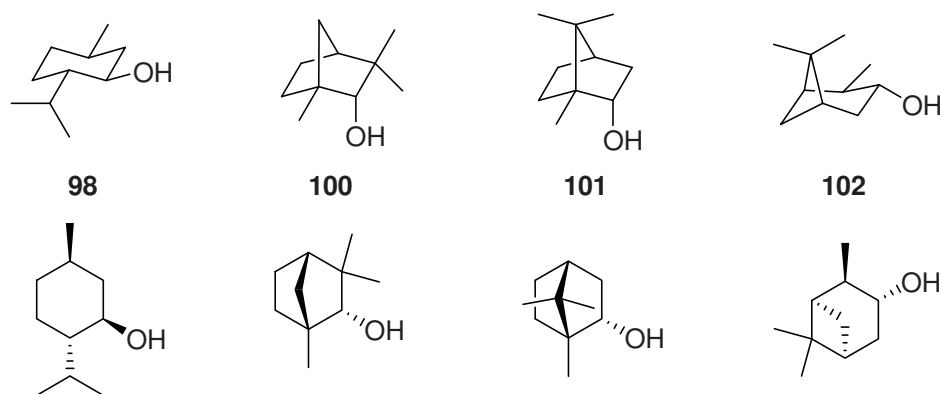


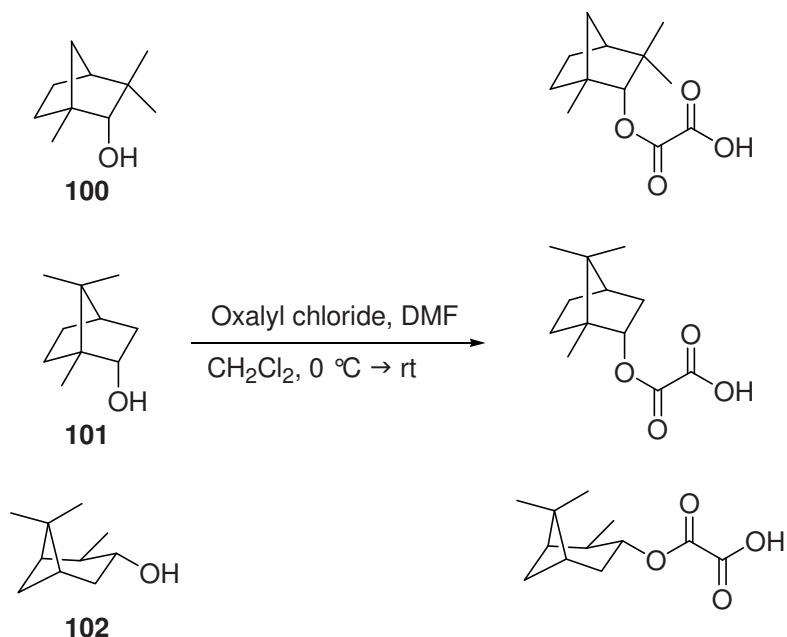
Figure 2.5. Commercially available terpenyl alcohols.

It turned out that for the terpenes tested, there is no general reaction to exchange the alcohol functionality for a halide. The reaction with zinc dichloride, which worked well for menthol, was not applicable to the other terpenes giving a mixture of unidentifiable products.

The chlorination of **101** and **102** has been described but the procedure involves a reaction in carbon tetrachloride.^[9] With the intention of an upscale upon a successful small scale synthesis, less problematic reagents were examined to find an alternative route.

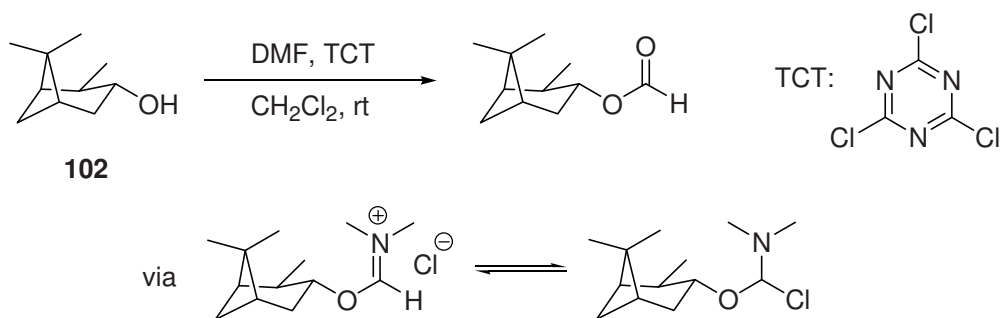
With thionyl chloride and *N,N*-dimethylformamide in dichloromethane the starting material was mostly consumed but no desired products could be isolated. Changing the solvent to diethyl ether or pyridine gave no improvement.

Oxalyl chloride in combination with *N,N*-dimethylformamide in dichloromethane did not lead to the desired haloterpenes, but rather formed oxalylic esters (Scheme 2.28).



Scheme 2.28. Reaction of terpenyl alcohols with oxalyl chloride.

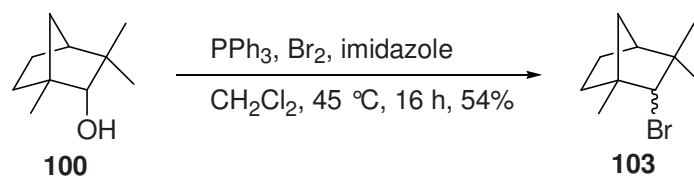
The combination of *N,N*-dimethylformamide and 2,4,6-trichloro[1,3,5]triazine (TCT)^[10] showed a related reactivity and after work up the corresponding formate was isolated instead of the desired halide (Scheme 2.29). Apparently, the intermediate alkoxyiminium chloride did not serve as a leaving group, remaining stable until aqueous work up.



Scheme 2.29. Reaction of isopinocampheol with 2,4,6-trichloro[1,3,5]triazine and DMF.

A procedure using trimethylsilyl chloride and lithium bromide in acetonitrile, reported for the conversion of norbornanol,^[11] gave no conversion at all.

The outcome of *Appel*-type reactions was dependent on the additives and the alcohols used. Whereas isopinocampheol **102** with triphenylphosphine in combination with *N*-chlorosuccinimide, *N*-bromosuccinimide, carbon tetrabromide or bromine gave each time no desired product, the reaction of fenchol **100** with triphenylphosphine and bromine in dichloromethane with imidazole as additive led to fenchyl bromide **103** in moderate yield (Scheme 2.30).



Scheme 2.30. *Appel*-type bromination of fenchol.

The reaction of borneol **101** and isopinocampheol **102** with 4-toluenesulfonic acid chloride and methylsulfonic acid chloride showed that only the latter reagent successfully generated the corresponding sulfonate ester. This compound showed only limited stability which indicated its reactivity. However, instead of undergoing substitution reactions with lithium halides in acetone or THF, only decomposition products were generated.

The notorious lack of product formation in the case of **101** and **102** posed the question whether an S_N2 -type reaction, for example under *Appel*-conditions, is even possible. The two geminal methyl groups in **101** and **102** are in proximity of a potential backside attack (Figure 2.6).

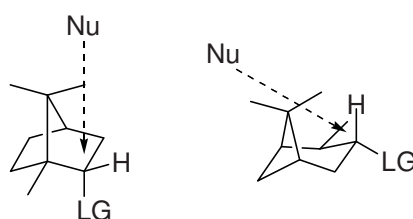
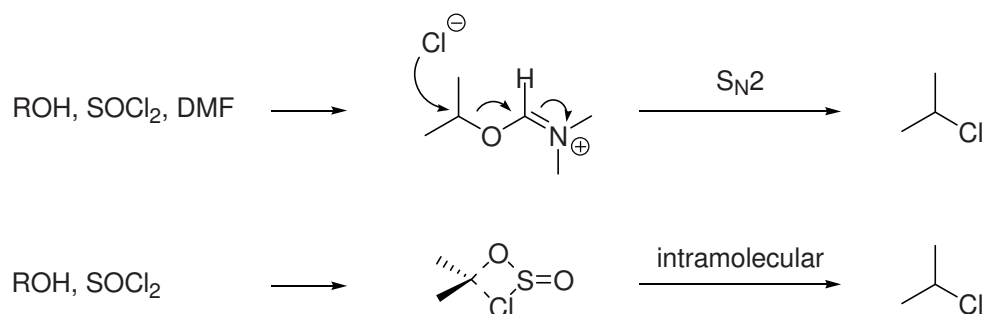


Figure 2.6. S_N2 -reactions on terpenes.

Therefore, the chlorination with thionyl chloride was carried out without additional *N,N*-dimethylformamide, since this reaction has been proposed to proceed via an intramolecular decomposition under certain conditions (Scheme 2.31).^[12]

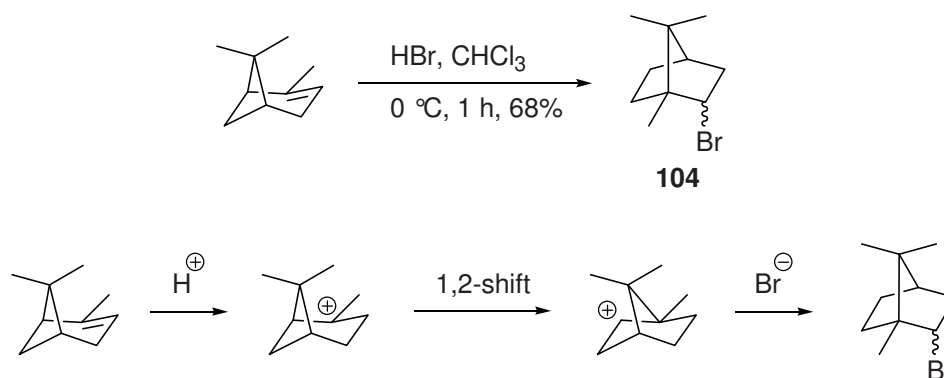


Scheme 2.31. Chlorination of alcohols with thionyl chloride.

The intramolecular pathway should be less affected by the sterics than the S_N2 -reaction, but the reactions with thionyl chloride gave no desired products. The use of phosphoryl trichloride or phosphorus pentachloride did not change the results. Finally, a S_N1 -type reaction was carried out. Unfortunately, treatment of the alcohols **101** and **102** with concentrated hydrobromic acid led either to decomposition products or recovery of starting material.

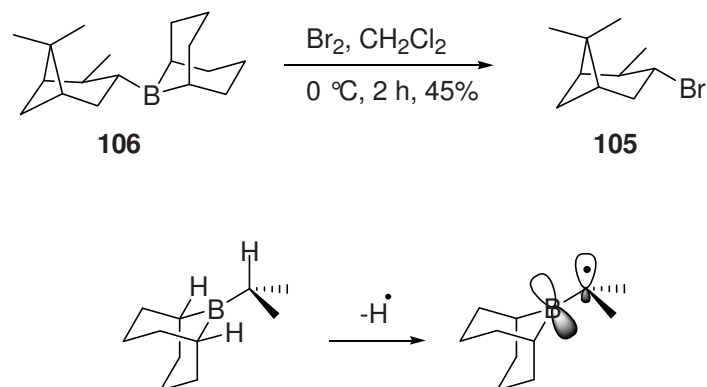
Since the functional group transformations in these alcohols were intractable, the focus turned to alternative synthetic routes.

The synthesis of bornyl bromide **104** was reported starting from pinene.^[13] Indeed; **104** could be generated when a solution of pinene in chloroform was aerated with hydrogen bromide. The mechanism proceeds via a diastereoselective 1,2-carbon shift (Scheme 2.32). After bulb-to-bulb distillation the bromide **104** was isolated in acceptable yield.



Scheme 2.32. Rearrangement of pinene under acidic conditions.

The final synthesis of the isopinocampheol derived bromide **105** was achieved by taking advantage of a reaction reported by *Brown* and co-workers.^[14] Alkyl boranes derived from 9-borabicyclo[3.3.1]nonane (9-BBN) gave the corresponding alkyl bromides after radical bromination. The starting material for the formation of **105** was commercially available Alpine-Borane® (**106**). Reaction with bromine under exclusion of light gave the bromide **105** in moderate yield (Scheme 2.33). The reaction is assumed to proceed via a free radical chain reaction.

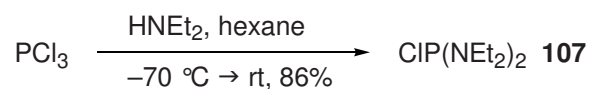


Scheme 2.33. Radical bromination of Alpine-Borane®.

The high selectivity in the reaction of the 9-BBN derived alkylboranes presumably originates from the conformation of the hydrogen atoms that can be abstracted. Only the radical formed in the α -position of the alkyl chain can be stabilized by the empty orbital of the boron-atom, whereas the single electron of a radical on the bicyclooctane moiety would occupy an orthogonal orbital without the possibility for stabilization.

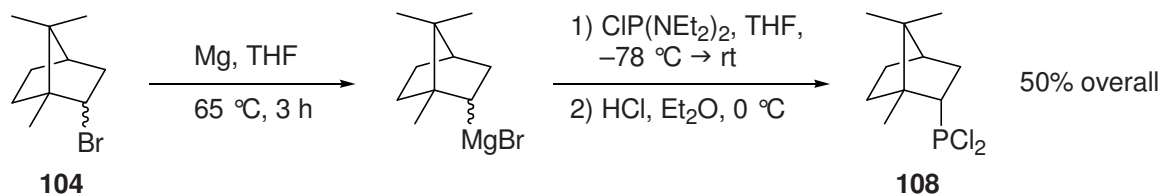
The next synthetic steps were the preparation of the *Grignard*-reagents, their conversion into phosphine dichlorides and the formation of the phosphine-SPO ligand.

The preparation of menthylphosphine dichloride **97** in diethyl ether shown in Scheme 2.26 has the synthetic advantage that, after the reaction of the menthyl-*Grignard*-reagent with phosphorus trichloride, the salts nicely precipitate and can easily be filtered off. Unfortunately, none of the bromides was reactive enough to form the metallated species under these conditions. Reaction of **104** with magnesium occurred in THF only at elevated temperature. However, the addition of this *Grignard*-reagent to phosphorus trichloride resulted in a poorly selective reaction and the salts formed did not precipitate. Purification of the product mixture was not possible due to the similar boiling points of the compounds formed. To avoid an unselective reaction, a less reactive phosphorus source was employed. Addition of four equivalents diethyl amine to phosphorus trichloride in hexane gave bis(diethylamino)phosphine chloride (**107**) in good yield (Scheme 2.34).



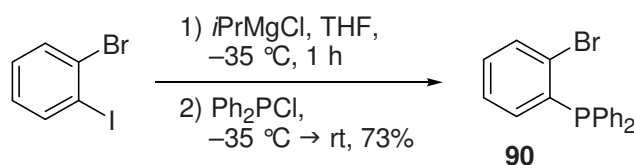
Scheme 2.34. Synthesis of bis(diethylamino)chlorophosphine.

This reagent, in combination with bornyl magnesium bromide, cleanly generated the intermediate diamminophosphine, and upon treatment with four equivalents of HCl the phosphine dichloride **108** was isolated in moderate yield after distillation (Scheme 2.35).



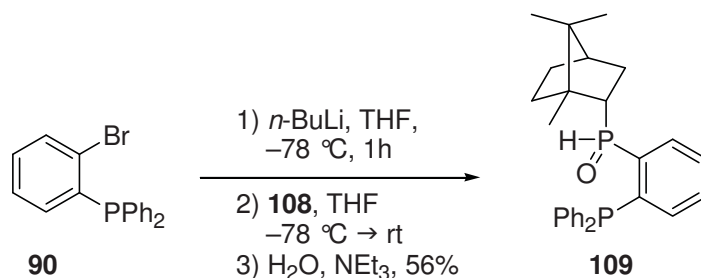
Scheme 2.35. Formation of bornylphosphine dichloride.

The phosphine building block for the formation of the bidentate ligand was prepared according to a literature procedure as shown in Scheme 2.36.^[15] Metalation of 2-bromo-1-iodobenzene with *iso*-propyl magnesium chloride at -30 °C in THF followed by reaction with diphenylphosphine chloride gave the phosphine **90** in acceptable yield.



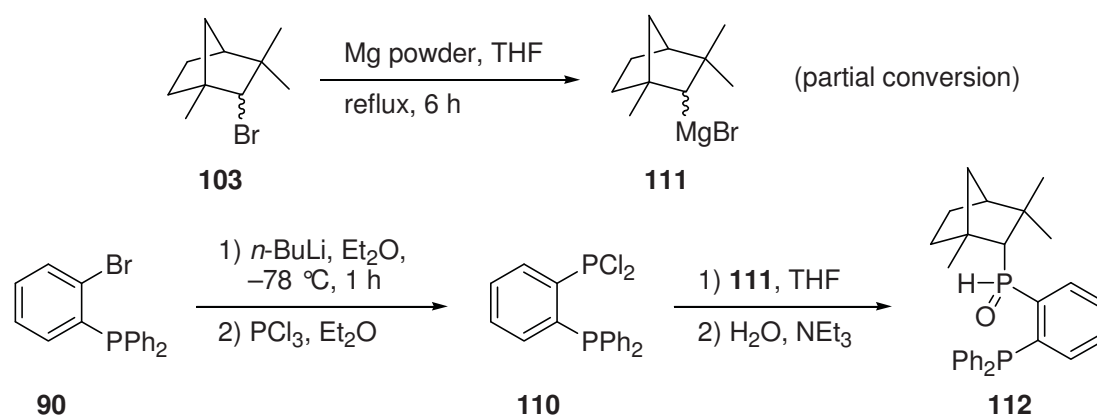
Scheme 2.36. Synthesis of (*ortho*-bromophenyl)diphenylphosphine.

Lithiation of **90** with *n*-butyllithium in THF at low temperature followed by addition of **108** and subsequent hydrolysis resulted in the formation of the secondary phosphine oxide **109** as a mixture of two diastereoisomers in almost equal amounts (Scheme 2.37). Separation of the diastereoisomers was achieved by chromatography and analysis by chiral HPLC showed an optical purity of 97% *ee* for both compounds (+)-**109** and (-)-**109**. Further purification by crystallization was not possible. The reduced enantiopurity was a result of the purity of the pinene starting material rather than partial racemization during the synthesis.



Scheme 2.37. Synthesis of a bornyl-SPO-phosphine ligand.

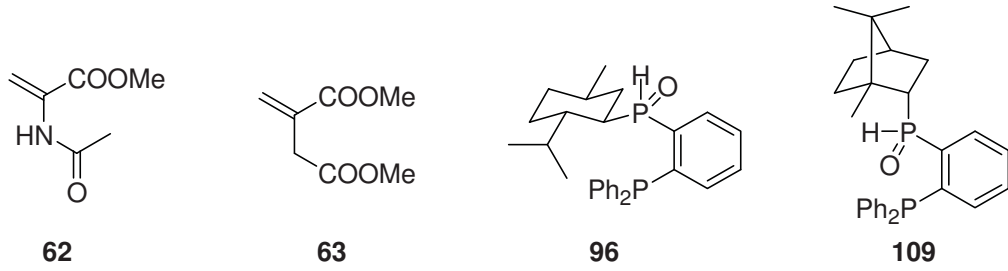
The formation of the *Grignard*-reagent from fenchyl bromide **103** was more problematic, since, even with magnesium powder at an elevated temperature and a longer reaction time, the formation of the metallated species could not be completed. As a consequence, the subsequent reaction with phosphorus trichloride gave a complex mixture of compounds and no isolatable product. Isopinocampheyl bromide **105** did not undergo reaction with magnesium at all. To circumvent the problematic formation of fenchylphosphine dichloride, the dichlorophosphine moiety was installed in reversed order (Scheme 2.38).



Scheme 2.38. Synthesis of a fenchyl-SPO-phosphine ligand.

Lithiation of **90** in diethyl ether resulted in a fine white suspension which then was added to phosphorus trichloride to give the phosphine dichloride **110** after evaporation of the solvent.^[19] This intermediate was not isolated, but rather directly treated with the fenchyl *Grignard*-reagent **111**. Again, the yield was very low and the secondary phosphine oxide **112** was isolated as an inseparable mixture of diastereoisomers.

With the two ligands (+)-**109** and (-)-**109** in hand, their performance in the Rh-catalyzed hydrogenation was briefly investigated. Dimethyl itaconate (**63**) and methyl acetamidoacrylate (**62**) were tested (Table 2.1).

Table 2.1. Asymmetric hydrogenation of olefins catalyzed by Rh-SPO-phosphine complexes.


Chemical structures shown above the table: **62** is methyl acrylate with an acetamido group at the 2-position; **63** is methyl itaconate; **96** is a menthyl-derived phosphine oxide ligand with a diphenylphosphino group; **109** is a menthyl-derived phosphine oxide ligand with a diphenylphosphino group in the opposite configuration to 96.

Entry ^a	Ligand	Substrate	conv. [%] ^b	ee [%] ^b
1	(+)- 109	63	>99	90 (<i>R</i>)
2	(-)- 109	63	>99	77 (<i>S</i>)
3	(+)- 109	62	>99	93 (<i>S</i>)
4	(-)- 109	62	>99	78 (<i>R</i>)
5	96	62	>99	97 (<i>S</i>)

^aReaction was carried out in methanol with 0.5 mol% [Rh(nbd)₂]BF₄ *in situ* precomplexed with 1.1 equivalents of ligand under 1 bar H₂ and 25 °C for 1 h. ^bDetermined by chiral GC.

The results nicely showed that the configuration at the secondary phosphine oxide determines the outcome of the hydrogenation reaction. In this respect, (-)-**109** represented the mismatched case for both substrates. The matched case complex was able to hydrogenate itaconate **63** with an enantiomeric excess of 90% (entry 1) and acrylate **62** with 93% *ee* (entry 3). Keeping in mind that the ligand itself was employed with an optical purity of 97% *ee*, the maximal possible selectivities would be slightly higher. The more selective catalyst was also more reactive. The measured turnover frequency (TOF) had, in the case of substrate **63**, values of 8000 h⁻¹ ((-)-**109**) and 12000 h⁻¹ ((+)-**109**). For the reduction of **62**, values of 1300 h⁻¹ ((-)-**109**) and 2700 h⁻¹ ((+)-**109**) were measured. Although these ligands were very active, they were outperformed by the menthol-derived ligand **96** which gave 97% *ee* with a TOF of 8000 h⁻¹ in the hydrogenation of itaconate **62**.

2.2.2 Hydroxyethyl-Functionalized Phosphines

The addition of a carbon nucleophile to a chlorophosphine generates P-chiral phosphines, instead of secondary phosphine oxides obtained by hydrolysis. This reaction proceeds with good diastereoselectivity and ligands such as the one shown in Figure 2.7 have been investigated at Solvias AG.

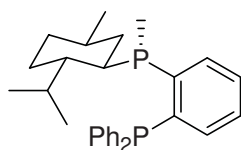
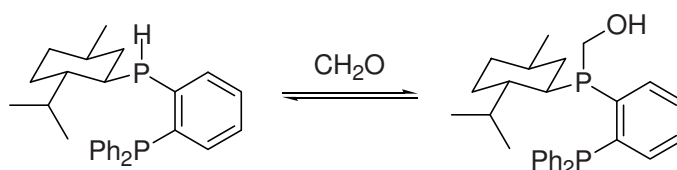


Figure 2.7. Menthol-derived P-chiral bisphosphine.

In a related project menthyl-derived bisphosphines with an additional functional group were studied (Scheme 2.39). It has been shown that internal hydroxy groups in chiral diphosphine ligands can have a beneficial influence on the enantioselectivity of the corresponding metal catalyst.^[17]

The combination of a secondary phosphine and formaldehyde generates a hydroxymethyl substituted phosphine.^[18] This reaction is reversible and, although the hydroxymethylphosphine can be isolated under certain conditions, the definite formation of a single metal complex for catalysis is not possible.



Scheme 2.39. Reversible formation of a hydroxymethylphosphine.

The installation of a functional group into the catalyst would allow for stereodiscrimination by secondary interactions like hydrogen bonding. To avoid reversibility, the carbon chain between this functional group and the phosphorus atom had to be extended. Employing a suitable nucleophilic building block – a similar reaction led to the ligand in Figure 2.7 – and subsequent synthetic transformations the formation of alcohols, esters or carboxylic acids seemed possible (Figure 2.8).

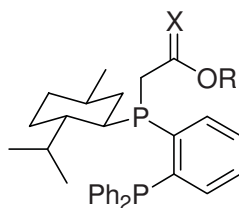
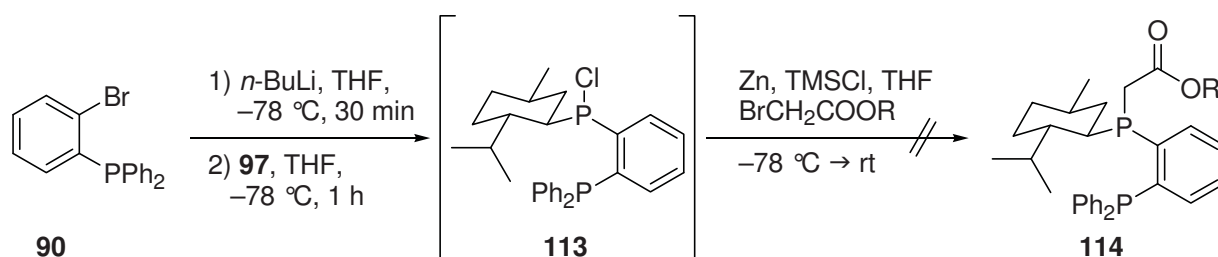


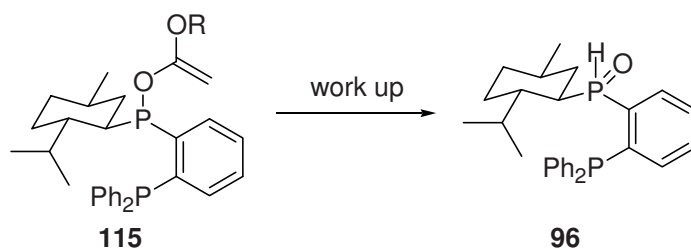
Figure 2.8. P-chiral functionalized diphosphines. R = H, alkyl; X = H₂, O.

The first synthetic approach was the formation of phosphine chloride **113**. This reaction proceeded with good stereoselectivity, as expected (Scheme 2.40).



Scheme 2.40. Reaction of a chlorophosphine with a *Reformatsky*-reagent. R = Et, *t*Bu.

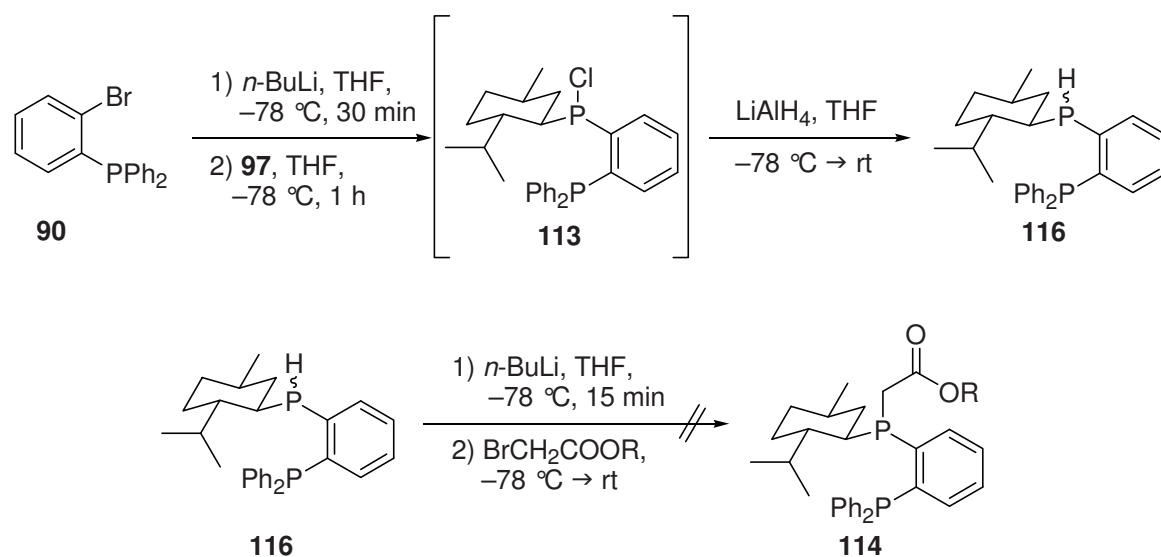
The addition of the *Reformatsky*-reagent^[19] did not lead to the desired ester **114**, instead only the secondary phosphine oxide **96** was isolated. The ³¹P-NMR-spectrum of the reaction mixture after the addition of the zinc ester-enolate, showed a resonance at 118 ppm, suggesting that formation of the phosphinite **115** took place. This water sensitive compound was then hydrolyzed during work-up, forming **96** (Scheme 2.41). Ethyl and *tert*-butyl ester enolates gave the same result as well, which reflects the oxophilicity of the phosphorus.



Scheme 2.41. Hydrolysis of a phosphinite. R = Et, *t*Bu.

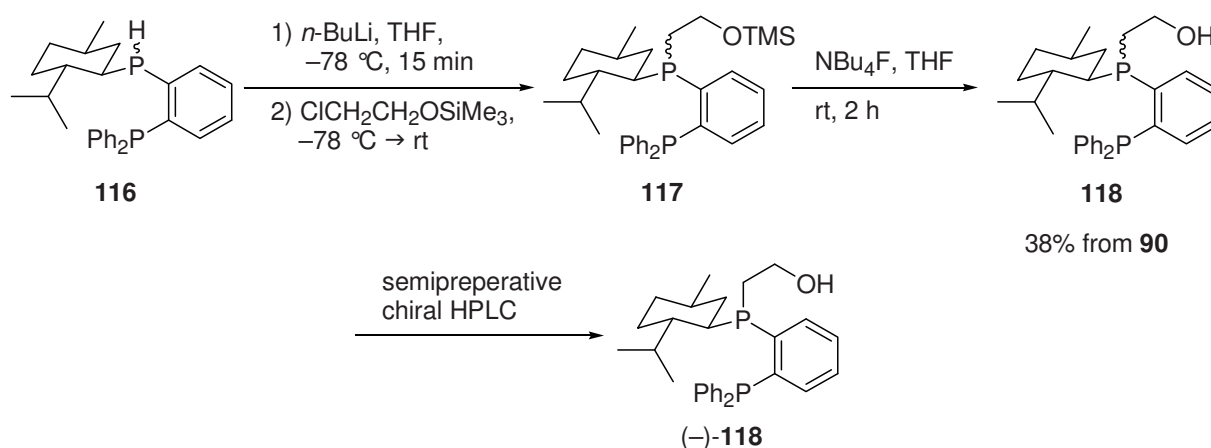
Reduction of the phosphine chloride **113** with lithium aluminium hydride gave the secondary phosphine **116**. During this transformation epimerization occurred at the phosphorus atom and the product was obtained as a mixture of diastereoisomers. Deprotonation with *n*-butyllithium resulted in a red solution that turned yellow after addition of the bromoacetate. However, the

apparent conversion of the phosphine anion gave an unidentifiable product mixture (Scheme 2.42).



Scheme 2.42. Alkylation of a secondary phosphine. R = Et, *t*Bu.

With a different electrophile the reaction worked better (Scheme 2.43). Addition of 2-chloroethoxytrimethylsilane gave the protected alcohol **117**. No diastereoselectivity was observed in the addition of the alkyl chain and the outcome was not affected by the base employed, such as LDA or *n*-butyllithium. Deprotection was achieved with tetrabutylammonium fluoride in THF and the hydroxy-functionalized phosphine **118** was isolated in 38% yield over four steps.



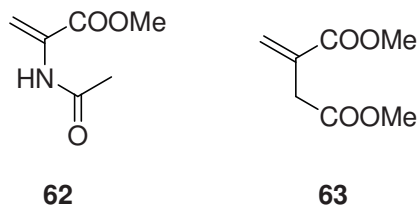
Scheme 2.43. Formation of a P-chiral hydroxyethyl-functionalized bisphosphine.

The reaction sequence was best carried out consecutively. Any attempts to purify the intermediates **116** and **117** resulted in lower overall yield. The two diastereoisomers then had

to be separated by semipreparative chiral HPLC. This procedure was problematic, since one diastereoisomer readily oxidized both during and after separation, and the recovery of (-)-**118** was not quantitative either.

Finally, ligand (-)-**118** was tested in the asymmetric hydrogenation in combination with $[\text{Rh}(\text{nbd})_2]\text{BF}_4$. The results are presented in Table 2.2.

Table 2.2. Rh-catalyzed asymmetric hydrogenation of olefins.

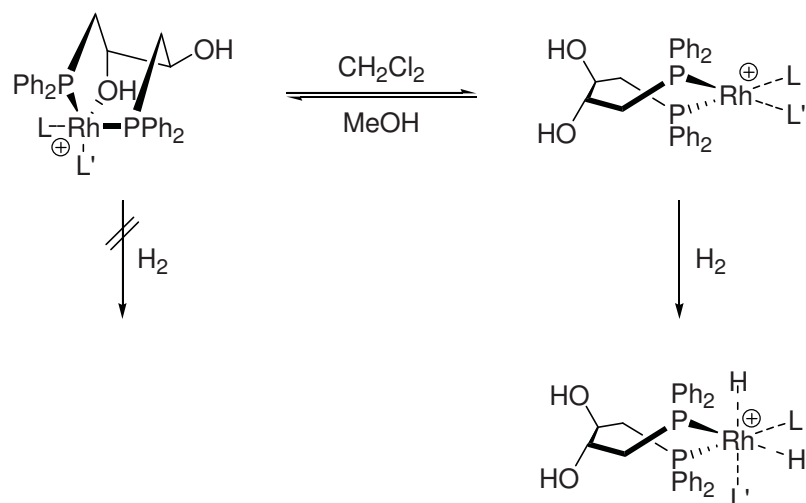


Entry ^a	Substrate	Reaction time	conv. [%] ^b	TOF [h ⁻¹]	ee [%] ^b
1	63	30 min	2	7	57
2	62	25 min	12	57	89

^aReaction was carried out in methanol with 0.5 mol% $[\text{Rh}(\text{nbd})_2]\text{BF}_4$ *in situ* precomplexed with 1.1 equivalent ligand (-)-**118** under 5 bar H₂ and 25 °C for 1 h. ^bDetermined by chiral GC.

The catalyst formed showed only low activity, resulting in a turnover frequency of 7 h⁻¹ in the reduction of dimethyl itaconate (**63**) and 57 h⁻¹ in the case of methyl acetamidoacrylate (**62**). Aside from the low conversion, the enantioselectivities were moderate to acceptable, generating an enantiomeric excess of 57% for itaconate **63** and 89% *ee* for acrylate **62**.

Among several hydroxy-functionalized bisphosphine ligands the difference in activity, as compared to the non-functionalized derivatives, varies depending on the ligand structure.^[17] The reaction rates usually either decrease or stay unaffected^[20] and rate acceleration is less common. In most cases this inhibition effect is believed to originate from the additional coordination of the hydroxy group to the rhodium atom. In these cases, the oxygen atom has to dissociate before dihydrogen addition can occur, and therefore slows down the catalytic turnover (Scheme 2.44).



Scheme 2.44. Influence of the hydroxy group on catalyst reactivity (L,L' = diolefin, MeOH, bidentate substrate).^[17]

Possibly, (–)-**118** is able to form a stable complex, therefore decreasing the rate of the reaction.

2.2.3 Conclusions

The synthesis of phosphine-SPO ligands was investigated. The 1,3-substitution pattern was shown to suffer from sensitivity of the phosphine towards oxygen, whereas the related 1,2-substituted compounds proved to be air-stable (Figure 2.9).

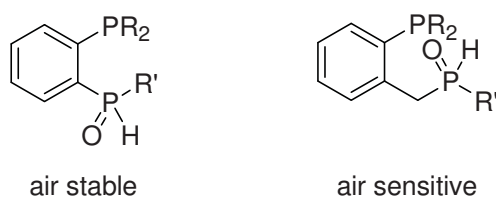


Figure 2.9. SPO-phosphine ligands.

A diastereoselective synthesis of secondary phosphine oxides was studied by employing a chiral phosphine dichloride. The preparation of menthylphosphine dichloride has been reported and proved to be a useful building block. Other terpenes were evaluated for their synthetic value in the diastereoselective preparation of secondary phosphine oxides. The straightforward functional group transformations in the case of menthol were not applicable to

the alcohols tested: fenchol, borneol and isopinocampheol. For each substrate a different synthetic procedure had to be used, and generally gave the corresponding bromides in only moderate yields. Furthermore, only bornyl bromide **104** could be transformed into the phosphine dichloride to access the secondary phosphine oxide **109** (Figure 2.10).

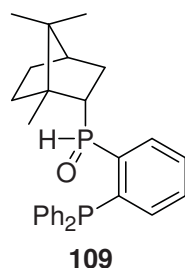


Figure 2.10. Bornyl-SPO-phosphine ligand

The results of the hydrogenation reactions showed that the bornyl-derived phosphine-SPO **109** can compete with the menthol derivative in terms of enantioselectivity, and a clear matched/mismatched case was observed for the two diastereoisomers. However, the lower activity in combination with the more tedious synthesis makes this system less attractive than the corresponding ligand prepared from menthol.

A hydroxyl-functionalized menthol-derived bisphosphine ligand was prepared in four consecutive steps (Figure 2.11). After purification by semipreparative chiral HPLC the performance of this ligand in the asymmetric hydrogenation was tested. The catalyst system exhibited low activity in the hydrogenation of dimethyl itaconate and methyl acetamidoacrylate, although the latter could be reduced with an enantiomeric excess of 89%.

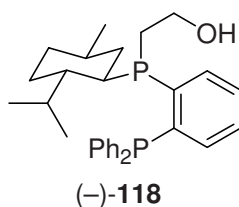


Figure 2.11. Hydroxyethyl-functionalized bisphosphine ligand.

2.2.4 References

- [1] a) B. Pugin, M. Lotz, H. Landert, A. Wyss, R. Aardom, B. Gschwend, A. Pfaltz, F. Spindler, PCT Int., Application WO 2009065784 (A1), 2009; b) B. Pugin, H. Landert, B. Gschwend, A. Pfaltz, F. Spindler, PCT Int., Application WO 2009065783 (A1), 2009.
- [2] G. Longoni, P. Chini, F. Canziani, P. Fantucci, *J. Chem. Soc. Sec. D: Chem. Commun.* **1971**, 10, 470.
- [3] T. E. Barder, S. L. Buchwald, *J. Am. Chem. Soc.* **2007**, 129, 5096-5101.
- [4] General mechanism: G. M. Kosolapoff, L. Maier, *Organic Phosphorus Compounds*; Wiley-Interscience: New York, **1972**, 3, 346; for $^3\text{O}_2$: a) M. M. Rauhut, H. A. Currier, *J. Org. Chem.* **1961**, 26, 4626-4628; b) H. D. Burkett, W. E. Hill, S. D. Worley, *Phosphorus and Sulfur* **1984**, 20, 169-172; for $^1\text{O}_2$: a) K. Nahm, Y. Li, J. D. Evanseck, K. N. Houk, C. S. Foote, *J. Am. Chem. Soc.* **1993**, 115, 4879-4884; b) S. Tsuji, M. Kondo, K. Ishiguro, Y. Sawaki, *J. Org. Chem.* **1993**, 58, 5055-5059; c) D. G. Ho, R. Gao, J. Celaje, H.-Y. Chung, M. Selke, *Science* **2003**, 302, 259-262.
- [5] G. Hägele, W. Kückelhaus, G. Tossing, J. Seega, R. K. Harris, C. J. Creswell, P. T. Jageland, *J. Chem. Soc. Dalton Trans.* **1987**, 795-805.
- [6] J. G. Smith, G. F. Wright, *J. Org. Chem.* **1952**, 17, 1116-1121.
- [7] J. Beckmann, D. Dakternieks, M. Dräger, A. Duthie, *Angew. Chem. Int. Ed.* **2006**, 45, 6509-6512.
- [8] a) M. Tanaka, I. Ogata, *Bull. Chem. Soc. Jpn.* **1975**, 48, 1094; b) N. F. Blank, K. C. McBroom, D. S. Glueck, W. S. Kassel, A. L. Rheingold, *Organometallics* **2006**, 25, 1742-1748.
- [9] A. Martinetti, F.-X. Buzin, L. Ricard, *J. Org. Chem.* **1997**, 62, 297-301.
- [10] L. De Luca, G. Giacomelli, A. Porcheddu, *Org. Lett.* **2002**, 4, 553-555.
- [11] G. A. Olah, B. Gupta, R. Malhotra, S. C. Narang, *J. Org. Chem.* **1980**, 45, 1638-1639.
- [12] M. B. Smith, J. March, *March's Advanced Organic Chemistry: Reactions, Mechanisms and Structure*, 6th Edition, Wiley-Interscience, **2007**, 468-469.
- [13] R. Krishnamurti, H. G. Kuivila, *J. Org. Chem.* **1986**, 51, 4947-4953.
- [14] H. C. Brown, C. F. Lane, N. M. De Lue, *Tetrahedron* **1988**, 44, 2773-2784.
- [15] S. Demay, M. Lotz, K. Polborn, P. Knochel, *Tetrahedron: Asymmetry* **2001**, 12, 909-914; for a different method see: D. Quintard, M. Keller, B. Breit, *Synthesis* **2004**, 905-908.
- [16] T. L. Schull, D. A. Knight, *Tetrahedron: Asymmetry* **1999**, 10, 207-211.
- [17] For a review see: A. Börner, *Eur. J. Inorg. Chem.* **2001**, 327-337.
- [18] a) O. Köhl, S. Blaurock, J. Sieler, E. Hey-Hawkins, *Polyhedron* **2001**, 20, 2171-2177; b) C. J. Curtis, A. Miedaner, R. Ciancanelli, W. W. Ellis, B. C. Noll, M. Rakowski DuBois, D. L. DuBois, *Inorg. Chem.* **2003**, 42, 216-227; c) A. A. Karasik, R. N. Naumov, Y. S. Spiridonova, O. G. Sinyashin, P. Lönnecke, E. Hey-Hawkins, *Z. Anorg. Allg. Chem.* **2007**, 633, 205-210.
- [19] S. Miki, K. Nakamoto, J.-I. Kawakami, S. Handa, S. Nuwa, *Synthesis* **2007**, 409-412.
- [20] J. Ward, A. Börner, H. B. Kagan, *Tetrahedron: Asymmetry* **1992**, 3, 849-852.

Chapter 3

P-Chiral Phosphino-Oxazolines as Ligands in the Iridium-Catalyzed Asymmetric Hydrogenation

3.1 Introduction

3.1.1 Historical Overview

Unlike the Rh- and Ru-catalyzed asymmetric hydrogenation of olefins bearing a coordinating functional group, as described in Section 1.1, which was introduced in the 1970's, the enantioselective reduction of unfunctionalized double bonds has been largely developed in the last ten years.^[1] Although the enantioselective hydrogenation of unfunctionalized terminal olefins with chiral metallocenes had been first reported by *Kagan* in 1979,^[2a] later by others,^[2] internal double bonds remained a challenge. In 1998, *Buchwald* published a chiral titanocene complex (Figure 3.1), which was able to hydrogenate a variety of unfunctionalized olefins with good enantioselectivities.^[3] However, these metallocenes had several drawbacks, such as tedious preparation, air-sensitivity and the high catalyst loading required.

These disadvantages were overcome when *Pfaltz* introduced iridium-based catalysts for the hydrogenation of unfunctionalized olefins,^[4] inspired by the work of *Crabtree* who had demonstrated the application of iridium complexes in the homogeneous hydrogenation of alkenes.^[5]

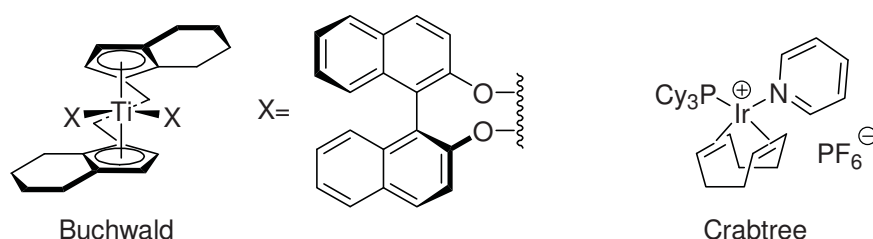
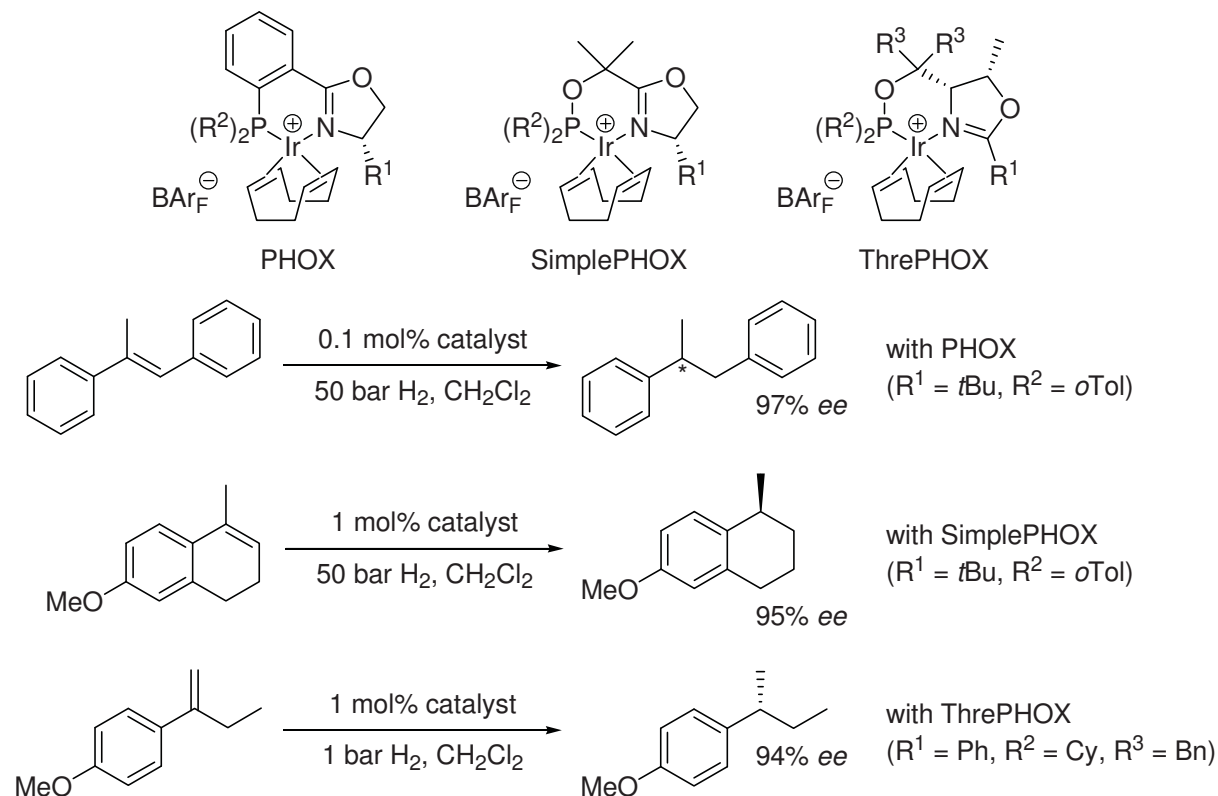


Figure 3.1. Complexes for the hydrogenation of unfunctionalized olefins.

The asymmetric version of *Crabtree's* catalyst, introduced by *Pfaltz*, contained a chiral oxazoline unit tethered to a phosphine (Scheme 3.1). These phosphino-oxazolines (PHOX) gave very good results in the hydrogenation of imines and unfunctionalized alkenes and were readily accessible since the stereogenic center is derived from commercially available chiral aminoalcohols. Today, several variants of the initial PHOX structure have been developed.^[6]

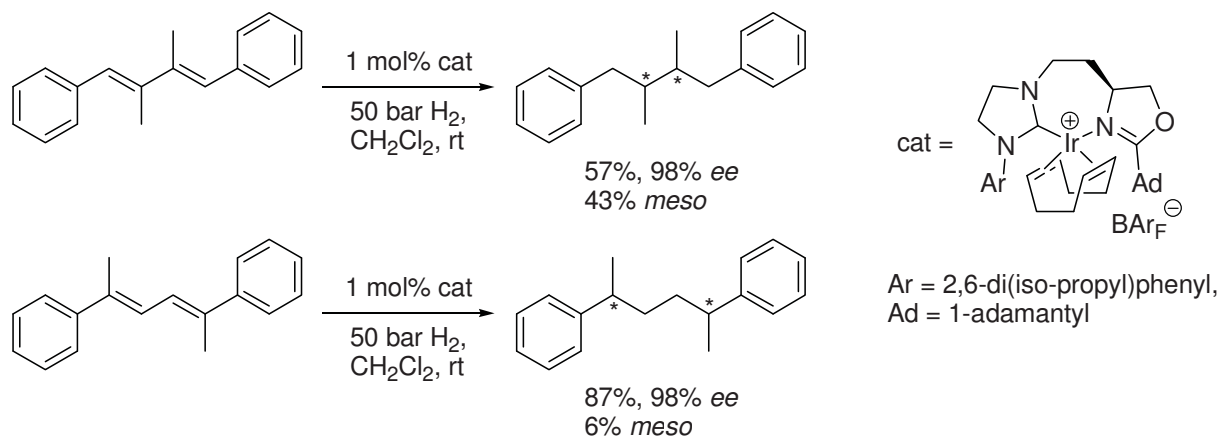
The phosphinite-containing complexes SimplePHOX^[7] and ThrePHOX^[8] are two examples of these that have been successfully applied in the hydrogenation of unfunctionalized olefins.



Scheme 3.1. Hydrogenation of unfunctionalized olefins with phosphino-oxazoline-Ir complexes.

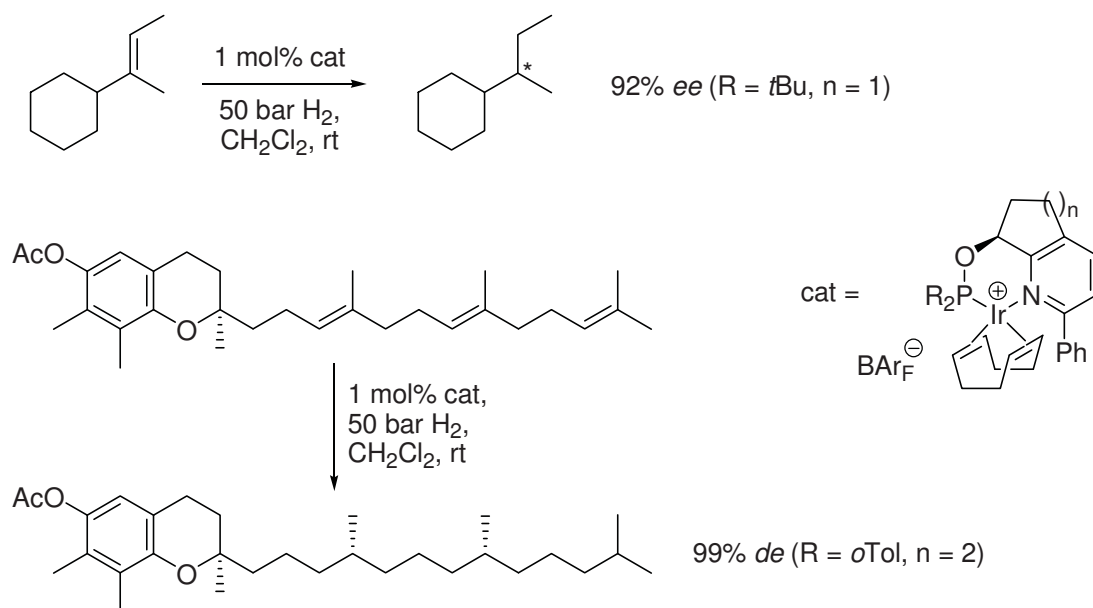
The complex types depicted in Scheme 3.1 were able to convert trisubstituted double bonds of different substitution patterns, terminal olefins and imines into their hydrogenation products with a high level of asymmetric induction at low catalyst loading. Nevertheless, the limitations of these catalysts became apparent with other substrate classes. The lack of any aromatic group reduced the enantioselectivity substantially, conjugated alkenes were poor substrates, and tetrasubstituted olefins showed low reactivity and selectivity in many cases. Further investigations into Ir-based systems resulted in the discovery of complexes which could overcome these limitations.

Iridium complexes of *N*-heterocyclic carbenes, reported by *Burgess*, hydrogenate conjugated double bonds with high enantioselectivity (Scheme 3.2), but the reaction is still problematic depending on the substitution pattern.^[9]



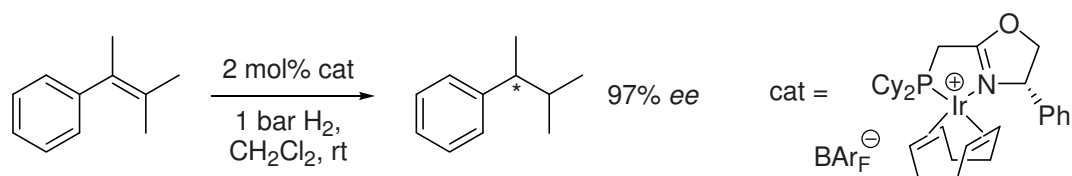
Scheme 3.2. Asymmetric hydrogenation of conjugated dienes.

Alkyl-substituted olefins were problematic substrates for a long time, since they lack any possibility of interaction with the catalyst except sterics. The development of tetrahydroquinoline-based phosphinite ligands by *Pfaltz*, which were also very selective with other substrates, gave catalysts exhibiting high enantioselectivity with these unfunctionalized compounds (Scheme 3.3).^[10] Applying these kinds of complexes (*E*)-1-cyclohexyl-1-methylpropene was hydrogenated with 97% *ee*, and even double bonds in a simple alkyl-chain as in the vitamin E precursor γ -tocotrienyl acetate were reduced with high selectivity.^[11]



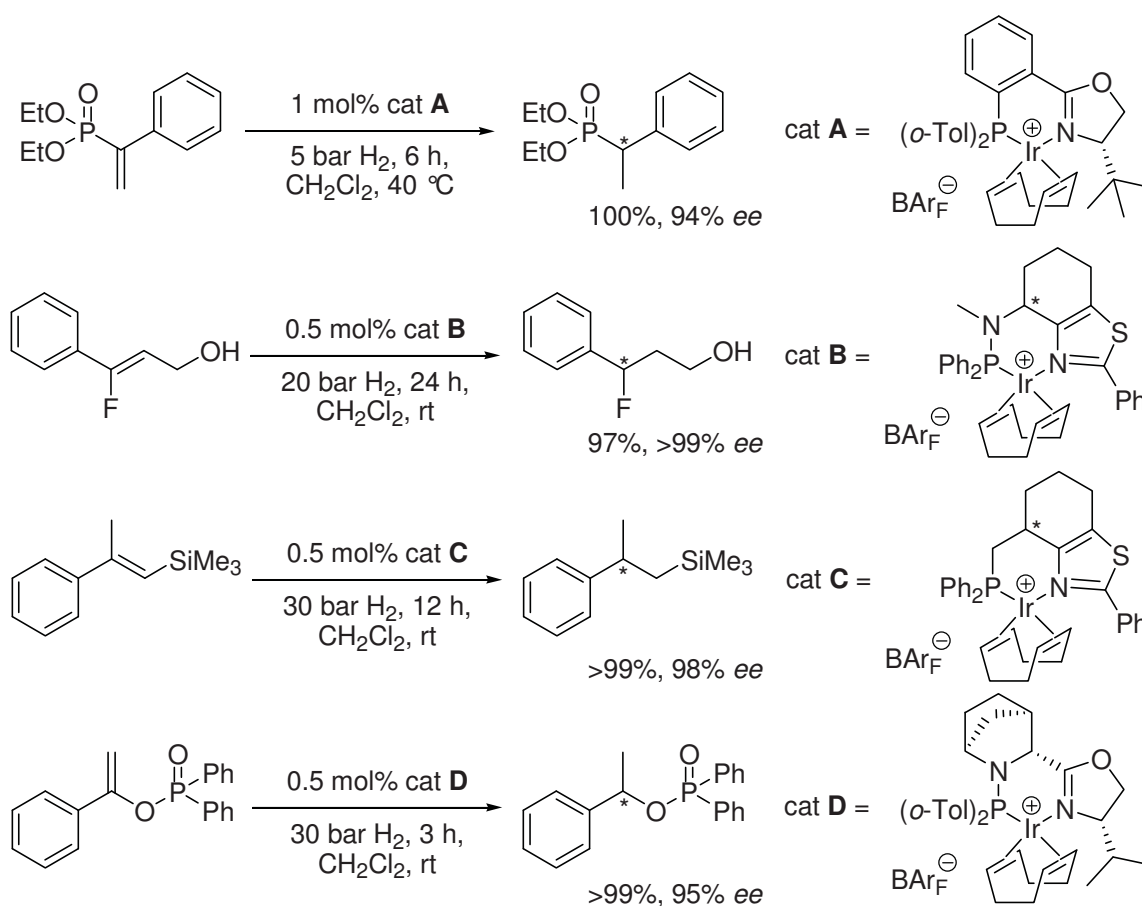
Scheme 3.3. Asymmetric hydrogenation of purely alkyl-substituted double bonds.

The reduction of tetrasubstituted alkenes with good selectivity was recently achieved, using a modified PHOX-catalyst with a reduced chelate-ring size. Among other tetrasubstituted olefins, the model-substrate shown in Scheme 3.4 could be hydrogenated with 97% *ee*.^[12]



Scheme 3.4. Asymmetric hydrogenation of a tetrasubstituted olefin.

Because of the high selectivity in the P,N-iridium-complex catalyzed asymmetric hydrogenation of unfunctionalized double bonds, this catalyst system has also been applied to alkenes with weakly coordinating functional groups (Scheme 3.5).^[13]



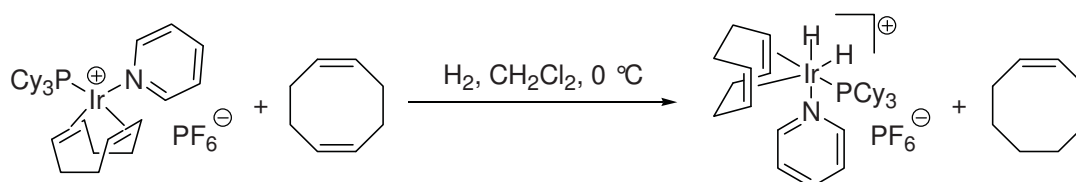
Scheme 3.5. Asymmetric hydrogenation of olefins with weakly coordinating functional groups.

For example, vinyl phosphates could be hydrogenated with Ir-PHOX catalysts,^[14] fluoroalkenes^[15] and unsaturated silanes^[16] were selectively reduced with thiazole-based complexes and enol phosphinates gave the reduced product with a phosphoramidite-oxazoline-iridium complex.^[17]

3.1.2 Mechanism

3.1.2.1 The Catalytic Cycle

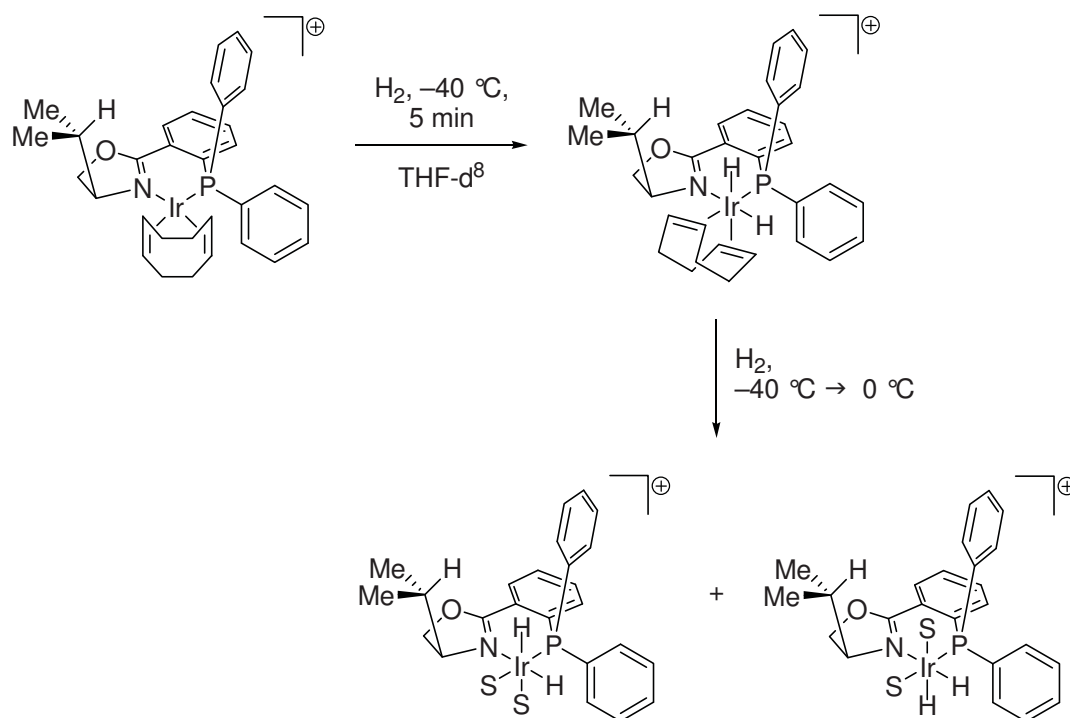
Unlike the Rh- and Ru-catalyzed asymmetric hydrogenation, the catalytic cycle of the iridium-catalyzed hydrogenation of unfunctionalized olfines is not yet fully understood.^[1a,6b,13,18] The first investigation in this field was performed by *Crabtree* who could identify a iridium-dihydride complex as a product of the exposure of $[\text{Ir}(\text{pyridine})\text{PCy}_3(\text{cod})]\text{PF}_6$ to dihydrogen in the presence of 1,5-cyclooctadiene (Scheme 3.6).^[19]



Scheme 3.6. Formation of a iridium-dihydride complex with *Crabtree's* catalyst.

Studies on chiral iridium-species were carried out with a PHOX-complex (Scheme 3.7).^[20] In THF the iridium-PHOX complex forms at low temperature a stable dihydride upon exposure to dihydrogen. This intermediate, even stable at $0\text{ }^\circ\text{C}$, was characterized by NMR-spectroscopy and the positions of the hydrides were confirmed to be both *cis* to the phosphorus atom as already described by *Crabtree*. At $-40\text{ }^\circ\text{C}$ the 1,5-cyclooctadiene ligand is still coordinated to the iridium-center, but upon raising the temperature under a hydrogen atmosphere the double bonds are hydrogenated and the formation of dihydride-solvate-complexes was observed. Two isomers were identified in the reaction mixture and the

hydrides were assigned to occupy positions *cis* to the phosphine ligand and *trans* to the nitrogen-atom.



Scheme 3.7. Observed dihydride species with Ir-PHOX complexes. S = THF.

The reaction had to be carried out in THF to obtain a clean reaction. In dichloromethane, the standard solvent for hydrogenation, the spectrum showed a complex mixture of hydrido complexes which could not be analyzed. Since the catalytic hydrogenation of unfunctionalized olefins does not proceed in coordinating solvents like THF, the prepared dihydride species could not be proven to be catalytically active. A computational study involving the iridium-PHOX complex shown in Scheme 3.7 and dichloromethane as solvent confirmed the observed dihydride species to be energetically favored over other possible isomers.^[20]

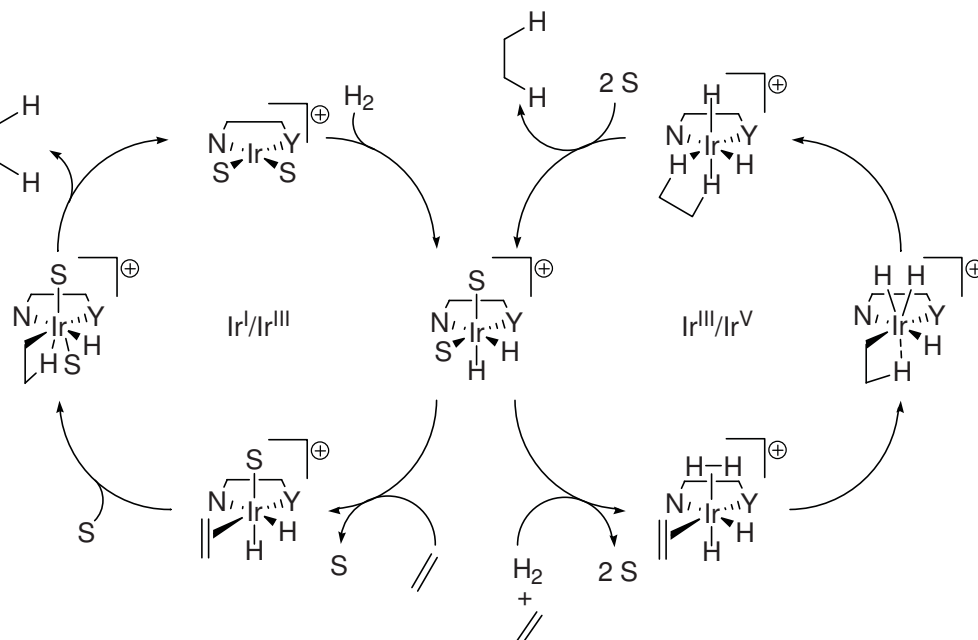
In order to gain insight into the full catalytic cycle, several groups have performed experimental and computational studies. Mechanistic pathways computed by *Brandt* and *Andersson*^[21] and by *Burgess* and *Hall*^[22] involve Ir^{III} and Ir^V intermediates. Their proposed catalytic cycle is shown in Scheme 3.8 (right hand side). Experimental evidence for a mechanism through Ir^I and Ir^{III} species (Scheme 3.8, left hand side) has been collected by mass spectrometry and NMR-spectroscopy. *Chen* used gas-phase MS to study the hydrogenation of styrene with an Ir-PHOX complex.^[23] The observed mass signals corresponded to species expected to be involved in the catalytic cycle. The authors found the

elementary steps to be reversible under gas-phase conditions and concluded from deuteration experiments the absence of polyhydrides as postulated for the Ir^{III}/Ir^V-cycle. *para*-Hydrogen induced polarization (PHIP) NMR-spectroscopy, carried out by *Buriak*, suggested that the hydrogen atoms are added pairwise, indicative of an Ir^I/Ir^{III}-mechanism.^[24] As noted by the authors, this experiment cannot exclude the non-pairwise hydrogen addition, operating as a parallel pathway.

There is no evidence to rule out one of the two proposed catalytic cycles. In view of the possibility, that, upon change of the catalyst, the substrate or reaction conditions, the relative energies of the intermediates shift to favor a different mechanism, both catalytic cycles could operate, with the dihydride-solvate complex as the common intermediate.

In the Ir^I/Ir^{III}-catalytic cycle the dihydride-solvate complex exchanges a solvent molecule for an alkene to form an olefin-dihydride species. Addition of one hydride to the double bond accompanied by coordination of a solvent molecule gives an alkyl-hydride complex. Reductive elimination forms the alkane and an Ir^I-solvate complex. Addition of dihydrogen regenerates the dihydride-solvate complex thus closing the catalytic cycle.

The Ir^{III}/Ir^V-mechanism is assumed to proceed via addition of dihydrogen and an olefin to the dihydride-solvate complex to give a polyhydride-species. This undergoes formation of an Ir^V-alkyl-trihydride complex followed by reductive elimination to liberate the hydrogenation product and reform the dihydride-solvate complex.

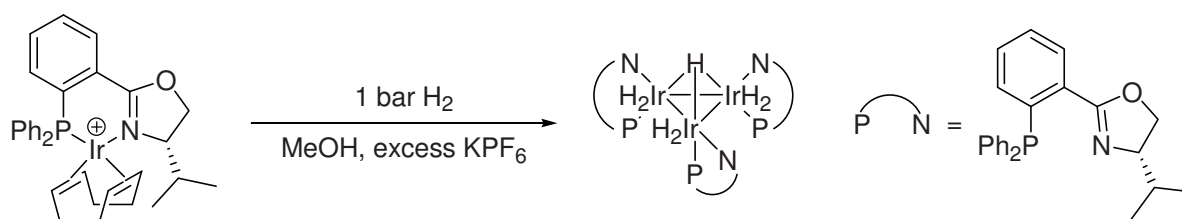


Scheme 3.8. Possible catalytic cycles for the Ir-catalyzed hydrogenation of unfunctionalized olefins.^[13] S = solvent, Y = phosphine or carbene.

Models have been developed to predict the enantioselectivity of a given complex.^[22, 25] In the examples described they are consistent with the observation that tetrasubstituted double bonds, trisubstituted alkenes with the two largest substituents in a *cis*-configuration and terminal olefins are all difficult substrates. Given that even these substrates can nowadays be hydrogenated with good enantioselectivity,^[6b] the general applicability of this model for ligand design is questionable at best.

3.1.2.2 The Counter-Ion Effect

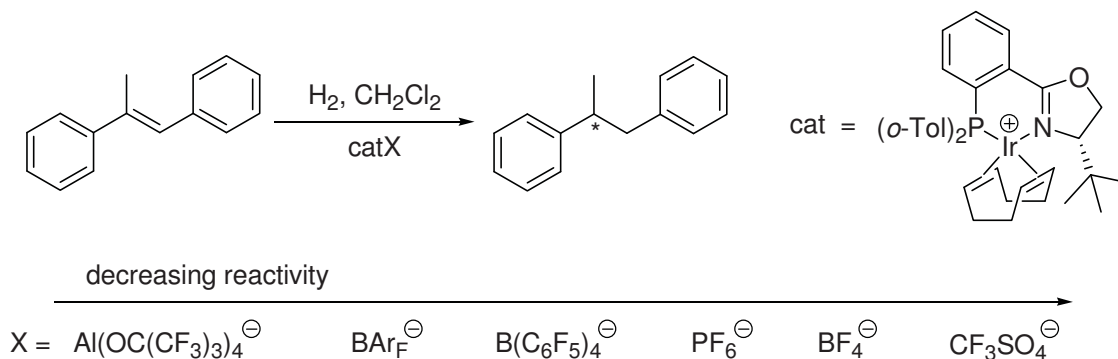
Initially, the iridium-catalyzed hydrogenation of unfunctionalized olefins required 4 mol% catalyst to obtain full conversion of the substrates.^[4a] The comparable high catalyst loading was necessary due to deactivation of the catalyst during the hydrogenation reaction. A similar behaviour had also been observed by *Crabtree* before and he identified a trimeric iridium complex as the catalytically inactive deactivation product.^[5b] NMR analysis also suggested the involvement of such hydride species in the deactivation of Ir-PHOX catalysts. In further studies this trimeric hydride-complex could be isolated and characterized by X-ray crystallography and NMR-spectroscopy (Scheme 3.9).^[26] Attempts to regenerate an active catalyst from this complex failed.



Scheme 3.9. Formation of a trimeric iridium-hydride complex.

The breakthrough to solve the problem of deactivation came by the introduction of a bulky, apolar and extremely weak coordinating counterion.^[27] Iridium-PHOX catalysts with tetrakis(3,5-bis(trifluoromethyl)phenyl)borate (BAR_F) as the counterion exhibited high stability under the reaction conditions and were less sensitive towards moisture. A kinetic study with different counterions showed that tetrakis(perfluoro-*tert*-butoxy)aluminate and

BAr_F were equally active while anions such as tetrafluoroborate and triflate gave only low conversion (Scheme 3.10).^[28]



Scheme 3.10. Counterion-dependent hydrogenation performance.

NMR-experiments involving pulse gradient spin-echo (PGSE) diffusion data and ^{19}F heteronuclear Overhauser effect spectroscopy (HOESY) of the precatalyst have been carried out,^[29] and the origin of this effect has been elucidated by kinetic studies.^[28]

Kinetic experiments showed a first order rate dependence on olefin concentration with the PF_6^- -counterion and a rate order close to zero with the BAr_F^- salt. The slower reaction of the alkene with the PF_6^- -containing catalyst may be explained by the specific interaction of the anion with the oxazoline unit blocking the approach of the olefin. The BAr_F^- -ion does not interfere with the alkene coordination, and therefore, the catalyst remains saturated with olefin even at low substrate concentration. Moreover, the slower reaction of the PF_6^- -salt with the olefin could explain its higher tendency for deactivation.^[6b] Assuming the deactivation is due to the formation of an inactive trimeric iridium-hydride complex, the important step during the catalytic cycle is the reaction of the Ir-hydride intermediate with the olefin. If this reaction is very fast, as is true for the BAr_F^- -salt, the hydrogenation dominates over the deactivation pathway. In the case of the PF_6^- -counterion, the olefin reacts more slowly and the deactivation pathway becomes an important competing process.

3.2 Objectives of this Work

As described in Section 2.2.1.1, the lithiated triarylphosphine **90** undergoes a highly stereoselective reaction with menthylphosphine dichloride (**97**). This addition reaction requires a sterically hindered nucleophile to proceed with good selectivity.^[30] Phenyloxazolines are structurally similar to **90** since both contain, when lithiated, quite a large substituent in the position *ortho* to the nucleophilic carbon atom (Figure 3.2).

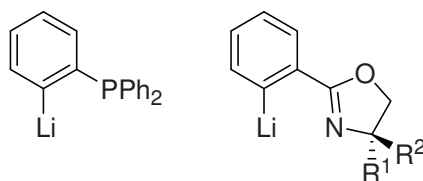
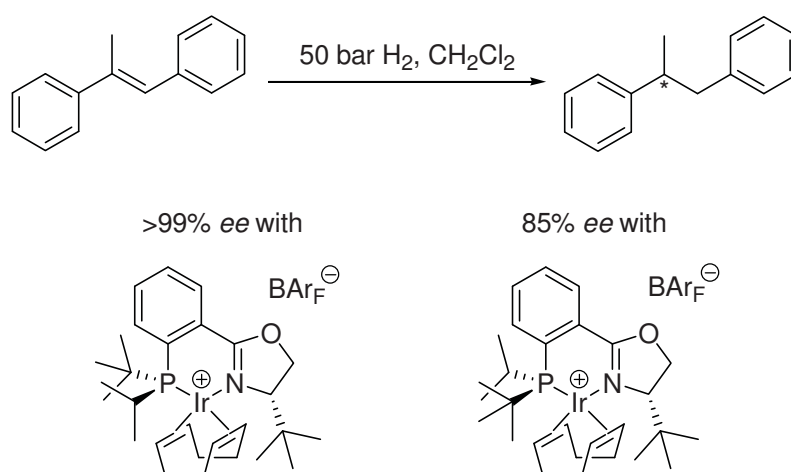


Figure 3.2. Structural similarities of lithiated **90** and lithiated phenyloxazolines.

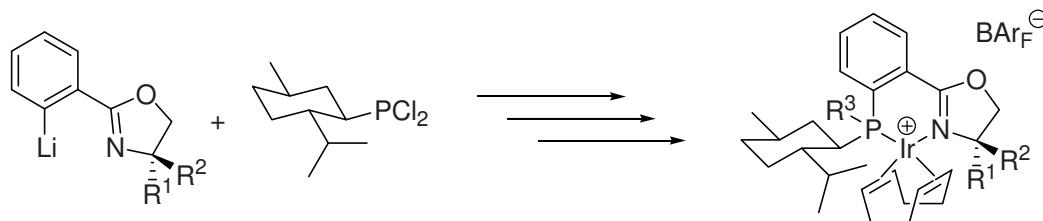
The reaction of phenyloxazolines with menthylphosphine dichloride would finally lead to PHOX-ligands with a stereogenic phosphorus atom. Ir-PHOX complexes with a chiral phosphorus atom have already been prepared and hydrogenation experiments have been carried out. The results showed that the stereogenic center at the oxazoline ring dominates the outcome of the reaction, whereas the configuration at the phosphorus atom plays a minor role but still leads to matched/mismatched effects (Scheme 3.11).^[31]



Scheme 3.11. Previous results with P-stereogenic PHOX-complexes.

However, the preparation of these ligands required the separation of the diastereoisomers by column chromatography or semipreparative chiral HPLC and therefore protection and

deprotection steps. A diastereoselective synthesis of P-stereogenic PHOX-ligands starting from a phosphine dichloride with a chiral menthyl substituent would avoid these separation steps and therefore simplify the preparation (Scheme 3.12).



Scheme 3.12. Synthetic strategy for the formation of menthyl-containing PHOX-ligands.

3.3 References

- [1] a) X. Cui, K. Burgess, *Chem. Rev.* **2005**, *105*, 3272-3296; b) K. Källström, I. Munslow, P. G. Andersson, *Chem. Eur. J.* **2006**, *12*, 3194-3200.
- [2] a) E. Cesarotti, R. Ugo, H. B. Kagan, *Angew. Chem.* **1979**, *91*, 842; b) L. A. Paquette, J. A. McKinney, M. L. McLaughlin, A. L. Rheingold, *Tetrahedron Lett.* **1986**, *27*, 5599; c) L.A. Paquette, M. R. Sivik, E. I. Bzowej, K. J. Stanton, *Organometallics* **1995**, *14*, 4865; d) R. L. Haltermann, K. P. C. Vollhardt, M. E. Welker, *J. Am. Chem. Soc.* **1987**, *109*, 8105; e) V. P. Conticello, L. Brard, M. A. Giardello, Y. Tsuji, M. Sabat, C. L. Stern, T. J. Marks, *J. Am. Chem. Soc.* **1992**, *114*, 2761; f) C. M. Haar, C. L. Stern, T. J. Marks, *Organometallics* **1996**, *15*, 1765; g) P. Beagly, P. J. Davies, A. J. Blacker, C. White, *Organometallics* **2002**, *21*, 5852.
- [3] R. D. Broene, S. L. Buchwald, *J. Am. Chem. Soc.* **1993**, *115*, 12569-12570.
- [4] a) A. Lightfoot, P. Schnider, A. Pfaltz, *Angew. Chem. Int. Ed.* **1998**, *37*, 2897-2899; b) A. Pfaltz, J. Blankenstein, R. Hilgraf, E. Hörmann, S. McIntyre, F. Menges, M. Schönleber, S. P. Smidt, B. Wüstenberg, N. Zimmermann, *Adv. Synth. Catal.* **2002**, *345*, 33-44.
- [5] a) R. H. Crabtree, H. Felkin, G. E. Morris, *J. Organomet. Chem.* **1977**, *141*, 205; b) R.H. Crabtree, *Acc. Chem. Res.* **1979**, *12*, 331.
- [6] a) S. Bell, A. Pfaltz in *Handbook of Homogeneous Hydrogenation*, J. G. de Vries, C. J. Elsevier Eds., Wiley-VHC, Weinheim, **2007**, 1029-1048; b) S. J. Roseblade, A. Pfaltz, *Acc. Chem. Res.* **2007**, *40*, 1402-1411.
- [7] S. P. Smidt, F. Menges, A. Pfaltz, *Org. Lett.* **2004**, *6*, 2023-2026.
- [8] a) J. Blankenstein, A. Pfaltz, *Angew. Chem. Int. Ed.* **2001**, *40*, 4445-4447; b) F. Menges, A. Pfaltz, *Adv. Synth. Catal.* **2002**, *334*, 4044.
- [9] a) X. Cui, K. Burgess, *J. Am. Chem. Soc.* **2003**, *125*, 14212; b) X. Cui, J. W. Ogle, K. Burgess, *Chem. Commun.* **2005**, 672-674.
- [10] S. Kaiser, S. P. Smidt, A. Pfaltz, *Angew. Chem. Int. Ed.* **2006**, *45*, 5194-5197.
- [11] S. Bell, B. Wüstenberg, S. Kaiser, F. Menges, T. Netscher, A. Pfaltz, *Science* **2006**, *311*, 642-644.
- [12] M. G. Schrems, E. Neumann, A. Pfaltz, *Angew. Chem. Int. Ed.* **2007**, *46*, 8274-8276.
- [13] T. L. Church, P. G. Andersson, *Coord. Chem. Rev.* **2008**, *252*, 513-531.
- [14] N. S. Goulioukina, T. M. Dolgina, G. N. Bondarenko, I. P. Beletskaya, M. M. Ilyin,

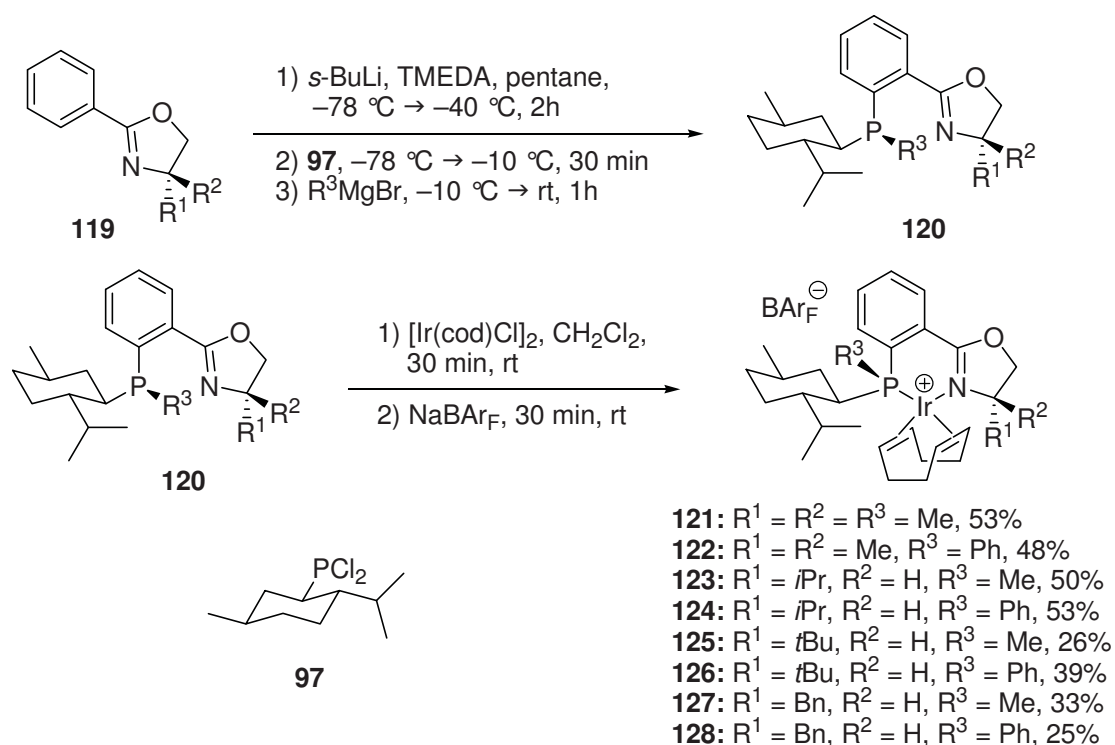
- V. A. Davankov, A. Pfaltz, *Tetrahedron: Asymmetry* **2003**, *14*, 1397.
- [15] M. Engman, J. S. Diesen, A. Paptchikhine, P. G. Andersson, *J. Am. Chem. Soc.* **2007**, *129*, 4536.
- [16] K. Källström, I. J. Munslow, C. Hedberg, P. G. Andersson, *Adv. Synth. Catal.* **2006**, *348*, 2575.
- [17] P. Cheruku, S. Gohil, P. G. Andersson, *Org. Lett.* **2007**, *9*, 1659.
- [18] S. J. Roseblade, A Pfaltz *C. R. Chimie*, **2007**, *10*, 178-187.
- [19] a) R. H. Crabtree, R. J. Uriarte, *Inorg. Chem.* **1983**, *22*, 4152; b) M. J. Burk, M. P. McGrath, R. Wheeler, R. H. Crabtree, *J. Am. Chem. Soc.* **1988**, *110*, 5034.
- [20] C. Mazet, S. P. Smidt, M. Meuwly, A. Pfaltz, *J. Am. Chem. Soc.* **2004**, *126*, 14176-14181.
- [21] P. Brandt, C. Hedberg, P. G. Andersson, *Chem. Eur. J.* **2003**, *9*, 339.
- [22] Y. Fan, X. Cui, K. Burgess, M. B. Hall, *J. Am. Chem. Soc.* **2004**, *126*, 16688.
- [23] R. Dietiker, P. Chen, *Angew. Chem. Int Ed.* **2004**, *43*, 5513.
- [24] L. D. Vázquez-Serrano, B. T. Owens, J. M. Burriak, *Chem. Commun.* **2002**, 2518.
- [25] a) K. Källström, C. Hedberg, P. Brandt, L. K. Hansen, P. G. Andersson, *J. Am. Chem. Soc.* **2004**, *126*, 14308; b) C. Hedberg, K. Källström, P. Brandt, L. K. Hansen, P. G. Andersson, *J. Am. Chem. Soc.* **2006**, *128*, 2995.
- [26] S. P. Smidt, A. Pfaltz, E. Martínez-Viviente, P. S. Pregosin, A. Albinati, *Organometallics* **2003**, *22*, 1000-1009.
- [27] For a review of anions of this type see: I. Krossing, I. Raabe, *Angew. Chem. Int. Ed.* **2004**, *43*, 2066-2090.
- [28] S. P. Smidt, N. Zimmermann, M. Studer, A. Pfaltz, *Chem. Eur. J.* **2004**, *10*, 4685-4693.
- [29] D. Drago, P. S. Pregosin, A. Pfaltz, *Chem. Commun*, **2002**, 286.
- [30] For an example of a less selective addition reaction see: G. Haegele, W. Kueckelhaus, G. Tossing, J. Seega, R. K. Harris, C. J. Creswell, P. T. Jageland, *J. Chem. Soc., Dalton Trans.: Inorg. Chem.* **1987**, 795-805.
- [31] S. P. Smidt, PhD-Thesis, *Iridium-Catalysed Enantioselective Hydrogenation – New P,N Ligands and Mechanistic Investigations*, **2003**, University of Basel.

3.2 Synthesis and Hydrogenation Experiments

3.2.1 Preparation of P-Chiral Phosphino-Oxazoline-Iridium Complexes

The synthesis started with the *ortho*-metalation of 2-phenyl-oxazolines **119** with *sec*-butyllithium and *N,N,N,N*-tetramethylethylenediamine in pentane. Addition of menthylphosphine dichloride (**97**), derived from (–)-menthol, followed by reaction with methylmagnesium or phenylmagnesium bromide gave the phosphino-oxazolines **120**. The introduction of larger groups with the corresponding *Grignard*-reagent was not possible. *iso*-Propylmagnesium bromide was too sterically hindered and no reaction occurred with the intermediate menthyl-phenyloxazoline-phosphine chloride. Due to the air-sensitivity of these phosphines they were not purified but only filtered through a plug of aluminium oxide. The ³¹P-NMR spectra of the phosphino-oxazolines basically showed only one signal in each case, indicating a stereoselective reaction. However, when the phosphino-oxazolines **120** were reacted with [Ir(cod)Cl]₂ and NaBAR_F, the overall yields of the corresponding iridium-complexes **121-128** only ranged between 25% and 50% (Scheme 3.13). An increased reaction time produced no improvement.

Complexes **121** and **122** contain the stereogenic phosphorus atom as the only stereogenic center. The results of hydrogenation reactions with these catalysts should clearly indicate the influence of the phosphorus atom configuration towards the enantioselectivity of the iridium-complex.



Scheme 3.13. Synthesis of iridium-phosphino-oxazoline complexes.

The complexes were isolated as single diastereoisomers and the absolute configuration was assigned according to the four X-ray structures obtained (Figure 3.3, Figure 3.4, Figure 3.5 and Figure 3.6).



Figure 3.3. Crystal structure of **123**. A second molecule in the unit cell, co-crystallized CH_2Cl_2 and the BAR_F -counterions are omitted for clarity.

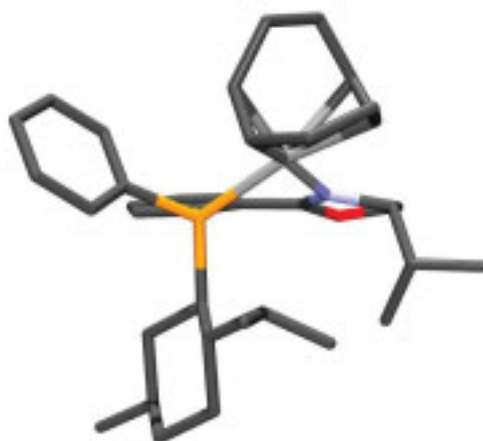


Figure 3.4. Crystal structure of **124**. A second molecule in the unit cell and the BAr_F -counterions are omitted for clarity.



Figure 3.5. Crystal structure of **125**. Three other molecules in the unit cell and the BAr_F -counterions are omitted for clarity.

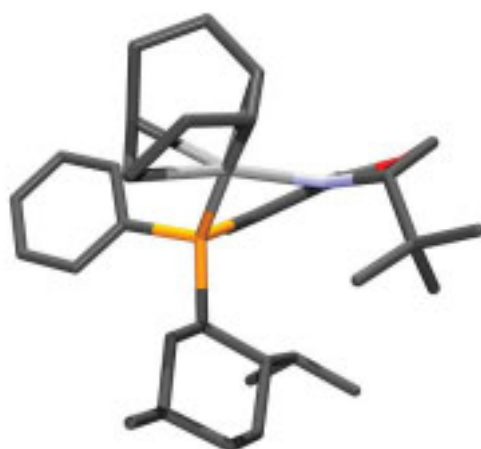
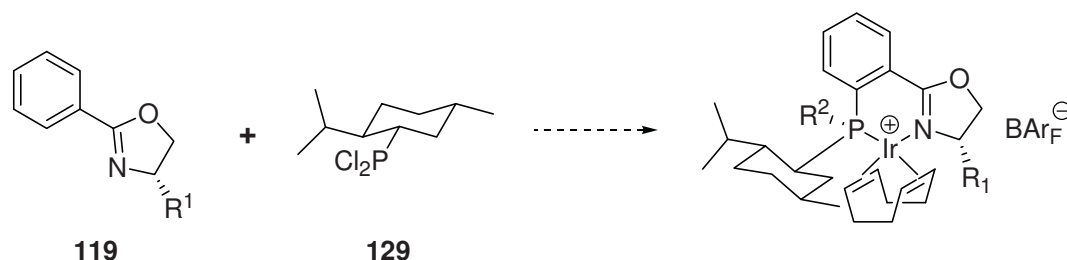


Figure 3.6. Crystal structure of **126**. A second molecule in the unit cell and the BAr_F -counterions are omitted for clarity.

In all cases, the menthyl group at the phosphorus atom and the substituent on the oxazoline ring show a *syn*-arrangement in the complex. The four solid state structures show similar geometries. The bite-angle is slightly larger in the complexes **124** and **126** (N-Ir-P: $\sim 87.5^\circ$) as compared to the methyl derivatives **123** and **125** (N-Ir-P: $\sim 85.5^\circ$).

The synthesis of diastereoisomeric ligands which should exhibit a *trans*-positioning of these groups was supposed to combine the already used phenyloxazolines **119** with menthylphosphine dichloride (**129**), derived from the menthyl chloride (**130**) prepared from (+)-menthol. As expected, the synthesis of **129** proceeded without deviation from the preparation of **97**. Unfortunately, the diastereoselectivity decreased tremendously in the next step and the phosphino-oxazolines were obtained as a 1:5 mixture of diastereoisomers. Neither the ligands nor the complexes could be purified by column chromatography or crystallization. An attempt to purify a borane protected phosphino-oxazoline by semipreparative chiral HPLC resulted in only a low amount of recovered compound. Moreover, the complexation following the deprotection step proceeded with very low yield and did not give a pure compound.



Scheme 3.14. Attempted synthesis of iridium-phosphinoxazoline complexes.

The diastereoselectivity of the addition reaction of menthylphosphine dichloride to phenyloxazolines with a stereogenic center shows a dependence on the combinations of the enantiomers employed, leading to a matched and mismatched case. Whereas the connection of the phosphine dichloride derived from (–)-menthol with oxazolines having (*S*)-configuration generates products of high diastereomeric purity, the employment of the enantiomeric phosphine dichloride results in a lower stereoselectivity. The high selectivity in the matched case is also an outcome of the inherent selectivity of the phosphine dichloride towards nucleophilic addition. When an achiral, bulky nucleophile, such as 1-(diphenylphosphino)-2-lithiobenzene, is used, the same configuration at the phosphorus-atom is generated as seen in the matched case reaction with phenyloxazolines (Figure 3.15).

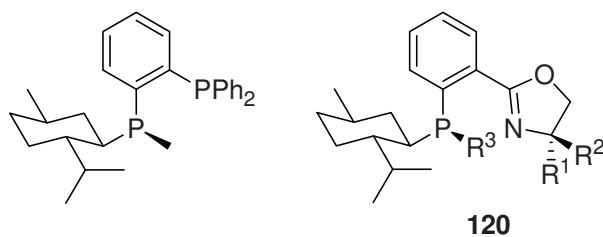


Figure 3.15. (–)-Menthyl-induced stereochemistry on the phosphorus atom.

3.2.2 Asymmetric Hydrogenation

The P-chiral phosphino-oxazoline-iridium complexes were employed in the asymmetric hydrogenation of various substrates (Figure 3.7).

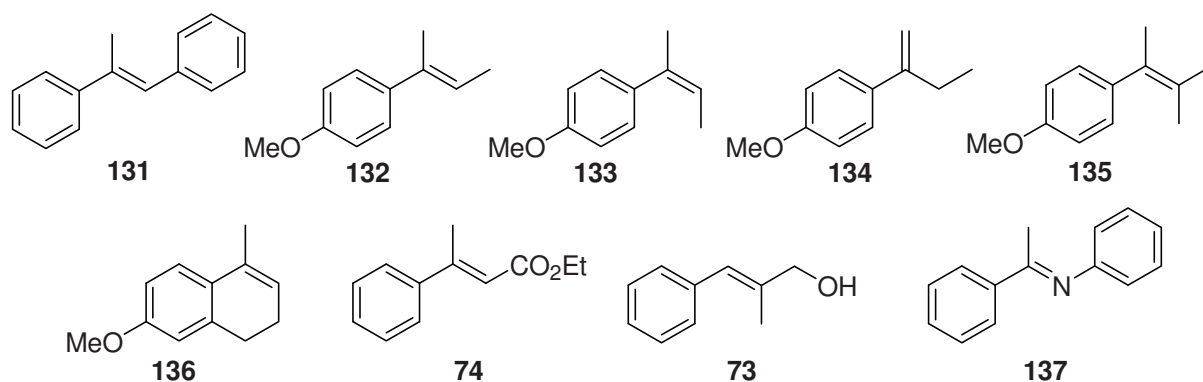
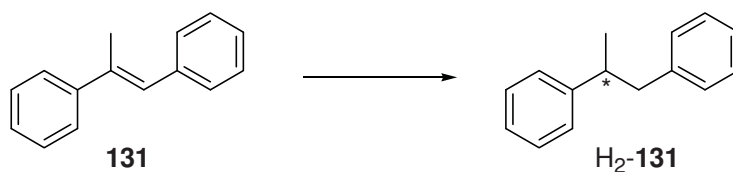


Figure 3.7. Substrates for the Ir-catalyzed asymmetric hydrogenation.

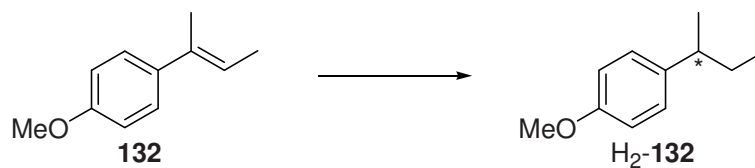
The substrate set consisted of unfunctionalized trisubstituted olefins with either different substitution patterns (**131**, **132**, **133**) or an endocyclic double bond (**136**). A terminal olefin (**134**) and a tetrasubstituted alkene (**135**) were also tested. Additionally, an α,β -unsaturated ester (**74**), an allylic alcohol (**73**) and a ketimine (**137**) were hydrogenated.

Table 3.1. Hydrogenation of *E*-1,2-diphenylpropene (**131**).

Entry ^a	Precatalyst	R	conv. [%] ^b	ee [%] ^c
1		Me (121)	84	rac.
2		Ph (122)	32	6 (<i>S</i>)
3		Me (123)	>99	78 (<i>R</i>)
4		Ph (124)	93	83 (<i>R</i>)
5		Me (125)	>99	63 (<i>R</i>)
6		Ph (126)	98	79 (<i>R</i>)
7		Me (127)	>99	46 (<i>R</i>)
8		Ph (128)	98	70 (<i>R</i>)

^aReaction was carried out in a 0.1 M CH₂Cl₂ solution with 1 mol% precatalyst at room temperature under 50 bar hydrogen pressure for 2 h. ^bDetermined by GC. ^cDetermined by chiral HPLC.

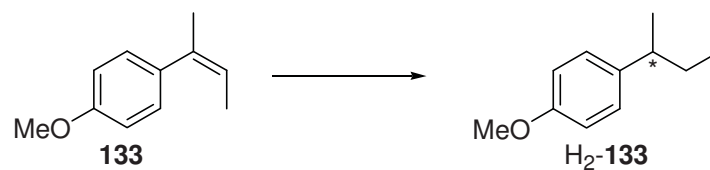
In the reduction of the stilbene **131**, the catalysts with a methyl-substituted phosphorus atom gave generally higher conversions than the phenyl-derivatives. The catalysts with a dimethyl-substituted oxazoline ring were of significantly reduced activity (Table 3.1, entries 1 and 2). These iridium complexes also showed almost no selectivity. Catalysts with a chiral center on the oxazoline ring performed better. Up to 83% *ee* were achieved with the *iso*-propyl-substituted complex **124** (entry 4). A phenyl substituent on the phosphorus atom generally led to higher enantioselectivities.

Table 3.2. Hydrogenation of *E*-2-(4-methoxyphenyl)-2-butene (**132**).

Entry ^a	Precatalyst	R	conv. [%] ^b	ee [%] ^b
1		Me (121)	>99	rac.
2		Ph (122)	>99	rac.
3		Me (123)	>99	85 (<i>R</i>)
4		Ph (124)	>99	76 (<i>R</i>)
5		Me (125)	>99	85 (<i>R</i>)
6		Ph (126)	>99	80 (<i>R</i>)
7		Me (127)	>99	90 (<i>R</i>)
8		Ph (128)	>99	83 (<i>R</i>)

^aReaction was carried out in a 0.1 M CH₂Cl₂ solution with 1 mol% precatalyst at room temperature under 50 bar hydrogen pressure for 2 h. ^bDetermined by chiral GC.

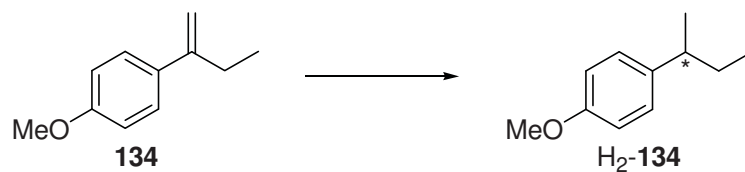
The olefin **132** was hydrogenated with complete conversion by all catalysts tested (Table 3.2). As observed before, the complexes with a geminal dimethyl group on the oxazoline gave no selective catalysts. In the other cases, a methyl-substituent on the phosphorus atom led to better selectivity than a phenyl-substituent. With the phenylalanine-derived complex **127** 90% *ee* were obtained (entry 7).

Table 3.3. Hydrogenation of *Z*-2-(4-methoxyphenyl)-2-butene (**133**).

Entry ^a	Precatalyst	R	conv. [%] ^b	ee [%] ^b
1		Me (121)	>99	8 (<i>S</i>)
2		Ph (122)	96	rac.
3		Me (123)	>99	rac.
4		Ph (124)	95	5 (<i>S</i>)
5		Me (125)	>99	9 (<i>R</i>)
6		Ph (126)	>99	12 (<i>R</i>)
7		Me (127)	>99	29 (<i>S</i>)
8		Ph (128)	>99	rac.

^aReaction was carried out in a 0.1 M CH₂Cl₂ solution with 1 mol% precatalyst at room temperature under 50 bar hydrogen pressure for 2 h. ^bDetermined by chiral GC.

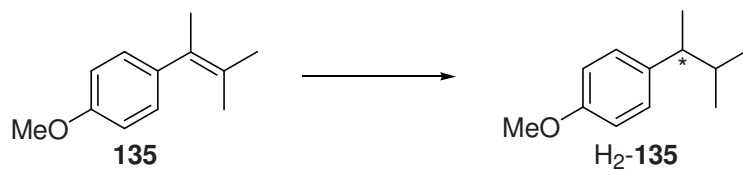
The *Z*-configured olefin **133** showed a distinctly different behaviour than its *E*-isomer **132** (Table 3.3). Although the conversions were usually complete, the selectivities were very low. Interestingly, the complexes with a *tert*-butyl-substituted oxazoline (**125**, **126**) favoured the same product configuration with both isomers **132** and **133** whereas complex **127** gave the opposite enantiomer.

Table 3.4. Hydrogenation of 2-(4-methoxyphenyl)-1-butene (**134**).

Entry ^a	Precatalyst	R	conv. [%] ^b	ee [%] ^b
1		Me (121)	>99	25 (<i>S</i>)
2		Ph (122)	>99	rac.
3		Me (123)	>99	74 (<i>S</i>).
4		Ph (124)	>99	63 (<i>S</i>)
5		Me (125)	>99	80 (<i>S</i>)
6		Ph (126)	>99	71 (<i>S</i>)
7		Me (127)	>99	87 (<i>S</i>)
8		Ph (128)	>99	84 (<i>S</i>)

^aReaction was carried out in a 0.1 M CH₂Cl₂ solution with 1 mol% precatalyst at room temperature under 1 bar hydrogen pressure for 2 h. ^bDetermined by chiral GC.

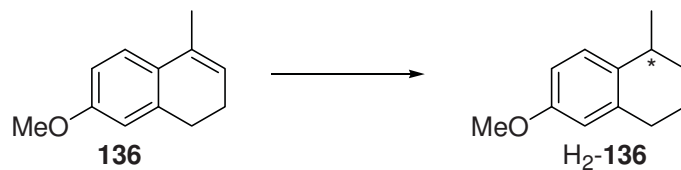
The hydrogenation of terminal olefin **134** was achieved at ambient pressure giving full conversion with all catalysts tested. The enantioselectivities of the dimethyloxazoline-derived catalysts were very low (Table 3.4 entries 1 and 2). On the other hand, up to 87% *ee* could be obtained with complex **127** (entry 7). A methyl-substituted phosphorus atom was beneficial for enantioselectivity. Reduction under 50 bar of hydrogen pressure gave only racemic product in every experiment.

Table 3.5. Hydrogenation of 2-(4-methoxyphenyl)-3-methyl-2-butene (**135**).

Entry ^a	Precatalyst	R	conv. [%] ^b	ee [%] ^b
1		Me (121)	16	8 (+)
2		Ph (122)	<1	-
3		Me (123)	<1	-
4		Ph (124)	4	9 (-)
5		Me (125)	<1	-
6		Ph (126)	<1	-
7		Me (127)	<1	-
8		Ph (128)	<1	-

^aReaction was carried out in a 0.1 M CH₂Cl₂ solution with 1 mol% precatalyst at room temperature under 50 bar hydrogen pressure for 2 h. ^bDetermined by chiral GC.

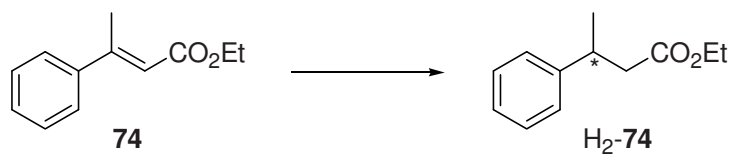
The tetrasubstituted olefin **135** showed only low reactivity towards the tested iridium complexes (Table 3.5). Only **121** and **124** gave measurable conversions accompanied by low selectivities.

Table 3.6. Hydrogenation of 7-methoxy-4-methyl-1,2-dihydro-naphthalene (**136**).

Entry ^a	Precatalyst	R	conv. [%] ^b	ee [%] ^c
1		Me (121)	60	13 (<i>S</i>)
2		Ph (122)	64	11 (<i>S</i>)
3		Me (123)	87	55 (<i>S</i>)
4		Ph (124)	84	44 (<i>S</i>)
5		Me (125)	73	39 (<i>S</i>)
6		Ph (126)	86	60 (<i>S</i>)
7		Me (127)	95	60 (<i>S</i>)
8		Ph (128)	96	50 (<i>S</i>)

^aReaction was carried out in a 0.1 M CH₂Cl₂ solution with 1 mol% precatalyst at room temperature under 50 bar hydrogen pressure for 2 h. ^bDetermined by GC. ^cDetermined by chiral HPLC.

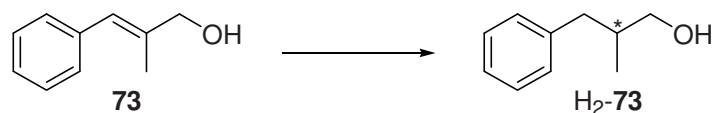
The hydrogenation results of the cyclic substrate **136** showed no clear trend (Table 3.6). On average, the conversions increase by changing the substitution on the oxazoline ring from dimethyl to *iso*-propyl, *tert*-butyl and benzyl. Comparing the substitution on the phosphorus atom with the same oxazoline group present, more active catalysts were also more selective but the preference of methyl or phenyl is different in each case. Again, the complexes with a dimethyl-substituted oxazoline exhibited significantly lower enantioselectivities (entries 1 and 2). The best result was achieved with complex **127** giving the hydrogenation product in 60% *ee* with 95% conversion (entry 7).

Table 3.7. Hydrogenation of ethyl *E*-2-methylcinnamate (**74**).

Entry ^a	Precatalyst	R	conv. [%] ^b	ee [%] ^b
1		Me (121)	84	72 (<i>R</i>)
2		Ph (122)	47	20 (<i>R</i>)
3		Me (123)	>99	86 (<i>R</i>)
4		Ph (124)	82	63 (<i>R</i>)
5		Me (125)	>99	91 (<i>R</i>)
6		Ph (126)	47	54 (<i>R</i>)
7		Me (127)	>99	79 (<i>R</i>)
8		Ph (128)	>99	69 (<i>R</i>)

^aReaction was carried out in a 0.1 M CH₂Cl₂ solution with 1 mol% precatalyst at room temperature under 50 bar hydrogen pressure for 2 h. ^bDetermined by chiral GC.

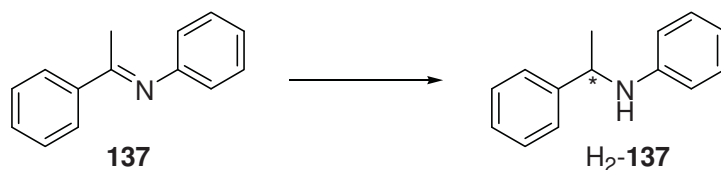
The asymmetric hydrogenation of ester **74** gave generally higher conversions with a methyl-substituted phosphorus atom, leading to full conversion except with complex **121** which still formed 84% of product (Table 3.7, entry 1). The more active catalysts also generated the saturated ester with higher enantioselectivities than the phenyl-derivatives. The best result was obtained with complex **125**, which gave full conversion and an enantiomeric excess of 91% (entry 5). Interestingly, the dimethylloxazoline-derived complex **121** gave not, as observed in the previous experiments, one of the least selective catalysts (entry 1). It outperformed all other phenyl-substituted complexes but was still inferior to the other methylphosphine-catalysts.

Table 3.8. Hydrogenation of ethyl *E*-2-methyl-3-phenylprop-2-enol (**73**).

Entry ^a	Precatalyst	R	conv. [%] ^b	ee [%] ^c
1		Me (121)	>99 ^d	n.d.
2 ^e		Me (121)	60 ^f	22 (–)
3		Ph (122)	>99 ^d	n.d.
4 ^e		Ph (122)	30 ^f	rac.
5		Me (123)	>99	87 (–)
6		Ph (124)	>99	80 (–)
7		Me (125)	>99 ^g	n.d.
8 ^e		Me (125)	92	67 (–)
9		Ph (126)	>99 ^g	n.d.
10 ^e		Ph (126)	>99	75 (–)
11		Me (127)	>99	83 (–)
12		Ph (128)	>99	80 (–)

^aReaction was carried out in a 0.1 M CH₂Cl₂ solution with 1 mol% precatalyst at room temperature under 50 bar hydrogen pressure for 2 h. ^bDetermined by GC. ^cDetermined by chiral HPLC. ^dMore than 80% side products were observed. ^eTFE as solvent. ^fUp to 10% side products were observed. ^g60% side products were observed.

In the hydrogenation of allylic alcohol **73**, clean conversions under standard conditions were only observed with the *iso*-propyl- (**123**, **124**) and benzyl-substituted (**127**, **128**) oxazolines (Table 3.8). To suppress the formation of side products in the other cases, 2,2,2-trifluoroethanol had to be used as solvent. 2,2,2-Trifluoroethanol as an additive was not sufficient. The conversions were usually complete except for the dimethyloxazoline-derived complexes. In most cases a methyl-substituted phosphorus atom was superior and the best selectivity was obtained with complex **123** with an enantiomeric excess of 87%.

Table 3.9. Hydrogenation of ethyl *E*-phenyl-(1-phenylethylidene)amine (**137**).

Entry ^a	Precatalyst	R	conv. [%] ^b	ee [%] ^c
1		Me (121)	>99	59 (<i>R</i>)
2		Ph (122)	>99	45 (<i>R</i>)
3		Me (123)	>99	71 (<i>R</i>)
4		Ph (124)	>99	77 (<i>R</i>)
5		Me (125)	>99	75 (<i>R</i>)
6		Ph (126)	>99	71 (<i>R</i>)
7		Me (127)	>99	55 (<i>R</i>)
8		Ph (128)	>99	62 (<i>R</i>)

^aReaction was carried out in a 0.1 M CH₂Cl₂ solution with 1 mol% precatalyst at room temperature under 50 bar hydrogen pressure for 2 h. ^bDetermined by GC. ^cDetermined by chiral HPLC.

The imine **137** was a very reactive substrate giving full conversion with all catalysts tested (Table 3.9). Changing between a methyl- and a phenyl-substituted phosphorus atom had an effect on the enantioselectivity of the catalyst but the impact was different for each oxazoline. The best selectivity was given by complex **124**, forming the amine product with 77% *ee*. As already seen in the reduction of the unsaturated ester **74**, the dimethyloxazoline-derived complexes **121** and **122** were only slightly inferior compared to the general observations made in the hydrogenation reactions with the other substrates.

Since the Ir-catalyzed reduction of imines has been proposed to proceed via different intermediates than the hydrogenation of unfunctionalized olefins,^[1] the chirality on the phosphorus atom has a different influence. Whereas the configuration of the phosphine seems to play a minor role in the hydrogenation of olefins, the selectivity obtained in the imine-reduction implies that the structures of the catalytic intermediates are substantially different. In this respect, the results of the hydrogenation of ester **74** (Table 3.7) also suggest alternative catalytic intermediates for the Ir-catalyzed reduction, because complex **121**, poorly selective in the other cases, was able to achieve 72% *ee*.

3.2.3 Influence of Temperature in the Reduction of 2-(4-Methoxyphenyl)-1-butene

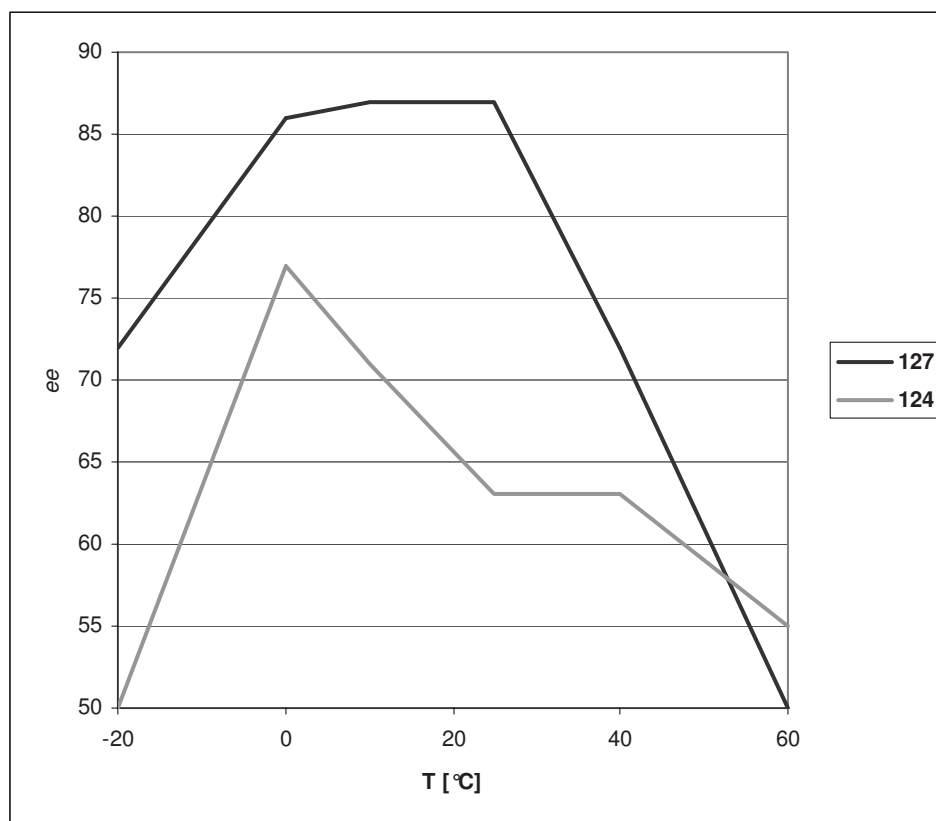


Figure 3.8. Temperature dependent enantioselectivity in the hydrogenation of **134**.

Table 3.10. Hydrogenation of **134** at variable temperature.

Entry ^a	T [°C]	Precatalyst	ee [%] ^c	Precatalyst	ee [%] ^c
1	-20		72		50
2	0		86		77
3	10		87		-
4	25		87		63
5 ^c	40		72		63
6 ^c	60		59		55

^aReaction was carried out in a 0.1 M CH₂Cl₂ solution with 1 mol% precatalyst under 1 bar hydrogen pressure for 2 h, giving full conversion in all cases. ^bDetermined by chiral GC. ^cClCH₂CH₂Cl as solvent.

Since the hydrogenation of the terminal olefin **134** with the types of catalysts tested in this work gave high enantioselectivities compared to other PHOX-ligands,^[2] a brief look at variable conditions was taken. Changing the temperature in the hydrogenation at ambient pressure had a pronounced effect on the selectivity (Figure 3.8, Table 3.10). Due to the boiling point of dichloromethane, reactions above room temperature had to be carried out in 1,2-dichloroethane. An experiment comparing these two reaction media at ambient temperature showed no solvent effect. Whereas up to 87% *ee* was obtained when the reaction was carried out with complex **127** at room temperature, lowering and increasing the temperature had a disadvantageous effect in the enantiomeric excess. The same trend was observed for complex **124** for which 77% *ee* were obtained at 0 °C and the selectivities were worse at -20 °C or room temperature.

Similar observations involving olefin **134** have already been made with Ir-phosphino-oxazolin catalysts.^[2] This behaviour seems to be a shared feature of the combination of substrate **134** and the phosphino-oxazoline catalyst system.

3.2.4 Conclusions

For all substrates tested there exist catalysts which are able to form the hydrogenation products with enantiomeric excesses above 95%.^[3] However, many of these iridium-based systems are structurally and electronically different from the tested phosphino-oxazoline-Ir-complexes and thus difficult to compare with the catalysts described in this chapter. Therefore the following comparison will focus only on the complexes structurally related to the catalysts tested.

The iridium complexes of menthol-derived P-chiral phosphino-oxazolines generally gave very active catalysts and in this respect reflect the behaviour of the established systems.^[3] Compared to previously reported results in the hydrogenation of olefins with Ir-phosphino-oxazoline complexes with^[4] or without^[5] a stereogenic phosphorus atom, the menthol derived ligands gave catalysts which were usually less enantioselective. However, in the case of the unsaturated ester **74** the selectivity was comparable, and the terminal olefin **134** was hydrogenated with higher enantiomeric excess (87% *ee*) than previously reported with phosphino-oxazoline-based complexes (76% *ee*).^[2]

Interestingly, the best menthol-derived catalyst in the hydrogenation of stilbene **131** and the structurally related imine **137** had a phenyl substituent on the phosphorus atom, whereas the other substrates gave better results with catalysts bearing a methyl group.

Iridium complexes **121** and **122**, having the only stereogenic center at the phosphorus atom, usually induced low enantioselectivities with the unfunctionalized olefins. The comparatively high asymmetric induction in the hydrogenation of the ester **74** and the imine **137** might originate from different types of catalytic intermediates as those operating in the reduction of unfunctionalized olefins.

Except for stilbene **131**, the experiments that gave a reasonable enantiomeric excess showed that the complexes having only an asymmetric phosphorus atom favored the formation of the same enantiomer as the catalysts with an additional stereogenic center on the oxazoline ring. The general experience that the configuration on the oxazoline ring has a dominating effect in the enantioselective hydrogenation over the influence of the phosphorus center, suggests that the complexes **123-128** represent the matched combination of the stereogenic centers. A final proof of this theory is still missing since the selective synthesis of the diastereomeric complexes could not be achieved.

The enantioselectivities in the reduction of the terminal olefin were shown to depend on the temperature applied. Reactions at low and high temperatures gave lower enantiomeric excesses than reactions at 0-25 °C.

3.2.5 References

- [1] F. Barrios-Landeros, A. Pfaltz, unpublished results.
- [2] S. McIntyre, E. Hörmann, F. Menges, S. P. Smidt, A. Pfaltz, *Adv. Synth. Catal.* **2005**, *347*, 282-288.
- [3] For an overview see: S. J. Roseblade, A. Pfaltz, *Acc. Chem. Res.* **2007**, *40*, 1402-1411.
- [4] S. P. Smidt, PhD-Thesis, *Iridium-Catalysed Enantioselective Hydrogenation – New P,N Ligands and Mechanistic Investigations*, **2003**, University of Basel.
- [5] K. Zhang, A. Pfaltz, unpublished results.

Chapter 4

Experimental

4.1 Working Techniques and Reagents

The synthetic procedures were performed in dried glassware under argon using Schlenk techniques. For the preparation of the hydrogenation experiments a glove box (MBraun Labmaster 130) was used.

Commercially available reagents were purchased from Acros, Aldrich, Fluka, Strem or TCI and used as received. *N,N,N,N*-Tetramethylethylenediamine and diethyl amine were distilled from calcium hydride. 1-Bromo-2-(*N,N*-dimethylamino)ethylferrocene (**3**)^[1] and 1-diphenylphosphino-3-ethyl-2-formylferrocene (**45**) were provided by Solvias AG. The chiral phenyl oxazolines **118** were prepared according literature procedures.^[2]

The solvents were distilled from calcium hydride (dichloromethane, triethylamine) or sodium (diethyl ether, pentane, tetrahydrofuran, toluene), collected from a purification column system (PureSolv, Innovative Technology Inc.), or purchased from Aldrich or Fluka in septum-sealed bottles over molecular sieves.

Column chromatographic purifications were performed on Fluka silica gel 60 (Buchs, particle size 40-63 nm). The eluents were of technical grade and distilled prior to use.

4.2 Analytical Methods

NMR-Spectroscopy (NMR): NMR spectra were measured on a Bruker Avance 400 (400 MHz) or a Bruker Avance 500 (500 MHz) spectrometer. The chemical shifts (δ) are given in ppm. ¹H and ¹³C spectra are referenced relative to tetramethylsilane ($\delta = 0$ ppm) using the solvent residual peaks (CDCl₃ 7.26 ppm, CD₂Cl₂ 5.32 ppm, C₆D₆ 7.15 ppm, CD₃OD 3.31 ppm) and the signals of the deuterated solvents (CDCl₃ 77.0 ppm, CD₂Cl₂ 53.1 ppm, C₆D₆ 128.02 ppm, CD₃OD 49.05 ppm), respectively as internal standards. ³¹P spectra are calibrated relative to 85% phosphoric acid ($\delta = 0$ ppm) as external standard. The assignment of ¹H and ¹³C signals was realized with the help of DEPT and two-dimensional correlation experiments (COSY, HMQC, HMBC and NOESY). Multiplets are assigned as s (singlet), d (doublet), t (triplet), q (quartet), quin (quintet), sep (septet), m (multiplet) and br (broad). If possible, signals were assigned pro-(*R*) (*C_R*, *H_R*) and pro-(*S*) (*C_S*, *H_S*) in terms of stereochemistry.

Infrared Spectroscopy (IR): Infrared spectra were collected on a Perkin Elmer 1600 series FTIR spectrometer. The spectra of liquids and oils were measured as thin films between two sodium chloride plates, those of solid samples as potassium bromide discs. The absorption bands are given in wavenumbers ($\tilde{\nu}$ [cm^{-1}]). The peak intensity is described by s (strong), m (medium) and w (weak).

Mass Spectrometry (MS): Mass spectra were measured by Dr. H. Nadig (Department of Chemistry, University of Basel) on a VG70-250 spectrometer (electron-impact ionization (EI)) or on a MAR 312 spectrometer (fast atom bombardment (FAB)). FAB was performed with 3-nitrobenzyl alcohol (NBA) as matrix.

ESI-MS spectra were measured by Mr. C. Ebner (Department of Chemistry, University of Basel) on a Finnigan MAT LCQ.

The signals are given in mass-to-charge ratios (m/z) with the relative intensity in brackets.

Elemental Analysis (EA): Elemental analyses were measured by Mr. W. Kirsch (Department of Chemistry, University of Basel) on a Leco CHN-900. The data are indicated in mass percent.

Melting Points (m.p.): Melting points were determined on a Gallenkamp melting point apparatus and are uncorrected.

Optical Rotations ($[\alpha]_D^{20}$): Optical rotations were measured on a Perkin Elmer Polarimeter 341 in a cuvette ($l = 1$ dm) at 20 °C. The concentration (c) is given in g/100 mL.

Gas Chromatography (GC): Gas chromatograms were collected on Carlo Erba HRGC Mega2 Series 800 (HRGS Mega 2) instruments. Achiral separations were performed on a Restek Rtx-1701 (30 m \times 0.25 mm \times 0.25 μm) and Macherey-Nagel Optima 5-Amin (30 m \times 0.25 mm \times 0.5 μm) column. Chiral separations were achieved on *ChiralDEX* γ -cyclodextrin TFA G-TA (30 m \times 0.25 mm \times 0.12 μm) and *Brechbühler* β -cyclodextrin DEtTButSil (SE54) (25 m \times 0.25 mm \times 0.25 μm) columns.

High Performance Liquid Chromatography (HPLC): HPLC analyses were measured on Shimadzu systems with SLC-10A system controller, CTO-10AC column oven, LC10-AD pump system, DGU-14A degasser and SPD-M10A diode array- or UV/VIS detector. Chiral

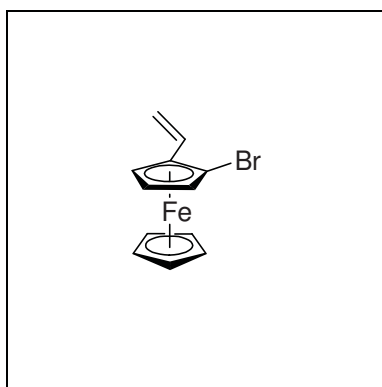
columns Chiracel AD-H, OD-H or OJ (2.6×250 mm) from Daicel Chemical Industries were used.

Semipreparative High Performance Liquid Chromatography (HPLC): Separations by semipreparative HPLC were performed on Shimadzu systems with SIL 10 Advp autosampler, CTO 10 Asvp column oven, LC 10 Atvp pump system, FCV 10 Alvp degasser and SPD M10 Avp diode array detector. A Daicel Chiracel AD (2×25 cm) column was used in this case.

Thin Layer Chromatography (TLC): TLC plates were obtained from Macherey-Nagel (Polygram SIL/UV254, 0.2 mm silica with fluorescence indicator). UV light (254 nm) or, when indicated, basic potassium permanganate solution were used for the visualization of the respective compounds.

4.3 Experimental Procedures

4.3.1 Preparation of Ferrocenephospholanes



(*S*)-(η⁵-2,4-cyclopentadien-1-yl)(η⁵-1-bromo-2-ethenyl-cyclopenta-2,4-dien-1-yl)iron (**4**)

A degassed solution of (*R,S_P*)-1-bromo-2-(*N,N*-dimethylamino)ethylferrocene (**3**) (3.00 g, 8.93 mmol) in Ac₂O (50 mL) was heated at 140 °C for 3.5 h. The solvent was evaporated under reduced pressure, the residue dissolved in Et₂O (40 mL), extracted 3 times with sat. aq. NaHCO₃ and dried over MgSO₄. The solvent was evaporated under reduced pressure and the residue purified by column chromatography (SiO₂, 10×5 cm, hexanes) to give the title compound **4** as a red liquid (2.30 g, 89%).

C₁₂H₁₁BrFe (290.96 g/mol)

¹H-NMR (C₆D₆): δ/ppm = 3.78 (t, ³J_{HH} = 2.5 Hz, 1H, C(Br)CHCH), 3.93 (s, 5H, Cp-CH), 4.16 (dd, ³J_{HH} = 2.5 Hz, ⁴J_{HH} = 1.5 Hz, 1H, C(Br)CCHCH), 4.27 (dd, ³J_{HH} = 2.5 Hz, ⁴J_{HH} =

1.5 Hz, 1H, C(Br)CH), 5.07 (dd, $^2J_{\text{HH}} = 1.5$ Hz, $^3J_{\text{HH}} = 10.6$ Hz, 1H, CHCH_EH_Z), 5.38 (dd, $^2J_{\text{HH}} = 1.5$ Hz, $^3J_{\text{HH}} = 17.7$ Hz, 1H, CHCH_EH_Z), 6.69 (dd, $^3J_{\text{HH}} = 10.6$ Hz, $^3J_{\text{HH}} = 17.7$ Hz, 1H, CHCH₂).

$^{13}\text{C}\{^1\text{H}\}$ -NMR (C₆D₆): $\delta/\text{ppm} = 63.5$ (s, C(Br)CCH), 67.2 (s, C(Br)CHCH), 71.1 (s, C(Br)CH), 72.1 (s, Cp-CH), 79.9 (s, CBr), 82.1 (s, C(Br)C), 113.1 (s, CH₂), 132.7 (s, CHCH₂).

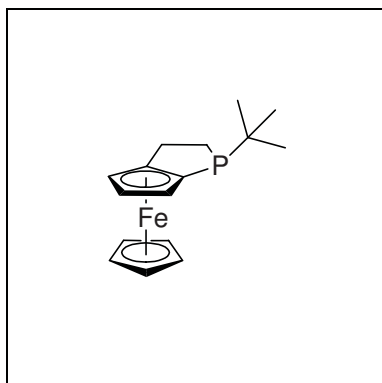
IR (NaCl): $\tilde{\nu}/\text{cm}^{-1} = 3091(\text{s}), 3008(\text{m}), 2981(\text{m}), 2925(\text{m}), 2857(\text{m}), 2700(\text{w}), 2461(\text{w}), 2251(\text{w}), 2189(\text{w}), 2111(\text{w}), 2054(\text{w}), 1963(\text{w}), 1894(\text{w}), 1778(\text{m}), 1722(\text{m}), 1629(\text{s}), 1461(\text{m}), 1409(\text{s}), 1387(\text{s}), 1327(\text{s}), 1289(\text{m}), 1250(\text{s}), 1167(\text{m}), 1106(\text{s}), 1060(\text{s}), 1028(\text{s}), 998(\text{s}), 953(\text{s}), 901(\text{s}), 820(\text{s}), 716(\text{s}), 648(\text{s})$.

MS (EI): $m/z(\%) = 293(14), 292(93), 291(17), 289(100), 208(34), 155(35), 154(41), 153(68), 152(32), 128(12), 89(13), 56(15)$.

$[\alpha]_{\text{D}}^{20} = +794$ ($c = 0.66$, CHCl₃ / 0.75% EtOH).

EA: calculated (%) for C₁₂H₁₁BrFe: C: 49.53, H: 3.81; measured: C: 49.56, H: 3.88.

R_f (SiO₂, hexane): 0.31.



(*S,S_p*)-(η⁵-2,4-cyclopentadien-1-yl)[(3a,4,5,6,6a-η)-1-*tert*-butyl-(1,2,3-trihydro-cyclopenta[*b*]phosphole-3a-yl]iron (**6**)

Procedure 1:

To a solution of **4** (302 mg, 1.04 mmol) in THF (5 mL) was added *n*-butyllithium (1.6 M in hexane, 0.70 mL, 1.12 mmol) at -78 °C. After 30 min this was added via cannula to a solution of *tert*-butylphosphine dichloride (190 mg, 1.19 mmol) in THF (5 mL). After additional 30 min LiAlH₄ (2 M in THF, 1.00 mL, 2.00 mmol) was added and the reaction mixture was allowed to warm up to -10 °C. 2 M aq. NaOH was added until no more gas was formed. The suspension was filtered over a pad of silica eluting with ethyl acetate and the solvent was evaporated under reduced pressure. The residue was dissolved in THF (5 mL) and a solution of *i*Pr₂NH (0.20 mL, 1.42 mmol) and *n*-butyllithium (1.6 M in hexane, 0.85 mL, 1.36 mmol) in THF (5 mL) (prepared at 0 °C) was added. The reaction mixture was stirred at room temperature for 18 h and then extracted with sat. aq. NaCl. The organic layer was dried over MgSO₄ and the solvent evaporated under reduced pressure. Purification by column

chromatography (SiO₂, 15×4 cm, hexanes:EtOAc:NEt₃ (300:1:3 → 100:1:1)) gave the title compound **6** (204 mg, 65%) as an orange oil which solidified on standing.

Procedure 2:

To a solution of **4** (950 mg, 3.26 mmol) in THF (20 mL) was added *n*-butyllithium (1.6 M in hexane, 2.30 mL, 3.68 mmol) at -78 °C. After 30 min a solution of *tert*-butylphosphine dichloride (575 mg, 3.62 mmol) in THF (10 mL) was added. After additional 30 min LiAlH₄ (1 M in THF, 5.00 mL, 5.00 mmol) was added and the reaction mixture was allowed to warm up to -30 °C. 2 M aq. NaOH was added until no more gas was formed. The suspension was filtered over a pad of silica eluting with ethyl acetate and the solvent was evaporated under reduced pressure. The residue was dissolved in THF (10 mL) and a solution of *i*Pr₂NH (0.60 mL, 4.25 mmol) and *n*-butyllithium (1.6 M in hexane, 2.60 mL, 4.16 mmol) in THF (5 mL) (prepared at 0 °C) was added. The reaction mixture was stirred at room temperature for 18 h and then extracted with sat. aq. NaCl. The organic layer was dried over MgSO₄ and the solvent evaporated under reduced pressure. Purification by column chromatography (SiO₂, 15×4 cm, hexanes:EtOAc:NEt₃ (300:1:3 to 100:1:1)) gave the title compound **6** (690 mg, 70%) as an orange oil which solidified on standing.

C₁₆H₂₁FeP (300.16 g/mol)

¹H-NMR (C₆D₆): δ/ppm = 0.93 (d, 9H, ³J_{HP} = 11.6 Hz, C(CH₃)₃), 1.95-2.01 (m, 1H, (CH₃)₃CPCH_RH_S), 2.32-2.50 (m, 3H, (CH₃)₃CPCH_RH_SCH₂), 3.97 (s, 5H, Cp-CH), 4.04 (dd, 1H, ³J_{HH} = 2.4 Hz, ⁴J_{HH} = 0.8 Hz, C(P)CCH), 4.10 (dd, 1H, ³J_{HH} = 2.4 Hz, ³J_{HH} = 2.2 Hz, C(P)CHCH), 4.19 (dd, 1H, ³J_{HH} = 2.2 Hz, ⁴J_{HH} = 0.8 Hz, C(P)CH).

¹³C{¹H}-NMR (C₆D₆): δ/ppm = 26.7 (d, ¹J_{CP} = 18.1 Hz, PCH₂), 27.4 (d, ²J_{CP} = 5.2 Hz, PCH₂CH₂), 27.5 (d, ²J_{CP} = 15.1 Hz, C(CH₃)₃), 31.1 (d, ¹J_{CP} = 18.1 Hz, C(CH₃)₃), 64.2 (s, C(P)CCH), 68.1 (d, ²J_{CP} = 15.5 Hz, C(P)CH), 70.1 (d, J_{CP} = 1.7 Hz, Cp-CH), 73.2 (d, ³J_{CP} = 1.7 Hz, C(P)CHCH), 83.1 (d, ²J_{CP} = 12.9 Hz, C(P)C), 99.3 (d, ¹J_{CP} = 0.9 Hz, CP).

³¹P{¹H}-NMR (C₆D₆): δ/ppm = -1.7 (s).

IR (KBr): $\tilde{\nu}$ /cm⁻¹ = 3087(m), 2935(s), 2855(s), 1761(w), 1694(w), 1641(m), 1464(s), 1410(m), 1389(m), 1358(m), 1278(m), 1217(w), 1179(m), 1139(w), 1103(m), 1053(w), 1004(m), 814(s), 692(w), 644(w), 505(m), 471(s).

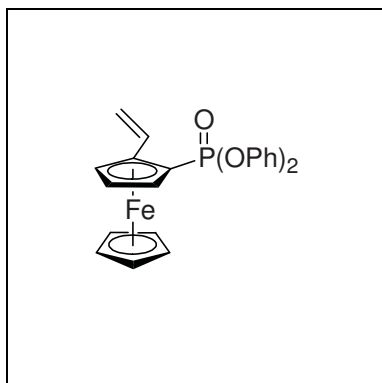
MS (FAB): *m/z*(%) = 300(26), 243(100), 177(7), 176(7), 151(6), 121(10).

[α]_D²⁰ = +70 (*c* = 0.27, CHCl₃ / 0.75% EtOH).

EA: calculated (%) for C₁₆H₂₁FeP: C: 64.02, H: 7.05; measured: C: 63.92, H: 6.82.

R_f (SiO₂, hexanes:EtOAc:NEt₃ (50:1:1)): 0.26.

m.p.: 66-70 °C.



(S)-(η⁵-2,4-cyclopentadien-1-yl)[η⁵-1-(diphenoxyphosphoryl)-2-ethenyl-cyclopenta-2,4-dien-1-yl]iron (10**)**

To a solution of **4** (740 mg, 2.54 mmol) in THF (10 mL) was added *n*-butyllithium (1.6 M in hexane, 1.75 mL, 2.80 mmol) at -78 °C. After 30 min this was added via cannula to a solution of diphenyl phosphoryl chloride (0.60 mL, 1.19 mmol) in THF (10 mL) at -78 °C. After 30 min water (2 mL) was added and the reaction mixture was allowed to warm up to room temperature. The organic layer was extracted with sat. aq. NaHCO₃ and sat. aq. NaCl, dried over MgSO₄ and the solvent was evaporated under reduced pressure. Column chromatography (SiO₂, 10×5 cm, hexanes:EtOAc (2:1)) gave the title compound **10** (957 mg, 85%) as an orange oil which crystallized upon treatment with hexane.

C₂₄H₂₁FeO₃P (444.24 g/mol)

¹H-NMR (CDCl₃): δ/ppm = 4.20 (s, 5H, Cp-CH), 4.48 (dt, ⁴J_{HP} = 2.6 Hz, ³J_{HH} = 2.6 Hz 1H, C(P)CHCH), 4.65-4.68 (m, 1H, C(P)CH), 4.76-4.80 (m, 1H, C(P)CCH), 5.16 (dd, ²J_{HH} = 1.4 Hz, ³J_{HH} = 10.8 Hz, 1H, CHCH_EH_Z), 5.46 (dd, ²J_{HH} = 1.4 Hz, ³J_{HH} = 17.5 Hz, 1H, CHCH_EH_Z), 6.95 (dd, ³J_{HH} = 10.8 Hz, ³J_{HH} = 17.5 Hz, 1H, CHCH₂), 7.10-7.35 (m, 10H, Ar-CH).

¹³C{¹H}-NMR (CDCl₃): δ/ppm = 64.4 (d, ¹J_{CP} = 217.6 Hz, CP), 68.6 (d, ³J_{CP} = 14.7 Hz, C(P)CCH), 71.2 (s, Cp-CH), 71.3 (d, ³J_{CP} = 15.0 Hz, C(P)CHCH), 74.0 (d, ²J_{CP} = 15.4 Hz, C(P)CH), 86.8 (d, ²J_{CP} = 16.5 Hz, C(P)C), 113.8 (s, CHCH₂), 120.6 (d, J_{CP} = 4.6 Hz, Ar-CH), 120.7 (d, J_{CP} = 4.5 Hz, Ar-CH), 124.9 (s, Ar-CH), 129.5 (s, Ar-CH), 129.6 (s, Ar-CH), 132.4 (s, CHCH₂), 150.6 (d, ²J_{CP} = 8.4 Hz, Ar-C), 150.7 (d, ²J_{CP} = 7.6 Hz, Ar-C).

³¹P{¹H}-NMR (CDCl₃): δ/ppm = 16.6 (s).

IR (KBr): $\tilde{\nu}$ /cm⁻¹ = 3097(m), 3056(w), 1950(w), 1828(w), 1778(w), 1745(w), 1661(w), 1622(w), 1589(m), 1486(s), 1406(m), 1261(s), 1211(s), 1184(s), 1078(m), 999(m), 930(s), 822(m), 756(s), 690(m), 570(m)517(m), 486(m).

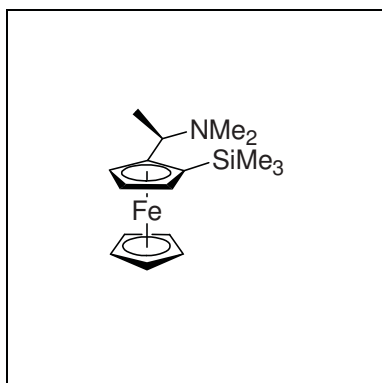
MS (EI): *m/z*(%) = 444(100), 285(5), 165(6), 121(5).

$[\alpha]_D^{20} = +599$ ($c = 0.34$, $\text{CHCl}_3 / 0.75\%$ EtOH).

EA: calculated (%) for $\text{C}_{24}\text{H}_{21}\text{FeO}_3\text{P}$: C: 64.89, H: 4.76; measured: C: 64.81, H: 4.84.

R_f (SiO_2 , hexanes:EtOAc (5:1)): 0.19.

m.p.: 76-78 °C.



(S,S_P)-(η^5 -2,4-cyclopentadien-1-yl)[η^5 -2-(1-dimethylaminoethyl)-1-trimethylsilyl-cyclopenta-2,4-dien-1-yl]iron (11**)**

To a solution of (*R*)-**1** (1.00 g, 3.89 mmol) in Et_2O (10 mL) was added *sec*-butyllithium (4.90 mL, 1.3 M in hexane/cyclohexane, 6.37 mmol) at 0 °C. After 4 h the solution was cooled to -78 °C

and trimethylsilyl chloride (0.70 mL, 5.46 mmol) was added and the reaction mixture was allowed to warm up to room temperature. After addition of water (2 mL), followed by extraction with sat. aq. NaHCO_3 and sat aq. NaCl , the organic layer was dried over MgSO_4 and the solvent was removed under reduced pressure. Column chromatography (SiO_2 , 10×5 cm, TBME: NEt_3 (1000:5)) gave the title compound **11** (1.18 g, 91%) as a dark orange oil.

$\text{C}_{17}\text{H}_{27}\text{FeNSi}$ (329.33 g/mol)

$^1\text{H-NMR}$ (C_6D_6): $\delta/\text{ppm} = 0.36$ (s, 9H, $\text{Si}(\text{CH}_3)_3$), 1.04 (d, $^3J_{\text{HH}} = 6.7$ Hz, 3H, CHCH_3), 1.99 (s, 6H, $\text{N}(\text{CH}_3)_2$), 3.80 (q, $^3J_{\text{HH}} = 6.7$ Hz, 1H, CHCH_3), 3.96 (s, 5H, Cp-CH), 4.03-4.01 (m, 1H, C(Si)CH), 4.10 (t, $^3J_{\text{HH}} = 2.3$ Hz, 1H, C(Si)CHCH), 4.11-4.13 (m, 1H, C(Si)CCH).

$^{13}\text{C}\{^1\text{H}\}$ -NMR (C_6D_6): $\delta/\text{ppm} = 0.3$ (s, $\text{Si}(\text{CH}_3)_3$), 7.7 (s, CHCH_3), 39.2 (s, $\text{N}(\text{CH}_3)_2$), 58.1 (s, CHCH_3), 69.1 (s, Cp-CH), 69.1 (s, C(Si)CHCH), 70.1 (s, C(Si)CCH), 72.0 (s, CSi), 75.1 (s, C(Si)CH), 96.6 (s, C(Si)C).

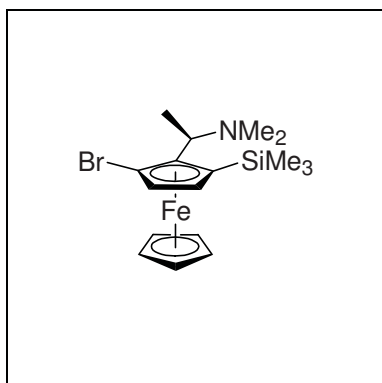
IR (NaCl): $\tilde{\nu}/\text{cm}^{-1} = 3093(\text{w})$, 2965(m), 2817(w), 2775(w), 1451(w), 1402(w), 1361(w), 1242(m), 1188(w), 1155(w), 1098(w), 1064(w), 1002(w), 931(w), 834(s), 755(w), 687(w).

MS (EI): $m/z(\%) = 401(5)$, 357(6), 331(5), 330(17), 329(67), 315(9), 314(34), 287(6), 286(24), 285(100), 284(16), 283(8), 271(5), 269(9), 258(13), 256(11), 243(8), 212(5), 121(7), 73(15), 72(19).

$[\alpha]_D^{20} = +17.9$ ($c = 0.65$, $\text{CHCl}_3 / 0.75\%$ EtOH).

EA: calculated for C₁₇H₂₇FeNSi: C: 62.00, H: 8.26, N: 4.25; measured: C: 62.12, H: 8.19, N: 4.04.

R_f (SiO₂, TBME:NEt₃ (1000:5)): 0.59.



(*S,R_p*)-[⁵-2,4-cyclopentadien-1-yl][⁵-1-bromo-2-(1-dimethylaminoethyl)-3-trimethylsilyl-cyclopenta-2,4-dien-1-yl]iron (**12**)

To a solution of **11** (633 mg, 1.92 mmol) in TBME (20 mL) was added *tert*-butyllithium (1.95 mL, 1.5 M in pentane, 2.93 mmol) at –30 °C. The reaction was allowed to warm up to 0 °C and stirred for 1 h. After cooling to –78 °C 1,2-dibromo-1,1,2,2-tetrafluoroethane (0.35 ml, 2.94 mmol) was added and the reaction mixture was allowed to warm to room temperature. The organic layer was extracted with water and sat. aq. NaCl and dried over MgSO₄. The solvent was removed under reduced pressure and purification by column chromatography (SiO₂, 10×4 cm, hexanes:EtOAc:NEt₃ (100:10:1)) gave the title compound **12** (415 mg, 53%) as an orange oil beside recovered starting material **11** (199 mg, 32%).

C₁₇H₂₆BrFeNSi (408.23 g/mol)

¹H-NMR (C₆D₆): δ/ppm = 0.26 (s, 9H, Si(CH₃)₃), 1.60 (d, ³J_{HH} = 7.0 Hz, 3H, CHCH₃), 2.08 (s, 6H, N(CH₃)₂), 3.72 (q, ³J_{HH} = 7.0 Hz, 1H, CHCH₃), 3.78 (d, ³J_{HH} = 2.4 Hz, 1H, C(Si)CH), 4.00 (s, 5H, Cp-CH), 4.35 (d, ³J_{HH} = 2.4 Hz, 1H, C(Br)CH).

¹³C{¹H}-NMR (C₆D₆): δ/ppm = 0.4 (s, Si(CH₃)₃), 11.6 (s, CHCH₃), 40.6 (s, N(CH₃)₂), 59.7 (s, CHCH₃), 71.6 (s, Cp-CH), 72.2 (s, CSi), 73.1 (s, C(Si)CH), 74.0 (s, C(Br)CH), 80.8 (s, BrC), 92.9 (s, C(Br)C).

IR (NaCl): $\tilde{\nu}$ /cm⁻¹ = 3096(w), 2955(s), 2899(m), 2856(m), 2819(m), 2776(m), 1770(w), 1715(w), 1645(w), 1451(m), 1404(w), 1375(m), 1246(s), 1219(m), 1188(w), 1155(w), 1107(m), 1063(m), 1002(w), 974(m), 935(w), 834(s), 756(m), 689(w).

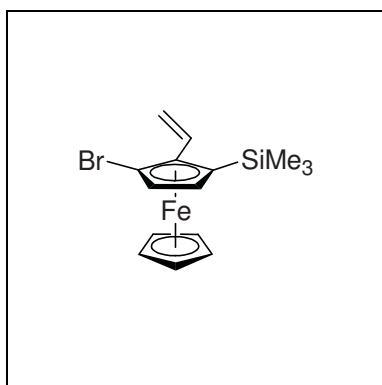
MS (EI): *m/z*(%) = 394(11), 392(11), 366(10), 365(64), 364(52), 363(68), 362(40), 339(15), 338(85), 337(19), 336(91), 242(6), 213(13), 197(9), 153(13), 147(6), 145(17), 139(8), 137(19), 135(22), 134(7), 133(18), 132(13), 131(20), 122(10), 121(94), 119(21), 109(7),

107(11), 105(16), 96(13), 93(7), 83(15), 73(91), 72(100), 71(13), 59(25), 57(7), 56(75), 45(25), 44(17), 43(20), 42(22).

$[\alpha]_D^{20} = +109$ ($c = 0.32$, $\text{CHCl}_3 / 0.75\%$ EtOH).

EA: calculated for $\text{C}_{17}\text{H}_{26}\text{BrFeNSi}$: C: 50.02, H: 6.42, N: 3.43; measured: C: 50.40, H: 6.34, N: 3.36.

R_f (SiO_2 , hexane:EtOAc:NEt₃ (100:10:1)): 0.20.



(R_P)-(η⁵-2,4-cyclopentadien-1-yl)[η⁵-1-bromo-2-ethenyl-3-trimethylsilyl-cyclopenta-2,4-dien-1-yl]iron (13**)**

A degassed solution of **12** (522 mg, 1.28 mmol) in Ac₂O (40 mL) was heated at 150 °C for 4 h. The solvent was evaporated under reduced pressure, the residue dissolved in Et₂O (30 mL), extracted 3 times with sat. aq. NaHCO₃ and dried

over MgSO₄. The solvent was evaporated under reduced pressure and the residue purified by column chromatography (SiO_2 , 10×5 cm, hexane) to give the title compound **13** (409 mg, 88%) as an orange liquid.

$\text{C}_{15}\text{H}_{19}\text{BrFeSi}$ (363.15 g/mol)

¹H-NMR (C_6D_6): $\delta/\text{ppm} = 0.21$ (s, 9H, Si(CH₃)₃), 3.80 (s, 1H, C(Si)CH), 3.97 (s, 5H, Cp-CH), 4.44 (s, 1H, C(Br)CH), 5.25 (d, ³J_{HH} = 11.2 Hz, 1H, CHCH_EH_Z), 5.70 (d, ³J_{HH} = 17.7 Hz, 1H, CHCH_EH_Z), 6.63 (dd, ³J_{HH} = 17.6 Hz, ³J_{HH} = 11.3 Hz, 1H, CHCH₂).

¹³C{¹H}-NMR (C_6D_6): $\delta/\text{ppm} = 0.5$ (s, Si(CH₃)₃), 69.5 (s, CSi), 72.1 (s, Cp-CH), 73.2 (s, C(Si)CH), 73.8 (s, C(Br)CH), 81.6 (s, CBr), 87.1 (s, C(Br)C), 117.1 (s, CHCH₂), 133.4 (s, CHCH₂).

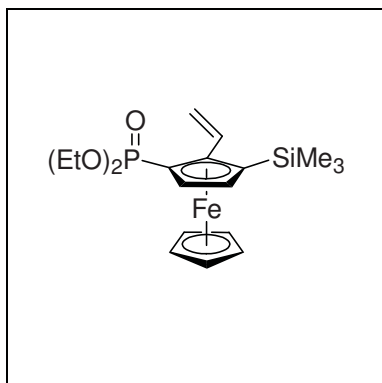
IR (NaCl): $\tilde{\nu}/\text{cm}^{-1} = 3096(\text{w})$, 2956(m), 2898(w), 1629(w), 1408(w), 1375(w), 1250(m), 1217(w), 1130(w), 1101(w), 980(w), 909(w), 835(s), 756(w), 690(w).

MS (EI): $m/z(\%) = 366(7)$, 365(22), 364(98), 363(23), 362(100), 360(6), 349(11), 347(11), 268(9), 211(6), 210(5), 209(10), 208(7), 197(19), 183(8), 181(5), 169(8), 154(5), 153(11), 152(7), 147(7), 145(8), 132(5), 131(7), 121(5), 73(30), 45(6).

$[\alpha]_D^{20} = +115.0$ ($c = 0.59$, $\text{CHCl}_3 / 0.75\%$ EtOH).

EA: calculated for $\text{C}_{15}\text{H}_{19}\text{BrFeSi}$: C: 49.61, H: 5.27; measured: C: 48.96, H: 5.34.

R_f (SiO_2 , hexanes): 0.50.



(*R_P*)-(η⁵-2,4-cyclopentadien-1-yl)[η⁵-1-diethoxyphosphoryl-2-ethenyl-3-trimethylsilyl-cyclopenta-2,4-dien-1-yl]iron (14**)**

To a solution of **13** (452 mg, 1.23 mmol) in THF (10 mL) was added *n*-butyllithium (0.85 mL, 1.6 M in hexane, 1.36 mmol) at $-78\text{ }^{\circ}\text{C}$ and stirred for 30 min. This solution then was added at $-78\text{ }^{\circ}\text{C}$ via cannula to diethyl phosphoryl chloride (0.21 mL, 1.46 mmol) in THF (10 mL). After 30 min water (2 mL) was added and the organic layer was extracted with sat. aq. NaHCO_3 and sat. aq. NaCl and dried over MgSO_4 . The solvent was evaporated under reduced pressure and the crude product was purified by column chromatography (SiO_2 , $15\times 5\text{ cm}$, hexanes:EtOAc (1:1 \rightarrow 1:4)) to give the title compound **14** (435 mg, 84%) as an orange oil.

$\text{C}_{19}\text{H}_{29}\text{FeO}_3\text{PSi}$ (420.34 g/mol)

¹H-NMR (C_6D_6): $\delta/\text{ppm} = 0.27$ (s, 9H, $\text{Si}(\text{CH}_3)_3$), 1.03 (t, $^3J_{\text{HH}} = 7.1\text{ Hz}$, 3H, OCH_2CH_3), 1.09 (t, $^3J_{\text{HH}} = 7.1\text{ Hz}$, 3H, OCH_2CH_3), 3.93-4.02 (m, 2H, OCH_2CH_3), 4.02-4.10 (m, 2H, OCH_2CH_3), 4.11 (t, $J = 2.5\text{ Hz}$, 1H, $\text{C}(\text{Si})\text{CH}$), 4.26 (s, 5H, Cp-CH), 4.76 (t, $J = 2.3\text{ Hz}$, 1H, $\text{C}(\text{P})\text{CH}$), 5.23 (dd, $^3J_{\text{HH}} = 11.2\text{ Hz}$, $^2J_{\text{HH}} = 1.6\text{ Hz}$, 1H, CHCH_EH_Z), 5.59 (dd, $^3J_{\text{HH}} = 17.7\text{ Hz}$, $^2J_{\text{HH}} = 1.6\text{ Hz}$, 1H, CHCH_EH_Z), 7.20 (dd, $^3J_{\text{HH}} = 17.7\text{ Hz}$, $^3J_{\text{HH}} = 11.2\text{ Hz}$, 1H, CHCH_2).

¹³C{¹H}-NMR (C_6D_6): $\delta/\text{ppm} = 0.8$ (s, $\text{Si}(\text{CH}_3)_3$), 16.4 (d, $^3J_{\text{CP}} = 6.5\text{ Hz}$, OCH_2CH_3), 16.6 (d, $^3J_{\text{CP}} = 6.1\text{ Hz}$, OCH_2CH_3), 61.4 (d, $^2J_{\text{CP}} = 5.8\text{ Hz}$, OCH_2CH_3), 61.5 (d, $^2J_{\text{CP}} = 6.0\text{ Hz}$, OCH_2CH_3), 71.2 (d, $^1J_{\text{CP}} = 208.4\text{ Hz}$, Cp), 71.4 (s, Cp-CH), 74.3 (d, $^3J_{\text{CP}} = 10.3\text{ Hz}$, CSi), 76.5 (d, $^2J_{\text{CP}} = 14.3\text{ Hz}$, $\text{C}(\text{P})\text{CH}$), 77.1 (d, $^3J_{\text{CP}} = 14.8\text{ Hz}$, $\text{C}(\text{Si})\text{CH}$), 92.8 (d, $^2J_{\text{CP}} = 15.2\text{ Hz}$, $\text{C}(\text{P})\text{C}$), 116.9 (s, CHCH_2), 134.6 (s, CHCH_2).

³¹P{¹H}-NMR (C_6D_6): $\delta/\text{ppm} = 21.9$ (s).

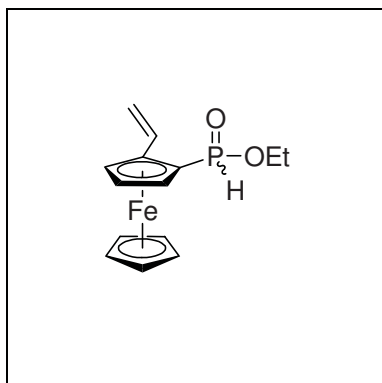
IR (KBr): $\tilde{\nu}/\text{cm}^{-1} = 3094(\text{w})$, 2978(m), 2903(w), 1741(w), 1629(w), 1442(w), 1396(w), 1249(s), 1217(m), 1162(w), 1133(w), 1104(w), 1054(s), 1031(s), 958(m), 838(s), 756(w), 688(w).

MS (EI): $m/z(\%) = 422(7)$, 421(26), 420(100), 418(6), 392(9), 347(5), 346(19), 283(5), 121(6).

$[\alpha]_D^{20} = -126.3$ ($c = 0.81$, $\text{CHCl}_3 / 0.75\%$ EtOH).

EA: calculated for $\text{C}_{19}\text{H}_{29}\text{FeO}_3\text{PSi}$: C: 54.29, H: 6.95; measured: C: 54.00, H: 7.10.

R_f (SiO_2 , hexanes:EtOAc (1:4)): 0.54.



(*S,R*_P)-(η⁵-2,4-cyclopentadien-1-yl)[η⁵-1-

(ethoxyphosphinoyl)-2-ethenyl-cyclopenta-2,4-dien-1-yl]iron

(*S,S*_P)-(η⁵-2,4-cyclopentadien-1-yl)[η⁵-1-

(ethoxyphosphinoyl)-2-ethenyl-cyclopenta-2,4-dien-1-yl]iron

(**16**)

To a solution of **4** (622 mg, 2.14 mmol) in THF (7 mL) was added *n*-butyllithium (1.6 M in hexane, 1.60 mL, 2.56 mmol) at -78 °C. After 30 min this was added to a solution of diethyl chlorophosphite (400 μL, 2.80 mmol) in THF (7 mL) at -78 °C. The reaction mixture was stirred for 1 h and then allowed to warm up to room temperature. The organic layer was extracted with sat. aq. NaHCO₃ and dried over MgSO₄. The crude product was purified by column chromatography (SiO₂, 15×4 cm, hexanes:EtOAc (1:10 to 0:1)) to give the title compound **16** as an orange oil as an almost 1:1 mixture of diastereoisomers (480 mg, 74%). If necessary the diastereoisomers can be separated by column chromatography (SiO₂, 15×4 cm, hexanes:EtOAc (1:2 → 1:20)).

C₁₄H₁₇FeO₂P (304.11 g/mol)

Diastereoisomer 1:

¹H-NMR (C₆D₆): δ/ppm = 0.98 (t, ³J_{HH} = 7.0 Hz, 3H, CH₃), 3.75-3.90 (m, 2H, CH₂CH₃), 4.01-4.08 (m, 1H, C(P)CHCH), 4.08 (s, 5H, Cp-CH), 4.17-4.21 (m, 1H, C(P)CH), 4.41-4.45 (m, 1H, C(P)CCH), 5.18 (dd, ³J_{HH} = 10.8 Hz, ²J_{HH} = 1.6 Hz, 1H, CHCH_EH_Z), 5.51 (dd, ³J_{HH} = 17.5 Hz, ²J_{HH} = 1.6 Hz, 1H, CHCH_EH_Z), 7.33 (dd, ³J_{HH} = 17.5 Hz, ³J_{HH} = 10.8 Hz, 1H, CHCH₂), 7.54 (d, ¹J_{HP} = 559.8 Hz, 1H, PH).

¹³C{¹H}-NMR (C₆D₆): δ/ppm = 16.4 (d, ³J_{CP} = 6.3 Hz, CH₃), 61.2 (d, ²J_{CP} = 6.0 Hz, CH₂CH₃), 68.6 (d, ¹J_{CP} = 145.4 Hz, CP), 68.7 (d, ³J_{CP} = 10.4 Hz, C(P)CCH), 71.2 (s, Cp-CH), 71.6 (d, ³J_{CP} = 2.9 Hz, C(P)CHCH), 71.8 (d, ²J_{CP} = 1.6 Hz, C(P)CH), 88.5 (d, ²J_{CP} = 12.0 Hz, C(P)C), 113.3 (s, CHCH₂), 133.5 (s, CHCH₂).

³¹P{¹H}-NMR (C₆D₆): δ/ppm = 41.6 (d, ¹J_{HP} = 560 Hz).

Diastereoisomer 2:

¹H-NMR (C₆D₆): δ/ppm = 0.98 (t, ³J_{HH} = 7.0 Hz, 3H, CH₃), 3.73-3.92 (m, 2H, CH₂CH₃), 4.05-4.09 (m, 1H, C(P)CHCH), 4.09 (s, 5H, Cp-CH), 4.34-4.38 (m, 1H, C(P)CCH), 4.68-4.72 (m, 1H, C(P)CH), 5.02 (dd, ³J_{HH} = 10.9 Hz, ²J_{HH} = 1.4 Hz, 1H, CHCH_EH_Z), 5.36 (dd, ³J_{HH} = 17.4 Hz, ²J_{HH} = 1.4 Hz, 1H, CHCH_EH_Z), 6.77 (dd, ³J_{HH} = 17.4 Hz, ³J_{HH} = 10.9 Hz, 1H, CHCH₂), 7.67 (d, ¹J_{HP} = 559.7 Hz, 1H, PH).

$^{13}\text{C}\{^1\text{H}\}$ -NMR (C_6D_6): $\delta/\text{ppm} = 16.4$ (d, $^3J_{\text{CP}} = 6.3$ Hz, CH_3), 61.2 (d, $^2J_{\text{CP}} = 5.9$ Hz, CH_2CH_3), 68.3 (d, $^1J_{\text{CP}} = 145.4$ Hz, CP), 69.5 (d, $^3J_{\text{CP}} = 11.2$ Hz, C(P)CCH), 71.2 (s, Cp-CH), 71.5 (d, $^3J_{\text{CP}} = 11.8$ Hz, C(P)CHCH), 74.1 (d, $^2J_{\text{CP}} = 12.0$ Hz, C(P)CH), 86.6 (d, $^2J_{\text{CP}} = 15.3$ Hz, C(P)C), 113.5 (s, CHCH₂), 132.9 (s, CHCH₂).

$^{31}\text{P}\{^1\text{H}\}$ -NMR (C_6D_6): $\delta/\text{ppm} = 38.0$ (d, $^1J_{\text{HP}} = 560$ Hz).

Diastereoisomeric mixture:

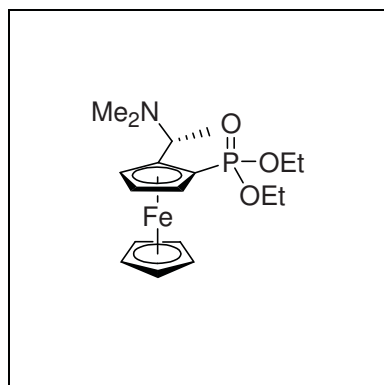
IR (NaCl): $\tilde{\nu}/\text{cm}^{-1} = 3459(\text{w})$, 3089(w), 2982(w), 2933(w), 2901(w), 1626(w), 1446(w), 1397(w), 1290(w), 1250(w), 1221(m), 1172(w), 1042(m), 995(m), 944(m), 824(w), 763(w), 725(w).

MS (EI): $m/z(\%) = 305(17)$, 304(100), 302(6), 276(29), 275(6), 274(5), 213(10), 212(57), 211(14), 210(18), 209(8), 193(5), 184(19), 147(10), 146(10), 145(9), 121(22), 119(8), 91(6), 89(5), 56(10).

$[\alpha]_D^{20} = +629$ ($c = 0.36$, $\text{CHCl}_3 / 0.75\%$ EtOH).

EA: calculated (%) for $\text{C}_{14}\text{H}_{17}\text{FeO}_2\text{P}$: C: 55.29, H: 5.63; measured: C: 52.46, H: 5.47 (oxidizes at ambient temperature, calculated for $\text{C}_{14}\text{H}_{17}\text{FeO}_3\text{P}$: C: 52.53, H: 5.35)

R_f (SiO_2 , hexanes:EtOAc (1:4)): 0.38 (dia1), 0.30 (dia2).



(*S,S_P*)-(η⁵-2,4-Cyclopentadien-1-yl)[η⁵-1-

(diethoxyphosphoryl)-2-(1-dimethylaminoethyl)-cyclopenta-2,4-dien-1-yl]iron (**18**)

To a solution of **3** (301 mg, 896 μmol) in THF (8 mL) was added *n*-butyllithium (0.70 mL, 1.6 M in hexane, 1.12 mmol) at -78 °C and stirred for 15 min. Diethyl phosphoryl chloride (0.17 mL, 1.18 mol) was added and stirring was continued for 45 min. Water (1 mL) and sat. aq. NaHCO_3 (4 mL) were added and the reaction mixture was allowed to warm up to room temperature. The organic layer was dried over MgSO_4 and the solvent was removed under reduced pressure. Purification by column chromatography (SiO_2 , 10×4 cm, acetone: NEt_3 (100:1)) gave the title compound **18** (325 mg, 92%) as an orange oil.

$C_{18}H_{28}FeNO_3P$ (393.2 g/mol)

1H -NMR (C_6D_6): $\delta/ppm = 1.07$ - 1.17 (m, 6H, OCH_2CH_3), 1.18 (d, $^3J_{HH} = 6.8$ Hz, 3H, $CHCH_3$), 2.15 (s, 6H, $N(CH_3)_2$), 3.99 - 4.02 (m, 1H, $C(P)CHCH$), 4.05 - 4.09 (m, 1H, $C(P)CCH$), 4.02 - 4.18 (m, 4H, OCH_2CH_3), 4.19 (s, 5H, Cp-CH), 4.44 - 4.47 (m, 1H, $C(P)CH$), 4.53 (q, $^3J_{HH} = 6.8$ Hz, 1H, $CHCH_3$).

$^{13}C\{^1H\}$ -NMR (C_6D_6): $\delta/ppm = 9.6$ (s, $CHCH_3$), 16.7 (d, $^3J_{CP} = 6.4$ Hz, OCH_2CH_3), 39.9 (s, $N(CH_3)_2$), 55.7 (s, $CHCH_3$), 60.5 (d, $^2J_{CP} = 6.0$ Hz, OCH_2CH_3), 61.9 (d, $^2J_{CP} = 5.5$ Hz, OCH_2CH_3), 67.6 (d, $^1J_{CP} = 211.7$ Hz, CP), 69.3 (d, $^3J_{CP} = 13.3$ Hz, $C(P)CHCH$), 70.0 (d, $^3J_{CP} = 14.8$ Hz, $C(P)CCH$), 70.9 (s, Cp-CH), 73.1 (d, $^2J_{CP} = 13.4$ Hz, $C(P)CH$), 95.5 (d, $^2J_{CP} = 17.5$ Hz, $C(P)C$).

$^{31}P\{^1H\}$ -NMR (C_6D_6): $\delta/ppm = 21.7$ (s).

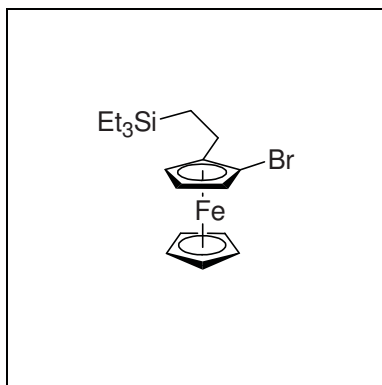
IR (NaCl): $\tilde{\nu}/cm^{-1} = 3095$ (w), 2975 (m), 2933 (w), 2817 (w), 2774 (w), 1708 (w), 1654 (w), 1451 (w), 1395 (w), 1366 (w), 1249 (m), 1171 (w), 1098 (w), 1034 (s), 958 (m), 816 (w), 790 (w), 755 (w).

MS (EI): $m/z(\%) = 394$ (6), 393 (27), 379 (21), 378 (100), 351 (11), 350 (56), 349 (28), 348 (9), 322 (12), 321 (7), 320 (8), 304 (7), 303 (7), 283 (5), 275 (5), 274 (7), 227 (7), 213 (12), 212 (6), 209 (14), 121 (9), 72 (10).

$[\alpha]_D^{20} = -1.0$ ($c = 0.77$, $CHCl_3 / 0.75\%$ EtOH).

EA: calculated (%) for $C_{18}H_{28}FeNO_3P$: C: 54.98, H: 7.18, N: 3.56; measured: C: 54.18, H: 7.24, N: 3.27.

R_f (SiO_2 , acetone:NEt₃ (100:1)): 0.13.



(S)-(η⁵-2,4-Cyclopentadien-1-yl)(η⁵-1-bromo-2-(2-(triethylsilyl)ethyl)-cyclopenta-2,4-dien-1-yl)iron (19)

To a solution of tris(pentafluorophenyl)borane (31 mg, 60 μmol) and triethylsilane (230 μL, 1.45 mmol) in CH_2Cl_2 (3 mL) was added a solution of **4** (350 mg, 1.20 mmol) in CH_2Cl_2 (4 mL) at room temperature. The reaction was stirred

for 20 h and filtered over a pad of silica. The solvent was evaporated under reduced pressure and the crude product was purified by column chromatography (SiO_2 , 15×3 cm, hexanes) to give the title compound **19** (426 mg, 87%) as an orange liquid.

$C_{18}H_{27}BrFeSi$ (407.25 g/mol)

1H -NMR (C_6D_6): $\delta/ppm = 0.56$ (q, $^3J_{HH} = 8.0$ Hz, 6H, $SiCH_2CH_3$), 0.81 (td, $^3J_{HH} = 14.1$ Hz, $^2J_{HH} = 4.9$ Hz, 1H, $SiCH_aH_bCH_2$), 0.90 (td, $^3J_{HH} = 14.3$ Hz, $^2J_{HH} = 4.7$ Hz, 1H, $SiCH_aH_bCH_2$), 1.00 (t, $^3J_{HH} = 8.0$ Hz, 9H, CH_3), 2.46 (td, $^3J_{HH} = 14.1$ Hz, $^2J_{HH} = 4.8$ Hz, 1H, $SiCH_2CH_aH_b$), 2.59 (td, $^3J_{HH} = 14.4$ Hz, $^2J_{HH} = 4.7$ Hz, 1H, $SiCH_2CH_aH_b$), 3.74 (s, 1H, $C(Br)CHCH$), 3.89 (s, 1H, $C(Br)CCH$), 4.00 (s, 5H, Cp-CH), 4.27 (s, 1H, $C(Br)CH$).

$^{13}C\{^1H\}$ -NMR (C_6D_6): $\delta/ppm = 3.6$ (s, $SiCH_2CH_3$), 7.8 (s, CH_3), 13.2 (s, $SiCH_2CH_2$), 23.2 (s, $SiCH_2CH_2$), 65.5 (s, $C(Br)CHCH$), 66.2 (s, $C(Br)CCH$), 69.9 (s, $C(Br)CH$), 71.3 (s, Cp-CH), 80.1 (s, CBr), 90.9 (s, $C(Br)C$).

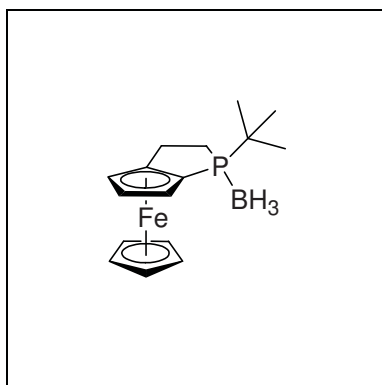
IR (NaCl): $\tilde{\nu}/cm^{-1} = 3095(m)$, 2951(s), 2908(s), 2878(s), 1766(w), 1715(w), 1650(w), 1460(m), 1414(m), 1380(w), 1305(w), 1237(m), 1177(w), 1103(m), 1059(w), 1006(m), 957(m), 887(w), 818(m), 774(m), 731(s).

MS (EI): $m/z(\%) = 410(6)$, 409(24), 408(98), 407(25), 406(100), 404(6), 299(5), 298(19), 212(22), 210(6), 121(6), 119(6), 115(10), 87(19), 59(14).

$[\alpha]_D^{20} = -5.0$ ($c = 0.88$, $CHCl_3 / 0.75\%$ EtOH).

EA: calculated for $C_{18}H_{27}BrFeSi$: C: 53.09, H: 6.68; measured: C: 53.19, H: 6.52.

R_f (SiO_2 , hexanes): 0.59.



(*S,S_p*)-(η⁵-2,4-Cyclopentadien-1-yl)[(3a,4,5,6,6a-η)-1-trihydroboranyl-1-*tert*-butyl-(1,2,3-trihydro-cyclopenta[*b*]phosphole-3a-yl)]iron (**22**)

To a solution of **6** (90.0 mg, 300 μmol) in THF (3 mL) was added BH_3 (0.50 mL, 1 M in THF, 500 μmol) at 0 °C. The solution was allowed to warm up to room temperature and the solvent was evaporated under reduced pressure. Column chromatography (SiO_2 , 10×3 cm, hexanes:EtOAc (10:1)) gave the title compound **22** (61.0 mg, 65%) as an orange solid.

$C_{16}H_{24}BF_6P$ (314.0 g/mol)

1H -NMR (C_6D_6): $\delta/ppm = 0.87$ (d, $^3J_{PH} = 13.3$ Hz, 9H, $C(CH_3)_3$), 1.30-2.00 (m, 3H, BH_3), 1.93-2.02 (m, 1H, $PCH_RH_SCH_2$), 2.02-2.12 (m, 1H, $PCH_2CH_RH_S$), 2.22-2.33 (m, 1H,

PCH₂CH_RH_S), 2.38-2.50 (m, 1H, PCH_RH_SCH₂), 3.88-3.92 (m, 1H, C(P)CCH), 4.01-4.05 (m, 1H, C(P)CHCH), 4.07-4.12 (m, 1H, C(P)CH), 4.19 (s, 5H, Cp-CH).

¹³C{¹H}-NMR (C₆D₆): δ/ppm = 25.3 (d, ²J_{CP} = 2.7 Hz, C(CH₃)₃), 25.6 (d, ²J_{CP} = 7.0 Hz, PCH₂CH₂), 26.2 (d, ¹J_{CP} = 32.7 Hz, PCH₂CH₂), 30.7 (d, ¹J_{CP} = 27.1 Hz, C(CH₃)₃), 64.8 (d, ³J_{CP} = 6.5 Hz, C(P)CCH), 66.3 (d, ²J_{CP} = 10.8 Hz, C(P)CH), 70.8 (s, Cp-CH), 74.3 (d, ³J_{CP} = 5.3 Hz, C(P)CHCH), 75.7 (d, ¹J_{CP} = 60.2 Hz, CP), 98.6 (d, ²J_{CP} = 14.3 Hz, C(P)C).

³¹P{¹H}-NMR (C₆D₆): δ/ppm = 58.7-59.8 (m).

IR (KBr): $\tilde{\nu}$ /cm⁻¹ = 3099(w), 2953(m), 2865(m), 2355(s), 2256(w), 1778(w), 1706(w), 1650(w), 1460(m), 1402(m), 1364(m), 1284(w), 1228(w), 1193(w), 1147(m), 1106(m), 1064(s), 1005(m), 938(w), 818(s), 763(w), 690(m), 640(w), 587(w), 551(w), 495(m), 462(w), 440(w), 408(w).

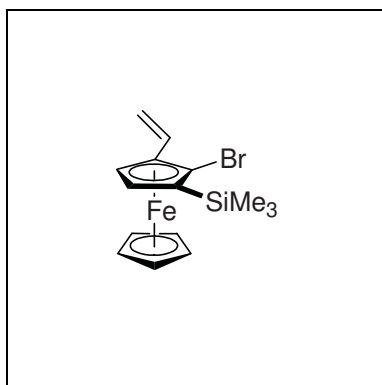
MS (EI): *m/z*(%) = 314(6), 301(6), 300(32), 244(16), 243(100), 242(7), 241(9).

$[\alpha]_D^{20} = -79$ (*c* = 0.37, CHCl₃ / 0.75% EtOH).

EA: calculated (%) for C₁₆H₂₄BFeP: C: 61.20, H: 7.70; measured: C: 60.74, H: 7.61.

R_f (SiO₂, Hex:EtOAc (10:1)): 0.19.

m.p.: 154-158 °C.



(*R*)-(η⁵-2,4-cyclopentadien-1-yl)(η⁵-2-bromo-1-trimethylsilyl-3-ethenyl-cyclopenta-2,4-dien-1-yl)iron (29**)**

To a solution of 2,2,6,6-tetramethylpiperidine (1.35 mL, 8.01 mmol) in THF (9 mL) was added *n*-butyllithium (5.00 mL, 1.6 M in hexane, 8.00 mmol) at 0 °C. After 30 min this solution was added dropwise to a solution of **4** (886 mg, 3.04 mmol) in

THF (15 mL) at -50 °C. The solution was kept between -40 and -30 °C for 2 h and then cooled down to -78 °C. To the dark red solution was added dropwise trimethylsilyl chloride (0.50 mL, 3.90 mmol). The solution was stirred for 2 h, then water (2 mL) was added and the solution was allowed to warm up to room temperature. The reaction mixture was extracted three times with sat. aq. NH₄Cl and dried over MgSO₄. The solvent was evaporated under reduced pressure and the residue was purified by column chromatography (SiO₂, 10×5 cm, hexanes) to give the title compound **29** (1.02 g, 92%) as a red oil which solidified at -20 °C.

$C_{15}H_{19}BrFeSi$ (363.15 g/mol)

1H -NMR (C_6D_6): $\delta/ppm = 0.34$ (s, 9H, $Si(CH_3)_3$), 3.91 (d, $^3J_{HH} = 2.7$ Hz, 1H, $C(Si)CH$), 3.96 (s, 5H, Cp-CH), 4.33 (d, $^3J_{HH} = 2.7$ Hz, 1H, $C(Si)CHCH$), 5.10 (dd, $^2J_{HH} = 1.6$ Hz, $^3J_{HH} = 10.9$ Hz, 1H, $CHCH_{E}H_Z$), 5.39 (dd, $^2J_{HH} = 1.6$ Hz, $^3J_{HH} = 17.5$ Hz, 1H, $CHCH_{E}H_Z$), 6.75 (dd, $^3J_{HH} = 10.9$ Hz, $^3J_{HH} = 17.5$ Hz, 1H, $CHCH_2$).

$^{13}C\{^1H\}$ -NMR (C_6D_6): $\delta/ppm = 0.0$ (s, $Si(CH_3)_3$), 65.8 (s, $C(Si)CHCH$), 72.1 (s, Cp-CH), 72.8 (s, $C(Si)CH$), 73.0 (s, CSi), 85.3 (s, $CCHCH_2$), 86.2 (s, CBr), 113.2 (s, $CHCH_2$), 132.9 (s, $CHCH_2$).

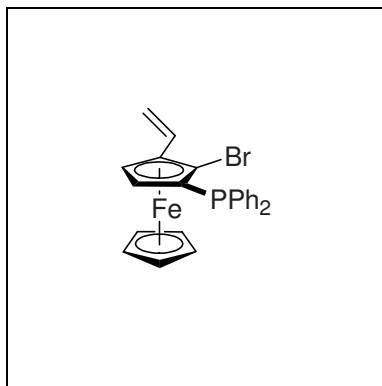
IR (NaCl): $\tilde{\nu}/cm^{-1} = 3090(m)$, 2956(s), 2898(m), 1703(w), 1628(m), 1459(w), 1406(m), 1327(w), 1282(m), 1249(s), 1146(s), 1107(m), 1055(w), 980(s), 909(s), 835(s), 756(m), 664(s).

MS (EI): $m/z(\%) = 365(20)$, 364(98), 363(21), 362(100), 360(5), 283(6), 281(6), 267(7), 225(5), 174(5), 147(29), 131(6), 121(12), 73(11).

$[\alpha]_D^{20} = +778$ ($c = 0.49$, $CHCl_3 / 0.75\%$ EtOH).

EA: calculated (%) for $C_{15}H_{19}BrFeSi$: C: 49.61, H: 5.27; measured: C: 49.63, H: 5.18.

R_f (SiO_2 , hexanes): 0.50.



(*R*)-(η⁵-2,4-cyclopentadien-1-yl)(η⁵-2-bromo-1-diphenylphosphino-3-ethenyl-cyclopenta-2,4-dien-1-yl)iron
(30)

To a solution of 2,2,6,6-tetramethylpiperidine (1.35 mL, 8.01 mmol) in THF (9 mL) was added *n*-butyllithium (5.00 mL, 1.6 M in hexane, 8.00 mmol) at 0 °C. After 30 min this solution was added dropwise to a solution of **4** (1.00 g, 3.44 mmol) in THF (15 mL) at -50 °C. The solution was kept between -40 and -30 °C for 2 h and then cooled down to -78 °C. To the dark red solution was added dropwise diphenylphosphine chloride (0.80 mL, 4.47 mmol). The solution was stirred for 2 h, then water (2 mL) was added and the solution was allowed to warm up to room temperature. The reaction mixture was extracted three times with sat. aq. NH_4Cl and dried over $MgSO_4$. The solvent was evaporated under reduced pressure and the residue was purified by column chromatography (SiO_2 , 15×5 cm, hexanes:EtOAc:NEt₃

(200:10:2)) and recrystallisation from hot hexane to give the title compound **30** (1.20 g, 74%) as an orange solid.

$C_{24}H_{20}BrFeP$ (475.14 g/mol)

1H -NMR (C_6D_6): $\delta/ppm = 3.72$ (d, $^3J_{HH} = 2.7$ Hz, 1H, C(P)CH); 3.97 (s, 5H, Cp-CH), 4.34 (d, $^3J_{HH} = 2.7$ Hz, 1H, C(P)CHCH), 5.08 (dd, $^3J_{HH} = 10.9$ Hz, $^2J_{HH} = 1.5$ Hz, 1H, CHCH_EH_Z), 5.40 (dd, $^3J_{HH} = 17.6$ Hz, $^2J_{HH} = 1.5$ Hz, 1H, CHCH_EH_Z), 6.74 (dd, $^3J_{HH} = 10.9$ Hz, $^3J_{HH} = 17.6$ Hz, 1H, CHCH₂), 6.96-7.03 (m, 3H, Ph-CH), 7.03-7.09 (m, 3H, Ph'-CH) 7.29-7.35 (m, 2H, Ph'-CH), 7.53-7.59 (m, 2H, Ph-CH).

$^{13}C\{^1H\}$ -NMR (C_6D_6): $\delta/ppm = 65.2$ (s, C(P)CHCH), 70.4 (d, $^2J_{CP} = 4.3$ Hz, C(P)CH), 73.4 (s, Cp-CH), 78.8 (d, $^2J_{CP} = 7.9$ Hz, C(Br)), 85.2 (d, $^3J_{CP} = 2.8$ Hz, CCHCH₂), 87.5 (d, $^1J_{CP} = 30.2$ Hz, C(P)C), 113.6 (s, CHCH₂), 128.2 (s, Ph-CH), 128.5 (d, $J_{CP} = 7.6$ Hz, Ph'-CH), 128.6 (d, $J_{CP} = 5.9$ Hz, Ph-CH), 129.4 (d, $J_{CP} = 0.7$ Hz, Ph'-CH), 132.6 (d, $J_{CP} = 18.4$ Hz, Ph'-CH), 132.7 (s, CHCH₂), 135.6 (d, $J_{CP} = 21.7$ Hz, Ph-CH), 137.7 (d, $^1J_{CP} = 11.4$ Hz, Ph'-C), 139.3 (d, $^1J_{CP} = 12.7$ Hz, Ph-C).

$^{31}P\{^1H\}$ -NMR (C_6D_6): $\delta/ppm = -22.4$ (s).

IR (KBr): $\tilde{\nu}/cm^{-1} = 3063$ (s), 3000(m), 1844(w), 1800(w), 1739(w), 1619(m), 1578(w), 1474(m), 1428(s), 1290(s), 1152(s), 1099(s), 1002(m), 973(s), 918(s), 819(s), 736(s), 693(s), 463(s).

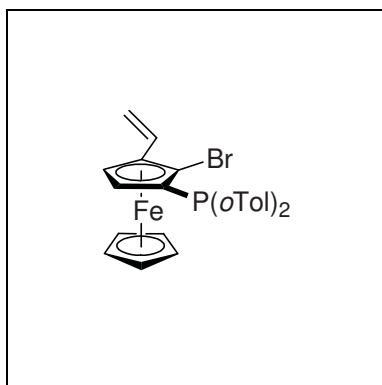
MS (EI): $m/z(\%) = 477$ (26), 476(96), 475(36), 473(100), 473(11), 394(10), 339(19), 273(12), 196(11), 183(13), 165(17), 153(17), 152(11).

$[\alpha]_D^{20} = +365$ ($c = 0.33$, $CHCl_3$ / 0.75% EtOH).

EA: calculated (%) for $C_{24}H_{20}BrFeP$: C: 60.67, H: 4.24; measured: C: 60.73, H: 4.20.

R_f (SiO_2 , hexanes:EtOAc:NEt₃ (100:5:1)): 0.42.

m.p.: 151-152 °C.



(R)-(η⁵-2,4-cyclopentadien-1-yl)(η⁵-2-bromo-1-di(*ortho*-tolyl)phosphino-3-ethenyl-cyclopenta-2,4-dien-1-yl)iron (31)

To a solution of 2,2,6,6-tetramethylpiperidine (2.00 mL, 11.9 mmol) in THF (9 mL) was added *n*-butyllithium (7.40 mL, 1.6 M in hexane, 11.8 mmol) at 0 °C. After 30 min this solution was added dropwise to a solution of **4** (1.42 g, 4.88 mmol) in

THF (20 mL) at –50 °C. The solution was kept between –40 and –30 °C for 5 h and then cooled down to –78 °C. To the dark red solution was added dropwise a solution of di(*o*-tolyl)phosphine chloride (1.56 g, 6.72 mmol) in THF (5 mL). The solution was stirred for 2 h, then water (2 mL) was added and the solution was allowed to warm up to room temperature. The reaction mixture was extracted three times with sat. aq. NH₄Cl and dried over MgSO₄. The solvent was evaporated under reduced pressure and the residue was purified by column chromatography (SiO₂, 10×5 cm, hexanes:EtOAc:NEt₃ (100:10:1)) to give the title compound **31** (2.44 g, 99%) as an orange solid.

C₂₆H₂₄BrFeP (503.19 g/mol)

¹H-NMR (C₆D₆): δ/ppm = 2.17 (d, ⁴J_{HP} = 1.3 Hz, 3H, *o*Tol'-CH₃), 2.81 (s, 3H, *o*Tol-CH₃), 3.91 (d, ³J_{HH} = 2.7 Hz, 1H, C(P)CH) 3.96 (s, 5H, Cp-CH), 4.40 (d, ³J_{HH} = 2.7 Hz, 1H, C(P)CHCH), 5.10 (dd, ³J_{HH} = 10.9 Hz, ²J_{HH} = 1.4 Hz, 1H, CHCH_EH_Z), 5.42 (dd, ³J_{HH} = 17.6 Hz, ²J_{HH} = 1.4 Hz, 1H, CHCH_EH_Z), 6.77 (dd, ³J_{HH} = 17.6 Hz, ³J_{HH} = 10.9 Hz, 1H, CHCH₂), 6.78-6.83 (m, 1H, *o*Tol-CH) 6.84-6.89 (m, 1H, *o*Tol'-CH), 6.89-6.95 (m, 1H, *o*Tol'-CH), 6.96-7.07 (m, 3H, *o*Tol-CH, *o*Tol'-CH), 7.16-7.20 (m, 1H, *o*Tol'-CH), 7.26-7.31 (m, 1H, *o*Tol-CH).

¹³C{¹H}-NMR (C₆D₆): δ/ppm = 20.9 (d, ³J_{CP} = 20.3 Hz, *o*Tol'-CH₃), 22.0 (d, ³J_{CP} = 24.8 Hz, *o*Tol-CH₃), 65.3 (d, ³J_{CP} = 1.2 Hz, C(P)CHCH), 71.0 (d, ²J_{CP} = 4.1 Hz, C(P)CH), 73.2 (d, J_{CP} = 0.7 Hz, Cp-CH) 78.8 (d, ¹J_{CP} = 7.1 Hz, C(P)C(Br)), 85.2 (d, ³J_{CP} = 2.8 Hz, CCHCH₂), 87.8 (d, ²J_{CP} = 30.6 Hz, C(Br)), 113.6 (s, CHCH₂), 126.1 (s, *o*Tol'-CH), 126.2 (d, J_{CP} = 1.8 Hz, *o*Tol-CH), 128.3 (s, *o*Tol'-CH), 129.6 (d, J_{CP} = 1.2 Hz, *o*Tol-CH), 130.2 (d, J_{CP} = 5.8 Hz, *o*Tol-CH), 130.4 (d, J_{CP} = 3.9 Hz, *o*Tol'-CH), 131.6 (d, J_{CP} = 1.6 Hz, *o*Tol'-CH), 132.8 (s, CHCH₂), 134.8 (d, J_{CP} = 10.8 Hz, *o*Tol-C), 136.7 (s, *o*Tol-CH), 139.0 (d, J_{CP} = 14.6 Hz, *o*Tol'-C), 140.5 (d, J_{CP} = 24.9 Hz, *o*Tol'-C), 143.8 (d, J_{CP} = 29.6 Hz, *o*Tol-C).

³¹P{¹H}-NMR (C₆D₆): δ/ppm = –41.5 (s).

IR (KBr): $\tilde{\nu}/\text{cm}^{-1} = 3054(\text{w}), 2967(\text{w}), 2921(\text{w}), 1917(\text{w}), 1794(\text{w}), 1772(\text{w}), 1739(\text{m}), 1694(\text{m}), 1644(\text{m}), 1561(\text{m}), 1539(\text{m}), 1511(\text{m}), 1456(\text{s}), 1289(\text{w}), 1267(\text{w}), 1150(\text{m}), 1100(\text{m}), 1000(\text{m}), 972(\text{m}), 900(\text{w}), 817(\text{m}), 750(\text{s}), 711(\text{w}), 672(\text{m})$.

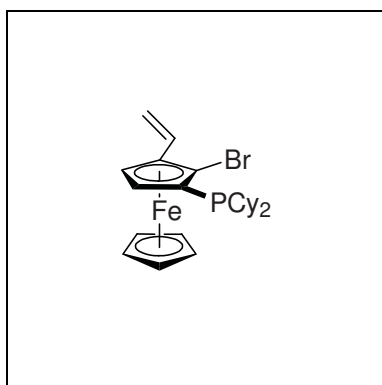
MS (EI): $m/z(\%) = 505(28), 504(95), 503(31), 502(100), 500(6), 439(6), 437(7), 367(8), 357(6), 302(17), 301(22), 290(6), 288(6), 287(9), 213(7), 212(10), 211.5(11), 211(17), 210(13), 209(15), 208(6), 207(10), 197(6), 196(16), 183(19), 179(13), 178(16), 165(15), 153(17), 152(11), 133(5), 121(9), 91(6)$.

$[\alpha]_D^{20} = +410$ ($c = 0.43$, $\text{CHCl}_3 / 0.75\% \text{ EtOH}$).

EA: calculated (%) for $\text{C}_{26}\text{H}_{24}\text{BrFeP}$: C: 62.06, H: 4.81; measured: C: 62.11, H: 4.85.

R_f (SiO_2 , hexanes:EtOAc:NEt₃ (100:5:1)): 0.23.

m.p.: 173-175 °C.



(R)-(η⁵-2,4-cyclopentadien-1-yl)(η⁵-2-bromo-1-dicyclohexylphosphino-3-ethenyl-cyclopenta-2,4-dien-1-yl)iron (32)

To a solution of 2,2,6,6-tetramethylpiperidine (1.60 mL, 9.50 mmol) in THF (5 mL) was added *n*-butyllithium (5.90 mL, 1.6 M in hexane, 9.44 mmol) at 0 °C. After 30 min this was added dropwise to a solution of **4** (1.06 g, 3.64 mmol) in THF (15 mL) at -50 °C. The solution was kept between -40 and -30 °C for 3 h and then cooled down to -78 °C. To the dark red solution was added dropwise dicyclohexylphosphine chloride (1.05 mL, 4.76 mmol). The solution was stirred for 2 h, then water (2 mL) was added and the solution was allowed to warm up to room temperature. The reaction mixture was extracted three times with sat. aq. NH₄Cl and dried over MgSO₄. The solvent was evaporated under reduced pressure and the residue was purified by column chromatography (SiO_2 , 10×5 cm, hexanes:EtOAc:NEt₃ (100:20:1)) to give the title compound **32** (1.74 g, 98%) as a sticky orange oil.

$\text{C}_{24}\text{H}_{32}\text{BrFeP}$ (487.24 g/mol)

¹H-NMR (C_6D_6): $\delta/\text{ppm} = 0.95\text{-}2.05$ (m, 21H, Cy-CH, Cy-CH₂), 2.29-2.37 (m, 1H, Cy-CHH), 4.02 (s, 5H, Cp-CH), 4.03 (d, ³J_{HH} = 2.8 Hz, 1H, C(P)CH), 4.41 (d, ³J_{HH} = 2.7 Hz, 1H, C(P)CHCH), 5.09 (dd, ³J_{HH} = 10.9 Hz, ²J_{HH} = 1.5 Hz, 1H, CHCH_EH_Z), 5.40 (dd,

$^3J_{\text{HH}} = 17.6$ Hz, $^2J_{\text{HH}} = 1.5$ Hz, 1H, CHCH_EH_Z), 6.79 (dd, $^3J_{\text{HH}} = 17.6$ Hz, $^3J_{\text{HH}} = 10.9$ Hz, 1H, CHCH₂).

$^{13}\text{C}\{^1\text{H}\}$ -NMR (C₆D₆): $\delta/\text{ppm} = 26.7$ (d, $J_{\text{CP}} = 1$ Hz, Cy-CH₂) 26.8 (d, $J_{\text{CP}} = 1$ Hz, Cy-CH₂), 27.7 (d, $J_{\text{CP}} = 8$ Hz, Cy-CH₂), 27.8 (d, $J_{\text{CP}} = 14$ Hz, Cy-CH₂), 27.9 (d, $J_{\text{CP}} = 11$ Hz, Cy-CH₂), 28.0 (d, $J_{\text{CP}} = 13$ Hz, Cy-CH₂), 30.5 (d, $J_{\text{CP}} = 10$ Hz, Cy-CH₂), 30.7 (d, $J_{\text{CP}} = 9$ Hz, Cy-CH₂), 31.5 (d, $J_{\text{CP}} = 16$ Hz, Cy-CH₂), 32.9 (d, $J_{\text{CP}} = 20$ Hz, Cy-CH₂), 34.2 (d, $^1J_{\text{CP}} = 13$ Hz, Cy-CH), 36.2 (d, $^1J_{\text{CP}} = 17$ Hz, Cy-CH), 64.6 (d, $^3J_{\text{CP}} = 1$ Hz, C(P)CHCH), 69.3 (d, $^2J_{\text{CP}} = 2$ Hz, C(P)CH), 73.6 (s, Cp-CH), 80.0 (d, $^2J_{\text{CP}} = 24$ Hz, CBr), 83.8 (d, $^1J_{\text{CP}} = 2$ Hz, CP), 87.3 (d, $^3J_{\text{CP}} = 26$ Hz, CCHCH₂), 113.2 (s, CHCH₂), 133.2 (s, CHCH₂).

$^{31}\text{P}\{^1\text{H}\}$ -NMR (C₆D₆): $\delta/\text{ppm} = -13.5$ (s).

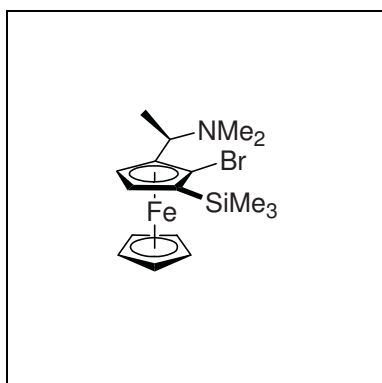
IR (KBr): $\tilde{\nu}/\text{cm}^{-1} = 3088(\text{w})$, 2922(s), 2848(s), 1702(w), 1628(m), 1558(w), 1446(m), 1408(w), 1290(m), 1152(w), 1107(w), 1000(m), 976(m), 898(m), 818(m), 656(w).

MS (EI): $m/z(\%) = 489(12)$, 488(44), 487(13), 486(46), 406(9), 405(7), 404(9), 403(5), 324(15), 323(94), 322(16), 321(100), 243(9), 241(5), 239(5), 185(7), 183(6), 153(5), 121(7), 55(5).

$[\alpha]_D^{20} = +499$ ($c = 0.37$, CHCl₃ / 0.75% EtOH).

EA: calculated (%) for C₂₄H₃₂BrFeP: C: 59.16, H: 6.62; measured: C: 59.88, H: 6.69.

R_f (SiO₂, hexanes:EtOAc:NEt₃ (100:5:1)): 0.22.



(*S,R_p*)-(η⁵-2,4-cyclopentadien-1-yl)(η⁵-2-bromo-3-(1-dimethylaminoethyl)-1-trimethylsilyl-cyclopenta-2,4-dien-1-yl)iron (**34**)

To a solution of 2,2,6,6-tetramethylpiperidine (0.50 mL, 2.97 mmol) in THF (4 mL) was added *n*-butyllithium (1.80 mL, 1.6 M in hexane, 2.88 mmol) at 0 °C. After 30 min this was added dropwise to a solution of **3** (336 mg, 1.00 mmol) in THF (4 mL) at -50 °C. The solution was kept between -40 and -30 °C for 3 h and then cooled down to -78 °C. To the dark red solution was added dropwise trimethylsilyl chloride (0.17 mL, 1.33 mmol). The solution was stirred for 2 h, then water (2 mL) was added and the solution was allowed to warm up to room temperature. The reaction mixture was extracted three times with sat. aq. NaHCO₃ and dried over MgSO₄. The solvent was evaporated under reduced pressure and the

residue was purified by column chromatography (SiO₂, 10×4 cm, hexanes:acetone:NEt₃ (80:20:1)) to give the title compound **34** (353 mg, 87%) as an orange oil.

C₁₇H₂₆BrFeNSi (408.23 g/mol)

¹H-NMR (C₆D₆): δ/ppm = 0.38 (s, 9H, Si(CH₃)₃), 1.31 (d, ³J_{HH} = 7.1 Hz, 3H, CHCH₃), 2.13 (s, 6H, N(CH₃)₂), 3.88 (d, ³J_{HH} = 2.5 Hz, 1H, C(Si)CH), 3.89 (q, ³J_{HH} = 7.1 Hz, 1H, CHCH₃), 3.95 (d, ³J_{HH} = 2.5 Hz, 1H, C(Si)CHCH), 3.98 (s, 5H, Cp-CH).

¹³C{¹H}-NMR (C₆D₆): δ/ppm = 0.01 (s, Si(CH₃)₃), 14.9 (s, CHCH₃), 40.9 (s, N(CH₃)₂), 56.5 (s, CHCH₃), 67.7 (s, C(Si)CHCH), 71.3 (s, C(Si)CHCH), 71.4 (s, Cp-CH), 71.8 (s, CSi), 86.4 (s, CBr), 91.5 (s, C(Br)CCH).

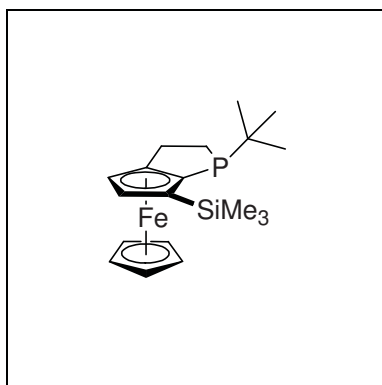
IR (NaCl): $\tilde{\nu}$ /cm⁻¹ = 3094(m), 2965(s), 2899(m), 2859(m), 2819(s), 2775(s), 1771(w), 1707(w), 1635(w), 1453(m), 1406(w), 1368(m), 1250(s), 1196(w), 1147(m), 1102(m), 1004(m), 976(m), 947(m), 905(w), 836(s), 756(m), 694(w), 632(m).

MS (EI): m/z(%) = 409(89), 407(91), 394(36), 392(37), 365(98), 363(100), 338(33), 336(34), 73(30), 72(38).

[α]_D²⁰ = +63 (c = 0.62, CHCl₃ / 0.75% EtOH).

EA: calculated for C₁₇H₂₆BrFeNSi: C: 50.02, H: 6.42, N: 3.43; measured: C: 50.43, H: 6.64, N: 3.67.

R_f (SiO₂, Hex:EtOAc:NEt₃ (33:66:1)): 0.14.



(*R,S_P*)-(η⁵-2,4-cyclopentadien-1-yl)[(3a,4,5,6,6a-η)-1-*tert*-butyl-6-trimethylsilyl-(1,2,3-trihydro-cyclopenta[*b*]phosphole-3a-yl]iron (**39**)

To a solution of **29** (476 mg, 1.31 mmol) in THF (10 mL) was added dropwise *n*-butyllithium (1.00 mL, 1.6 M in hexane, 1.60 mmol) at -78 °C. After 30 min this was added via cannula at -78 °C to a solution of *tert*-butylphosphine dichloride (252 mg, 1.58 mmol) in THF (10 mL). After 1 h a solution of LiAlH₄ (1.65 mL, 2 M in THF, 3.30 mmol) was added and the reaction mixture was allowed to warm up to room temperature during 3 h, then 2 M aq. NaOH was added until no more gas was formed. The suspension was filtered over a pad of silica eluting with ethyl acetate and the solvent was evaporated under reduced pressure. The residue

was dissolved in THF (10 mL) and a solution of $i\text{Pr}_2\text{NH}$ (0.25 mL, 1.77 mmol) and n -butyllithium (1.10 mL, 1.6 M in hexane, 1.76 mmol) in THF (5 mL) (prepared at 0 °C) was added. The solution was heated at 70 °C for 15 h. It was extracted three times with sat. aq. NaCl and dried over MgSO_4 . The solvent was removed under reduced pressure and column chromatography (SiO_2 , 15×4 cm, hexanes:EtOAc: NEt_3 (100:2:1)) gave the title compound **39** (367 mg, 75%) as an orange oil.

$\text{C}_{19}\text{H}_{29}\text{FePSi}$ (372.34 g/mol)

$^1\text{H-NMR}$ (C_6D_6): δ/ppm = 0.41 (s, 9H, $\text{Si}(\text{CH}_3)_3$), 1.94 (d, $^3J_{\text{HP}}$ = 11.3 Hz, 9H, $\text{C}(\text{CH}_3)_3$), 1.95-2.05 (m, 1H, $\text{PCH}_R\text{H}_S\text{CH}_2$), 2.30-2.50 (m, 3H, $\text{PCH}_R\text{H}_S\text{CH}_2$), 3.93 (s, 5H, Cp-CH), 4.11 (d, $^3J_{\text{HH}}$ = 2.1 Hz, 1H, $\text{C}(\text{Si})\text{CH}$), 4.26 (d, $^3J_{\text{HH}}$ = 2.2 Hz, 1H, $\text{C}(\text{Si})\text{CHCH}$).

$^{13}\text{C}\{^1\text{H}\}\text{-NMR}$ (C_6D_6): δ/ppm = 1.0 (d, $^4J_{\text{CP}}$ = 3.0 Hz, $\text{Si}(\text{CH}_3)_3$), 27.2 (d, $^1J_{\text{CP}}$ = 19.8 Hz, PCH_2CH_2), 27.2 (d, $^2J_{\text{CP}}$ = 1.1 Hz, PCH_2CH_2), 28.4 (d, $^2J_{\text{CP}}$ = 14.3 Hz, $\text{C}(\text{CH}_3)_3$), 31.9 (d, $^1J_{\text{CP}}$ = 19.7 Hz, $\text{C}(\text{CH}_3)_3$), 67.6 (s, $\text{C}(\text{Si})\text{CHCH}$), 70.7 (d, J_{CP} = 0.9 Hz, Cp-CH), 72.0 (d, $^2J_{\text{CP}}$ = 16.3 Hz, CSi), 79.2 (d, $^3J_{\text{CP}}$ = 2.2 Hz, $\text{C}(\text{Si})\text{CH}$), 89.1 (d, $^1J_{\text{CP}}$ = 18.6 Hz, $\text{C}(\text{Si})\text{C}$), 102.5 (s, $\text{C}(\text{Si})\text{CC}$).

$^{31}\text{P}\{^1\text{H}\}\text{-NMR}$ (C_6D_6): δ/ppm = -0.6 (s).

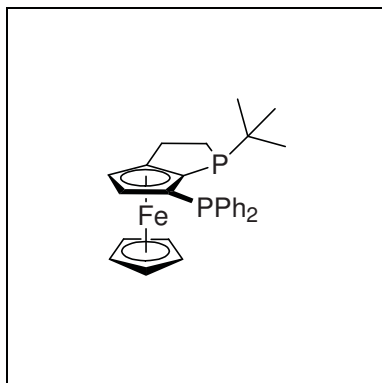
IR (NaCl): $\tilde{\nu}/\text{cm}^{-1}$ = 3090(m), 2950(s), 2897(s), 2859(s), 1742(w), 1650(w), 1462(m), 1412(m), 1360(w), 1249(s), 1182(w), 1123(m), 1054(w), 1001(m), 940(w), 837(s), 755(m), 693(m).

MS (EI): $m/z(\%)$ = 372(10), 317(5), 316(20), 315(100), 313(5), 241(7), 73(13).

$[\alpha]_D^{20}$ = +66 (c = 0.65, CHCl_3 / 0.75% EtOH).

EA: calculated (%) for $\text{C}_{19}\text{H}_{29}\text{FePSi}$: C: 61.29, H: 7.85; measured: C: 61.45, H: 7.80.

R_f (SiO_2 , hexanes:EtOAc: NEt_3 (100:2:1)): 0.27.



(*R,S_P*)-(η⁵-2,4-cyclopentadien-1-yl)[(3a,4,5,6,6a-η)-1-tert-butyl-6-diphenylphosphino-(1,2,3-trihydro-cyclopenta[*b*]phosphole-3a-yl]iron (40**)**

To a solution of **30** (1.32 g, 2.78 mmol) in THF (20 mL) was added dropwise n -butyllithium (2.10 mL, 1.6 M in hexane, 3.36 mmol) at -78 °C. After 30 min this was added via cannula to a solution of *tert*-butylphosphine dichloride (630 mg, 3.96 mmol) in THF (20 mL) at

–78 °C. After 1 h a solution of LiAlH₄ (4.00 mL, 2 M in THF, 8.00 mmol) was added and the reaction mixture was allowed to warm up to –20 °C during 3 h, then 2 M aq. NaOH was added until no more gas was formed. The suspension was filtered over a pad of silica eluting with ethyl acetate and the solvent was evaporated under reduced pressure. The residue was dissolved in THF (20 mL) and a solution of *i*Pr₂NH (0.55 mL, 3.90 mmol) and *n*-butyllithium (2.40 mL, 1.6 M in hexane, 3.84 mmol) in THF (6 mL) (prepared at 0 °C) was added. After 40 h at room temperature it was extracted three times with sat. aq. NaCl and dried over MgSO₄. The solvent was removed under reduced pressure and purification by column chromatography (SiO₂, 15×5 cm, hexanes:EtOAc:NEt₃ (300:10:3)) and recrystallization from MeOH gave the title compound **40** (940 mg, 70%) as a yellow solid.

C₂₈H₃₀FeP₂ (484.33 g/mol)

¹H-NMR (C₆D₆): δ/ppm = 0.89 (d, *J*_{HP} = 11.6 Hz, 9H, C(CH₃)₃), 1.98-2.08 (m, 1H, PCH_RH_SCH₂), 2.32-2.62 (m, 3H, PCH_RH_SCH₂), 3.83 (s, 5H, Cp-CH), 4.14 (d, ³*J*_{HH} = 2.3 Hz, 1H, Ph₂PCCH), 4.23 (d, ³*J*_{HH} = 2.3 Hz, 1H, Ph₂PCCHCH), 6.98 (t, *J*_{HH} = 7.2 Hz, 1H, Ph-CH) 7.01-7.08 (m, 5H, Ph-CH, Ph'-CH), 7.39 (t, *J*_{HH} = 7.0 Hz, 2H, Ph-CH), 7.64-7.72 (m, 2H, Ph'-CH).

¹³C{¹H}-NMR (C₆D₆): δ/ppm = 26.8 (d, *J*_{CP} = 17.6 Hz, PCH₂), 27.9 (d, *J*_{CP} = 4.6 Hz, PCH₂CH₂), 28.1 (dd, *J*_{CP} = 14.7 Hz, *J*_{CP} = 2.0 Hz, C(CH₃)₃), 31.9 (d, *J*_{CP} = 20.0 Hz, C(CH₃)₃), 67.5 (s br, Ph₂PCCHCH), 71.6 (d, *J*_{CP} = 1.3 Hz, Cp-CH), 76.4 (dd, *J*_{CP} = 5.1 Hz, *J*_{CP} = 0.5 Hz, Ph₂PCCH), 90.9 (dd, *J*_{CP} = 36.8 Hz, *J*_{CP} = 19.6 Hz, Ph₂PC), 102.5 (d, *J*_{CP} = 6.3 Hz, Ph₂PCC), 102.5 (d, *J*_{CP} = 6.5 Hz, Ph₂PCCC), 127.8 (s, Ph-CH), 128.2 (d, *J*_{CP} = 8.2 Hz, Ph'-CH), 128.2 (d, *J*_{CP} = 5.7 Hz, Ph-CH), 129.1 (s, Ph'-CH), 132.8 (d, *J*_{CP} = 17.8 Hz, Ph-CH), 135.8 (d, *J*_{CP} = 22.1 Hz, Ph'-CH), 139.6 (d, *J*_{CP} = 11.0 Hz, Ph'-C), 142.1 (d, *J*_{CP} = 11.2 Hz, Ph-C).

³¹P{¹H}-NMR (C₆D₆): δ/ppm = –22.3 (d, ³*J*_{PP} = 14.0 Hz, PPh₂), 0.1 (d, ³*J*_{PP} = 14.0 Hz, PC(CH₃)₃),

IR (KBr): $\tilde{\nu}$ /cm⁻¹ = 3049(m), 2925(s), 2853(s), 1952(w), 1884(w), 1813(w), 1757(w), 1706(w), 1649(w), 1582(w), 1462(m), 1431(m), 1358(m), 1279(w), 1227(w), 1180(w), 1128(m), 1099(m), 998(m), 815(s), 743(s), 695(s), 578(w), 503(m).

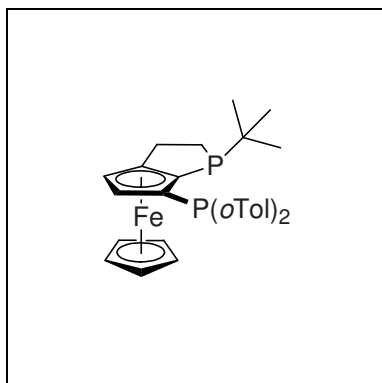
MS (EI): *m/z*(%) = 485(5), 484(17), 428(27), 427(100), 242(12), 241(12), 212(5), 183(6).

$[\alpha]_D^{20}$ = –319 (*c* = 0.39, CHCl₃ / 0.75% EtOH).

EA: calculated (%) for C₂₈H₃₀FeP₂: C: 69.44, H: 6.24; measured: C: 69.39, H: 6.38.

R_f (SiO₂, hexanes:EtOAc:NEt₃ (100:10:1)): 0.5.

m.p.: 168-170 °C.



(*R,S_p*)-(η⁵-2,4-cyclopentadien-1-yl)[(3a,4,5,6,6a-η)-1-*tert*-butyl-6-di(*ortho*-tolyl)phosphino-(1,2,3-trihydro-cyclopenta[*b*]phosphole-3a-yl)]iron (41**)**

To a solution of **31** (1.00 g, 1.99 mmol) in THF (7 mL) was added dropwise *n*-butyllithium (1.60 mL, 1.6 M in hexane, 2.56 mmol) at -78 °C. After 30 min this was added via cannula to a solution of *tert*-butylphosphine dichloride (400 mg, 2.52 mmol) in THF (10 mL) at -78 °C. After 1 h a solution of LiAlH₄ (2.90 mL, 2 M in THF, 5.80 mmol) was added and the reaction mixture was allowed to warm up to 0 °C during 3 h, then 2 M aq. NaOH was added until no more gas was formed. The suspension was filtered over a pad of silica eluting with ethyl acetate and the solvent was evaporated under reduced pressure. The residue was dissolved in THF (10 mL) and a solution of *i*Pr₂NH (0.35 mL, 2.48 mmol) and *n*-butyllithium (1.50 mL, 1.6 M in hexane, 2.40 mmol) in THF (3 mL) (prepared at 0 °C) was added. The solution was heated at 60 °C for 10 h. It was extracted three times with sat. aq. NaCl and dried over MgSO₄. The solvent was removed under reduced pressure and column chromatography (SiO₂, 15×5 cm, hexanes:CH₂Cl₂:NEt₃ (50:50:1)) gave the title compound **41** (579 mg, 57%) as a yellow foam.

C₃₀H₃₄FeP₂ (512.38 g/mol)

¹H-NMR (C₆D₆): δ/ppm = 0.88 (d, *J*_{HP} = 11.5 Hz, 9H, C(CH₃)₃), 2.00-2.08 (m, 1H, PCHHCH₂), 2.18 (d, *J* = 1.0 Hz, 3H, *o*Tol-CH₃) 2.37-2.62 (m, 3H, PCHHCH₂), 2.93 (s, 3H, *o*Tol-CH₃), 3.82 (s, 5H, Cp-CH), 4.29 (d, ³*J*_{HH} = 2.2 Hz, 1H, (*o*Tol)₂PCCHCH), 4.38 (d, ³*J*_{HH} = 2.1 Hz, 1H, (*o*Tol)₂PCCH), 6.82-6.91 (m, 2H, *o*Tol-CH), 6.98-7.09 (m, 4H, *o*Tol-CH), 7.35-7.39 (m, 1H, *o*Tol-CH), 7.39-7.44 (m, 1H, *o*Tol-CH).

¹³C{¹H}-NMR (C₆D₆): δ/ppm = 21.1 (d, *J*_{CP} = 19.8 Hz, *o*Tol-CH₃), 22.3 (d, *J*_{CP} = 26.5 Hz, *o*Tol-CH₃), 26.7 (d, *J*_{CP} = 17.5 Hz, PCH₂CH₂), 27.9 (d, *J*_{CP} = 4.5 Hz, PCH₂CH₂), 28.0 (dd, *J*_{CP} = 14.6 Hz, *J*_{CP} = 2.3 Hz, C(CH₃)₃), 32.1 (d, *J*_{CP} = 20.1 Hz, C(CH₃)₃), 67.8 (s, (*o*Tol)₂PCCHCH), 71.2 (s, Cp-CH), 76.0 (dd, *J*_{CP} = 14.3 Hz, ³*J*_{CP} = 10.9 Hz, (*o*Tol)₂PC), 76.4 (d, *J*_{CP} = 4.5 Hz, (*o*Tol)₂PCCH), 91.9 (dd, *J*_{CP} = 39.2 Hz, *J*_{CP} = 19.3 Hz, (*o*Tol)₂PCC), 102.6 (d, *J*_{CP} = 6.9 Hz, (*o*Tol)₂PCCC), 125.6 (s, *o*Tol-CH), 125.8 (s, *o*Tol-CH), 128.0 (s, *o*Tol-CH), 129.3 (s, *o*Tol-CH), 130.2 (d, *J*_{CP} = 6.6 Hz, *o*Tol-CH), 130.3 (d, *J*_{CP} = 4.4 Hz, *o*Tol-CH), 132.2 (s, *o*Tol-CH), 135.8 (d, *J*_{CP} = 2.7 Hz, *o*Tol-CH), 136.7 (d, *J*_{CP} = 9.3 Hz, *o*Tol-C), 140.6

(d, $J_{CP} = 24.3$ Hz, *o*Tol-C), 141.7 (d, $J_{CP} = 12.6$ Hz, *o*Tol-C), 143.5 (d, $J_{CP} = 31.4$ Hz, *o*Tol-C).

$^{31}\text{P}\{^1\text{H}\}$ -NMR (C_6D_6): $\delta/\text{ppm} = -43.4$ (d, $^3J_{PP} = 16.8$ Hz, $P(o\text{Tol})_2$), 0.2 (d, $^3J_{PP} = 16.8$ Hz, $\text{PC}(\text{CH}_3)_3$).

IR (KBr): $\tilde{\nu}/\text{cm}^{-1} = 3053(\text{m}), 3003(\text{w}), 2929(\text{s}), 2856(\text{m}), 1919(\text{w}), 1846(\text{w}), 1803(\text{w}), 1774(\text{w}), 1705(\text{w}), 1587(\text{w}), 1460(\text{m}), 1416(\text{w}), 1378(\text{w}), 1381(\text{w}), 1276(\text{w}), 1226(\text{w}), 1194(\text{w}), 1130(\text{m}), 1053(\text{w}), 1001(\text{w}), 816(\text{m}), 750(\text{s}), 719(\text{w}), 581(\text{w}), 511(\text{w}), 452(\text{s})$.

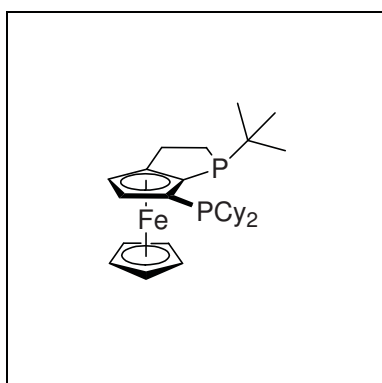
MS (EI): $m/z(\%) = 513(7), 512(17), 457(5), 456(30), 455(100), 453(6), 243(6), 242(8), 241(11)$.

$[\alpha]_D^{20} = -240$ ($c = 0.42$, $\text{CHCl}_3 / 0.75\%$ EtOH).

EA: calculated (%) for $\text{C}_{30}\text{H}_{34}\text{FeP}_2$: C: 70.32, H: 6.69; measured: C: 70.25, H: 6.70.

R_f (SiO_2 , hexanes: CH_2Cl_2 : NEt_3 (50:50:1)): 0.34.

m.p.: 71-76 °C.



(*R,S_p*)-(η⁵-2,4-cyclopentadien-1-yl)[(3a,4,5,6,6a-η)-1-*tert*-butyl-6-dicyclohexylphosphino-(1,2,3-trihydro-cyclopenta[*b*]phosphole-3a-yl)]iron (42)

To a solution of **32** (1.73 g, 3.55 mmol) in THF (10 mL) was added dropwise *n*-butyllithium (2.90 mL, 1.6 M in hexane, 4.64 mmol) at -78 °C. After 30 min this was added via cannula to a solution of *tert*-butylphosphine dichloride (734 mg, 4.62 mmol) in THF (10 mL) at -78 °C. After 1 h a solution of LiAlH_4 (5.10 mL, 2 M in THF, 10.2 mmol) was added and the reaction mixture was allowed to warm up to 0 °C during 3 h, then 2 M aq. NaOH was added until no more gas was formed. The suspension was filtered over a pad of silica eluting with ethyl acetate and the solvent was evaporated under reduced pressure. The residue was dissolved in THF (15 mL) and a solution of *i*Pr₂NH (0.750 mL, 5.32 mmol) and *n*-butyllithium (3.30 mL, 1.6 M in hexane, 5.28 mmol) in THF (5 mL) (prepared at 0 °C) was added. The solution was heated at 60 °C for 10 h. It was extracted three times with sat. aq. NaCl and dried over MgSO_4 . The solvent was removed under reduced pressure and column chromatography (SiO_2 , 15×5 cm hexanes: Et_2O : NEt_3 (100:10:1)) gave the title compound **42** (879 mg, 50%) as an orange solid.

$C_{28}H_{42}FeP_2$ (496.43 g/mol)

1H -NMR (C_6D_6): δ /ppm = 1.12 (d, J_{HP} = 11.0 Hz, 9H, $C(CH_3)_3$), 1.15-2.60 (m, 26H, Cy-CH, PCH_2CH_2), 4.03 (s, 5H, Cp-CH), 4.20 (s, 1H, Cy_2PCCH), 4.25 (s, 1H, Cy_2PCCH).

$^{13}C\{^1H\}$ -NMR (C_6D_6): δ /ppm = 26.9 (dd, J_{CP} = 10.3 Hz, J_{CP} = 1.0 Hz, Cy- CH_2), 27.1 (d, J_{CP} = 16.6 Hz, PCH_2CH_2), 27.6 (d, J_{CP} = 9.8 Hz, PCH_2CH_2), 27.7 (d, J_{CP} = 4.5 Hz, Cy- CH_2), 27.9 (d, J_{CP} = 10.8 Hz, Cy- CH_2), 27.9 (d, J_{CP} = 6.9 Hz, Cy- CH_2), 28.5 (d, J_{CP} = 12.9 Hz, Cy- CH_2), 29.2 (dd, J_{CP} = 14.2 Hz, $^5J_{CP}$ = 3.2 Hz, $C(CH_3)_3$), 30.2 (s, Cy- CH_2), 31.0 (s br, Cy- CH_2), 31.4 (d, J_{CP} = 15.3 Hz, Cy- CH_2), 32.3 (d, J_{CP} = 21.4 Hz, $C(CH_3)_3$), 32.4 (d, J_{CP} = 14.6 Hz, Cy- CH_2), 33.2 (d, J_{CP} = 18.7 Hz, Cy- CH_2), 35.9 (d, J_{CP} = 12.5 Hz, PCH), 38.6 (d, J_{CP} = 16.5 Hz, PCH), 66.6 (d, J_{CP} = 1.8 Hz, Cy_2PCCH), 71.0 (s, Cy_2PCC), 71.5 (d, J_{CP} = 1.2 Hz, Cp-CH), 71.9 (s, Cy_2PC), 78.1 (s br, $Cy_2PCCHCH$), 100.2 (dd, J_{CP} = 4.5 Hz, J_{CP} = 0.9 Hz, $C(P)C(P)C$).

$^{31}P\{^1H\}$ -NMR (C_6D_6): δ /ppm = -11.6 (s br, PCy_2), 1.9 (d, $^3J_{PP}$ = 7.0 Hz, $PC(CH_3)_3$).

IR (KBr): $\tilde{\nu}$ /cm $^{-1}$ = 3078(w), 2920(s), 2848(s), 1636(w), 1544(w), 1443(m), 1413(w), 1358(w), 1265(w), 1175(w), 1126(m), 1047(w), 1001(m), 885(w), 848(w), 818(m), 693(w).

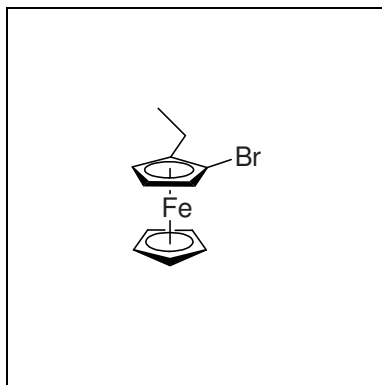
MS (EI): m/z (%) = 497(5), 496(14), 441(5), 440(31), 439(100), 437(6), 331(6), 275(13), 274(6), 244(5), 243(8), 242(5), 241(17).

$[\alpha]_D^{20}$ = -79 (c = 0.090, $CHCl_3$ / 0.75% EtOH).

EA: calculated (%) for $C_{28}H_{42}FeP_2$: C: 67.74, H: 8.53; measured: C: 67.70, H: 8.46.

R_f (SiO_2 , hexanes:EtOAc:NEt $_3$ (100:10:1)): 0.29.

m.p.: 170-175 °C.



(S)-(η 5 -2,4-Cyclopentadien-1-yl)(η 5 -1-bromo-2-ethylcyclopenta-2,4-dien-1-yl)iron (**44**)

A solution of **4** (340 mg, 1.17 mmol) in EtOAc (15 mL) containing palladium on charcoal (30 mg, 10% Pd, moistened with 50% H $_2$ O) was shaken under dihydrogen atmosphere at ambient pressure for 5 h. After filtration the solvent was evaporated under reduced pressure. Column chromatography (SiO_2 , 10×4 cm, hexanes) gave the title compound **44** (331 mg, 97%) as an orange liquid.

$C_{12}H_{13}BrFe$ (292.98 g/mol)

1H -NMR (C_6D_6): $\delta/ppm = 1.04$ (t, $^3J_{HH} = 7.5$ Hz, 3H, CH_3), 2.27 (dq, $^2J_{HH} = 15.0$ Hz, $^3J_{HH} = 7.5$ Hz, 1H, CHH), 2.37 (dq, $^2J_{HH} = 15.0$ Hz, $^3J_{HH} = 7.5$ Hz, 1H, CHH), 3.70 (t, $^3J_{HH} = 2.5$ Hz, 1H, $C(Br)CHCH$), 3.75-3.78 (m, 1H, $C(Br)CCH$), 3.95 (s, 5H, Cp- CH), 4.24 (dd, $^3J_{HH} = 2.3$ Hz, $^4J_{HH} = 1.5$ Hz, 1H, $C(Br)CH$).

$^{13}C\{^1H\}$ -NMR (C_6D_6): $\delta/ppm = 14.7$ (s, CH_3), 21.7 (s, CH_2), 65.5 (s, $C(Br)CHCH$), 65.9 (s, $C(Br)CCH$), 69.3 (s, $C(Br)CH$), 71.3 (s, Cp- CH), 80.3 (s, CBr), 89.4 (s, CEt).

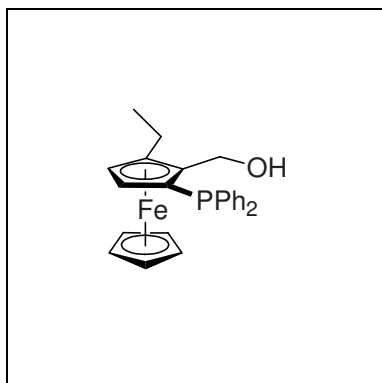
IR (NaCl): $\tilde{\nu}/cm^{-1} = 3094(m)$, 2966(s), 2930(m), 2870(m), 1771(w), 1719(w), 1652(w), 1463(m), 1387(m), 1304(w), 1168(w), 1106(m), 1072(m), 1001(m), 931(m), 818(s).

MS (EI): $m/z(\%) = 295(15)$, 294(93), 293(19), 292(100), 290(7), 279(11), 277(11), 213(20), 212(18), 210(9), 208(5), 197(6), 157(10), 147(7), 146(7), 142(6), 141(13), 137(8), 135(9), 129(6), 121(24), 115(8), 92(14), 91(20), 81(5), 65(11), 56(34).

$[\alpha]_D^{20} = -2.0$ ($c = 0.58$, $CHCl_3 / 0.75\%$ EtOH).

EA: calculated (%) for $C_{12}H_{13}BrFe$: C: 49.19, H: 4.47; measured: C: 49.56, H: 4.64.

R_f (SiO_2 , hexanes): 0.47.



(S)-(η⁵-2,4-Cyclopentadien-1-yl)(η⁵-1-diphenylphosphino-3-ethyl-2-hydroxymethyl-cyclopenta-2,4-dien-1-yl)iron (46**)**

To a solution of **45** (300 mg, 704 μ mol) in THF (10 mL) was added $LiAlH_4$ (400 μ L, 2 M in THF, 800 μ mol) at 0 °C. After 30 min 2 M aq. NaOH was added until no more gas was formed, the organic layer was dried over $MgSO_4$ and the solvent was

evaporated under reduced pressure. Column chromatography (SiO_2 , 15×4 cm, hexanes:EtOAc (4:1 → 2:1)) gave the title compound **46** (262 mg, 87%) as a yellow oil which solidified on standing.

$C_{25}H_{25}FeOP$ (428.28 g/mol)

1H -NMR (C_6D_6): $\delta/ppm = 1.12$ (t, $^3J_{HH} = 7.5$ Hz, 3H, CH_3), 1.15 (ddd, $^3J_{HH} = 7.2$ Hz, $^3J_{HH} = 4.9$ Hz, $^5J_{HP} = 1.3$ Hz, 1H, OH), 2.16-2.26 (m, 1H, $CHHCH_3$), 2.32-2.42 (m, 1H, $CHHCH_3$), 3.69 (dd, $^3J_{HH} = 2.5$ Hz, $^3J_{HP} = 1.0$ Hz, 1H, Ph_2PCCH), 3.86 (s, 5H, Cp- CH), 4.06

(d, $^3J_{\text{HH}} = 2.5$ Hz, 1H, Ph₂PCCHCH), 4.46 (dd, $^2J_{\text{HH}} = 12.2$ Hz, $^3J_{\text{HH}} = 7.2$ Hz, 1H, CHHOH), 4.74 (ddd, $^2J_{\text{HH}} = 12.2$ Hz, $^3J_{\text{HH}} = 4.9$ Hz, $^4J_{\text{HP}} = 2.6$ Hz, 1H, CHHOH), 6.91-7.02 (m, 3H, Ph-CH), 7.03-7.11 (m, 3H, Ph'-CH), 7.35-7.41 (m, 2H, Ph-CH), 7.56-7.62 (m, 2H, Ph'-CH).

$^{13}\text{C}\{^1\text{H}\}$ -NMR (C₆D₆): $\delta/\text{ppm} = 15.4$ (s, CH₃), 21.3 (s, CH₂CH₃), 58.4 (d, $^3J_{\text{CP}} = 10.5$ Hz, CH₂OH), 69.6 (d, $^2J_{\text{CP}} = 4.0$ Hz, Ph₂PCCH), 69.9 (s, Ph₂PCCHCH), 70.3, (s, Cp-CH), 76.7 (d, $^2J_{\text{CP}} = 7.2$ Hz, CCH₂OH), 90.9 (d, $^1J_{\text{CP}} = 23.3$ Hz, Ph₂PC), 94.1 (d, $^3J_{\text{CP}} = 3.5$ Hz, CEt), 128.3 (s, Ph-CH), 128.4 (d, $J_{\text{CP}} = 7.7$ Hz, Ph-CH), 128.6 (d, $J_{\text{CP}} = 5.8$ Hz, Ph'-CH), 129.2 (s, Ph'-CH), 132.8 (d, $J_{\text{CP}} = 18.2$ Hz, Ph-CH), 135.4 (d, $J_{\text{CP}} = 21.0$ Hz, Ph'-CH), 137.9 (d, $^1J_{\text{CP}} = 9.8$ Hz, Ph'-C), 141.1 (d, $^1J_{\text{CP}} = 11.4$ Hz, Ph-C).

$^{31}\text{P}\{^1\text{H}\}$ -NMR (C₆D₆): $\delta/\text{ppm} = -8.78$ (s).

IR (KBr): $\tilde{\nu}/\text{cm}^{-1} = 3446(\text{s}), 3066(\text{m}), 3020(\text{w}), 2960(\text{m}), 2923(\text{m}), 2868(\text{m}), 1585(\text{w}), 1477(\text{m}), 1434(\text{s}), 1368(\text{m}), 1307(\text{w}), 1277(\text{w}), 1241(\text{w}), 1184(\text{w}), 1154(\text{m}), 1131(\text{w}), 1107(\text{m}), 1068(\text{w}), 1000(\text{m}), 966(\text{s}), 822(\text{s}), 748(\text{s}), 701(\text{s}), 505(\text{s}), 485(\text{m}), 446(\text{m})$.

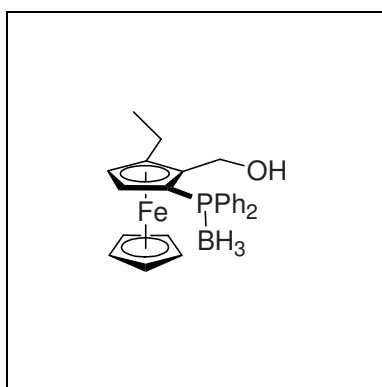
MS (EI): $m/z(\%) = 429(29), 428(100), 426(7), 291(18), 290(78), 289(32), 275(9), 261(8), 197(6), 183(20), 181(12), 167(5), 166(6), 165(11)$.

EA: calculated for C₂₅H₂₅FeOP: C: 70.11, H: 5.88; measured: C: 70.03, H: 5.90.

$[\alpha]_{\text{D}}^{20} = -212$ ($c = 0.098$, CHCl₃ / 0.75% EtOH).

R_{f} (SiO₂, hexanes:EtOAc (4:1)): 0.21.

m.p.: 124-126 °C.



(S)-(η⁵-2,4-Cyclopentadien-1-yl)(η⁵-1-boranyl(diphenyl)phosphino-3-ethyl-2-hydroxymethyl-cyclopenta-2,4-dien-1-yl)iron (**47**)

To a solution of **46** (200 mg, 425 μmol) in THF (5 mL) was added BH₃ (1.00 mL, 1 M in THF, 1.00 mol). After 3 h the reaction mixture was extracted with sat. aq. NaHCO₃, dried over MgSO₄ and the solvent was evaporated under reduced pressure. Column chromatography (SiO₂, 10×4 cm, hexanes:EtOAc (2:1)) gave the title compound **47** (205 mg, 99%) as a yellow oil which solidified glass-like upon standing.

$C_{25}H_{28}BFeOP$ (442.12 g/mol)

1H -NMR (C_6D_6): $\delta/ppm = 1.07$ (t, $^3J_{HH} = 7.5$ Hz, 3H, CH_3), 1.60-2.60 (m br, 3H, BH_3), 1.83 (t, $^3J_{HH} = 6.5$ Hz, 1H, OH), 2.05-2.17 (m, 1H, $CHHCH_3$), 2.24-2.35 (m, 1H, $CHHCH_3$), 3.73 (dd, $^3J_{HP} = 2.4$ Hz, $^3J_{HH} = 2.4$ Hz, 1H, EtCCHCH), 3.99 (s, 5H, Cp-CH), 4.04 (d, $^3J_{HH} = 2.4$ Hz, 1H, EtCCH), 4.36 (dd, $^2J_{HH} = 12.5$ Hz, $^3J_{HH} = 6.9$ Hz, 1H, CHHOH), 5.03 (dd, $^2J_{HH} = 12.5$ Hz, $^3J_{HH} = 6.0$ Hz, 1H, CHHOH), 6.86-6.96 (m, 3H, Ph-CH), 6.96-7.08 (m, 3H, Ph'-CH), 7.56-7.66 (m, 2H, Ph-CH), 7.72-7.82 (m, 2H, Ph'-CH).

$^{13}C\{^1H\}$ -NMR (C_6D_6): $\delta/ppm = 15.3$ (s, CH_3), 21.0 (s, CH_2CH_3), 57.1 (s, CH_2OH), 69.2 (d, $^1J_{CP} = 63.0$ Hz, EtCCC), 70.7 (d, $^3J_{CP} = 5.8$ Hz, EtCCH), 71.0 (s, Cp-CH), 71.7 (d, $^2J_{CP} = 3.8$ Hz, EtCCHCH), 90.5 (d, $^2J_{CP} = 14.4$ Hz, EtCC), 95.5 (d, $^3J_{CP} = 7.1$ Hz, EtC), 128.4 (d, $J_{CP} = 10.0$ Hz, Ph'-CH), 128.6 (d, $J_{CP} = 9.9$ Hz, Ph-CH), 130.8 (d, $J_{CP} = 2.2$ Hz, Ph-CH), 131.0 (d, $J_{CP} = 2.2$, Ph'-CH), 131.4 (d, $^1J_{CP} = 60.2$ Hz, Ph'-C), 132.7 (d, $^1J_{CP} = 57.2$ Hz, Ph-C), 132.9 (d, $J_{CP} = 9.4$ Hz, Ph-CH), 133.8 (d, $J_{CP} = 9.5$ Hz, Ph'-CH).

$^{31}P\{^1H\}$ -NMR (C_6D_6): $\delta/ppm = 28.6$ -30.0 (m).

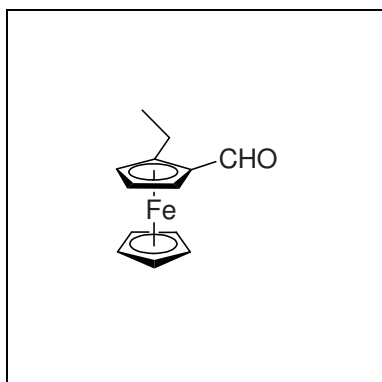
IR (KBr): $\tilde{\nu}/cm^{-1} = 3446$ (m), 3056(m), 2965(m), 2932(m), 2873(m), 2387(s), 22.67(w), 1972(w), 1897(w), 1654(w), 1479(m), 1436(m), 1376(m), 1314(m), 1275(m), 1154(m), 1106(s), 1062(s), 978(m), 823(m), 742(s), 697(s), 646(m), 595(w), 499(s).

MS (FAB): $m/z(\%) = 443$ (5), 442(18), 441(7), 430(5), 429(30), 428(100), 427(10), 426(9), 425(7), 412(16), 411(48), 409(5), 345(9), 335(13), 333(5), 291(7), 290(18), 289(8), 227(8), 211(5), 185(6), 183(15), 165(8), 136(6), 121(6), 91(8), 77(7), 56(6), 39(5).

$[\alpha]_D^{20} = -207.0$ ($c = 0.67$, $CHCl_3 / 0.75\%$ EtOH).

EA: calculated for $C_{25}H_{28}BFeOP$: C: 67.92, H: 6.38; measured: C: 67.75, H: 6.43.

R_f (SiO_2 , hexanes:EtOAc (2:1)): 0.51.



(S)-(η⁵-2,4-Cyclopentadien-1-yl)(η⁵-2-ethyl-1-formyl-cyclopenta-2,4-dien-1-yl)iron (**48**)

To a solution of **44** (600 mg, 2.05 mmol) in THF (8 mL) was added *n*-butyllithium (1.50 mL, 1.6 M in hexane, 2.40 mmol) at -78 °C. After 20 min DMF (220 μ L, 2.86 mmol) was added and the solution was allowed to warm up to room temperature. The

reaction mixture was extracted twice with water and dried over $MgSO_4$. The solvent was

evaporated under reduced pressure and column chromatography (SiO₂, 15×4 cm, hexanes:EtOAc (5:1)) gave the title compound **48** (457 mg, 92%) as a red liquid which solidified upon storage at 5 °C.

C₁₃H₁₄FeO (242.09 g/mol)

¹H-NMR (C₆D₆): δ/ppm = 1.04 (t, ³J_{HH} = 7.5 Hz, 3H CH₃), 2.38 (dq, ²J_{HH} = 15.0 Hz, ³J_{HH} = 7.5 Hz, 1H, CHHCH₃), 2.59 (dq, ²J_{HH} = 15.0 Hz, ³J_{HH} = 7.5 Hz, 1H, CHHCH₃), 3.85 (s, 5H, Cp-CH), 3.99 (t, ³J_{HH} = 2.5 Hz, 1H, EtCCHCH), 4.04 (s br, 1H, EtCCH), 4.46 (s br, 1H, EtCCCH), 10.00 (s, 1H, CHO).

¹³C{¹H}-NMR (C₆D₆): δ/ppm = 15.6 (s, CH₃), 21.4 (s, CH₂), 70.1 (s, Cp-CH), 70.3 (s, EtCCCH), 70.7 (s, EtCCHCH), 72.8 (s, EtCCH), 77.5 (s, CCHO), 93.6 (s, EtC), 192.4 (s, CHO).

IR (KBr): $\tilde{\nu}/\text{cm}^{-1}$ = 3086(w), 2966(w), 2926(w), 2866(w), 2796(w), 2728(w), 1671(s), 1439(m), 1408(w), 1383(w), 1362(w), 1312(w), 1278(m), 1188(w), 1151(w), 1104(w), 1038(w), 1001(m), 823(m), 744(m), 533(w), 492(m).

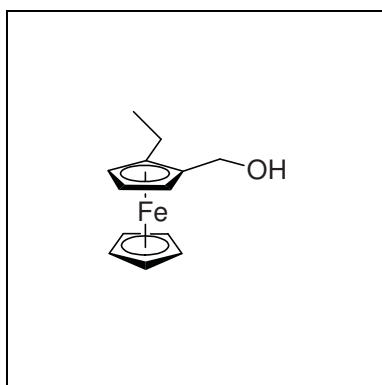
MS (EI): $m/z(\%)$ = 243(16), 242(100), 214(14), 213(35), 212(16), 199(25), 148(21), 122(13), 121(30), 56(15).

$[\alpha]_D^{20} = -168$ ($c = 0.26$, CHCl₃ / 0.75% EtOH).

EA: calculated for C₁₃H₁₄FeO: C: 64.50, H: 5.83; measured: C:64.37, H:5.76.

R_f (SiO₂, hexanes:EtOAc (5:1)): 0.40.

m.p.: 43-44 °C.



(S)-(η⁵-2,4-Cyclopentadien-1-yl)(η⁵-2-ethyl-1-hydroxymethyl-cyclopenta-2,4-dien-1-yl)iron (**49**)

To a solution of **48** (457 mg, 1.89 mmol) in THF (5 mL) was added LiAlH₄ (2.0 mL, 1 M in THF, 2.00 mmol) at 0 °C. After 20 min 2 M aq. NaOH was added until no more gas was formed, the organic layer was dried over MgSO₄ and the solvent was

evaporated under reduced pressure. Column chromatography (SiO₂, 15×4 cm, hexanes:EtOAc (2:1)) gave the title compound **49** (424 mg, 92%) as a yellow oil which solidified on standing.

$C_{13}H_{16}FeO$ (244.11 g/mol)

1H -NMR (C_6D_6): $\delta/ppm = 1.06$ (t, $^3J_{HH} = 7.5$ Hz, 3H, CH_3), 1.07 (dd, $^3J_{HH} = 6.9$ Hz, $^3J_{HH} = 4.6$ Hz, 1H, OH), 2.10-2.28 (m, 2H, CH_2CH_3), 3.86 (t, $^3J_{HH} = 2.4$ Hz, 1H, EtCCHCH), 3.88 (s, 5H, Cp-CH) 3.99-4.02 (m, 1H, EtCCH), 4.08-4.11 (m, 1H, EtCCCH), 4.15 (dd, $^2J_{HH} = 11.9$ Hz, $^3J_{HH} = 4.6$ Hz, 1H, CHHOH), 4.26 (dd, $^2J_{HH} = 11.9$ Hz, $^3J_{HH} = 6.9$ Hz, 1H, CHHOH).

$^{13}C\{^1H\}$ -NMR (C_6D_6): $\delta/ppm = 15.4$ (s, CH_3), 21.0 (s, CH_2CH_3), 59.4 (s, CH_2OH), 66.1 (s, EtCCHCH), 68.3 (s, EtCCH), 68.5 (s, EtCCCH), 69.0 (s, Cp-CH), 86.4 (s, EtCC), 90.3 (s, EtC).

IR (KBr): $\tilde{\nu}/cm^{-1} = 3261$ (s), 3091(m), 2963(m), 2926(m), 2867(m), 1743(w), 1687(w), 1636(w), 1468(w), 1448(w), 1415(w), 1373(w), 1315(m), 1278(m), 1196(w), 1134(w), 1103(m), 1034(w), 992(s), 814(s), 764(w), 682(m), 547(w), 485(m), 444(w).

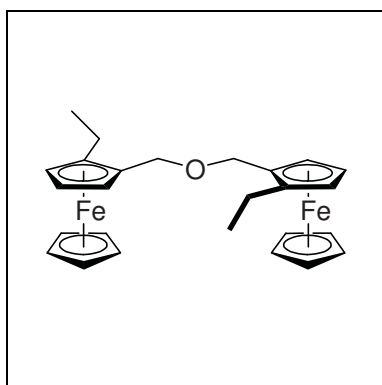
MS (EI): $m/z(\%) = 245$ (16), 244(100), 242(7), 226(20), 179(11), 161(6), 139(5), 138(62), 121(8), 106(14), 105(10), 91(29), 56(6).

$[\alpha]_D^{20} = +35.0$ ($c = 0.44$, $CHCl_3 / 0.75\%$ EtOH).

EA: calculated for $C_{13}H_{16}FeO$: C: 63.96, H: 6.61; measured: C: 63.78, H: 6.52.

R_f (SiO_2 , hexanes:EtOAc (2:1)): 0.48.

m.p.: 66-68 °C.



(*S,S*)-Di(2-ethylferrocen-1-yl)methyl ether (50)

To a solution of **49** (100 mg, 410 μ mol) and *p*-toluenesulfonyl chloride (80 mg, 419 μ mol) in CH_2Cl_2 (5 mL) was added triethyl amine (60 μ L, 434 μ mol) at room temperature. After 4 h the solvent was evaporated and the crude product was purified by column chromatography (SiO_2 , 15 \times 4 cm, hexanes:EtOAc

(10:1)) to give the title compound **50** (58 mg, 60%) as an orange oil which solidified upon storage at 5 °C.

$C_{26}H_{30}Fe_2O$ (470.21 g/mol)

$^1\text{H-NMR}$ (C_6D_6): $\delta/\text{ppm} = 1.15$ (t, $^3J_{\text{HH}} = 7.5$ Hz, 6H, CH_3), 2.20-2.43 (m, 4H, CH_2CH_3), 3.91-3.93 (m, 2H, EtCCHCH), 3.93 (s, 10H, Cp-CH), 3.95-3.98 (m, 2H, EtCCH), 4.14-4.17 (m, 2H, EtCCCH), 4.15 (d, $^2J_{\text{HH}} = 11.2$ Hz, 2H, CHHO), 4.44 (d, $^2J_{\text{HH}} = 11.2$ Hz, 2H, CHHO).

$^{13}\text{C}\{^1\text{H}\}\text{-NMR}$ (C_6D_6): $\delta/\text{ppm} = 15.4$ (s, CH_3), 21.2 (s, CH_2CH_3), 66.2 (s, EtCCHCH), 66.8 (s, CH_2O), 68.4 (s, EtCCH), 69.2 (s, Cp-CH), 70.0 (s, EtCCCH), 82.5 (s, EtCC), 91.0 (EtC).

IR (NaCl): $\tilde{\nu}/\text{cm}^{-1} = 3092(\text{m})$, 2963(s), 2932(s), 2866(m), 2235(w), 2050(w), 1919(w), 1761(w), 1699(w), 1636(w), 1453(s), 1344(m), 1276(m), 1193(w), 1137(m), 1105(m), 1044(s), 1002(s), 956(w), 884(w), 815(s), 758(m).

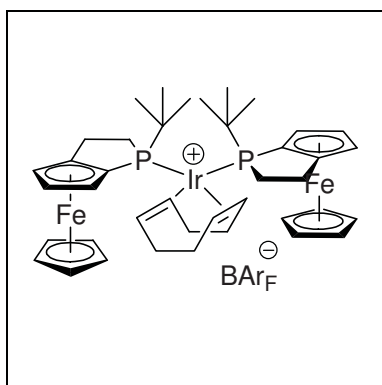
MS (EI): $m/z(\%) = 472(6)$, 471(33), 470(100), 268(7), 258(6), 235(11), 228(20), 227(91), 226(10), 225(7), 212(13), 193(6), 186(5), 121(13).

$[\alpha]_D^{20} = +13.5$ ($c = 0.45$, $\text{CHCl}_3 / 0.75\%$ EtOH).

EA: calculated for $\text{C}_{26}\text{H}_{30}\text{Fe}_2\text{O}$: C: 66.41, H: 6.43; measured: C: 66.12, H: 6.54.

R_f (SiO_2 , hexanes:EtOAc (10:1)): 0.56.

m.p.: 20-25 °C.



(*S,S*),(*S,S*)- $\{(\eta^4\text{-}1,5\text{-cyclooctadiene})\text{-bis}\{(\eta^5\text{-}2,4\text{-cyclopentadien-}1\text{-yl})[(3a,4,5,6,6a\text{-}\eta)\text{-}1\text{-tert-butyl-(}1,2,3\text{-trihydro-cyclopenta}[b]\text{phosphole-}3a\text{-yl)]\text{iron}\}\text{-iridium(I)}\}\text{-tetrakis[}3,5\text{-bis(trifluoromethyl)phenyl]borat (67)}$

$[\text{Ir}(\text{cod})\text{Cl}]_2$ (14.6 mg, 21.7 μmol) was dissolved in CH_2Cl_2 (1 mL) and a solution of **6** (26.0 mg, 86.7 μmol) in CH_2Cl_2 (1 mL) was added. After 10 min NaBARF (45.0 mg, 50.8 μmol) was added and the resulting mixture was stirred at room temperature for 1 h. The solvent was evaporated under reduced pressure and purification by column chromatography (SiO_2 , 2×10 cm) first by elution of the side products with TBME and then of the product with CH_2Cl_2 followed by recrystallization from CH_2Cl_2 /hexanes gave **67** (51.0 mg, 67%) as a brown-orange solid.

$\text{C}_{72}\text{H}_{66}\text{BF}_{24}\text{Fe}_2\text{IrP}_2$ (1764 g/mol)

$^1\text{H-NMR}$ (CD_2Cl_2): $\delta/\text{ppm} = 1.27$ (d, $J = 14.1$ Hz, 18H, $\text{C}(\text{CH}_3)_3$), 1.79-1.92 (m, 2H, cod- CH_2), 2.12-2.45 (m, 6H, cod- CH_2), 2.63-2.88 (m, 6H, CH_2), 2.97-3.08 (m, 2H, CH_2), 4.16 (s,

10H, Cp-CH), 4.27-4.31 (m, 2H, CH), 4.45-4.55 (m, 4H, CH, cod-CH), 4.58-4.62 (m, 2H, CH), 6.57-6.65 (m, 2H, cod-CH), 7.56 (s, 4H, BAr_F-CH), 7.70-7.75 (m, 8H, BAr_F-CH).

¹³C{¹H}-NMR (CD₂Cl₂): δ/ppm = 26.3 (s, cod-CH₂), 26.4-26.6 (m, CH₂), 29.2-29.3 (m, C(CH₃)₃), 31.3-31.8 (m, CH₂), 36.3-36.5 (m, cod-CH₂), 40.3-40.6 (m, C(CH₃)₃), 63.9-64.1 (m, CH), 67.5-67.7 (m, CH), 70.0 (s, Cp-CH), 74.9-75.2 (m, cod-CH), 75.5-75.7 (m, CH), 76.7-77.3 (m, CP), 91.2-91.4 (m, cod-CH), 99.4-99.7 (m, C(P)C), 117.0-117.2 (m, BAr_F-CH), 124.3 (q, ¹J_{CF} = 272 Hz, BAr_F-CF₃), 127.9-129.1 (m, BAr_F-C), 134.5 (s, BAr_F-CH), 161.4 (q, ¹J_{BC} = 50.0 Hz, BAr_F-CB).

³¹P{¹H}-NMR (CD₂Cl₂): δ/ppm = 31.7 (s).

IR (KBr): $\tilde{\nu}$ /cm⁻¹ = 2961(m), 2874(w), 1613(w), 1466(w), 1355(s), 1278(s), 1128(s), 1005(w), 889(w), 835(w), 713(w), 675(w).

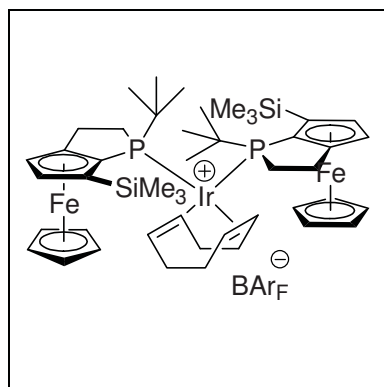
MS (ESI): *m/z*(%) = 902(47), 901(100), 900(32), 899(73), 897(7).

EA: calculated (%) for C₇₂H₆₆BF₂₄Fe₂IrP₂: C: 49.03, H: 3.77; measured: C: 49.03, H: 3.76.

[α]_D²⁰ = -10 (*c* = 0.074, CHCl₃ / 0.75% EtOH).

R_f (SiO₂, hexanes:CH₂Cl₂ (1:2)): 0.28.

m.p.: 235-240 °C (dec.).



(*R,S_P*),(*R,S_P*)-{(η⁴-1,5-cyclooctadiene)-bis{(η⁵-2,4-cyclopentadien-1-yl)[(3*a*,4,5,6,6*a*-η)-1-*tert*-butyl-6-trimethylsilyl-(1,2,3-trihydro-cyclopenta[*b*]phosphole-3*a*-yl]iron}-iridium(I)}-tetrakis[3,5-bis(trifluoromethyl)phenyl]borat (**68**)

[Ir(cod)Cl]₂ (20.0 mg, 29.8 μmol) was dissolved in CH₂Cl₂ (1 mL) and a solution of **39** (45.0 mg, 121 μmol) in CH₂Cl₂ (1 mL) was added. After 10 min NaBAr_F (63.0 mg, 71.1 μmol) was added and the resulting mixture was stirred at room temperature for 6 h. The solvent was evaporated under reduced pressure and purification by column chromatography (SiO₂, 2×10 cm) first by elution of the side products with TBME and then of the product with CH₂Cl₂ followed by recrystallization from CH₂Cl₂/hexanes gave **68** (55.0 mg, 48%) as a red-brown solid.

C₇₈H₈₂BF₂₄Fe₂IrP₂Si₂ (1908 g/mol)

$^1\text{H-NMR}$ (CD_2Cl_2): $\delta/\text{ppm} = 0.39$ (s, 18H, $\text{Si}(\text{CH}_3)_3$), 1.30 (d, $^3J_{\text{HP}} = 13.9$ Hz, 18H, $\text{C}(\text{CH}_3)_3$), 1.65-1.79 (m, 2H, cod- CHH), 2.00-2.23 (m, 4H, cod- CHH), 2.32-2.45 (m, 2H, cod- CHH), 2.67-2.87 (m, 6H, CH_2CHH), 3.01-3.13 (m, 2H, CH_2CHH), 4.15 (s, 10H, Cp- CH), 4.19-4.30 (m, 2H, cod- CH), 4.70 (d, $^3J_{\text{HH}} = 2.6$ Hz, 2H, CHCH), 4.74-4.77 (m, 2H, CHCH), 6.10-6.18 (m, 2H, cod- CH), 7.56 (s, 4H, BAr_F - CH), 7.70-7.75 (m, 8H, BAr_F - CH).

$^{13}\text{C}\{^1\text{H}\}$ -NMR (CD_2Cl_2): $\delta/\text{ppm} = 3.1$ (s, $\text{Si}(\text{CH}_3)_3$), 25.4-25.6 (m, CH_2CH_2), 26.3 (s, cod- CH_2), 29.4 (s, cod- CH_2), 29.9-30.1 (m, $\text{C}(\text{CH}_3)_3$), 32.2-32.6 (m, cod- CH_2), 36.3-36.5 (m, CH_2CH_2), 40.0 (d, $^1J_{\text{CP}} = 21.4$ Hz, $\text{C}(\text{CH}_3)_3$), 67.4-67.5 (m, CHCH), 69.7-70.0 (m, cod- CH), 70.1 (s, Cp- CH), 79.2 (d, $^1J_{\text{CP}} = 43.1$ Hz, $\text{C}(\text{Si})\text{C}$), 85.7-85.8 (m, CHCH), 87.7-87.9 (m, cod- CH), 104.0-104.4 (m, $\text{C}(\text{Si})\text{CC}$), 117.0-117.2 (m, BAr_F - CH), 124.3 (d, $^1J_{\text{CF}} = 272$ Hz, BAr_F - CF_3), 127.9-129.1 (m, BAr_F - C), 134.5 (s, BAr_F - CH), 161.4 (q, $^1J_{\text{BC}} = 50.0$ Hz, BAr_F - CB).

$^{31}\text{P}\{^1\text{H}\}$ -NMR (CD_2Cl_2): $\delta/\text{ppm} = 49.4$ (s).

IR (KBr): $\tilde{\nu}/\text{cm}^{-1} = 2958(\text{m})$, 1612(w), 1467(w), 1355(m), 1278(s), 1128(s), 1005(w), 889(w), 837(w), 712(w), 676(w).

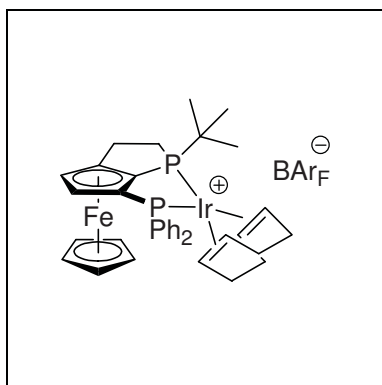
MS (ESI): $m/z(\%) = 1047(21)$, 1046(51), 1045 (97), 1044(39), 1043(59), 1041(8), 675(8), 674(35), 673 (100), 672(25), 671(65), 670(6), 669(15), 667(7).

EA: calculated (%) for $\text{C}_{78}\text{H}_{82}\text{BF}_{24}\text{Fe}_2\text{IrP}_2\text{Si}_2 \cdot \text{CH}_2\text{Cl}_2$: C: 47.60, H: 4.25; measured: C: 47.96, H: 4.05.

$[\alpha]_D^{20} = +13$ ($c = 0.081$, CHCl_3 / 0.75% EtOH).

R_f (SiO_2 , hexanes: CH_2Cl_2 (1:2)): 0.28.

m.p.: 140-150 °C (dec.).



(*R,S*)-{(η^4 -1,5-cyclooctadiene)-{(η^5 -2,4-cyclopentadien-1-yl)[(3a,4,5,6,6a- η)-1-*tert*-butyl-6-diphenylphosphino-(1,2,3-trihydro-cyclopenta[*b*]phosphole-3a-yl)iron}-iridium(I)}-tetrakis[3,5-bis(trifluoromethyl)phenyl]borat (69)

$[\text{Ir}(\text{cod})\text{Cl}]_2$ (40.0 mg, 59.5 μmol) was dissolved in CH_2Cl_2 (1 mL) and a solution of **40** (58.0 mg, 120 μmol) in CH_2Cl_2 (1 mL) was added. After 10 min NaBAr_F (110 mg, 124 μmol) was added and the resulting mixture was stirred at room temperature for 1 h. The solvent was evaporated under reduced pressure and purification by column chromatography (SiO_2 , 2×10 cm) first by elution of the

side products with TBME and then of the product with CH₂Cl₂ followed by recrystallization from CH₂Cl₂/hexanes gave **69** (170 mg, 86%) as an orange solid.

C₆₈H₅₄BF₂₄FeIrP₂ (1648 g/mol)

¹H-NMR (CD₂Cl₂): δ/ppm = 0.88 (d, J_{HP} = 15.3 Hz, 9H, C(CH₃)₃) 1.80-1.90 (m, 1H, cod-CH₂), 1.92-2.06 (m, 2H, cod-CH₂), 2.11-2.23 (m, 2H, cod-CH₂), 2.29-2.43 (m, 3H, cod-CH₂), 2.75-2.85 (m, 1H, CHHCH₂), 2.87-3.16 (m, 3H, CHHCH₂), 4.20-4.28 (m, 1H, cod-CH), 4.31 (s, 5H, Cp-CH), 4.96-5.00 (m, 1H, CH), 5.00-5.08 (m, 1H, cod-CH), 5.14-5.22 (m, 2H, cod-CH), 5.51-5.55 (m, 1H, CH), 7.36-7.44 (m, 3H, Ph-CH), 7.48-7.59 (m, 9H, Ph-CH, BAr_F-CH), 7.70-7.76 (m, 8H, BAr_F-CH), 7.83-7.90 (m, 2H, Ph-CH).

¹³C{¹H}-NMR (CD₂Cl₂): δ/ppm = 28.4 (d, J_{CP} = 5.6 Hz, C(CH₃)₃), 29.3-29.5 (m, cod-CH₂), 30.0 (d, J_{CP} = 25.3 Hz, CH₂), 31.0 (d, J_{CP} = 8.6 Hz, CH₂), 31.1-31.2 (m, cod-CH₂), 31.8-32.1 (m, cod-CH₂), 38.7 (d, J_{CP} = 17.7 Hz, C(CH₃)₃), 68.2 (dd, J_{CP} = 58.6 Hz, J_{CP} = 22.1 Hz, Ph₂PC), 73.5 (d, J_{CP} = 6.6 Hz, CH), 73.8 (s, Cp-CH), 75.3-75.5 (m, CH), 77.8 (d, J_{CP} = 11.1 Hz, cod-CH), 78.1 (d, J_{CP} = 8.6 Hz, cod-CH), 79.1 (d, J_{CP} = 14.2 Hz, cod-CH), 79.3 (d, J_{CP} = 13.6 Hz, cod-CH), 96.9-97.2 (m, C), 99.9 (d, J_{CP} = 55.2 Hz, C), 117.0-117.3 (m, BAr_F-CH), 124.4 (q, ¹J_{CF} = 272 Hz, BAr_F-CF₃), 128.3-129.0 (m, BAr_F-C), 128.7 (d, J_{CP} = 10.1 Hz, Ph-CH), 126.9 (d, J_{CP} = 10.0 Hz, Ph-CH), 130.2 (d, J_{CP} = 52.6 Hz, Ph-C), 130.7-130.9 (m, Ph-CH), 131.2 (d, J_{CP} = 11.5 Hz, Ph-CH), 131.4 (d, J_{CP} = 9.4 Hz, Ph-CH), 134.5 (s, BAr_F-CH), 137.0 (d, J_{CP} = 41.5 Hz, Ph-C), 161.8 (q, ¹J_{BC} = 49.9 Hz, BAr_F-CB).

³¹P{¹H}-NMR (CD₂Cl₂): δ/ppm = 11.2 (d, J_{PP} = 9.5 Hz), 29.4 (d, J_{PP} = 9.5 Hz).

IR (KBr): $\tilde{\nu}$ /cm⁻¹ = 2991(w), 2933(w), 1613(w), 1466(w), 1436(w), 1355(m), 1278(s), 1128(s), 1006(w), 889(w), 838(w), 744(w), 707(w), 677(w).

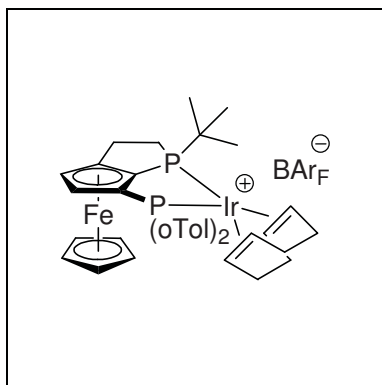
MS (ESI): *m/z*(%) = 787(6), 786(36), 785 (100), 784(30), 783(70), 782(5), 781(10).

EA: calculated (%) for C₆₈H₅₄BF₂₄FeIrP₂•CH₂Cl₂: C: 47.82, H: 3.26; measured: C: 47.92, H: 3.32.

$[\alpha]_D^{20} = -80$ (*c* = 0.065, CHCl₃ / 0.75% EtOH).

R_f (SiO₂, hexanes:CH₂Cl₂ (1:2)): 0.28.

m.p.: 235-240 °C.



(*R,S_P*)-{(η⁴-1,5-cyclooctadiene)-{(η⁵-2,4-cyclopentadien-1-yl)[(3a,4,5,6,6a-η)-1-*tert*-butyl-6-di(*ortho*-toluy)lphosphino-(1,2,3-trihydro-cyclopenta[*b*]phosphole-3a-yl]iron}-iridium(I)}-tetrakis[3,5-bis(trifluoromethyl)phenyl]borat (70)

[Ir(cod)Cl]₂ (40.0 mg, 59.5 μmol) was dissolved in CH₂Cl₂ (1 mL) and a solution of **41** (62.0 mg, 121 μmol) in CH₂Cl₂ (1 mL) was added. After 10 min NaBAR_F (110 mg, 124 μmol) was added and the resulting mixture was stirred at room temperature for 1 h. The solvent was evaporated under reduced pressure and purification by column chromatography (SiO₂, 2×10 cm) first by elution of the side products with TBME and then of the product with CH₂Cl₂ followed by recrystallization from CH₂Cl₂/hexanes gave **70** (161 mg, 81%) as an orange solid.

C₇₀H₅₈BF₂₄FeIrP₂ (1676 g/mol)

¹H-NMR (CD₂Cl₂, two conformers): δ/ppm = 1.07 (d, *J* = 15.1 Hz, 9H, C(CH₃)₃ minor), 1.18 (d, *J* = 15.0 Hz, 9H, C(CH₃)₃ major), 1.80-2.50 (m, 7H major, 7H minor, CH₂), 1.84 (s, 3H, CH₃ major), 1.87 (s, 3H, CH₃ major), 1.90 (s, 3H, CH₃ minor), 2.08 (s, 3H, CH₃ minor), 2.57-2.72 (m, 1H major, CH₂), 2.77-2.86 (m, 1H major, 1H minor, CH₂), 2.88-3.19 (m, 3H major, 4H minor, CH₂), 3.99 (s, 5H major, Cp-CH), 4.21 (s, 5H minor, Cp-CH), 4.40-4.73 (m, 3H major, 1H minor), 4.82-4.85 (m, 1H minor), 4.92-5.00 (m, 1H minor), 5.02-5.10 (m, 2H minor), 5.13-5.21 (m, 1H major), 5.44-5.47 (m, 1H major, CH), 5.47-5.55 (m, 1H major, 1H minor, CH), 7.07-7.13 (m, 1H minor, *o*Tol-CH), 7.18-7.38 (m, 5H major, 3H minor, *o*Tol-CH), 7.47-7.70 (m, 2H major, 3H minor, *o*Tol-CH), 7.56 (s, 4H major, 4H minor, BAR_F-CH), 7.73 (s, 8H major, 8H minor, BAR_F-CH), 9.05 (ddd, *J* = 15.7 Hz, *J* = 7.6 Hz, *J* = 1.4 Hz, 1H, *o*Tol-CH major), 9.16 (ddd, *J* = 13.8 Hz, *J* = 7.6 Hz, *J* = 1.8 Hz, 1H, *o*Tol-CH minor).

¹³C{¹H}-NMR (CD₂Cl₂): δ/ppm = 21.1 (d, *J* = 4.9 Hz), 21.3 (d, *J* = 2.8 Hz), 21.8 (d, *J* = 3.6 Hz), 22.2 (d, *J* = 3.8 Hz), 26.3-26.5 (m), 26.9-27.0 (m), 28.1 (d, *J* = 5.2 Hz), 28.8 (d, *J* = 5.3 Hz), 30.0-30.7 (m), 31.7-31.9 (m), 32.3-32.4 (m), 36.5-36.7 (m), 37.9 (d, *J* = 5.3 Hz), 38.9 (d, *J* = 17.5 Hz), 40.2 (d, *J* = 18.8 Hz), 67.1 (d, *J* = 23.1 Hz), 69.6 (d, *J* = 17.5 Hz), 72.4 (d, *J* = 7.0 Hz), 72.6 (d, *J* = 13.5 Hz), 73.0 (s), 73.8 (s), 75.3-75.4 (m), 75.9-76.0 (m), 79.8 (d, *J* = 11.1 Hz), 83.4 (d, *J* = 7.0 Hz), 83.5-83.7 (m), 84.6 (d, *J* = 2.0 Hz), 97.7 (t, *J* = 11.8 Hz), 102.4 (dd, *J* = 54.5 Hz, *J* = 38.1 Hz), 117.0-117.3 (m, BAR_F-CH), 124.3 (q, ¹J_{CF} = 272 Hz, BAR_F-CF₃), 124.9 (d, *J* = 11.3 Hz), 125.7 (d, *J* = 14.6 Hz), 126.1 (d, *J* = 8.6 Hz), 127.7 (d,

$J = 50.3$ Hz), 128.8-129.2 (m, BAr_F-C), 130.6 (d, $J = 2.0$ Hz), 131.3 (d, $J = 2.3$ Hz), 131.4 (d, $J = 2.7$ Hz), 131.6 (d, $J = 7.8$ Hz), 131.8 (d, $J = 2.5$ Hz), 132.1 (d, $J = 6.2$ Hz), 132.5 (d, $J = 9.0$ Hz), 132.7-133.2 (m), 134.5 (s, BAr_F-CH), 136.1 (d, $J = 14.2$ Hz), 137.9 (d, $J = 24.7$ Hz), 138.8 (d, $J = 11.6$ Hz), 140.8 (d, $J = 82.8$ Hz), 140.9 (d, $J = 90.0$ Hz), 141.3 (s), 161.5 (q, $^1J_{CB} = 49.8$ Hz, BAr_F-CB).

$^{31}\text{P}\{^1\text{H}\}$ -NMR (CD₂Cl₂, two conformers): $\delta/\text{ppm} = 13.5$ (d, $J_{PP} = 9.0$ Hz, minor), 18.3 (d, $J_{PP} = 8.1$ Hz, major), 29.8 (d, $J_{PP} = 9.0$ Hz, minor), 30.9 (d, $J_{PP} = 8.1$ Hz, major).

IR (KBr): $\tilde{\nu}/\text{cm}^{-1} = 2940(\text{m}), 2948(\text{m}), 2889(\text{w}), 1611(\text{w}), 1463(\text{w}), 1355(\text{s}), 1278(\text{s}), 1128(\text{s}), 1006(\text{w}), 889(\text{w}), 837(\text{w}), 753(\text{w}), 713(\text{w}), 675(\text{w})$.

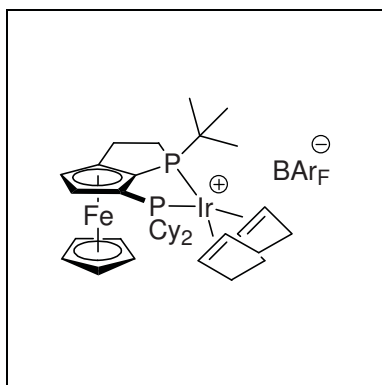
MS (ESI): $m/z(\%) = 815(8), 814(41), 813(100), 812(26), 811(63)$.

EA: calculated (%) for C₇₀H₅₈BF₂₄FeIrP₂: C: 50.17, H: 3.49; measured: C: 50.24, H: 3.52.

$[\alpha]_D^{20} = -180$ ($c = 0.075$, CHCl₃ / 0.75% EtOH).

R_f (SiO₂, hexanes:CH₂Cl₂ (1:2)): 0.28.

m.p.: 215-220 °C (dec.).



(*R,S*)-{(η^4 -1,5-cyclooctadiene)-{(η^5 -2,4-cyclopentadien-1-yl)}[(3a,4,5,6,6a- η)-1-*tert*-butyl-6-dicyclohexylphosphino-(1,2,3-trihydro-cyclopenta[*b*]phosphole-3a-yl)iron]-iridium(I)}-tetrakis[3,5-bis(trifluoromethyl)phenyl]borat (71)

[Ir(cod)Cl]₂ (40.0 mg, 59.5 μmol) was dissolved in CH₂Cl₂ (1 mL) and a solution of **42** (60.0 mg, 121 μmol) in CH₂Cl₂ (1 mL) was added. After 10 min NaBAr_F (130 mg, 147 μmol) was added and the resulting mixture was stirred at room temperature for 1 h. The solvent was evaporated under reduced pressure and purification by column chromatography (SiO₂, 2 \times 10 cm) first by elution of the side products with TBME and then of the product with CH₂Cl₂ followed by recrystallization from CH₂Cl₂/hexanes gave **71** (163 mg, 83%) as an orange solid.

C₆₈H₆₆BF₂₄FeIrP₂ (1660 g/mol)

^1H -NMR (CD₂Cl₂): $\delta/\text{ppm} = 0.95$ -2.37 (m, 29H, Cy-CH, Cy-CH₂, cod-CH₂), 1.23 (d, $J_{HP} = 15.0$ Hz, 9H, C(CH₃)₃), 2.35-2.43 (m, 1H, Cy-CHH), 2.67-3.02 (m, 4H, PCH₂CH₂),

4.35 (s, 5H, Cp-CH), 4.53-4.62 (m, 1H, cod-CH), 4.64-4.67 (m, 1H, cod-CH), 4.67-4.75 (m, 1H, CHCH), 4.75-4.84 (m, 1H, CHCH), 5.29 (d, $J = 2.0$ Hz, 1H, cod-CH), 5.42-5.51 (m, 1H, cod-CH), 7.56 (s, 4H, BAr_F-CH), 7.70-7.75 (m, 8H, BAr_F-CH).

¹³C{¹H}-NMR (CD₂Cl₂): δ /ppm = 25.3 (d $J_{CP} = 6.0$ Hz, Cy-CH₂), 27.1 (d, $J_{CP} = 13.4$ Hz, Cy-CH₂), 27.3 (d, $J_{CP} = 12.8$ Hz, Cy-CH₂), 27.5 (d, $J_{CP} = 5.8$ Hz, Cy-CH₂), 27.6 (d, $J_{CP} = 5.7$ Hz, Cy-CH₂), 28.4-28.5 (m, cod-CH₂), 29.3 (d, $J_{CP} = 5.6$ Hz, C(CH₃)₃), 29.4-29.6 (m), 29.8 (d, $J_{CP} = 7.2$ Hz, Cy-CH₂), 30.2 (d, $J_{CP} = 24.3$ Hz, PCH₂CH₂), 30.4 (d, $J_{CP} = 4.9$ Hz, PCH₂CH₂), 31.0 (d, $J_{CP} = 8.8$ Hz, Cy-CH₂), 32.0-32.2 (m, cod-CH₂), 33.8-33.9 (m, Cy-CH₂), 36.9 (d, $J_{CP} = 17.6$ Hz, C(CH₃)₃), 42.0 (d, $J_{CP} = 23.1$ Hz, Cy-CH), 49.2 (d, $J_{CP} = 17.3$ Hz, Cy-CH), 70.8 (dd, $J_{CP} = 47.6$ Hz, $J_{CP} = 22.4$ Hz, Cy₂PC), 72.6 (s, Cp-CH), 73.0 (d, $J_{CP} = 11.0$ Hz, CHCH), 74.5 (dd, $J_{CP} = 5.9$ Hz, $J_{CP} = 1.8$ Hz, cod-CH), 75.0 (d, $J_{CP} = 7.0$ Hz, cod-CH), 75.5 (d, $J_{CP} = 12.0$ Hz, CHCH), 79.0 (d, $J_{CP} = 14.5$ Hz, cod-CH), 79.4 (d, $J_{CP} = 8.1$ Hz, cod-CH), 95.8 (t, $J_{CP} = 11.8$ Hz, Cy₂PCCC), 100.4 (dd, $J_{CP} = 55.9$ Hz, $J_{CP} = 36.8$ Hz, Cy₂PCC), 117.0-117.3 (m, BAr_F-CH), 124.3 (q, $J_{CF} = 272$ Hz, BAr_F-CF₃), 128.0-129.1 (m, BAr_F-C), 134.5 (s, BAr_F-CH), 160.9 (q, $J_{CB} = 49.8$ Hz, BAr_F-CB).

³¹P{¹H}-NMR (CD₂Cl₂): δ /ppm = 12.8 (d, $J_{PP} = 10.1$ Hz), 36.4 (d, $J_{PP} = 10.1$ Hz).

IR (KBr): $\tilde{\nu}$ /cm⁻¹ = 2940(m), 2860(w), 1611(w), 1455(w), 1355(s), 1277(s), 1128(s), 1003(w), 890(w), 837(w), 713(w), 676(w).

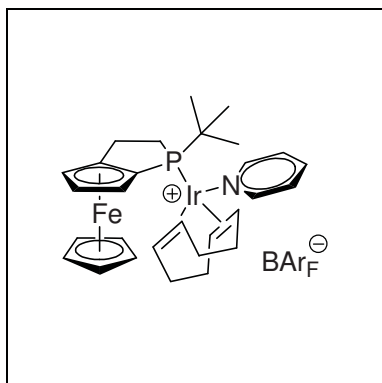
MS (ESI): m/z (%) = 799(6), 798(37), 797(100), 796(28), 795(68), 793(8).

EA: calculated (%) for C₆₈H₆₆BF₂₄FeIrP₂: C: 49.20, H: 4.01; measured: C: 49.13, H: 3.93.

$[\alpha]_D^{20} = -10$ ($c = 0.072$, CHCl₃ / 0.75% EtOH).

R_f (SiO₂, hexanes:CH₂Cl₂ (2:1)): 0.28.

m.p.: 235-240 °C (dec.).



(*S,S_P*)-{(η⁴-1,5-cyclooctadiene)-(η⁵-2,4-cyclopentadien-1-yl)}[(3a,4,5,6,6a-η)-1-*tert*-butyl-(1,2,3-trihydro-cyclopenta[*b*]phosphole-3a-yl)]iron-pyridine-iridium(I)-tetrakis[3,5-bis(trifluoromethyl)phenyl]borat (**75**)

[Ir(cod)Py₂]*BAR_F* (100 mg, 75.6 μmol) was dissolved in CH₂Cl₂ (3 mL) and a solution of **6** (22.0 mg 73.3 μmol) in CH₂Cl₂ (1 mL) was added. After 1 h the solution was filtered over a pad of SiO₂ and recrystallized from CH₂Cl₂/hexanes to give **75** (75.0 mg, 66%) as an orange solid.

C₆₁H₅₀BF₂₄FeIrNP (1543 g/mol)

¹H-NMR (333 K, CDCl₃): δ/ppm = 0.97 (d, ²J_{HP} = 14.6 Hz, 9H, C(CH₃)₃), 1.35-1.70 (m, 1H CH₂), 1.77-2.14 (m, 3H, CH₂), 2.16-2.32 (m, 2H, CH₂), 2.33-2.60 (m, 5H, CH₂), 2.61-2.74 (m, 1H, CH₂), 3.82 (s br, 1H, CH), 3.98-4.16 (m, 2H, cod-CH), 4.19-4.32 (m, 1H, cod-CH), 4.38 (s, 5H, Cp-CH), 4.45 (s, 1H, CH), 4.46 (s, 1H, CH), 4.53-4.72 (m, 1H, cod-CH), 7.47-7.57 (m, 6H, *BAR_F*-CH, Py-CH), 7.73 (s, 8H, *BAR_F*-CH), 7.77 (t, J_{HH} = 7.6 Hz, 1H, Py-CH), 8.81 (s, 2H, Py-CH).

¹³C{¹H}-NMR (333 K, CDCl₃): δ/ppm = 28.0 (s, C(CH₃)₃), 65.4 (s, CH), 65.4 (s, cod-CH), 68.1 (d, J_{CP} = 10.4 Hz, CH), 70.6 (s, Cp-CH), 75.7 (s, cod-CH), 75.8 (s, CH), 90.3-91.0 (m, cod-CH), 91.2-91.5 (m, cod-CH), 117.4-117.6 (m, *BAR_F*-CH), 124.7 (q, ¹J_{CF} = 272.3 Hz, *BAR_F*-CF₃), 126.8 (s, Py-CH), 128.5-129.5 (m, *BAR_F*-C), 134.9 (s, *BAR_F*-CH), 139.2 (s, Py-CH), 151.1 (s, Py-CH), 161.9 (q, ¹J_{CB} = 50.0 Hz, *BAR_F*-CB). (all secondary and quaternary signals were not detected).

³¹P{¹H}-NMR (333 K, CDCl₃): 30.4-30.8 (m).

IR (KBr): $\tilde{\nu}$ /cm⁻¹ = 2954(m), 1610(m), 1455(w), 1357(s), 1278(s), 1130(s), 889(m), 836(w), 755(w), 712(m), 675(m).

MS (ESI): *m/z*(%) = 681(30), 680(100), 679(21), 678(66).

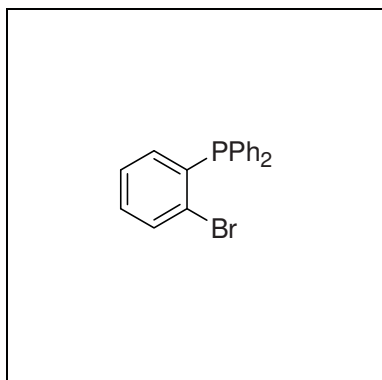
EA: calculated (%) for C₆₁H₅₀BF₂₄FeIrNP: C: 47.49, H: 3.27, N: 0.91; measured: C: 47.26, H: 3.11, N: 0.78.

[α]_D²⁰ = -54.2 (*c* = 0.78, CHCl₃ / 0.75% EtOH).

R_f (SiO₂, CH₂Cl₂): 0.77.

m.p.: 210- 215 °C (dec).

4.3.2 Preparation of Terpene-Derived Phosphorus Compounds



1-Bromo-2-(diphenylphosphino)benzene^[3] (**90**)

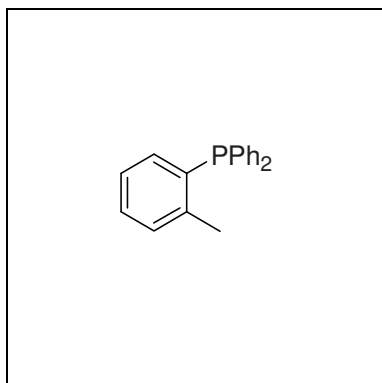
To a solution of 2-bromo-1-iodobenzene (4.40 g, 15.5 mmol) in THF (10 mL) was added *i*PrMgCl (7.70 mL, 2 M in THF, 15.4 mmol) while keeping the temperature below $-35\text{ }^{\circ}\text{C}$. The solution was stirred for 1 h at $-35\text{ }^{\circ}\text{C}$ then diphenylphosphine chloride (3.45 mL, 18.6 mmol) was added while keeping the temperature below $-30\text{ }^{\circ}\text{C}$. After 45 min at $-30\text{ }^{\circ}\text{C}$ the solution was allowed to warm up to room temperature. Water (1 mL) was added and the solvent was removed under reduced pressure. The residue was dissolved in EtOAc (20 mL) and extracted with sat. aq. NaHCO_3 and sat aq. NaCl . The solution was dried over MgSO_4 and the solvent was removed under reduced pressure. The resulting oil was overlaid with EtOH and sonicated. The formed solid was filtered, washed twice with cold EtOH and dried under vacuum to give the title compound **90** (3.55 g, 73%) as a white solid.

$\text{C}_{18}\text{H}_{14}\text{BrP}$ (341.19 g/mol)

$^1\text{H-NMR}$ (CD_2Cl_2): $\delta/\text{ppm} = 6.76\text{--}6.80$ (m, 1H, $\text{C}(\text{Br})\text{CH}$), $7.20\text{--}7.26$ (m, 2H, $\text{C}(\text{Br})\text{CHCHCH}$), $7.26\text{--}7.31$ (m, 4H, Ph-CCH), $7.34\text{--}7.42$ (m, 6H, Ph-CCHCHCH), $7.59\text{--}7.63$ (m, 1H, $\text{C}(\text{Br})\text{CCH}$).

$^{13}\text{C}\{^1\text{H}\}\text{-NMR}$ (CD_2Cl_2): $\delta/\text{ppm} = 127.2$ (s, $\text{C}(\text{Br})\text{CCHCH}$), 128.3 (d, $^3J_{\text{CP}} = 7.2$ Hz, Ph-CCHCH), 128.7 (s, Ph-CCHCHCH), 129.4 (d, $^1J_{\text{CP}} = 30.9$ Hz, $\text{C}(\text{P})\text{C}(\text{Br})$), 129.9 (s, $\text{C}(\text{Br})\text{CHCH}$), 132.6 (d, $^2J_{\text{CP}} = 2.3$ Hz, $\text{C}(\text{Br})\text{C}(\text{P})\text{CH}$), 133.6 (d, $^2J_{\text{CP}} = 20.4$ Hz, Ph-CCH), 134.2 (s, $\text{C}(\text{Br})\text{CH}$), 135.6 (d, $^1J_{\text{CP}} = 11.1$ Hz, Ph-C), 138.6 (d, $^2J_{\text{CP}} = 12.3$ Hz, CBr).

$^{31}\text{P}\{^1\text{H}\}\text{-NMR}$ (CD_2Cl_2): $\delta/\text{ppm} = -4.6$ (s).



1-(Diphenylphosphino)-2-methylbenzene^[4] (**92**)

Magnesium turnings (261 mg, 10.7 mmol) were stirred under argon for 2 h and then overlaid with THF (30 mL). Three drops of 1,2-dibromoethane were added followed by a few drops of a solution containing 2-bromotoluene (1.30 mL, 10.8 mmol) in THF (5 mL). Upon start of the reaction the remaining solution of 2-bromotoluene in THF was added drop-wise. The reaction mixture was heated to reflux until all magnesium was dissolved. The reaction mixture was cooled to $-78\text{ }^{\circ}\text{C}$ and a solution of diphenylphosphine chloride (2.00 mL, 11.1 mmol) in THF (2 mL) was added drop-wise. The reaction mixture was stirred overnight at room temperature and extracted twice with sat. aq. NaCl and dried over MgSO_4 . The solvent was removed under reduced pressure and the crude product oil treated with EtOH. The formed solid was filtered and washed with cold ethanol and the supernatant was concentrated and purified by column chromatography (SiO_2 , $3 \times 15\text{ cm}$, hexanes:EtOAc (1:0 \rightarrow 5:1)) to give the title compound **92** (2.95 g combined yield, 99%) as a white solid.

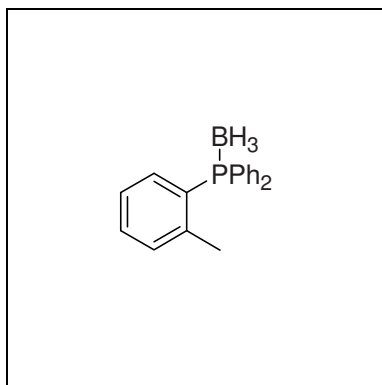
$\text{C}_{19}\text{H}_{17}\text{P}$ (278.33 g/mol)

$^1\text{H-NMR}$ (CD_2Cl_2): $\delta/\text{ppm} = 2.39$ (s, 3H, CH_3), 6.78 (dd, $^3J_{\text{HH}} = 7.3\text{ Hz}$, $^3J_{\text{HP}} = 4.7\text{ Hz}$, 1H, CC(P)CH), 7.09 (t, $^3J_{\text{HH}} = 7.3\text{ Hz}$, 1H, C(P)CCHCH), 7.20-7.30 (m, 6H, C(P)CCHCHCH , Ph-CCH), 7.32-7.38 (m, 6H, Ph-CCHCHCH).

$^{13}\text{C}\{^1\text{H}\}\text{-NMR}$ (CD_2Cl_2): $\delta/\text{ppm} = 20.6$ (d, $^3J_{\text{CP}} = 21.2\text{ Hz}$, CH_3), 125.6 (s, CC(P)CHCH), 128.2 (d, $^3J_{\text{CP}} = 7.0\text{ Hz}$, Ph-CCHCH), 128.3 (s, C(P)CCHCH), 128.4 (s, Ph-CCHCHCH), 129.7 (d, $^3J_{\text{CP}} = 4.5\text{ Hz}$, C(P)CCH), 132.3 (s, CC(P)CH), 133.6 (d, $^2J_{\text{CP}} = 19.9\text{ Hz}$, Ph-CCH), 135.8 (d, $^1J_{\text{CP}} = 12.3\text{ Hz}$, C(P)C), 136.1 (d, $^1J_{\text{CP}} = 10.7\text{ Hz}$, Ph-C), 141.9 (d, $^2J_{\text{CP}} = 25.4\text{ Hz}$, CCH_3).

$^{31}\text{P}\{^1\text{H}\}\text{-NMR}$ (CD_2Cl_2): $\delta/\text{ppm} = -13.1$ (s).

R_f (SiO_2 , hexanes): 0.18.



1-(Boranyldiphenylphosphino)-2-methylbenzene (**95**)

To a solution of **92** (200 mg, 725 μmol) in THF (5 mL) was added $\text{BH}_3\cdot\text{THF}$ (1.00 mL, 1 M in THF, 1.00 mmol) at room temperature. After 30 min the solvent was evaporated, the residue dissolved in TBME and filtered. After removal of the solvent under reduced pressure the crude product was recrystallized from TBME to give the title compound **95** (182 mg, 87%) as a white solid.

$\text{C}_{19}\text{H}_{20}\text{BP}$ (290.15 g/mol)

$^1\text{H-NMR}$ (CD_2Cl_2): δ/ppm = 0.85-1.70 (m, 3H, BH_3), 2.24 (s, 3H, CH_3), 7.05 (dd, $^2J_{\text{HP}} = 11.8$ Hz, $^3J_{\text{HH}} = 7.9$ Hz, 1H, $\text{CC}(\text{P})\text{CH}$), 7.17 (t, $^3J_{\text{HH}} = 7.5$ Hz, 1H, $\text{CC}(\text{P})\text{CHCH}$), 7.26-7.31 (m, 1H, $\text{C}(\text{P})\text{CCH}$), 7.43 (t, $^3J_{\text{HH}} = 7.5$ Hz, $\text{C}(\text{P})\text{CCHCH}$), 7.45-7.51 (m, 4H, Ph-CCHCH), 7.51-7.58 (m, 2H, Ph-CCHCHCH), 7.59-7.65 (m, 4H, Ph-CCH).

$^{13}\text{C}\{^1\text{H}\}\text{-NMR}$ (CD_2Cl_2): δ/ppm = 21.9 (d, $^3J_{\text{CP}} = 4.9$ Hz, CH_3), 125.5 (d, $^3J_{\text{CP}} = 9.6$ Hz, $\text{CC}(\text{P})\text{CHCH}$), 127.5 (d, $^1J_{\text{CP}} = 55.4$ Hz, $\text{C}(\text{P})\text{C}$), 128.5 (d, $^3J_{\text{CP}} = 10.1$ Hz, Ph-CCHCH), 128.7 (d, $^1J_{\text{CP}} = 56.0$ Hz, Ph-C), 130.9 (d, $^4J_{\text{CP}} = 2.4$ Hz, Ph-CCHCHCH), 131.0 (d, $^4J_{\text{CP}} = 2.3$ Hz, $\text{C}(\text{P})\text{CCHCH}$), 131.5 (d, $^3J_{\text{CP}} = 8.8$ Hz, $\text{C}(\text{P})\text{CCH}$), 132.8 (d, $^2J_{\text{CP}} = 9.4$ Hz, Ph-CCH), 133.8 (d, $^2J_{\text{CP}} = 8.7$ Hz, $\text{CC}(\text{P})\text{CH}$), 142.5 (d, $^2J_{\text{CP}} = 10.3$ Hz, CCH_3).

$^{31}\text{P}\{^1\text{H}\}\text{-NMR}$ (CD_2Cl_2): δ/ppm = 20.0-21.5 (m).

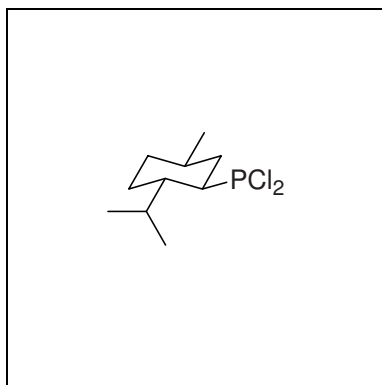
IR (KBr): $\tilde{\nu}/\text{cm}^{-1}$ = 3219(m), 3050(m), 2379(s), 2343(s), 2256(m), 1967(w), 1898(w), 1818(w), 1772(w), 1590(w), 1479(m), 1470(m), 1435(s), 1387(w), 1333(w), 1312(w), 1285(w), 1205(w), 1135(m), 1105(s), 1063(s), 1027(m), 999(w), 806(w), 755(s), 741(s), 713(s), 696(s), 676(m), 621(m), 603(s), 551(w), 515(s), 498(s), 455(m), 442(m).

MS (EI): $m/z(\%)$ = 287(11), 286(6), 277(21), 276(100), 275(74), 197(12), 166(5), 165(16).

EA: calculated (%) for $\text{C}_{19}\text{H}_{20}\text{BP} \cdot 1/3 \text{H}_2\text{O}$: C: 77.06, H: 7.03; measured: C: 76.92, H: 6.94.

R_f (SiO_2 , hexanes:EtOAc, 10:1): 0.40.

m.p.: 144-146 $^\circ\text{C}$.



(1*S*,2*R*,4*R*)-2-(Dichlorophosphino)-1-isopropyl-4-methylcyclohexane^[5] (97)

Magnesium turnings (3.34 g, 139 mmol) were stirred overnight under argon and then overlaid with Et₂O (5 mL). 0.5 mL of a solution of **99** (7.95 g, 45.4 mmol) in Et₂O (45 mL) were added followed by 0.05 mL 1,2-dibromoethane. Upon start of the reaction the remaining solution of **99** in Et₂O was added while keeping the reaction mixture at reflux. After complete addition, the reaction mixture was heated to reflux for 1 h then allowed to cool down to room temperature and the formed suspension was dissolved by addition of THF (1 mL). The *Grignard*-solution was added via a filter-paper equipped cannula to a solution of PCl₃ (15.0 mL, 172 mmol) in Et₂O (15 ml) at 0 °C. The formed white suspension was allowed to warm up to room temperature and filtered under argon. The solvent was removed under reduced pressure and the crude product was distilled to give the title compound **97** (6.63 g, 61%) as a colorless liquid.

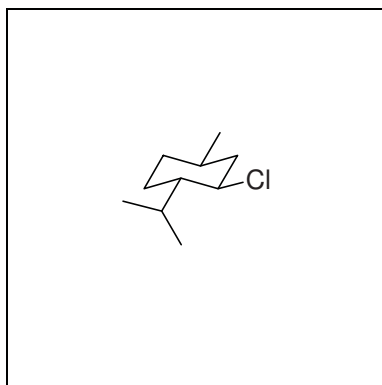
C₁₀H₁₉PCl₂ (241.14 g/mol)

¹H-NMR (CD₂Cl₂): δ/ppm = 0.90 (d, ³J_{HH} = 6.8 Hz, 3H, CH₃), 0.96 (d, ³J_{HH} = 6.8 Hz, 3H, CH₃), 0.97 (d, ³J_{HH} = 6.5 Hz, 3H, CH₃), 1.10-1.28 (m, 3H), 1.36-1.54 (m, 2H), 1.74-1.83 (m, 2H), 1.97 (dtd, ¹J_{HP} = 27.1 Hz, J_{HH} = 11.2 Hz, J_{HH} = 3.1 Hz, 1H, C(P)H), 2.22-2.32 (m, 2H).

¹³C{¹H}-NMR (CD₂Cl₂): δ/ppm = 15.1 (d, ⁴J_{CP} = 2.0 Hz, CH₃), 20.9 (s, CH₃), 21.9 (s, CH₃), 24.7 (d, J_{CP} = 6.4 Hz, CH₂), 28.1 (d, J_{CP} = 24.7 Hz, CH), 32.0 (s, CH₂), 32.6 (d, J_{CP} = 2.0 Hz, CH), 34.3 (s, CH₂), 44.2 (d, J_{CP} = 8.8 Hz, CH), 49.6 (d, ¹J_{CP} = 52.7 Hz, C(P)H).

³¹P{¹H}-NMR (CD₂Cl₂): δ/ppm = 212.7 (s).

b.p.: 74 °C (0.08 mbar).

**(1*S*,2*R*,4*R*)-2-Chloro-1-isopropyl-4-methylcyclohexane**^[6]**(99)**

Zinc dichloride (75.0 g, 550 mmol) was dissolved in conc. HCl (36-38%, 51 mL) while cooling in an ice bath. (-)-Menthol (26.0 g 166 mmol) was added and the reaction mixture was heated at 35 °C for 6 h. The reaction mixture was allowed to

cool down to room temperature, the layers were separated and the aqueous layer was extracted with hexane (50 mL). The combined organic layers were extracted with water (25 mL) and conc. H₂SO₄ (6 × 20 mL) until the extract was colorless. The organic layer was washed with water (5 × 20 mL) and dried over MgSO₄. The solvent was removed under reduced pressure and the crude product was distilled to give the title compound **99** (24.8 g, 85%) as a colorless liquid.

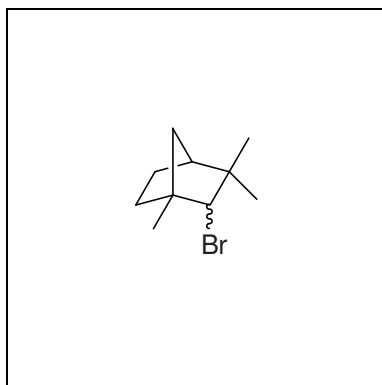
C₁₀H₁₉Cl (174.71 g/mol)

¹H-NMR (CDCl₃): δ/ppm = 0.77 (d, ³J_{HH} = 6.9 Hz, 3H, CH₃CHCH₃), 0.85-0.95 (m, 1H, CH₃CHCHHCH₂), 0.92 (d, ³J_{HH} = 7.2 Hz, 3H, CH₃CHCH₃), 0.92 (d, ³J_{HH} = 5.9 Hz, 3H, CH₃), 0.97-1.08 (m, 1H, CH₃CHCH₂CHH), 1.33-1.50 (m, 3H, CHC(Cl)HCHHCH), 1.67-1.75 (m, 2H, CHHCHH), 2.20-2.26 (m, 1H, C(Cl)HCHH), 2.35 (sepd, ³J_{HH} = 7.0 Hz, ³J_{HH} = 3.0 Hz, 1H, CH₃CHCH₃), 3.78 (td, ³J_{HH} = 11.1 Hz, ³J_{HH} = 4.2 Hz, 1H, C(Cl)H).

¹³C{¹H}-NMR (CDCl₃): δ/ppm = 15.1 (s, CH₃CHCH₃), 21.0 (CH₃CHCH₃), 21.9 (s, CH₃), 24.2 (CH₃CHCH₂CH₂), 27.1 (s, CH₃CHCH₃), 33.4 (s, CH₃CH), 34.2 (CH₃CHCH₂CH₂), 46.7 (s, C(Cl)HCH₂), 50.4 (s, C(Cl)HCH), 63.9 (s, C(Cl)H).

[α]_D²⁰ = -45.8 (c = 2.50, CHCl₃ / 0.75% EtOH).

b.p.: 92-95 °C (12 mbar).



**(1R,2RS,4S)-2-Bromo-1,3,3-trimethyl-bicyclo[2.2.1]heptane
(103)**

To a solution of triphenylphosphine (12.4 g, 47.3 mmol) and imidazole (3.20 g, 47.1 mmol) in CH_2Cl_2 (50 mL) was added bromine (2.40 mL, 46.8 mmol) while keeping the temperature below 10 °C. (+)-Fenchol (7.00 g, 45.5 mmol) dissolved in CH_2Cl_2 (10 mL) was added and the suspension was heated to reflux for 15 h. After cooling down to room temperature the reaction mixture was extracted with water and sat. aq. NaCl and dried over MgSO_4 . The solution was concentrated under reduced pressure, hexanes were added and the solution filtered. The filtrate was concentrated under reduced pressure and again filtered. After removal of the solvent under reduced pressure, the crude product was distilled to give the title compound **103** (5.29 g, 54%) as a colorless liquid.

$\text{C}_{10}\text{H}_{17}\text{Br}$ (217.15 g/mol)

$^1\text{H-NMR}$ (CDCl_3): δ/ppm = 1.04 (s, 3H, CH_3CCH_3), 1.07-1.12 (m, 1H, CCHHCH), 1.17 (s, 3H, CH_3CCH_3), 1.21 (s, 3H, CCH_3), 1.23-1.32 (m, 1H, CCHHCH₂), 1.41-1.51 (m, 1H, CCH₂CHH), 1.61-1.69 (m, 2H, CCHHCHH), 1.78-1.81 (m, 1H, CH), 1.81-1.86 (m, 1H, CCHHCH), 3.77 (d, $^4J_{\text{HH}} = 2.3$ Hz, 1H, C(Br)H).

$^{13}\text{C}\{^1\text{H}\}\text{-NMR}$ (CDCl_3): δ/ppm = 25.5 (s, CCH₂CH₂), 26.2 (s, CH_3CCH_3), 21.8 (s, CCH₃), 31.3 (s, CH_3CCH_3), 35.7 (s, CCH₂CH₂), 41.5 (s, CCH₂CH), 44.2 (s, CCH₃), 49.7 (s, CH), 50.6 (s, CH_3CCH_3), 76.8 (s, C(Br)H).

IR (NaCl): $\tilde{\nu}/\text{cm}^{-1}$ = 2958(s), 2872(s), 1740(w), 1661(w), 1459(s), 1380(m), 1319(w), 1231(m), 1157(w), 1105(w), 956(w), 902(m), 857(w), 819(m), 715(m), 678(w).

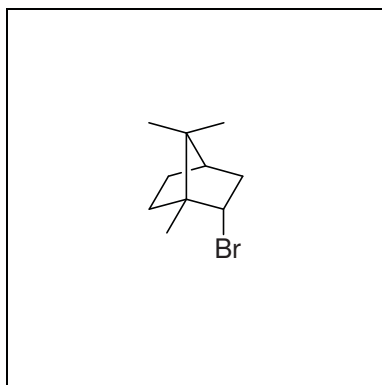
MS (EI): $m/z(\%)$ = 218 (3), 216(3), 203(14), 201(14), 137(30), 136(6), 123(15), 121(12), 109(13), 107(6), 95(25), 93(22), 82(8), 81(100), 80(17), 79(21), 77(9), 69(12), 67(14), 55(10), 41(14), 39(7).

EA: calculated (%) for $\text{C}_{10}\text{H}_{17}\text{Br}$: C: 55.31, H: 7.89; measured: C: 56.38, H: 7.99.

$[\alpha]_D^{20} = -5.0$ ($c = 0.64$, CHCl_3 / 0.75% EtOH).

R_f (SiO_2 , hexanes, KMnO_4): 0.8.

b.p.: 74-76 °C (2 mbar).



(1*R*,2*S*,4*S*)-2-Bromo-1,7,7-trimethyl-bicyclo[2.2.1]heptane^[7]
(104)

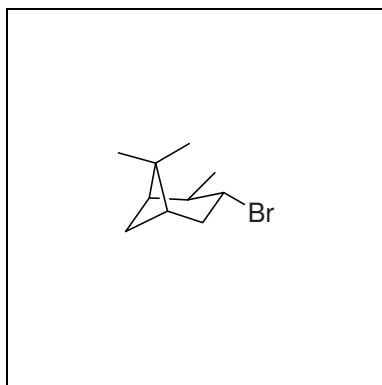
A solution of (-)- α -Pinene (34.0 g, 250 mmol) in CHCl_3 (300 mL) was aerated with hydrogen bromide (generated by slow hydrolysis of PBr_3 (30 mL, 319 mmol)) while keeping the temperature at 0 °C. When the solution turned yellow the introduction of HBr was stopped and the solution degassed with a stream of argon. The solvent was evaporated under reduced pressure and the residue purified by Kugelrohr-distillation (100 °C, 0.1 mbar) and recrystallization from methanol to give the title compound **104** (37.0 g, 68%) as a white solid.

$\text{C}_{10}\text{H}_{17}\text{Br}$ (217.15 g/mol)

$^1\text{H-NMR}$ (CDCl_3): δ/ppm = 0.86 (s, 3H, CH_3), 0.88 (s, 3H, $\text{C}_\text{R}\text{H}_3\text{CC}_\text{S}\text{H}_3$), 0.96 (s, 3H, $\text{C}_\text{R}\text{H}_3\text{CC}_\text{S}\text{H}_3$), 1.27 (ddd, $J_{\text{HH}} = 12.4$ Hz, $J_{\text{HH}} = 9.5$ Hz, $J_{\text{HH}} = 4.5$ Hz, 1H $\text{CHCH}_\text{R}\text{H}_\text{S}\text{CH}_2$), 1.37-1.47 (m, 1H, $\text{CHCH}_2\text{CH}_\text{R}\text{H}_\text{S}$), 1.53 (dd, $J_{\text{HH}} = 14.0$ Hz, $J_{\text{HH}} = 4.5$ Hz, 1H $\text{CHCH}_\text{R}\text{H}_\text{S}\text{CH}_2$), 1.66 (t, $J_{\text{HH}} = 4.5$ Hz, 1H CH_2CHCH_2), 1.69-1.80 (m, 1H $\text{C}(\text{Br})\text{HCH}_\text{R}\text{H}_\text{S}$), 2.06 (ddd, $J_{\text{HH}} = 13.5$ Hz, $J_{\text{HH}} = 9.5$ Hz, $J_{\text{HH}} = 4.4$ Hz, 1H, $\text{CHCH}_2\text{CH}_\text{R}\text{H}_\text{S}$), 2.47-2.57 (m, 1H, $\text{C}(\text{Br})\text{HCH}_\text{R}\text{H}_\text{S}$), 4.32 (ddd, $J_{\text{HH}} = 10.6$ Hz, $J_{\text{HH}} = 4.4$ Hz, $J_{\text{HH}} = 2.8$ Hz, 1H, $\text{C}(\text{Br})\text{H}$).

$^{13}\text{C}\{^1\text{H}\}\text{-NMR}$ (CDCl_3): δ/ppm = 13.7 (s, CH_3), 18.5 (s, $\text{C}_\text{S}\text{H}_3\text{CC}_\text{R}\text{H}_3$), 20.9 (s, $\text{C}_\text{S}\text{H}_3\text{CC}_\text{R}\text{H}_3$), 28.1 (s, CHCH_2CH_2), 30.4 (s, CHCH_2CH_2), 40.8 (s, $\text{C}(\text{Br})\text{HCH}_2$), 45.0 (s, CH_2CHCH_2), 47.0 (s, CH_3CCH_3), 50.9 (s, $\text{C}(\text{Br})\text{HC}$), 62.9 (s, $\text{C}(\text{Br})\text{H}$).

$[\alpha]_D^{20} = -32.0$ ($c = 2.00$, CHCl_3 / 0.75% EtOH).



**(1R,2R,3R,5S)-3-Bromo-2,6,6-trimethyl-
bicyclo[3.1.1]heptane (105)**

From a solution of (*R*)-Alpine-Borane (20.0 mL, 0.5 M in THF, 10.0 mmol) the solvent was evaporated under reduced pressure. The residue was dissolved in CH₂Cl₂ (10 mL) and cooled in an ice bath. Under the exclusion of light bromine (0.56 mL, 10.9 mmol) was added. After 30 min the cooling bath was removed and the reaction mixture was stirred for another 2 h. After addition of 2 M aq. NaOH while cooling the aqueous layer was extracted with CH₂Cl₂. The combined organic layers were washed with sat. aq. NaCl and dried over MgSO₄. The solvent was evaporated under reduced pressure and the residue was bulb-to-bulb condensed under vacuum (40 °C → liq. N₂). The crude product was distilled to give the title compound **105** (970 mg, 45%) as a colorless liquid.

C₁₀H₁₇Br (217.15 g/mol)

¹H-NMR (CDCl₃): δ/ppm = 1.00 (s, 3H, C_RH₃CC_SH₃), 1.13 (d, *J*_{HH} = 7.2 Hz, 3H, CHCH₃), 1.21 (s, 3H, C_RH₃CC_SH₃), 1.22 (d, *J*_{HH} = 9.7 Hz, 1H, CHCH_RH_SCH) 1.87 (td, *J*_{HH} = 6.0 Hz, *J*_{HH} = 1.8 Hz, 1H, CH₃CHCH), 1.96 (tdd, *J*_{HH} = 6.0 Hz, *J*_{HH} = 3.6 Hz, *J*_{HH} = 2.5 Hz, 1H, C(Br)HCH₂CH), 2.43-2.48 (m, 1H, CHCH_RH_SCH), 2.46-2.51 (m, 1H, C(Br)HCH_RH_S), 2.59 (quind, *J*_{HH} = 7.2 Hz, *J*_{HH} = 1.8 Hz, 1H, C(Br)HCH), 2.67-2.76 (m, 1H, C(Br)HCH_RH_S), 4.39 (dt, *J*_{HH} = 9.8 Hz, *J*_{HH} = 7.0 Hz, 1H, C(Br)H).

¹³C{¹H}-NMR (CDCl₃): δ/ppm = 20.2 (s, CHCH₃), 23.8 (s, C_RH₃CC_SH₃), 28.0 (s, C_RH₃CC_SH₃), 35.2 (s, CHCH₂CH), 38.9 (s, C), 40.9 (s, C(Br)HCH₂), 43.3 (s, C(Br)HCH₂CH), 49.3 (s, CH₃CHCH), 49.4 (CH₃CH), 52.8 (s, C(Br)H).

IR (NaCl): $\tilde{\nu}$ /cm⁻¹ = 2923(s), 1706(m), 1455(m), 1376(m), 1287(w), 1204(m), 865(w), 779(w), 685(m).

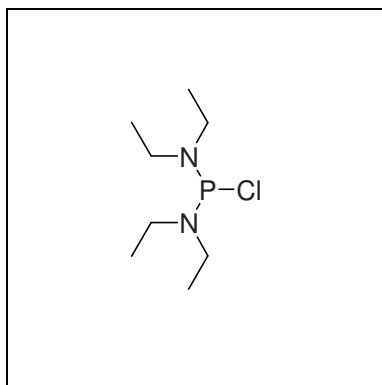
MS (EI): *m/z*(%) = 203(1), 201(1), 138(6), 137(73), 136(9), 96(5), 95(39), 94(13), 93(43), 92(9), 91(12), 84(5), 83(67), 82(10), 81(100), 80(14), 79(20), 77(12), 69(58), 68(9), 67(21), 56(6), 55(41), 43(10), 41(39), 39(12).

EA: calculated (%) for C₁₀H₁₇Br: C: 55.31, H: 7.89; measured: C: 56.85, H: 8.01.

$[\alpha]_D^{20}$ = -46.5 (*c* = 1.40, CHCl₃ / 0.75% EtOH).

*R*_f (SiO₂, hexanes, KMnO₄): 0.80.

b.p.: 72 °C (2 mbar).


Bis(diethylamino)phosphine chloride^[8] (107)

To a solution of phosphorus trichloride (5.25 mL, 60.2 mmol) in hexane (120 mL) was added a solution of diethylamine (25 mL, 240 mmol) in hexane (25 mL) while keeping the temperature below $-60\text{ }^{\circ}\text{C}$. After complete addition the solution was allowed to warm up to room temperature and filtered under argon. After evaporation of the solvent under reduced pressure the crude product was distilled to give the title compound **107** (10.9 g, 86%) as a colorless liquid.

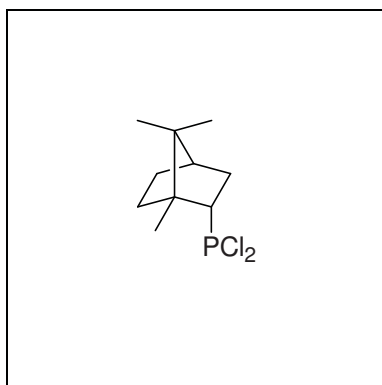
$\text{C}_8\text{H}_{20}\text{ClN}_2\text{P}$ (210.70 g/mol)

$^1\text{H-NMR}$ (CD_2Cl_2): $\delta/\text{ppm} = 1.12$ (t, $^3J_{\text{HH}} = 7.1$ Hz, 12H, CH_3), 3.15 (s br, 8H, CH_2).

$^{13}\text{C}\{^1\text{H}\}\text{-NMR}$ (CD_2Cl_2): $\delta/\text{ppm} = 13.3$ (d, $^3J_{\text{CP}} = 4.8$ Hz, CH_3), 40.7 (d, $^2J_{\text{CP}} = 17.9$ Hz, CH_2).

$^{31}\text{P}\{^1\text{H}\}\text{-NMR}$ (CD_2Cl_2): $\delta/\text{ppm} = 156.8$ (s).

b.p.: $60\text{ }^{\circ}\text{C}$ (0.15 mbar).


(1R,2S,4S)-2-(Dichlorophosphino)-1,7,7-trimethylbicyclo[2.2.1]heptane (108)

Magnesium turnings (565 mg, 23.5 mmol) were stirred under argon for 2 h and then overlaid with THF (20 mL). A small portion of iodine was added and after disappearance of the color the suspension was heated to reflux. A solution of **104** (4.80 g, 22.1 mmol) in THF (10 mL) was added drop-wise and after complete addition the reaction mixture was heated for another hour. The reaction mixture was allowed to cool down to room temperature and the solution was added via a filter-paper equipped cannula to a solution of **107** (4.75 mL, 22.5 mmol) in THF (10 mL) at $-78\text{ }^{\circ}\text{C}$. After 15 min the reaction mixture was allowed to warm up to room temperature and concentrated to half volume under reduced pressure. While cooling in an ice bath HCl (46 mL, 2 M in Et_2O , 92.0 mmol) was added. The ice bath was removed and pentane (10 mL) was added. After 20 min the suspension was filtered and the solvent was removed under reduced pressure. The crude product was distilled to give the title compound **108** (2.81 g, 50%) as a colorless liquid.

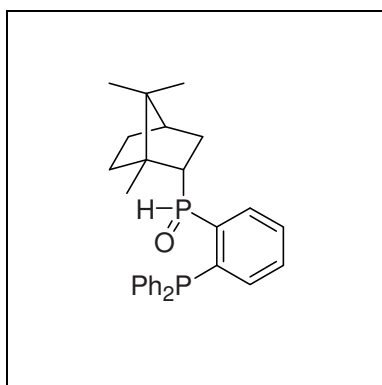
$C_{10}H_{17}Cl_2P$ (239.12 g/mol)

1H -NMR (CD_2Cl_2): $\delta/ppm = 0.89$ (s, 3H, $C_RH_3CC_5H_3$), 0.94 (s, 3H, $C_RH_3CC_5H_3$), 1.07 (s, 3H, CH_3CCH_2), 1.18-1.30 (m, 1H, $CCH_2CH_RH_S$), 1.25-1.39 (m, 1H, $PCHCH_RH_S$), 1.50-1.64 (m, 1H, $CCH_RH_SCH_2$), 1.72-1.80 (m, 1H, $CCH_RH_SCH_2$), 1.75-1.79 (m, 1H, CH_2CHCH_2), 1.76-1.88 (m, 1H, $CCH_2CH_RH_S$), 2.13-2.26 (m, 1H, $PCHCH_RH_S$), 2.67 (dddd, $J = 11.5$ Hz, $J = 5.4$ Hz, $J = 3.5$ Hz, $J = 1.7$ Hz, 1H, CHP).

$^{13}C\{^1H\}$ -NMR (CD_2Cl_2): $\delta/ppm = 15.2$ (s, CH_3CCH_2), 17.8 (s, $C_RH_3CC_5H_3$), 18.0 (d, $^4J_{CP} = 1.4$ Hz, $C_RH_3CC_5H_3$), 28.8 (s, $CHCH_2CH_2$), 31.3 (d, $^3J_{CP} = 29.1$ Hz, $CHCH_2CH_2$), 33.4 (d, $^2J_{CP} = 21.8$ Hz, $PCHCH_2$), 44.3 (d, $^3J_{CP} = 2.1$ Hz, CH_2CHCH_2), 49.4 (d, $^2J_{CP} = 9.9$ Hz, $PCHC$), 50.6 (d, $^3J_{CP} = 2.9$ Hz, CH_3CCH_3), 56.5 (d, $^1J_{CP} = 49.4$ Hz, CHP).

$^{31}P\{^1H\}$ -NMR (CD_2Cl_2): $\delta/ppm = 195.7$ (s).

b.p.: 57-60 °C (0.1 mbar).



(2-Diphenylphosphinophenyl)((1R,2S,4S)-1,7,7-trimethylbicyclo[2.2.1]heptan-2-yl)phosphine oxide (109)

To a solution of **90** (272 mg, 866 μ mol) in THF (5 mL) was added at -78 °C *n*-butyllithium (0.55 mL, 1.6 M in hexane, 880 μ mol). After 1 h this solution was transferred via cannula to a solution containing **108** (207 mg, 866 μ mol) in THF (5 mL) at -78 °C. After 15 min the cooling bath was removed and the reaction mixture was allowed to warm up to room temperature. The solution was added to a mixture of triethyl amine (2 mL) and water (8 mL). EtOAc (10 mL) and sat. aq. $NaHCO_3$ (15 mL) were added and the aqueous layer was extracted with EtOAc. The combined organic layers were washed with sat. aq. $NaCl$ and dried over $MgSO_4$. The solvent was evaporated under reduced pressure and the crude product was purified by column chromatography (SiO_2 , 23 \times 3 cm, hexanes:EtOAc (1:1)) to give the two separable diastereoisomers of title compound **109** (125 mg + 90 mg, 56% combined yield) as white foams.

(+)-109:

$C_{28}H_{32}OP_2$, 446.50 g/mol

1H -NMR (C_6D_6): $\delta/ppm = 0.54$ (s, 3H, $C_RH_3CC_SH_3$), 0.66 (s, 3H, $C_RH_3C_SCH_3$), 1.00 (s, 3H, $C(P)HCCH_3$), 1.27-1.36 (m, 1H, $CHCH_RH_SCH_2$), 1.32-1.46 (m, 1H, $C(P)HCH_RH_S$), 1.40-1.50 (m, 1H, $CHCH_2CH_RH_S$), 1.41-1.45 (m, 1H, $CHCH_2CH_2$), 1.54-1.68 (m, 2H, $CHCH_RH_SCH_2$, $C(P)HCH_RH_S$), 2.56 (ddd, $J_{HH} = 13.1$ Hz, $J_{HH} = 9.3$ Hz, $J_{HH} = 3.4$ Hz, 1H $CHCH_2CH_RH_S$), 2.68-2.78 (m, 1H, $C(P)H$), 6.83 (t, $J_{HH} = 7.5$ Hz, 1H, $Ph_2PCCHCH$), 6.97-7.06 (m, 7H, $Ph-CH$), 7.00-7.06 (m, 1H, $Ph_2PCCHCHCH$), 7.15-7.25 (m, 2H, Ph_2PCCH , $Ph-CH$), 7.32-7.37 (m, 2H, $Ph-CH$), 8.03 (dddd, $J = 12.6$ Hz, $J = 7.5$ Hz, $J = 3.3$ Hz, $J = 1.1$ Hz, 1H, Ph_2PCCCH), 8.22 (dt, $^1J_{PH} = 466.3$ Hz, $J = 4.5$ Hz, 1H, PH).

$^{13}C\{^1H\}$ -NMR (C_6D_6): $\delta/ppm = 15.8$ (s, $C(P)HCCH_3$), 18.3 (s, CH_3CCH_3), 18.3 (s, CH_3CCH_3), 28.4 (s, $CHCH_2CH_2$), 30.8 (s br, $C(P)HCH_2$), 31.5 (d, $^3J_{CP} = 9.0$ Hz, $CHCH_2CH_2$), 44.1 (dd, $^1J_{CP} = 73.1$ Hz, $^4J_{CP} = 7.2$ Hz, $C(P)H$), 45.4 (d, $^3J_{CP} = 4.5$ Hz, $CHCH_2CH_2$), 50.0 (d, $^3J_{CP} = 3.0$ Hz, CH_3CCH_3), 50.5 (d, $^2J_{CP} = 10.6$ Hz, $C(P)HC$), 128.9 (s, $Ph-CH$), 128.9 (d, $J_{CP} = 2.2$ Hz, $Ph-CH$), 129.0 (d, $J_{CP} = 1.6$ Hz, $Ph-CH$), 129.2 (s, $Ph-CH$), 129.5 (d, $J_{CP} = 10.8$ Hz, $Ph_2PCCHCHCH$), 131.6 (d, $J_{CP} = 2.3$ Hz, $Ph_2PCCHCH$), 133.1 (t, $J_{CP} = 9.7$ Hz, Ph_2PCCCH), 133.5 (d, $J_{CP} = 19.0$ Hz, $Ph-CH$), 134.5 (d, $J_{CP} = 20.0$ Hz, $Ph-CH$), 135.4 (d, $J_{CP} = 8.9$ Hz, Ph_2PCCH), 136.2 (d, $^1J_{CP} = 10.9$ Hz, $Ph-C$), 137.1 (d, $^1J_{CP} = 10.6$ Hz, $Ph-C$), 139.9 (dd, $^1J_{CP} = 89.8$ Hz, $^2J_{CP} = 30.3$ Hz, Ph_2PCC), 140.1 (dd, $J_{CP} = 18.8$ Hz, $J_{CP} = 10.1$ Hz, Ph_2PC).

$^{31}P\{^1H\}$ -NMR (C_6D_6): $\delta/ppm = -19.8$ (d, $^3J_{PP} = 52.4$ Hz, PPh_2), 24.7 (d, $^3J_{PP} = 52.4$ Hz, PHO).

IR (KBr): $\tilde{\nu}/cm^{-1} = 3050(w)$, 2982(w), 2949(m), 2870(m), 1479(m), 1455(m), 1433(m), 1389(w), 1310(w), 1179(s), 1110(m), 914(m), 938(m), 832(m), 743(s), 694(s).

MS (EI): $m/z(\%) = 310(18)$, 309(100), 183(18).

EA: calculated (%) for $C_{28}H_{32}OP_2$: C: 75.32, H: 7.22; measured: C: 74.16, H: 7.26.

$[\alpha]_D^{20} = +63.0$ ($c = 0.35$, $CHCl_3$ / 0.75% EtOH).

R_f (SiO_2 , hexanes:EtOAc (1:1)): 0.36.

m.p.: 52-62 °C.

(-)-109:

$C_{28}H_{32}OP_2$, 446.50 g/mol

1H -NMR (C_6D_6): $\delta/ppm = 0.24$ (s, 3H, $C_RH_3CC_5H_3$), 0.68 (s, 3H, $C_RH_3CC_5H_3$), 1.03 (s, 3H, $C(P)HCCH_3$), 1.30-1.46 (m, 2H, $C(P)HCH_RH_S$, $CHCH_2CH_RH_S$), 1.49 (t, $J_{HH} = 4.1$ Hz, 1H, $CHCH_2CH_2$), 1.61-1.76 (m, 2H, $CHCH_2CH_2$), 1.96 (ddd, $J_{HP} = 18.3$ Hz, $J_{HH} = 12.3$ Hz, $J_{HH} = 5.9$ Hz, 1H, $C(P)HCH_RH_S$), 2.13-2.20 (m, 1H, $C(P)H$), 2.92 (ddd, $J_{HH} = 12.8$ Hz, $J_{HH} = 9.0$ Hz, $J_{HH} = 3.9$ Hz, 1H, $CHCH_2CH_RH_S$), 6.94 (t, $J_{HH} = 7.5$ Hz, 1H, $Ph_2PCCHCH$), 6.96-7.03 (m, 6H, $Ph-CH$), 7.04-7.08 (m, 1H, Ph_2PCCH), 7.08-7.15 (m, 5H, $Ph_2PCCHCHCH$, $Ph-CH$), 8.48-8.56 (m, 1H, Ph_2PCCCH), 8.68 (dd, $J_{PH} = 470.4$ Hz, $J_{HH} = 4.5$ Hz, 1H, PH).

$^{13}C\{^1H\}$ -NMR (C_6D_6): $\delta/ppm = 15.1$ (d, $J_{CP} = 1.9$ Hz, $C(P)HCCH_3$), 18.0 (s, $C_RH_3CC_5H_3$), 18.5 (s, $C_RH_3CC_5H_3$), 27.1 (s, $C(P)HCH_2$), 28.2 (s, $CHCH_2CH_2$), 31.8 (d, $J_{CP} = 6.6$ Hz, $CHCH_2CH_2$), 44.9 (dd, $J_{CP} = 73.0$ Hz, $J_{CP} = 4.7$ Hz, $C(P)H$), 45.6 (d, $J_{CP} = 3.8$ Hz, $CHCH_2CH_2$), 49.8 (d, $J_{CP} = 2.2$ Hz, CH_3CCH_3), 50.1 (d, $J_{CP} = 11.1$ Hz, $C(P)HC$), 128.9 (d, $J_{CP} = 6.8$ Hz, $Ph-CH$), 129.1 (s, $Ph-CH$), 129.2 (d, $J_{CP} = 7.8$ Hz, $Ph-CH$), 129.7 (d, $J_{CP} = 10.3$ Hz, $Ph_2PCCHCHCH$), 131.6 (d, $J_{CP} = 2.1$ Hz, $Ph_2PCCHCH$), 133.7 (d, $J_{CP} = 19.8$ Hz, $Ph-CH$), 133.9 (d, $J_{CP} = 19.5$ Hz, $Ph-CH$), 134.2 (dd, $J_{CP} = 9.4$ Hz, $J_{CP} = 7.4$ Hz, Ph_2PCCCH), 135.3 (d, $J_{CP} = 8.9$ Hz, Ph_2CCH), 135.6 (d, $^1J_{CP} = 9.3$ Hz, $Ph-C$), 136.8 (d, $^1J_{CP} = 10.3$ Hz, $Ph-C$), 137.9 (dd, $J_{CP} = 16.4$ Hz, $J_{CP} = 9.6$ Hz, Ph_2PC), 140.0 (dd, $J_{CP} = 91.6$ Hz, $J_{CP} = 28.7$ Hz, Ph_2PCC).

$^{31}P\{^1H\}$ -NMR (C_6D_6): $\delta/ppm = -23.2$ (d, $^3J_{PP} = 71.6$ Hz, PPh_2), 9.9 (d, $^3J_{PP} = 71.6$ Hz, PHO).

IR (KBr): $\tilde{\nu}/cm^{-1} = 3051(w)$, 2983(w), 2948(m), 2871(m), 1478(m), 1449(m), 1433(m), 1389(w), 1311(w), 1184(s), 1110(m), 1027(w), 997(w), 903(m), 816(m), 743(s), 695(s).

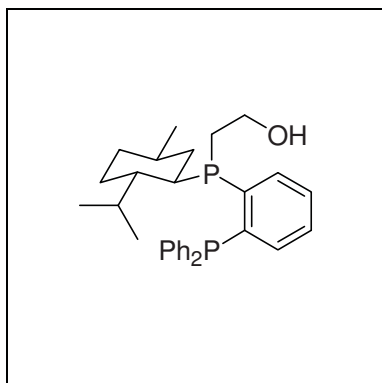
MS (EI): $m/z(\%) = 310(19)$, 309(100), 183(20).

EA: calculated (%) for $C_{28}H_{32}OP_2$: C: 75.32, H: 7.22; measured: C: 73.99, H: 7.19.

$[\alpha]_D^{20} = -81.0$ ($c = 0.36$, $CHCl_3$ / 0.75% EtOH).

R_f (SiO_2 , hexanes:EtOAc (1:1)): 0.48.

m.p.: 55-65 °C.



(2-Diphenylphosphinophenyl)((1*S*,2*R*,4*R*)-1-iso-propyl-4-methylcyclohex-2-yl)(2-hydroxyethyl)phosphine (118**)**

To a solution of **90** (700 mg, 2.23 mmol) in THF (20 mL) was added *n*-butyllithium (1.5 mL, 1.6 M in hexane, 2.40 mmol) at –78 °C. After 1 h this solution was transferred via cannula to a solution containing **97** (546 mg, 2.27 mmol) in THF (5 mL) at –

78 °C. After 1 h LiAlH₄ (90 mg, 2.37 mmol) was added and the solution was allowed to warm up to room temperature. Water (5 mL), aq. HCl (1 M, 2 mL) and EtOAc (10 mL) were added and the aqueous layer was extracted with EtOAc. The combined organic layers were washed with sat. aq. NaCl and dried over MgSO₄. The solvent was evaporated under reduced pressure and the residue dissolved in THF (12 mL). The solution was cooled down to –78 °C and *n*-butyllithium (1.5 mL, 1.6 M in hexane, 2.40 mmol) was added. After 15 min (2-chloroethoxy)trimethylsilane (0.5 mL, 3.08 mmol) was added and the reaction mixture was allowed to warm up to room temperature overnight. Ethanol (5 mL) was added and the solvent was evaporated under reduced pressure to give light yellow foam which was dissolved in THF (15 mL). Tetrabutylammonium fluoride • 3 H₂O (1.00 g, 3.17 mmol) was added and the solution was stirred for 2 h. EtOAc (10 mL) and water (10 mL) were added and the aqueous layer was extracted with EtOAc. The combined organic layers were washed with water and sat. aq. NaCl and dried over MgSO₄. The solvent was evaporated under reduced pressure and the crude product was purified by column chromatography (SiO₂, 23×4 cm, CH₂Cl₂:EtOAc (100:1 → 10:1)) to give the title compound **118** (402 mg, 38%) as a mixture of two diastereoisomers.

Separation of the diastereoisomers was achieved by semi-preparative chiral HPLC (AD, hexane:*i*PrOH (97:3)), whereupon the first eluting diastereoisomer quickly oxidized and could not be used for catalysis or proper analysis.

C₃₀H₃₈OP₂ (476.57)

¹H-NMR (CD₂Cl₂): δ/ppm = 0.70-0.90 (m, 13H, CH₃, CH₂, CH), 1.10-1.20 (m, 1H, CH), 1.24-1.36 (m, 1H, CH₂), 1.56-1.72 (m, 2H, CH₂, CH₂), 1.72-1.82 (m, 1H, CH), 1.82-1.95 (m, 1H, CH₂), 2.10-2.21 (m, 1H, CH₂), 2.25-2.38 (m, 1H, CH), 3.48-3.65 (m, 2H, CH₂), 6.94-7.01 (m, 1H, Ar-CH), 7.16-7.28 (m, 5H, Ar-CH), 7.28-7.38 (m, 7H, Ar-CH), 7.48-7.56 (m, 1H, Ar-CH).

$^{13}\text{C}\{^1\text{H}\}$ -NMR (CD_2Cl_2): $\delta/\text{ppm} = 15.3$ (d, $J_{\text{CP}} = 5.0$ Hz, CH_3), 21.1 (s, CH_3), 21.9 (s, CH_3), 24.4 (dd, $J_{\text{CP}} = 19.0$ Hz, $J_{\text{CP}} = 8.0$ Hz, $\text{CH}_2\text{CH}_2\text{OH}$), 25.0 (d, $J_{\text{CP}} = 8.0$ Hz, CH_2), 28.2 (d, $J_{\text{CP}} = 20.4$ Hz, CH), 33.1 (d, $J_{\text{CP}} = 2.3$ Hz, CH), 34.7 (s, CH_2), 35.9 (d, $J_{\text{CP}} = 3.3$ Hz, CH_2), 37.7 (dd, $J_{\text{CP}} = 15.0$ Hz, $J_{\text{CP}} = 5.2$ Hz, CH), 45.9 (d, $J_{\text{CP}} = 10.5$ Hz, CH), 59.9 (d, $J_{\text{CP}} = 24.7$ Hz, CH_2OH), 127.9 (s, Ar-CH), 128.0 (s, Ar-CH), 128.1 (s, Ar-CH), 128.1 (s, Ar-CH), 128.2 (s, Ar-CH), 128.3 (s, Ar-CH), 131.4 (d, $J_{\text{CP}} = 7.3$ Hz, Ar-CH), 133.1 (d, $J_{\text{CP}} = 19.2$ Hz, Ar-CH), 133.5 (d, $J_{\text{CP}} = 19.7$ Hz, Ar-CH), 134.2 (d, $J_{\text{CP}} = 6.6$ Hz, Ar-CH), 136.9 (d, $J_{\text{CP}} = 5.4$ Hz, Ar-C), 137.3 (d, $J_{\text{CP}} = 6.6$ Hz, Ar-C), 142.6 (d, $J_{\text{CP}} = 9.8$ Hz, Ar-C), 142.9 (d, $J_{\text{CP}} = 9.6$ Hz, Ar-C).

$^{31}\text{P}\{^1\text{H}\}$ -NMR (CD_2Cl_2): $\delta/\text{ppm} = -38.6$ (d, $^3J_{\text{PP}} = 143.5$ Hz), -19.1 (d, $^3J_{\text{PP}} = 143.5$ Hz).

IR (KBr): $\tilde{\nu}/\text{cm}^{-1} = 3381(\text{s})$, 3055(m), 2950(s), 2925(s), 2869(s), 1963(w), 1897(w), 1822(w), 1712(w), 1633(w), 1586(w), 1437(s), 1372(m), 1182(s), 1118(s), 1043(s), 1000(m), 745(s), 696(s), 545(s), 510(m).

MS (EI): $m/z(\%) = 476(4)$, 431(4), 353(5), 338(24), 337(100), 309(10), 294(7), 293(14), 215(4), 184(4), 183(29).

EA: calculated (%) for $\text{C}_{30}\text{H}_{38}\text{OP}_2 \cdot \text{H}_2\text{O}$: C: 72.85, H: 8.15; measured: C: 72.92, H: 7.68.

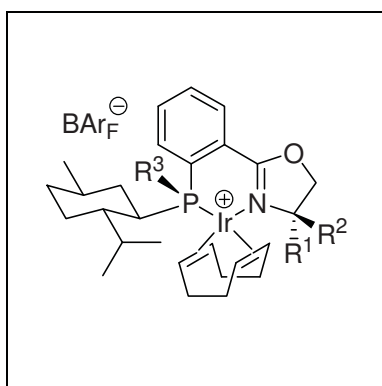
$[\alpha]_D^{20} = -153$ ($c = 0.16$, $\text{CHCl}_3 / 0.75\%$ EtOH).

R_f (SiO_2 , CH_2Cl_2 :EtOAc (10:1)): 0.4.

m.p.: 90-97 °C.

HPLC (AD-H, *n*-hexane:*i*PrOH (97:3), 0.5 mL/min, 20 °C): $t_R/\text{min} = 15.2$, 22.8.

4.3.3 Preparation of P-Chiral Iridium-PHOX Complexes

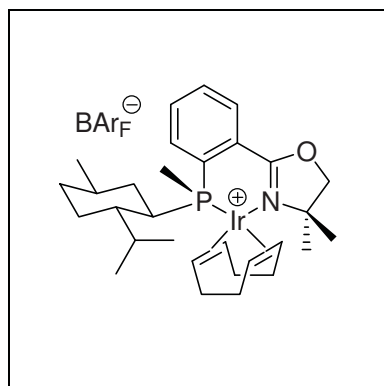


General procedure for the preparation of the P,N-iridium complexes (121-128)

To a solution of the oxazoline and *N,N,N,N*-tetramethylethylenediamine (100 μL , 668 μmol) in pentane (10 mL) was added *sec*-butyllithium (600 μL , 1.3 M in hexane, 960 μmol) at -78 °C. The reaction mixture was stirred for 2 h,

97 (200 mg, 830 μmol) was added and after additional 30 min the suspension was allowed to warm up to -10 °C. The reaction mixture was cooled to -78 °C and the corresponding

Grignard-reagent was added. After warming up to room temperature $\text{Na}_2\text{SO}_4 \cdot 12 \text{H}_2\text{O}$ was added and the solution was filtered over a pad of Al_2O_3 eluting with Et_2O . The solvent was evaporated under reduced pressure to give a yellow oil which was dissolved in CH_2Cl_2 (3.5 mL) and added to a solution of $[\text{Ir}(\text{cod})\text{Cl}]_2$ (177 mg, 264 μmol) in CH_2Cl_2 (1.5 mL) at room temperature. After 30 min NaBAr_F (500 mg, 564 μmol) was added and the solution was stirred for 1 h. The solvent was evaporated under reduced pressure and the crude product was purified by column chromatography (SiO_2 , 3×15 cm). Elution of the side products with TBME and then of the product with CH_2Cl_2 followed by recrystallization from CH_2Cl_2 /hexanes gave the desired complexes.



[(η^4 -1,5-Cyclooctadiene)-{(R_P)-4,4-dimethyl-2-[2'-((1*S*,2*R*,4*R*)-1-*iso*-propyl-4-methylcyclohex-2-yl)methylphosphinyl)-phenyl]-4,5-dihydrooxazole}-iridium(I)]-tetrakis[3,5-bis(trifluoromethyl)phenyl]borat (121)

The iridium-complex was prepared according to the general procedure from 4,4-dimethyl-2-phenyl-oxazoline (90.0 μL , 527 μmol) and MeMgBr (400 μL , 3 M in Et_2O , 1.20 mmol) to give the title compound **121** (428 mg, 53%) as an orange solid.

$\text{C}_{62}\text{H}_{58}\text{BF}_4\text{IrNOP}$ (1523.09 g/mol)

$^1\text{H-NMR}$ (CD_2Cl_2): δ/ppm = 0.50-0.62 (m, 1H, Men-*CHH*), 0.66 (d, $^3J_{\text{HH}} = 6.5$ Hz, 3H, CH_3CHCH_3), 0.75-0.84 (m, 2H, Men-*CHH*, Men-*CHH*), 1.08 (d, $^3J_{\text{HH}} = 6.7$ Hz, 3H, CHCH_3), 1.09 (d, $^3J_{\text{HH}} = 6.7$ Hz, 3H, CH_3CHCH_3), 1.08-1.23 (m, 3H, C(P)*HCH*, *CHCH}_3*, Men-*CHH*), 1.41-1.46 (m, 1H, cod-*CHH*), 1.45 (s, 3H, CH_3CCH_3), 1.49 (d, $^2J_{\text{HP}} = 8.5$ Hz, 3H, PCH_3), 1.61-1.74 (m, 2H, cod-*CHH*, Men-*CHH*), 1.69 (s, 3H, CH_3CCH_3), 1.76-1.84 (m, 1H, Men-*CHH*), 1.88-1.92 (m, 1H, cod-*CHH*), 2.08-2.36 (m, 6H, C(P)*H*, cod-*CHH*, cod- CH_2 , cod-*CH}_2*), 2.46-2.55 (m, 1H, CH_3CHCH_3), 3.38-3.45 (m, 1H, cod-*CH*), 3.50-3.56 (m, 1H, cod-*CH*), 4.26 (d, $^2J_{\text{HH}} = 9.0$ Hz, 1H, O*CHH*), 4.46 (d, $^2J_{\text{HH}} = 9.0$ Hz, 1H, O*CHH*), 5.12-5.23 (m, 2H, cod-*CH*, cod-*CH*), 7.31-7.37 (m, 1H, C(P)*CH*), 7.57 (s, 4H, BAr_F -*CH*), 7.56-7.66 (m, 2H, C(P)*CHCHCH*), 7.73 (s, 8H, BAr_F -*CH*), 7.81-7.84 (m, 1H, C(P)*CCH*).

^{13}C -NMR (CD_2Cl_2): $\delta/\text{ppm} = -4.0$ (d, $^1J_{\text{CP}} = 35.0$ Hz, PCH_3), 17.6 (s, CH_3CHCH_3), 21.4 (s, CHCH_3), 21.7 (s, CH_3CHCH_3), 25.2 (d, $J_{\text{CP}} = 10.5$ Hz, Men- CH_2), 27.0 (d, $J_{\text{CP}} = 1.7$ Hz, cod- CH_2), 27.6 (s, CH_3CCH_3), 27.8 (s, CH_3CCH_3), 29.0 (d, $J_{\text{CP}} = 2.2$ Hz, cod- CH_2), 29.9 (d, $^4J_{\text{CP}} = 7.2$ Hz, CH_3CHCH_3), 31.7 (d, $J_{\text{CP}} = 1.7$ Hz, cod- CH_2), 33.1 (d, $^3J_{\text{CP}} = 8.7$ Hz, CHCH_3), 33.4 (s, Men- CH_2), 34.6 (d, $J_{\text{CP}} = 4.2$ Hz, cod- CH_2), 36.9 (d, $J_{\text{CP}} = 6.4$ Hz, Men- CH_2), 39.9 (d, $^1J_{\text{CP}} = 26.7$ Hz, C(P)H), 43.8 (s, C(P)HCH), 60.3 (s, cod- CH), 62.1 (s, cod- CH), 73.0 (s, OCH_2C), 82.5 (s, OCH_2C), 89.1 (d, $J_{\text{CP}} = 12.7$ Hz, cod- CH), 91.5 (d, $J_{\text{CP}} = 11.4$ Hz, cod- CH), 117.0-117.2 (m, $\text{BAr}_\text{F}\text{-CH}$), 124.3 (q, $^1J_{\text{CF}} = 272.4$ Hz, $\text{BAr}_\text{F}\text{-CF}_3$), 126.8 (d, $^1J_{\text{CP}} = 41.6$ Hz, C(P)C), 128.1-129.0 (m, $\text{BAr}_\text{F}\text{-C}$), 128.8 (s, C(P)CH), 129.6 (d, $^2J_{\text{CP}} = 12.5$ Hz, C(P)C), 130.4 (d, $^3J_{\text{CP}} = 7.3$ Hz, C(P)CCH), 130.5 (d, $^4J_{\text{CP}} = 1.7$ Hz, C(P)CCHCH), 133.3 (d, $^3J_{\text{CP}} = 6.0$ Hz, C(P)CHCH), 134.5 (s, $\text{BAr}_\text{F}\text{-CH}$), 161.4 (q, $^1J_{\text{CB}} = 49.8$ Hz, $\text{BAr}_\text{F}\text{-CB}$), 165.7 (d, $^3J_{\text{CP}} = 6.1$ Hz, NCO).

^{31}P -NMR (CD_2Cl_2): $\delta/\text{ppm} = 4.26$ (s).

IR (KBr): $\tilde{\nu}/\text{cm}^{-1} = 2962(\text{m})$, 2933(m), 2893(m), 1608(m), 1567(w), 1463(w), 1355(s), 1278(s), 1128(s), 998(w), 965(w), 888(m), 839(w), 741(w), 714(m), 676(m).

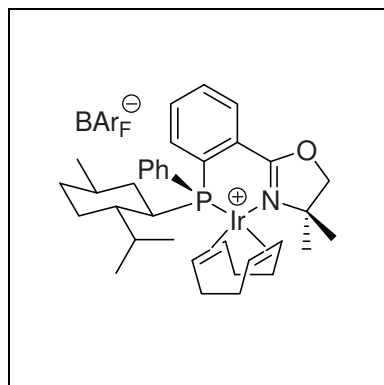
MS (ESI): $m/z(\%) = 661(27)$, 660(100), 659(20), 658(56), 550(20), 548(15).

EA: calculated (%) for $\text{C}_{62}\text{H}_{58}\text{BF}_{24}\text{IrNOP}$: C: 48.89, H: 3.84, N: 0.92; measured: C: 48.97, H: 3.74, N: 0.87.

$[\alpha]_{\text{D}}^{20} = -155$ ($c = 0.22$, $\text{CHCl}_3 / 0.75\%$ EtOH).

R_f (SiO_2 , hexanes: CH_2Cl_2 (1:1)): 0.18.

m.p.: 191-195 $^\circ\text{C}$.



[(η^4 -1,5-Cyclooctadiene)-{(S_P)-4,4-dimethyl-2-[2'-((1S,2R,4R)-1-iso-propyl-4-methylcyclohex-2-yl)phenylphosphinyl)-phenyl]-4,5-dihydrooxazole}-iridium(I)]-tetrakis[3,5-bis(trifluoromethyl)phenyl]borat (122)

The iridium-complex was prepared according to the general procedure from 4,4-dimethyl-2-phenyl-oxazoline (90.0 μL , 527 μmol) and PhMgBr (1.20 mL, 1 M in THF, 1.20 mmol) to give the title compound **122** (405 mg, 48%) as a red solid.

$C_{67}H_{60}BF_{24}IrNOP$ (1585.15 g/mol)

1H -NMR (CD_2Cl_2): $\delta/ppm = 0.61$ (d, $^3J_{HH} = 6.8$ Hz, 3H, CH_3CHCH_3), 0.79 (d, $^3J_{HH} = 6.6$ Hz, 3H, CH_3CHCH_3), 0.83-0.90 (m, 1H, Men- CHH), 0.91 (d, $^3J_{HH} = 6.3$ Hz, 3H, CH_3), 1.12-1.40 (m, 6H, cod- CH_2 , cod- CHH , cod- CHH , CH_3CHCH_3 , C(P)HCH), 1.48 (s, 3H, CH_3CCH_3), 1.55-1.80 (m, 3H, Men- CHH , cod- CHH , cod- CHH), 1.84 (s, 3H, CH_3CCH_3), 1.92-2.40 (m, 7H, $CHCH_3$, Men- CH_2 , Men- CHH , Men- CHH , cod- CH_2), 1.62-2.78 (m, 2H, C(P)H, cod- CH), 3.89-3.95 (m, 1H, cod- CH), 4.23 (d, $^2J_{HH} = 8.9$ Hz, 1H, OCHH), 4.48 (d, $^2J_{HH} = 8.9$ Hz, 1H, OCHH), 4.87-4.95 (m, 1H, cod- CH), 5.36-5.42 (m, 1H, cod- CH), 7.42-7.82 (m, 1H, C(P)CHCH), 7.51-7.67 (m, 11H, BArF- CH , Ph- CH , C(P)CHCHCH), 7.74 (s, 8H, BArF- CH), 7.97 (dd, $^3J_{HH} = 7.8$ Hz, $^4J_{HP} = 3.6$ Hz, 1H, C(P)CCH).

$^{13}C\{^1H\}$ -NMR (CD_2Cl_2): $\delta/ppm = 16.3$ (s, CH_3CHCH_3), 20.8 (s, CH_3CHCH_3), 22.0 (s, CH_3), 25.2 (d, $J_{CP} = 9.5$ Hz, Men- CH_2), 25.5 (s, cod- CH_2), 26.5 (s, CH_3CCH_3), 27.2 (s, cod- CH_2), 28.4 (s, CH_3CCH_3), 31.3 (s, CH_3CHCH_3), 33.4 (s, cod- CH_2), 33.5 (s, CH_3CH), 33.8 (d, $J_{CP} = 13.4$ Hz, Men- CH_2), 35.8 (d, $J_{CP} = 4.6$ Hz, cod- CH_2), 41.6-42.0 (m, Men- CH_2), 42.6 (d, $^1J_{CP} = 21.2$ Hz, C(P)H), 43.6 (d, $^2J_{CP} = 3.1$ Hz, C(P)HCH), 62.6 (s, cod- CH), 64.5 (cod- CH), 73.2 (s, CH_3CCH_3), 82.9 (s, OCH $_2$), 84.3 (d, $J_{CP} = 14.1$ Hz, cod- CH), 90.8 (d, $J_{CP} = 9.4$ Hz, cod- CH), 117.0-117.3 (m, BArF- CH), 123.5 (d, $^1J_{CP} = 50.0$ Hz, Ph- C), 124.3 (q, $^1J_{CF} = 272.5$ Hz, BArF- CF_3), 128.1-129.1 (m, BArF- C , C(P)C), 128.4 (d, $J_{CP} = 9.5$ Hz, Ph- CH), 130.8 (d, $^3J_{CP} = 7.6$ Hz, C(P)CCH), 131.0 (d, $^4J_{CP} = 1.9$ Hz, C(P)CCHCH), 131.4 (d, $J_{CP} = 2.2$ Hz, Ph- CH), 131.7 (d, $^2J_{CP} = 13.8$ Hz, C(P)C), 132.4 (d, $^2J_{CP} = 6.2$ Hz, C(P)CH), 132.9 (d, $J_{CP} = 13.7$ Hz, Ph- CH), 133.0 (d, $^3J_{CP} = 5.7$ Hz, C(P)CHCH), 161.4 (q, $^1J_{BC} = 49.8$ Hz, BArF- CB), 166.3 (d, $^3J_{CP} = 6.4$ Hz, NCO).

$^{31}P\{^1H\}$ -NMR (CD_2Cl_2): $\delta/ppm = 19.2$ (s).

IR (KBr): $\tilde{\nu}/cm^{-1} = 2961(m)$, 2933(m), 2025(w), 1610 (m), 1462(w), 1355(s), 1278(s), 1127(s), 999(w), 963(w), 889(m), 839(w), 743(m), 712(m), 676(m), 529(w).

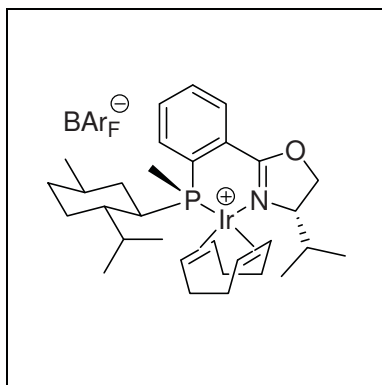
MS (ESI): $m/z(\%) = 723(8)$, 722(20), 721(9), 720(12), 613(32), 612(100), 611(23), 610(77), 609(5), 608(12), 606(5).

EA: calculated (%) for $C_{67}H_{60}BF_{24}IrNOP$: C: 50.77, H: 3.82, N: 0.88; measured: C: 50.38, H: 3.86, N: 0.82.

$[\alpha]_D^{20} = -120$ ($c = 0.22$, $CHCl_3 / 0.75\%$ EtOH).

R_f (SiO_2 , hexanes: CH_2Cl_2 (1:1)): 0.12.

m.p.: 138-143 °C.



[(η^4 -1,5-Cyclooctadiene)-{(4*S*,*R*_P)-4-*iso*-propyl-2-[2'-((1*S*,2*R*,4*R*)-1-*iso*-propyl-4-methylcyclohex-2-yl)methylphosphinyl]-phenyl]-4,5-dihydrooxazole}-iridium(I)]-tetrakis[3,5-bis(trifluoromethyl)phenyl]borat
(**123**)

The iridium-complex was prepared according to the general procedure from (*S*)-4-*iso*-propyl-2-phenyl-oxazoline (100 mg, 529 μ mol) and MeMgBr (400 μ L, 3 M in Et₂O, 1.20 mmol) to give the title compound **123** (409 mg, 50%) as a red solid.

C₆₃H₆₀BF₂₄IrNOP (1537.11 g/mol)

¹H-NMR (CD₂Cl₂): δ /ppm = 0.55-0.66 (m, 1H, Men-CHH), 0.66 (d, ³J_{HH} = 6.5 Hz, 3H, CH₃), 0.70-0.84 (m, 2H, Men-CHH, Men-CHH), 0.94 (d, ³J_{HH} = 6.7 Hz, 3H, Men-CH₃CHCH₃), 1.09 (d, ³J_{HH} = 6.7 Hz, 3H, CH₃CHCH₃), 1.10 (d, ³J_{HH} = 6.8 Hz, 3H, CH₃CHCH₃), 1.10-1.15 (m, 1H, Men-CHCH₃), 1.12 (d, ³J_{HH} = 7.1 Hz, 3H, Men-CH₃CHCH₃), 1.15-1.23 (m, 1H, CH(P)CH), 1.51 (d, ²J_{HP} = 8.4 Hz, 3H, PCH₃), 1.65-1.93 (m, 5H, cod-CHH, cod-CHH, Men-CHH, Men-CH₂), 1.98-2.41 (m, 8H, cod-CHH, cod-CHH, cod-CH₂, cod-CH₂, C(P)H, Men-CH₃CHCH₃), 2.81-2.89 (m, 1H, CH₃CHCH₃), 3.31-3.37 (m, 1H, cod-CH), 3.72-3.79 (m, 1H, cod-CH), 4.15 (ddd, ³J_{HH} = 10.0 Hz, ³J_{HH} = 4.2 Hz, ³J_{HH} = 2.3 Hz, 1H, CHN), 4.46 (t, ³J_{HH} = 9.8 Hz, 1H, OCH_RH_S), 4.53-4.60 (m, 1H, cod-CH), 4.66 (dd, ²J_{HH} = 9.6 Hz, ³J_{HH} = 4.3 Hz, 1H, OCH_RH_S), 4.94-5.01 (m, 1H, cod-CH), 7.38-7.45 (m, 1H, C(P)CH), 7.57 (s, 4H, BAr_F-CH), 7.60 (tt, ³J_{HH} = 7.7 Hz, ⁴J_{HH} = 1.2 Hz, 1H, C(P)CCHCH), 7.65 (tt, ³J_{HH} = 7.5 Hz, ⁴J_{HH} = 1.2 Hz, 1H, C(P)CHCH), 7.73 (s, 8H, BAr_F-CH), 8.09 (ddd, ³J_{HH} = 7.6 Hz, ⁴J_{HP} = 3.8 Hz, ⁴J_{HH} = 1.4 Hz, 1H, C(P)CCH).

¹³C{¹H}-NMR (CD₂Cl₂): δ /ppm = -3.31 (d, ¹J_{CP} = 33.8 Hz, PCH₃), 14.2 (s, Men-CH₃CHCH₃), 16.9 (s, CH₃CHCH₃), 19.0 (s, Men-CH₃CHCH₃), 21.4 (s, CHCH₃), 21.6 (s, CH₃CHCH₃), 25.2 (d, ¹J_{CP} = 10.6 Hz, Men-CH₂), 28.4 (d, ¹J_{CP} = 1.8 Hz, cod-CH₂), 29.4 (d, ¹J_{CP} = 2.0 Hz, cod-CH₂), 30.3 (d, ⁴J_{CP} = 7.0 Hz, CH₃CHCH₃), 31.5 (s, Men-CH₃CHCH₃), 31.6 (d, ¹J_{CP} = 2.9 Hz, cod-CH₂), 32.9 (d, ¹J_{CP} = 6.1 Hz, cod-CH₂), 33.0 (s, CHCH₃), 33.3 (s, Men-CH₂), 36.5 (d, ¹J_{CP} = 6.5 Hz, Men-CH₂), 41.0 (d, ¹J_{CP} = 28.1 Hz, C(P)H), 43.2 (s, C(P)HCH), 60.5 (s, cod-CH), 64.6 (s, cod-CH), 68.4 (s, OCH₂), 69.9 (s, NCH), 91.0 (d, ¹J_{CP} = 11.4 Hz, cod-CH), 92.6 (d, ¹J_{CP} = 12.9 Hz, cod-CH), 117.0-117.2 (m, BAr_F-CH), 124.3 (q, ¹J_{CF} = 272 Hz, BAr_F-CF₃), 127.3 (d, ²J_{CP} = 11.5 Hz, C(P)C), 128.0-129.0 (m, BAr_F-C), 129.9

(d, $^1J_{\text{CP}} = 40.3$ Hz, C(P)C), 130.8 (s, C(P)CH), 131.0 (s, C(P)CCHCH), 133.0 (d, $^3J_{\text{CP}} = 7.3$ Hz, C(P)CCH), 133.5 (d, $^3J_{\text{CP}} = 6.1$ Hz, C(P)CHCH), 134.5 (s, BAr_F-CH), 161.4 (q, $^1J_{\text{BC}} = 49.9$ Hz, BAr_F-CB), 164.3 (d, $^3J_{\text{CP}} = 5.1$ Hz, NCO).

$^{31}\text{P}\{^1\text{H}\}$ -NMR (CD₂Cl₂): $\delta/\text{ppm} = 1.4$ (s).

IR (KBr): $\tilde{\nu}/\text{cm}^{-1} = 2962(\text{m}), 2932(\text{m}), 2888(\text{m}), 1785(\text{w}), 1606(\text{m}), 1463(\text{w}), 1355(\text{s}), 1278(\text{s}), 1128(\text{s}), 1001(\text{w}), 961(\text{w}), 887(\text{m}), 839(\text{w}), 714(\text{m}), 676(\text{m}), 579(\text{w}), 518(\text{w}), 448(\text{w})$.

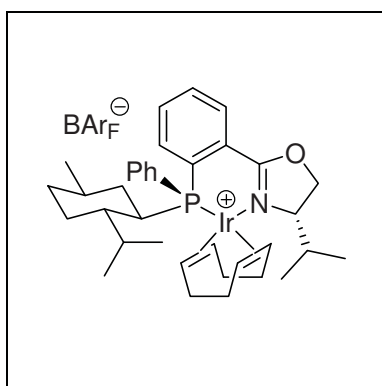
MS (ESI): $m/z(\%) = 676(5), 675(34), 674(100), 673(20), 672(62), 562(13), 560(14), 558(7)$.

EA: calculated (%) for C₆₃H₆₀BF₂₄IrNOP: C: 49.23, H: 3.93, N: 0.91; measured: C: 49.24, H: 3.92, N: 0.91.

$[\alpha]_{\text{D}}^{20} = -108$ ($c = 0.24$, CHCl₃ / 0.75% EtOH).

R_f (SiO₂, hexanes:CH₂Cl₂ (1:1)): 0.18.

m.p.: 193-197 °C.



[(η^4 -1,5-Cyclooctadiene)-{(4*S*,*S*_P)-4-*iso*-propyl-2-[2'-((1*S*,2*R*,4*R*)-1-*iso*-propyl-4-methylcyclohex-2-yl)phenylphosphinyl)-phenyl]-4,5-dihydrooxazole}-iridium(I)]-tetrakis[3,5-bis(trifluoromethyl)phenyl]borat (124)

The iridium-complex was prepared according to the general procedure from (*S*)-4-*iso*-propyl-2-phenyl-oxazoline (100 mg, 529 μmol) and PhMgBr (1.20 mL, 1 M in THF, 1.20 mmol) to give the title compound **124** (447 mg, 53%) as a red solid.

C₆₈H₆₂BF₂₄IrNOP (1599.18 g/mol)

^1H -NMR (CD₂Cl₂): $\delta/\text{ppm} = 0.80$ -0.90 (m, 1H, Men-CHH), 0.84 (d, $^3J_{\text{HH}} = 6.6$ Hz, 3H, CH₃), 0.88 (d, $^3J_{\text{HH}} = 6.4$ Hz, 3H, Ox-CH₃CHCH₃), 0.89 (d, $^3J_{\text{HH}} = 6.9$ Hz, 3H, Men-CH₃CHCH₃), 0.91 (d, $^3J_{\text{HH}} = 8.0$ Hz, 3H, Men-CH₃CHCH₃), 1.04 (d, $^3J_{\text{HH}} = 7.0$ Hz, 3H, Ox-CH₃CHCH₃), 1.12-1.26 (m, 2H, Men-CHH, Men-CHH), 1.30-1.49 (m, 2H, CHCH₃, cod-CHH), 1.51-1.88 (m, 5H, C(P)HCH, Men-CHH, Men-CHH, cod-CHH, cod-CHH), 2.08-2.43 (m, 7H, Ox-CH₃CHCH₃, Men-CHH, cod-CH₂, cod-CH₂, cod-CH), 2.44-2.54 (m, 2H, Men-CH₃CHCH₃,

cod-CH), 2.66-2.76 (m, 1H, C(P)H), 3.36-3.42 (m, 1H, cod-CH), 4.16-4.21 (m, 1H, NCH), 4.43 (t, $^2J_{\text{HH}} = 9.3$ Hz, 1H, OCH_RH_S), 4.70 (dd, $^2J_{\text{HH}} = 9.6$ Hz, $^3J_{\text{HH}} = 2.6$ Hz, 1H, OCH_RH_S), 4.76-4.83 (m, 2H, cod-CH, cod-CH), 7.41-7.53 (m, 6H, Ph-CH, C(P)CH), 7.56-7.61 (m, 1H, C(P)CHCH), 7.57 (s, 4H, BAr_F-CH), 7.65-7.71 (m, 1H, C(P)CCHCH), 7.73 (s, 8H, BAr_F-CH), 8.36 (dd, $^3J_{\text{HH}} = 7.8$ Hz, $^4J_{\text{HH}} = 4.0$ Hz, 1H, C(P)CCH).

$^{13}\text{C}\{^1\text{H}\}$ -NMR (CD₂Cl₂): $\delta/\text{ppm} = 15.0$ (s, Ox-CH₃CHCH₃), 16.9 (s, Men-CH₃CHCH₃), 18.7 (s, Ox-CH₃CHCH₃), 21.3 (s, Men-CH₃CHCH₃), 21.6 (s, CH₃), 25.7 (d, $J_{\text{CP}} = 9.5$ Hz, Men-CH₂), 26.7 (s, cod-CH₂), 29.0 (s, cod-CH₂), 29.5 (d, $^3J_{\text{CP}} = 3.6$ Hz, Men-CH₃CHCH₃), 31.3 (s, cod-CH₂), 31.7 (s, Ox-CH₃CHCH₃), 33.3 (s, Men-CH₂), 33.7 (d, $^3J_{\text{CP}} = 13.3$ Hz, CHCH₃), 34.6 (d, $J_{\text{CP}} = 4.3$ Hz, cod-CH₂), 40.3 (d, $J_{\text{CP}} = 1.8$ Hz, Men-CH₂), 43.9 (d, $^2J_{\text{CP}} = 3.4$ Hz, C(P)HCH), 45.0 (d, $^1J_{\text{CP}} = 23.3$ Hz, C(P)H), 61.6 (s, cod-CH), 67.0 (s, cod-CH), 67.9 (s, OCH₂), 70.0 (s, NCH), 88.4 (d, $J_{\text{CP}} = 12.2$ Hz, cod-CH), 93.1 (d, $J_{\text{CP}} = 11.2$ Hz, cod-CH), 117.0-117.3 (m, BAr_F-CH), 124.3 (q, $^1J_{\text{CF}} = 272$ Hz, BAr_F-CF₃), 125.6 (d, $^1J_{\text{CP}} = 49.4$ Hz, Ph-C), 128.1-129.1 (m, C(P)C, BAr_F-C), 128.2 (d, $J_{\text{CP}} = 9.8$ Hz, Ph-CH), 129.0 (d, $^2J_{\text{CP}} = 12.8$ Hz, C(P)C), 131.0 (d, $J_{\text{CP}} = 2.2$ Hz, Ph-CH), 131.9 (d, $^4J_{\text{CP}} = 2.1$ Hz, C(P)CCHCH), 132.2 (d, $J_{\text{CP}} = 8.3$ Hz, Ph-CH), 132.8 (d, $^3J_{\text{CP}} = 6.3$ Hz, C(P)CHCH), 133.5 (d, $^3J_{\text{CP}} = 7.9$ Hz, C(P)CCH), 134.5 (s, BAr_F-CH), 136.7 (s, C(P)CH), 161.4 (q, $^1J_{\text{BC}} = 49.8$ Hz, BAr_F-CB), 164.5 (d, $^3J_{\text{CP}} = 6.0$ Hz, NCO).

$^{31}\text{P}\{^1\text{H}\}$ -NMR (CD₂Cl₂): $\delta/\text{ppm} = 18.3$ (s).

IR (KBr): $\tilde{\nu}/\text{cm}^{-1} = 2964(\text{m}), 2933(\text{m}), 2882(\text{m}), 1607(\text{m}), 1565(\text{w}), 1463(\text{w}), 1355(\text{s}), 1278(\text{s}), 1127(\text{s}), 1002(\text{w}), 967(\text{w}), 889(\text{m}), 839(\text{w}), 743(\text{w}), 712(\text{m}), 677(\text{m}), 544(\text{w})$.

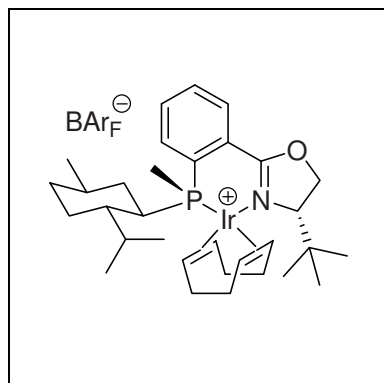
MS (ESI): $m/z(\%) = 738(6), 737(37), 736(100), 735(29), 734(65), 732(5), 627(6), 626(25), 625(16), 624(51), 623(20), 622(75), 621(9), 620(30), 618(5)$.

EA: calculated (%) for C₆₈H₆₂BF₂₄IrNOP: C: 51.07, H: 3.91, N: 0.88; measured: C: 50.96, H: 3.90, N: 0.76.

$[\alpha]_{\text{D}}^{20} = -84$ ($c = 0.25$, CHCl₃ / 0.75% EtOH).

R_{f} (SiO₂, hexanes:CH₂Cl₂ (1:1)): 0.18.

m.p.: 146-155 °C.



[(η^4 -1,5-Cyclooctadiene)-{(4*S*,*R*_P)-4-*tert*-butyl-2-[2'-((1*S*,2*R*,4*R*)-1-*iso*-propyl-4-methylcyclohex-2-yl)methylphosphinyl]-phenyl]-4,5-dihydrooxazole}-iridium(I)]-tetrakis[3,5-bis(trifluoromethyl)phenyl]borat
(125)

The iridium-complex was prepared according to the general procedure from (*S*)-4-*tert*-butyl-2-phenyl-oxazoline (107 mg, 527 μ mol) and MeMgBr (400 μ L, 3 M in Et₂O, 1.20 mmol) to give the title compound **125** (212 mg, 26%) as an orange foam.

C₆₄H₆₂BF₂₄IrNOP (1551.15 g/mol)

¹H-NMR (CD₂Cl₂): δ /ppm = 0.48-0.60 (m, 1H, Men-CHH), 0.64 (d, ³J_{HH} = 6.5 Hz, 3H, CHCH₃), 0.76-0.82 (m, 2H, Men-CHH, Men-CHH), 1.02 (d, ³J_{HH} = 6.7 Hz, 3H, CH₃CHCH₃), 1.04-1.26 (m, 3H, Men-CHH, CHCH₃, C(P)HCH), 1.07 (d, ³J_{HH} = 6.8 Hz, 3H, CH₃CHCH₃), 1.14 (s, 9H, C(CH₃)₃), 1.50-1.60 (m, 1H, cod-CHH), 1.55 (d, ²J_{HP} = 8.2 Hz, 3H, PCH₃), 1.62-1.72 (m, 2H, Men-CHH, cod-CHH), 1.75-1.83 (m, 1H, Men-CHH), 1.98-2.28 (m, 4H, cod-CH₂, cod-CHH, cod-CHH), 2.35-2.48 (m, 3H, cod-CH₂, CH₃CHCH₃), 2.50-2.59 (m, 1H, CHP), 3.48-3.60 (m, 2H, cod-CH, cod-CH), 3.96 (dd, ³J_{HH} = 9.5 Hz, ³J_{HH} = 3.3 Hz, 1H, NCHCH₂), 4.46 (t, ²J_{HH} = ³J_{HH} = 9.7 Hz, 1H, NCHCH_RH_S), 4.56-4.63 (m, 1H, cod-CH), 4.75 (dd, ²J_{HH} = 9.8 Hz, ³J_{HH} = 3.3 Hz, 1H, NCHCH_RH_S), 4.87-4.96 (m, 1H, cod-CH), 7.40-7.46 (m, 1H, C(P)CH), 7.57 (s, 4H, BAR_F-CH), 7.57-7.62 (m, 1H, C(P)CCHCH), 7.62-7.67 (m, 1H, C(P)CHCH), 7.73 (s, 8H, BAR_F-CH), 8.14 (dd, ³J_{HH} = 7.7 Hz, ⁴J_{HH} = 3.7 Hz, 1H, C(P)CCH).

¹³C{¹H}-NMR (CD₂Cl₂): δ /ppm = -1.4 (d, ¹J_{CP} = 34.5 Hz, PCH₃), 17.6 (s, CH₃CHCH₃), 21.4 (s, CHCH₃), 21.8 (s, CH₃CHCH₃), 25.6 (s, C(CH₃)₃), 25.7 (d, J_{CP} = 10.4 Hz, Men-CH₂), 26.2 (d, J_{CP} = 1.8 Hz, cod-CH₂), 29.6 (d, J_{CP} = 2.0 Hz, cod-CH₂), 29.7 (d, ³J_{CP} = 6.3 Hz, CH₃CHCH₃), 31.0 (d, J_{CP} = 1.8 Hz, cod-CH₂), 33.0 (d, ³J_{CP} = 9.1 Hz, CHCH₃), 33.2 (s, Men-CH₂), 34.2 (s, C(CH₃)₃), 35.2 (d, J_{CP} = 4.1 Hz, cod-CH₂), 38.1 (d, J_{CP} = 6.2 Hz, Men-CH₂), 41.4 (d, ¹J_{CP} = 26.3 Hz, C(P)H), 43.6 (s, C(P)HCH), 60.8 (s, cod-CH), 62.1 (s, cod-CH), 70.1 (s, NCHCH₂), 74.0 (s, NCHCH₂), 91.0 (d, J_{CP} = 12.5 Hz, cod-CH), 94.6 (d, J_{CP} = 11.8 Hz, cod-CH), 117.0-117.3 (m, BAR_F-CH), 124.3 (q, ¹J_{CF} = 272.4 Hz, BAR_F-CF₃), 128.0 (d, ²J_{CP} = 11.6 Hz, C(P)C), 128.1-129.0 (m, BAR_F-C), 130.0 (d, ¹J_{CP} = 40.4 Hz, C(P)C), 131.0 (d, ⁴J_{CP} = 1.9 Hz, PCCCHCH), 131.1 (s, C(P)CH), 133.0 (d, ³J_{CP} = 7.5 Hz, C(P)CCH), 133.6 (d,

$^3J_{\text{CP}} = 6.0$ Hz, C(P)CHCH), 134.5 (s, BAr_F-CH), 161.4 (q, $^1J_{\text{BC}} = 49.8$ Hz, BAr_F-CB), 164.6 (d, $^3J_{\text{CP}} = 4.6$ Hz, NCO).

$^{31}\text{P}\{^1\text{H}\}$ -NMR (CD₂Cl₂): $\delta/\text{ppm} = 1.3$ (s).

IR (KBr): $\tilde{\nu}/\text{cm}^{-1} = 2964(\text{m}), 2933(\text{m}), 2884(\text{m}), 1609(\text{m}), 1598(\text{m}), 1354(\text{s}), 1277(\text{s}), 1163(\text{s}), 1125(\text{s}), 1001(\text{w}), 967(\text{w}), 879(\text{m}), 839(\text{m}), 744(\text{w}), 714(\text{m}), 682(\text{m}), 667(\text{m})$.

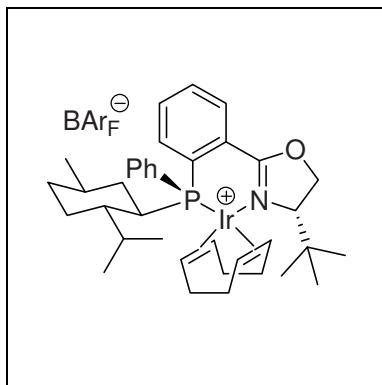
MS (ESI): $m/z(\%) = 689(35), 688(100), 687(18), 686(60), 578(7), 577(7), 576(21), 574(14)$.

EA: calculated (%) for C₆₄H₆₂BF₂₄IrNOP: C: 49.56, H: 4.03, N: 0.90; measured: C: 49.68, H: 4.05, N: 0.75.

$[\alpha]_D^{20} = -125$ ($c = 0.24$, CHCl₃ / 0.75% EtOH).

R_f (SiO₂, hexanes:CH₂Cl₂ (1:4)): 0.78.

m.p.: 186-193 °C.



[(η^4 -1,5-Cyclooctadiene)-{(4*S*,*S*_P)-4-*tert*-butyl-2-[2'-((1*S*,2*R*,4*R*)-1-*iso*-propyl-4-methylcyclohex-2-yl)phenylphosfinyl]-phenyl]-4,5-dihydrooxazole}-iridium(I)]-tetrakis[3,5-bis(trifluoromethyl)phenyl]borat (**126**)

The iridium-complex was prepared according to the general procedure from (*S*)-4-*tert*-butyl-2-phenyl-oxazoline (107 mg, 527 μmol) and PhMgBr (1.20 mL, 1 M in THF, 1.20 mmol) to give the title compound **126** (324 mg, 38%) as an orange foam.

C₆₉H₆₄BF₂₄IrNOP (1613.22 g/mol)

^1H -NMR (CD₂Cl₂): $\delta/\text{ppm} = 0.56$ (d, $^3J_{\text{HH}} = 6.6$ Hz, 3H, CH₃CHCH₃), 0.70 (d, $^3J_{\text{HH}} = 6.8$ Hz, 3H, CH₃CHCH₃), 0.80-1.00 (m, 2H, cod-CHH, Men-CHH), 0.93 (d, $^3J_{\text{HH}} = 6.5$ Hz, 3H, CH₃), 1.13 (s, 9H, C(CH₃)₃), 1.17-1.48 (m, 3H, Men-CHH, Men-CHH, CH₃CHCH₃), 1.49-1.64 (m, 2H, CHCH₃, C(P)HCH), 1.65-1.84 (m, 4H, Men-CHH, Men-CHH, cod-CH₂), 1.96-2.05 (m, 1H, cod-CHH), 2.12-2.20 (m, 1H, cod-CHH), 2.28-2.56 (m, 5H, cod-CH₂, cod-CHH, cod-CH, Men-CHH), 3.04-3.14 (m, 1H, C(P)H), 3.91-3.97 (m, 1H, cod-CH), 4.15 (dd, $^3J_{\text{HH}} = 8.6$ Hz, $^3J_{\text{HH}} = 1.8$ Hz, 1H, CHN), 4.42 (t, $J_{\text{HH}} = 9.2$ Hz, 1H, OCH_RH_S), 4.75-4.84 (m, 2H, cod-CH, OCH_RH_S), 4.95-5.10 (m, 1H, cod-CH), 7.43-7.56 (m, 7H, Ph-CH, C(P)CHCH),

7.58 (s, 4H, BAr_F-CH), 7.60-7.65 (m, 1H, C(P)CCHCH), 7.73 (s, 8H, BAr_F-CH), 8.37 (dd, ³J_{HH} = 8.0 Hz, ⁴J_{HH} = 4.1 Hz, 1H, C(P)CCH).

¹³C{¹H}-NMR (CD₂Cl₂): δ/ppm = 15.9 (s, CH₃CHCH₃), 20.9 (s, CH₃CHCH₃), 22.1 (s, CH₃), 24.6 (s, cod-CH₂), 25.0 (d, J_{CP} = 9.7 Hz, Men-CH₂), 25.5 (s, C(CH₃)₃), 27.5 (s, cod-CH₂), 28.2 (d, ³J_{CP} = 2.6 Hz, CH₃CHCH₃), 32.6 (s, cod-CH₂), 33.3 (d, ³J_{CP} = 14.9 Hz, CHCH₃), 33.3 (d, J_{CP} = 1.1 Hz, Men-CH₂), 34.8 (s, C(CH₃)₃), 36.5 (d, J_{CP} = 4.2 Hz, cod-CH₂), 42.0 (d, J_{CP} = 6.2 Hz, Men-CH₂), 43.2 (d, ¹J_{CP} = 21.9 Hz, C(P)H), 43.4 (d, ²J_{CP} = 2.6 Hz, C(P)HCH), 64.1 (s, cod-CH), 64.7 (s, cod-CH), 69.4 (s, OCH₂), 73.5 (s, NCH), 88.5 (d, J_{CP} = 14.2 Hz, cod-CH), 93.8 (d, J_{CP} = 9.8 Hz, cod-CH), 117.0-117.2 (m, BAr_F-CH), 124.3 (q, ¹J_{CF} = 272 Hz, BAr_F-CF₃), 128.1-129.0 (m, BAr_F-C, C(P)C), 128.3 (d, J_{CP} = 9.8 Hz, Ph-CH), 128.9 (d, ¹J_{CP} = 41.4 Hz, Ph-C), 130.0 (d, ¹J_{CP} = 37.6 Hz, C(P)C), 130.9 (d, J_{CP} = 2.3 Hz, Ph-CH), 131.8 (d, ⁴J_{CP} = 2.1 Hz, C(P)CCHCH) 132.1 (d, J_{CP} = 8.8 Hz, Ph-CH), 133.1 (d, ³J_{CP} = 7.4 Hz, C(P)CCH), 133.2 (d, ³J_{CP} = 5.9 Hz, C(P)CHCH), 134.5 (s, BAr_F-CH), 136.3 (s, C(P)CH), 161.4 (q, ¹J_{BC} = 49.8 Hz, BAr_F-CB), 165.4 (d, ³J_{CP} = 5.8 Hz, NCO)

³¹P{¹H}-NMR (CD₂Cl₂): δ/ppm = 16.6 (s).

IR (KBr): $\tilde{\nu}$ /cm⁻¹ = 2965(m), 2931(m), 2891(m), 2878(m), 1609 (m), 1354(s), 1277(s), 1162(s), 1125(s), 1001(w), 971(w), 886 (m), 839(m), 744(w), 714(m), 682(m), 668(m).

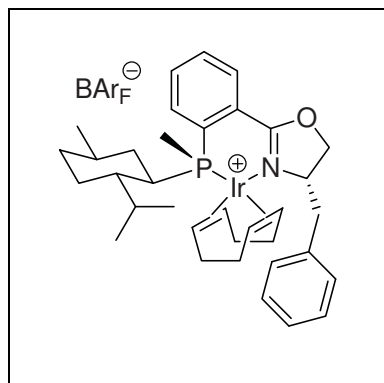
MS (ESI): *m/z* = 751(44), 750(100), 749(30), 748(63), 640(29), 638(76), 637(14), 636(47), 634(11), 632(7).

EA: calculated (%) for C₆₉H₆₄BF₂₄IrNOP: C: 51.37, H: 4.00, N: 0.87; measured: C: 51.32, H: 3.95, N: 0.75.

[α]_D²⁰ = -51 (*c* = 0.22, CHCl₃ / 0.75% EtOH).

R_f (SiO₂, hexanes:CH₂Cl₂ (1:4)): 0.78.

m.p.: 183-191 °C.



[(η^4 -1,5-Cyclooctadiene)-{(4*S*,*R*_P)-4-benzyl-2-[2'-((1*S*,2*R*,4*R*)-1-*iso*-propyl-4-methylcyclohex-2-yl)methylphosphinyl]-phenyl]-4,5-dihydrooxazole}-iridium(I)]-tetrakis[3,5-bis(trifluoromethyl)phenyl]borat (127)

The iridium-complex was prepared according to the general procedure from (*S*)-4-benzyl-2-phenyl-oxazoline (115 mg, 485 μ mol), **97** (148 mg, 614 μ mol) and MeMgBr (350 μ L, 3 M in Et₂O, 1.05 mmol) to give the title compound **127** (257 mg, 33%) as an orange foam.

C₆₇H₆₀BF₂₄IrNOP (1585.16 g/mol)

¹H-NMR (CD₂Cl₂): δ /ppm = 0.60-0.71 (m, 1H, Men-CHH), 0.70 (d, ³J_{HH} = 6.5 Hz, 3H, CHCH₃), 0.74-0.85 (m, 2H, Men-CHH, cod-CHH), 1.08 (d, ³J_{HH} = 6.7 Hz, 3H, CH₃CHCH₃), 1.12 (d, ³J_{HH} = 6.8 Hz, 3H, CH₃CHCH₃), 1.15-1.25 (m, 3H, Men-CHH, cod-CHH, C(P)HCH), 1.56 (d, ²J_{HP} = 8.4 Hz, 3H, PCH₃), 1.64-1.74 (m, 2H, cod-CHH, cod-CHH), 1.78-1.90 (m, 2H, Men-CHH, cod-CHH), 2.05-2.45 (m, 7H, Men-CH₂, C(P)H, cod-CH₂, cod-CHH, cod-CHH), 2.72-2.80 (m, 1H, CHHPh), 2.92-3.01 (m, 1H, CH₃CHCH₃), 3.49-3.55 (m, 1H, cod-CH), 3.59 (d, ²J_{HH} = 13.4 Hz, 1H, CHHPh), 3.71-3.78 (m, 1H, cod-CH), 4.46-4.53 (m, 2H, NCH_RH_SCH), 4.49-4.63 (m, 1H, NCH_RH_SCH), 4.70-4.76 (m, 1H, cod-CH), 5.10-5.17 (m, 1H, cod-CH), 7.20-7.24 (m, 2H, Ph-CH), 7.31-7.37 (m, 1H, Ph-CH), 7.37-7.42 (m, 2H, Ph-CH), 7.42-7.47 (m, 1H, C(P)CH), 7.56 (s, 4H, BAR_F-CH), 7.58-7.64 (m, 1H, C(P)CCHCH), 7.64-7.70 (m, 1H, C(P)CHCH), 7.73 (s, 8H, BAR_F-CH), 8.06 (dd, ³J_{HH} = 7.4 Hz, ⁴J_{HP} = 3.6 Hz, 1H, C(P)CCH).

¹³C{¹H}-NMR (CD₂Cl₂): δ /ppm = -3.12 (d, ¹J_{CP} = 33.8 Hz, PCH₃), 17.8 (s, CHCH₃), 21.4 (s, CH₃CHCH₃), 21.7 (s, CH₃CHCH₃), 25.2 (d, J_{CP} = 10.5 Hz, Men-CH₂), 27.5 (s, cod-CH₂), 30.4 (d, ³J_{CP} = 6.7 Hz, CH₃CHCH₃), 30.4 (s, cod-CH₂), 30.5 (d, J_{CP} = 2.2 Hz, cod-CH₂), 32.7 (d, ³J_{CP} = 8.8 Hz, CHCH₃), 33.2 (s, cod-CH₂), 34.1 (d, J_{CP} = 3.8 Hz, Men-CH₂), 36.5 (d, J_{CP} = 6.3 Hz, Men-CH₂), 41.0 (d, ¹J_{CP} = 28.1 Hz, C(P)H), 42.8 (s, C(P)HCH), 43.1 (s, CH₂Ph), 61.7 (s, cod-CH), 64.7 (s, cod-CH), 66.4 (s, NCHCH₂), 72.4 (s, NCHCH₂), 90.2 (d, J_{CP} = 12.0 Hz, cod-CH), 93.2 (d, J_{CP} = 12.2 Hz, cod-CH), 117.0-117.3 (m, BAR_F-CH), 124.3 (q, ¹J_{CF} = 272.3 Hz, BAR_F-CF₃), 127.4 (d, ²J_{CP} = 11.6 Hz, C(P)C), 127.6 (s, Ph-CH), 128.0-129.0 (m, BAR_F-C), 128.3 (s, Ph-CH), 129.1 (s, Ph-CH), 129.5 (d, ¹J_{CP} = 40.9 Hz, C(P)C), 130.6 (s, C(P)CH), 131.0 (d, ⁴J_{CP} = 1.7 Hz, C(P)CCHCH), 132.6 (d, ³J_{CP} = 7.3 Hz,

C(P)CCH), 133.6 (d, $^3J_{CP} = 6.1$ Hz, C(P)CHCH), 134.5 (s, BAr_F-CH), 161.4 (q, $^1J_{BC} = 49.8$ Hz, BAr_F-CB), 164.7 (d, $^3J_{CP} = 5.4$ Hz, NCO).

$^{31}\text{P}\{^1\text{H}\}$ -NMR (CD₂Cl₂): $\delta/\text{ppm} = 2.1$ (s).

IR (KBr): $\tilde{\nu}/\text{cm}^{-1} = 2960(\text{m}), 2929(\text{m}), 2890(\text{m}), 2875(\text{m}), 1609$ (m), 1354(s), 1277(s), 1163(s), 1124(s), 1000(w), 972(w), 886 (m), 839(m), 744(w), 713(m), 682(m), 668(m).

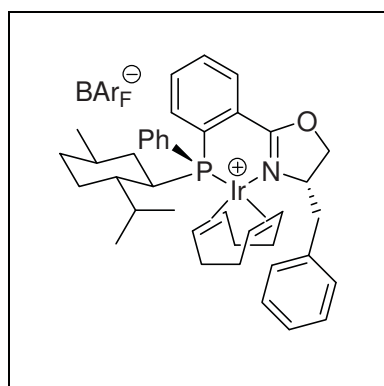
MS (ESI): $m/z(\%) = 724(5), 723(34), 722(100), 721(27), 720(60), 612(15), 611(9), 610(38), 609(9), 608(24), 606(7)$.

EA: calculated (%) for C₆₇H₆₀BF₂₄IrNOP: C: 50.77, H: 3.82, N: 0.88; measured: C: 50.85, H: 3.84, N: 0.78.

$[\alpha]_D^{20} = -114$ ($c = 0.23$, CHCl₃ / 0.75% EtOH).

R_f (SiO₂, hexanes:CH₂Cl₂ (1:4)): 0.68.

m.p.: 72-78 °C.



[(η^4 -1,5-Cyclooctadiene)-{(4*S*,*S*_P)-4-benzyl-2-[2'-((1*S*,2*R*,4*R*)-1-*iso*-propyl-4-methylcyclohex-2-yl)phenylphosphinyl]-phenyl]-4,5-dihydrooxazole}-iridium(I)]-tetrakis[3,5-bis(trifluoromethyl)phenyl]borat (128)

The iridium-complex was prepared according to the general procedure from (*S*)-4-benzyl-2-phenyl-oxazoline (112 mg, 473 μmol), **97** (170 mg, 705 μmol) and PhMgBr (1.20 mL, 1 M in THF, 1.20 mmol) to give the title compound **128** (195 mg, 25%) as a red foam.

C₇₂H₆₂BF₂₄IrNOP (1647.23 g/mol)

^1H -NMR (CD₂Cl₂): $\delta/\text{ppm} = 0.72$ (d, $^3J_{\text{HH}} = 6.8$ Hz, 3H, CH₃CHCH₃), 0.75-0.80 (m, 1H, Men-CHH), 0.78 (d, $^3J_{\text{HH}} = 6.6$ Hz, 3H, CH₃CHCH₃), 0.95 (d, $^3J_{\text{HH}} = 6.5$ Hz, 3H, CHCH₃), 1.07-1.42 (m, 5H, Men-CH₂, Men-CHH, cod-CHH, C(P)HCH), 1.45-1.80 (m, 5H, Men-CHH, Men-CHH, cod-CHH, cod-CHH, CHCH₃), 1.89-1.97 (m, 1H, CH₃CHCH₃), 2.08-2.18 (m, 2H, cod-CH, cod-CHH), 2.29-2.35 (m, 2H, cod-CH₂), 2.43-2.50 (m, 2H, cod-CH₂), 2.78-2.86 (m, 1H, CHHPh), 2.88-2.92 (m, 1H, C(P)H), 3.54 (d, $^2J_{\text{HH}} = 13.6$ Hz, 1H, CHHPh), 3.65-3.70 (m, 1H, cod-CH), 4.43 (t, $J_{\text{HH}} = 8.9$ Hz, 1H, OCH_RH_SCH), 4.54-4.61 (m, 1H, OCH₂CH), 4.64 (dd,

$^2J_{\text{HH}} = 9.3$ Hz, $^3J_{\text{HH}} = 2.8$ Hz, 1H, $\text{OCH}_R\text{H}_S\text{CH}$), 4.95-5.02 (m, 2H, cod-CH, cod-CH), 7.22 (d, $^3J_{\text{HH}} = 7.1$ Hz, 2H, $\text{CH}_2\text{Ph-CH}$), 7.32-7.37 (m, 1H, $\text{CH}_2\text{Ph-CH}$), 7.37-7.43 (m, 2H, $\text{CH}_2\text{Ph-CH}$), 7.43-7.53 (m, 5H, PPh-CH), 7.56 (s, 4H, $\text{BAr}_F\text{-CH}$), 7.60-7.65 (m, 2H, C(P)CHCH), 7.70-7.75 (m, 1H, C(P)CCHCH), 7.74 (s, 8H, $\text{BAr}_F\text{-CH}$), 8.38 (dd, $^3J_{\text{HH}} = 7.8$ Hz, $^4J_{\text{HH}} = 3.7$, 1H, C(P)CCH).

$^{13}\text{C}\{^1\text{H}\}$ -NMR (CD_2Cl_2): $\delta/\text{ppm} = 16.5$ (s, CH_3CHCH_3), 20.8 (s, CH_3CHCH_3), 22.2 (s, CHCH_3), 25.2 (d, $J_{\text{CP}} = 8.8$ Hz, Men- CH_2), 25.7 (s, cod- CH_2), 27.8 (s, cod- CH_2), 28.1 (s, CH_3CHCH_3), 29.4 (s, Men- CH_2), 32.5 (s, cod- CH_2), 33.1 (s, Men- CH_2), 33.9 (d, $^3J_{\text{CP}} = 15.8$ Hz, CHCH_3), 36.0 (d, $J_{\text{CP}} = 4.1$ Hz, cod- CH_2), 42.5 (s, CH_2Ph), 43.4 (d, $^1J_{\text{CP}} = 23.4$ Hz, C(P)H), 43.7 (d, $^2J_{\text{CP}} = 5.5$ Hz, C(P)HCH), 62.8 (s, cod-CH), 66.4 (s, NCHCH_2), 66.9 (s, cod-CH), 71.3 (s, NCHCH_2), 88.0 (d, $J_{\text{CP}} = 13.2$ Hz, cod-CH), 93.8 (d, $J_{\text{CP}} = 10.6$ Hz, cod-CH), 117.0-117.3 (m, $\text{BAr}_F\text{-CH}$), 124.3 (q, $^1J_{\text{CF}} = 272.4$ Hz, $\text{BAr}_F\text{-CF}_3$), 125.9 (d, $^1J_{\text{CP}} = 50.2$ Hz, PPh-C), 126.6 (d, $^1J_{\text{CP}} = 38.9$ Hz, C(P)C), 127.6 (s, $\text{CH}_2\text{Ph-CH}$), 128.0-129.0 (m, $\text{BAr}_F\text{-C}$), 128.2 (d, $J_{\text{CP}} = 10.0$ Hz, PPh-CH), 128.3 (s, $\text{CH}_2\text{Ph-CH}$), 129.1 (s, $\text{CH}_2\text{Ph-CH}$), 129.9 (d, $^2J_{\text{CP}} = 12.9$ Hz, C(P)C), 131.0 (d, $J_{\text{CP}} = 2.1$ Hz, PPh-CH), 131.5 (d, $J_{\text{CP}} = 8.3$ Hz, PPh-CH), 132.1 (d, $^4J_{\text{CP}} = 1.9$ Hz, C(P)CCHCH), 132.9 (d, $^3J_{\text{CP}} = 6.3$ Hz, C(P)CHCH), 133.5 (d, $^3J_{\text{CP}} = 7.7$ Hz, C(P)CCH), 134.1 (s, $\text{CH}_2\text{Ph-C}$), 134.5 ($\text{BAr}_F\text{-CH}$), 135.9 (s, C(P)CH), 161.4 (q, $^1J_{\text{BC}} = 49.9$ Hz, $\text{BAr}_F\text{-CB}$), 165.1 (d, $^3J_{\text{CP}} = 6.1$ Hz, NCO).

$^{31}\text{P}\{^1\text{H}\}$ -NMR (CD_2Cl_2): $\delta/\text{ppm} = 19.9$ (s).

IR (KBr): $\tilde{\nu}/\text{cm}^{-1} = 2961(\text{m})$, 2930(m), 2891(m), 2877(m), 1609 (m), 1354(s), 1277(s), 1163(s), 1124(s), 1000(w), 979(w), 887 (m), 839(m), 744(w), 713(m), 682(m), 668(m).

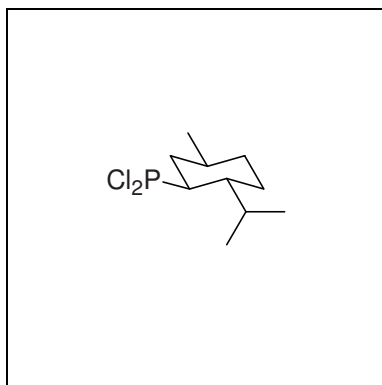
MS (ESI): $m/z(\%) = 786(7)$, 785(41), 784(100), 783(27), 782(61), 780(7), 675(5), 674(17), 673(8), 672(31), 671(6), 670(25), 668(7).

EA: calculated (%) for $\text{C}_{72}\text{H}_{62}\text{BF}_{24}\text{IrNOP}$: C: 52.50, H: 3.79, N: 0.85; measured: C: 52.13, H: 3.88, N: 0.70.

$[\alpha]_D^{20} = -138$ ($c = 0.14$, $\text{CHCl}_3 / 0.75\%$ EtOH).

R_f (SiO_2 , hexanes: CH_2Cl_2 (1:4)): 0.84.

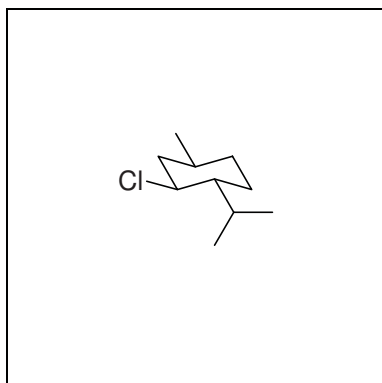
m.p.: 78-84 °C.



(1*R*,2*S*,4*S*)-2-(Dichlorophosphino)-1-isopropyl-4-methylcyclohexane (129)

In analogy to the formation of **97**, its enantiomer was prepared from **130** (4.00 g, 22.9 mmol) to give the title compound **129** (2.65 g, 48%) as a colorless liquid.

The analytical data measured were identical to **97**.



(1*R*,2*S*,4*S*)-2-Chloro-1-isopropyl-4-methylcyclohexane (130)

In analogy to the formation of **99**, its enantiomer was prepared from (+)-menthol (10.0 g, 64.0 mmol) to give the title compound **130** (6.70 g, 60%) as a colorless liquid.

The analytical data measured were identical to **99** except for the optical rotation.

$[\alpha]_D^{20} = +45.7$ ($c = 2.10$, $\text{CHCl}_3 / 0.75\%$ EtOH).

4.3.4 Preparation of Single Crystals

Complexes for X-ray studies were prepared by combining a solution of the ligand in CH_2Cl_2 (1 mL) with a solution of the metal source in CH_2Cl_2 (1 mL) at room temperature:

51: Prepared from **6** (38.0 mg, 127 μmol) and $[\text{Rh}(\text{kbd})\text{Cl}]_2$ (27.0 mg, 58.6 μmol).

52: Prepared from **6** (24.5 mg, 81.7 μmol) and $[\text{Pd}(\text{MeCN})_2\text{Cl}_2]$ (10.0 mg, 38.6 μmol).

53: Prepared **39** (38.4 mg, 103 μmol) and $[\text{Pd}(\text{MeCN})_2\text{Cl}_2]$ (13.0 mg, 50.2 μmol).

54: Prepared from **6** (16.0 mg, 53.3 μmol) and $[\text{Rh}(\text{kbd})_2]\text{BF}_4$ (9.50 mg, 25.4 μmol).

55: Prepared from **40** (24.0 mg, 49.6 μmol) and $[\text{Rh}(\text{kbd})\text{Cl}]_2$ (11.0 mg, 47.7 μmol).

56: Prepared from **40** (24.3 mg, 50.2 μmol) and $[\text{Pd}(\text{MeCN})_2\text{Cl}_2]$ (13.0 mg, 50.2 μmol).

Single crystals of the complexes **51**, **52**, **53**, **54**, **55**, **56**, **69**, **70**, **71**, **75**, **123**, **124**, **125** and **126** could be grown by slow diffusion of hexane into a solution of the corresponding complex in CH_2Cl_2 carried out in a closed NMR-tube.

In case of the ferrocenephospholanes **6**, **40**, **42** and **43** single crystals were obtained by recrystallization from hot methanol.

4.3.5 Procedure for the Competition Experiments

In a NMR-tube $[\text{M}(\text{diene})\text{Cl}]_2$ (2 μmol) and **40** (4 μmol) were dissolved in CD_3OD or CD_2Cl_2 (0.5 mL). In the case of CD_3OD sonication was needed to achieve dissolution. After 15 minutes NMR-spectra were recorded and the second portion of $[\text{M}(\text{diene})\text{Cl}]_2$ (2 μmol) was added. After additional 15 minutes the obtained solution was analyzed by NMR-spectroscopy and ESI-MS.

4.3.6 Hydrogenation Procedures

4.3.6.1 Automated Parallel Hydrogenations (SYMYX)

The experiments were performed at Solvias AG in Basel.

The preparation of the reactions was carried out in a glove box under inert atmosphere. The catalyst precursors were prepared *in situ* by mixing 1,2-dichloroethane solutions of the ligands with ethanol solutions of the metal sources. After stirring for 10 minutes, the solvent was evaporated to dryness under reduced pressure. The solvent of choice was added and the solution distributed to the vials (1.2 mL) via a robotic cannula. The substrate solution in the same solvent was added to the vials resulting in a final volume of approximately 0.5 mL. The vials were placed in a heated orbital shaker, set under 1 bar of hydrogen and shaken for the required time at room temperature. The reaction mixtures were analyzed by chiral GC (Lipodex E and Chirasil-L-val).

4.3.6.2 Hydrogenations with Iridium-Complexes

For the hydrogenation experiments the solvents were degassed prior to use by three freeze-pump-thaw cycles. In the cases of dichloromethane and 1,2-dichloroethane the solvents were stored over aluminium oxide and filtered through a syringe filter before usage.

Procedure for the hydrogenation at elevated pressure:

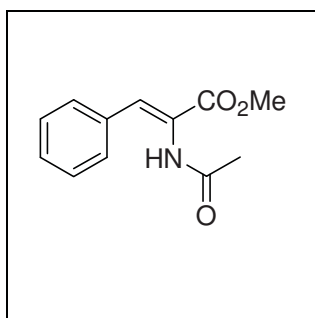
The preparation of the reactions was carried out in a glove box under inert atmosphere. The substrate (100 μmol) and the catalyst (1 μmol or 0.5 μmol) were dissolved in the appropriate solvent (1 mL) and the solution was filled into glass vials (2 mL) containing stirring bars. Up to four vials were placed in an autoclave (60 mL) which was closed in the glove box. The autoclave was pressurized with H_2 and placed on a stirring plate for the time indicated. After pressure release the solvent was evaporated under a stream of nitrogen. The residue was filtered over a short pad of SiO_2 eluting with heptane/ Et_2O (1:1) and the filtrate was analyzed by GC and HPLC.

Procedure for the hydrogenation at ambient pressure:

The preparation of the reactions was carried out in a glove box under inert atmosphere. The substrate (100 μmol) and the catalyst (1 μmol) were dissolved in the appropriate solvent (1 mL) and the solution was filled into glass vials (2 mL) containing stirring bars. The vials were placed in a flask equipped with a 24/40 joint which was closed in the glove box with a rubber septum. A H_2 -filled balloon equipped with a needle was put on the septum, the flask was flushed with H_2 by pulling vacuum and placed on a stirring plate for the time indicated. After removal of the septum the solvent was evaporated under a stream of nitrogen. The residue was filtered over a short plug of SiO_2 eluting with heptane/ Et_2O (1:1) and the filtrate was analyzed by GC and HPLC.

For reactions at elevated or low temperature the flask containing the reaction vials was immersed in an oil or cooling bath for 30 minutes prior to the exposure to hydrogen. Reactions above room temperature were conducted in 1,2-dichloroethane.

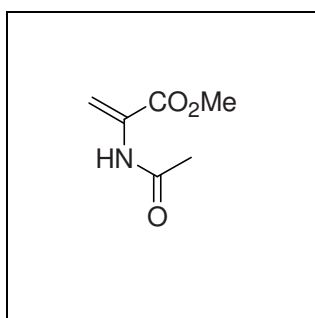
4.3.6.3 Analytical Data of Hydrogenation Substrates



Methyl 2-acetamidocinnamate (**59**):

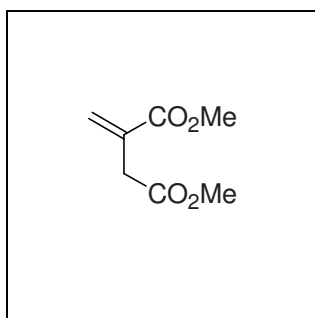
GC (Restek Rtx-1701 (30 m × 0.25 mm × 0.25 μm), 60 kPa He, (100 °C - 2 min - 7 K/min - 250 °C - 10 min)): t_R = 23.8 min (H₂-**59**), 27.3 min (**59**).

HPLC (Daicel Chiracel OD-H, (2.6×250 mm), heptane/*iso*-propanol = 90:10, 0.5 mL/min, 20 °C, 215 nm): t_R = 21.1 min ((*R*)-H₂-**59**), 28.6 min ((*S*)-H₂-**59**).



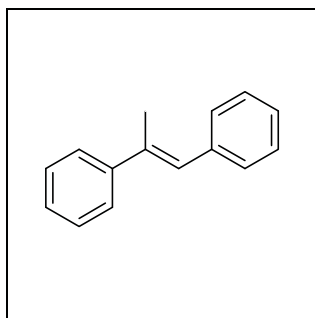
Methyl 2-acetamidoacrylate (**62**):

GC (Brechtbühler β-cyclodextrin DEtTButSil (SE54) (25 m × 0.25 mm × 0.25 μm), 60 kPa H₂, (90 °C - 20 min - 30 K/min - 180 °C - 10 min)): t_R = 12.2 min (**62**), 13.6 min ((*S*)-H₂-**62**), 17.6 min ((*R*)-H₂-**62**).



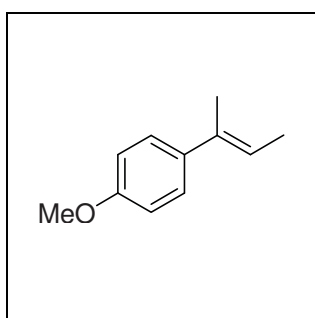
Dimethyl itaconate (**63**):

GC (Chiraldex γ-cyclodextrin TFA G-TA (30 m × 0.25 mm × 0.12 μm), 60 kPa H₂, (80 °C - 20 min - 30 K/min - 160 °C - 10 min)): t_R = 21.7 min ((*R*)-H₂-**63**), 22.4 min ((*S*)-H₂-**63**), 24.4 min (**63**).

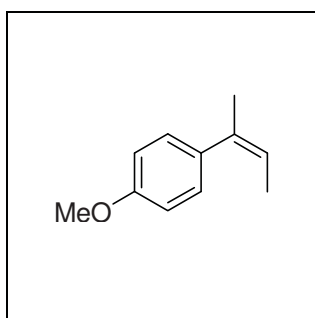
*E*-1,2-Diphenylpropene (**131**):

GC (Restek Rtx-1701 (30 m × 0.25 mm × 0.25 μm), 60 kPa He, (100 °C - 2 min - 7 K/min - 250 °C - 10 min)): t_R = 18.2 min (H₂-**131**), 21.4 min (**131**).

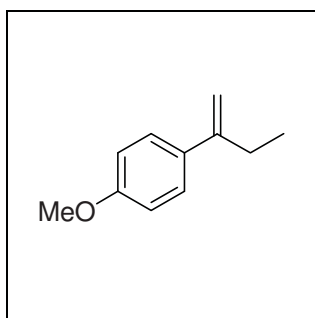
HPLC (Daicel Chiracel OJ, (2.6×250 mm), heptane/*iso*-propanol = 99:1, 0.5 mL/min, 20 °C, 220 nm): t_R = 15.6 min ((*R*)-H₂-**131**), 23.8 min ((*S*)-H₂-**131**).

*E*-2-(4-Methoxyphenyl)-2-butene (**132**):

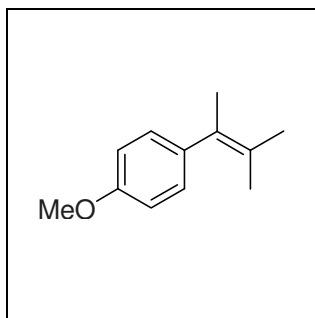
GC (*Chiral*dex γ-cyclodextrin TFA G-TA (30 m × 0.25 mm × 0.12 μm), 60 kPa H₂, (60 °C - 30 min - 5 K/min - 100 °C - 20 K/min - 160 °C - 10 min)): t_R = 38.4 min ((*S*)-H₂-**132**), 38.6 min ((*R*)-H₂-**132**), 41.2 min (**132**).

*Z*-2-(4-Methoxyphenyl)-2-butene (**133**):

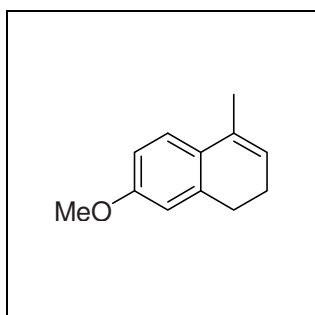
GC (*Chiral*dex γ-cyclodextrin TFA G-TA (30 m × 0.25 mm × 0.12 μm), 60 kPa H₂, (60 °C - 30 min - 5 K/min - 100 °C - 20 K/min - 160 °C - 10 min)): t_R = 38.4 min ((*S*)-H₂-**133**), 38.6 min ((*R*)-H₂-**133**), 39.3 min (**133**).

2-(4-Methoxyphenyl)-1-butene (**134**):

GC (*Chiral*dex γ-cyclodextrin TFA G-TA (30 m × 0.25 mm × 0.12 μm), 60 kPa H₂, (60 °C - 30 min - 5 K/min - 100 °C - 20 K/min - 160 °C - 10 min)): t_R = 38.4 min ((*S*)-H₂-**134**), 38.6 min ((*R*)-H₂-**134**), 40.3 min (**134**).

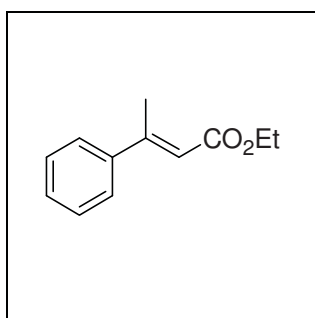
2-(4-Methoxyphenyl)-3-methyl-2-butene (**135**):

GC (*Brechbühler* β -cyclodextrin DEtTButSil (SE54) (25 m \times 0.25 mm \times 0.25 μ m), 60 kPa H₂, (80 °C - 1 K/min - 110 °C - 10 K/min - 160 °C - 2 min)): t_R = 20.9 min ((+)-H₂-**135**), 21.8 min ((-)-H₂-**135**), 25.1 min (**135**).

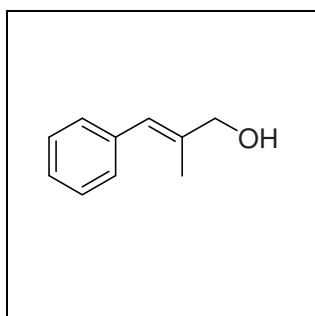
7-Methoxy-4-methyl-1,2-dihydro-naphthalene (**136**):

GC (Restek Rtx-1701 (30 m \times 0.25 mm \times 0.25 μ m), 60 kPa He, (100 °C - 2 min - 7 K/min - 250 °C - 10 min)): t_R = 17.0 min (H₂-**136**), 19.7 min (**136**).

HPLC (Daicel Chiracel OD-H, (2.6 \times 250 mm), heptane, 0.5 mL/min, 20 °C, 215 nm): t_R = 20.4 min ((*R*)-H₂-**136**), 27.0 min ((*S*)-H₂-**136**).

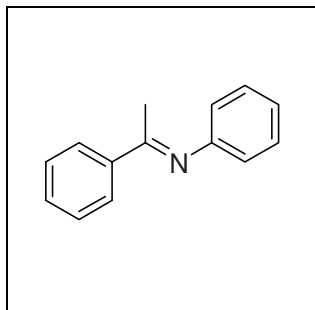
Ethyl *E*-2-methylcinnamate (**74**):

GC (*Chiraldex* γ -cyclodextrin TFA G-TA (30 m \times 0.25 mm \times 0.12 μ m), 60 kPa H₂, (85 °C - 50 min - 10 K/min - 160 °C)): t_R = 42.9 min ((*R*)-H₂-**74**), 44.9 min ((*S*)-H₂-**74**), 57.0 min (**74**).

*E*-2-Methyl-3-phenylprop-2-enol (**73**):

GC (Restek Rtx-1701 (30 m \times 0.25 mm \times 0.25 μ m), 60 kPa He, (100 °C - 2 min - 7 K/min - 250 °C - 10 min)): t_R = 14.6 min (H₂-**73**), 16.5 min (**73**).

HPLC (Daicel Chiracel OD-H, (2.6×250 mm), heptane/*iso*-propanol = 95:5, 0.5 mL/min, 40 °C, 200 nm): t_R = 15.3 min ((+)-H₂-**73**), 17.5 min ((-)-H₂-**73**).



E-Phenyl-(1-phenylethylidene)amine (**137**):

GC (Macherey-Nagel Optima 5-Amin (30 m × 0.25 mm × 0.5 μm), 60 kPa He, (150 °C - 7 K/min - 250 °C - 10 min)): t_R = 12.8 min (H₂-**137**), 13.2 min (**137**).

HPLC (Daicel Chiracel OD-H, (2.6×250 mm), heptane/*iso*-propanol = 99:1, 0.5 mL/min, 20 °C, 210 nm): t_R = 24.6 min ((*S*)-H₂-**137**), 33.0 min ((*R*)-H₂-**137**).

4.4 References

- [1] J. W. Han, N. Tokunaga, T. Hayashi, *Helv. Chim. Acta* **2002**, *85*, 3848-3854.
- [2] a) B. T. Hahn, K. Schwekendiek, F. Glorius, B. Gschwend, A. Pfaltz. *Org. Synth.* **2008**, *85*, 267-277; b) M. R. Krout, J. T. Mohr, B. M. Stoltz, A. Schumacher, A. Pfaltz, *Org. Synth.* **2009**, *86*, 181-193.
- [3] S. Demay, M. Lotz, K. Polborn, P. Knochel, *Tetrahedron: Asymmetry* **2001**, *12*, 909-914.
- [4] A.-E. Wang, J.-H. Xie, L.-X. Wang, Q.-L. Zhou, *Tetrahedron* **2005**, *61*, 259-266.
- [5] M. Hidai, H. Mizuta, H. Yagi, Y. Nagai, K. Hata, Y. Uccida, *J. Organomet. Chem.* **1982**, *232*, 89-98.
- [6] J. G. Smith, G. F. Wright, *J. Org. Chem.* **1952**, *17*, 1116-1121.
- [7] R. Krishnamurti, H. G. Kuivila, *J. Org. Chem.* **1986**, *51*, 4947-4953.
- [8] P. G. Chantrell, C. A. Pearce, C. R. Toyer, R. Twaits, *J. Appl. Chem.* **1964**, *14*, 563.

Chapter 5

Appendix

5.1 Crystallographic Data

The X-ray structures were measured by Mr. Markus Neuburger (Department of Chemistry, University of Basel) on a Nonius KappaCCD diffractometer, solved using direct methods (SIR92^[1]) and refined with Crystals^[2] by Mr. Markus Neuburger, Dr. Silvia Schaffner and Mr. Marcus Schrems (Department of Chemistry, University of Basel). Hydrogen atoms were added geometrically.

	6	40
formula	C ₁₆ H ₂₁ Fe ₁ P ₁	C ₂₈ H ₃₀ Fe ₁ P ₂
M _r [g mol ⁻¹]	300.16	484.34
shape	plate	plate
color	orange	dark orange
crystal system	orthorhombic	monoclinic
space group	P 2 ₁ 2 ₁ 2 ₁	P 2 ₁
crystal size [mm ³]	0.05 · 0.10 · 0.20	0.08 · 0.12 · 0.16
<i>a</i> [Å]	6.3275(1)	10.5728(1)
<i>b</i> [Å]	10.4666(1)	19.8434(2)
<i>c</i> [Å]	22.1949(3)	11.7855(1)
α [°]	90	90
β [°]	90	99.0002(6)
γ [°]	90	90
<i>V</i> [Å ³]	1469.91(3)	2442.16(4)
<i>Z</i>	4	4
<i>F</i> (000)	632	1016
Θ range for data collection [°]	1.835-30.021	1.749-30.036
ρ_{calcd} [g cm ⁻³]	1.356	1.317
absorption coeff. μ [mm ⁻¹]	1.115	0.762
measured reflections	15358	28272
independent reflections	4296 (merging <i>r</i> = 0.045)	14289 (merging <i>r</i> = 0.049)
used reflections ^[b]	2985	9729
parameters refined	164	560
<i>R</i> ^[c]	0.0274	0.0307
<i>R</i> _w ^[d]	0.0316	0.0645
goodness of fit	0.9429	0.9479

[a] All data were collected using Mo *K*_α ($\lambda = 0.71073$ Å) at 173 K. [b] Observation criterion: $I > 3\sigma(I)$. [c] $R = \sum |F_0| - |F_C| / \sum |F_0|$. [d] $R_w = \{\sum [w(F_0 - F_C)^2] / \sum [w(F_0)^2]\}^{1/2}$.

	42	43
formula	C ₂₈ H ₄₂ Fe ₁ P ₂	C ₃₈ H ₅₆ Fe ₂ P ₂ Si ₂
M _r [g mol ⁻¹]	496.44	742.68
shape	plate	plate
color	orange	dark orange
crystal system	orthorhombic	orthorhombic
space group	P 2 ₁ 2 ₁ 2 ₁	P 2 ₁ 2 ₁ 2 ₁
crystal size [mm ³]	0.07 · 0.10 · 0.20	0.12 · 0.21 · 0.30
<i>a</i> [Å]	11.12420(10)	11.68110(10)
<i>b</i> [Å]	11.83570(10)	15.08110(10)
<i>c</i> [Å]	19.5664(2)	22.0190(2)
α [°]	90	90
β [°]	90	90
γ [°]	90	90
<i>V</i> [Å ³]	2576.17(4)	3878.95(5)
<i>Z</i>	4	4
<i>F</i> (000)	1064	1576
θ range for data collection [°]	2.011-27.883	1.637-30.056
ρ_{calcd} [g cm ⁻³]	1.280	1.272
absorption coeff. μ [mm ⁻¹]	0.723	0.917
measured reflections	21963	39326
independent reflections	6144 (merging <i>r</i> = 0.038)	11351 (merging <i>r</i> = 0.072)
used reflections ^[b]	5259	8347
parameters refined	281	398
<i>R</i> ^[c]	0.0244	0.0265
<i>R</i> _w ^[d]	0.0313	0.0339
goodness of fit	0.9848	0.9390

[a] All data were collected using Mo *K*_α ($\lambda = 0.71073$ Å) at 173 K. [b] Observation criterion: $I > 3\sigma(I)$. [c] $R = \sum ||F_0| - |F_C|| / \sum |F_0|$. [d] $R_w = \{\sum [w(F_0 - F_C)^2] / \sum [w(F_0)^2]\}^{1/2}$.

	51	52
formula	C ₂₃ H ₂₉ Cl ₁ Fe ₁ P ₁ Rh ₁	C ₃₂ H ₄₂ Cl ₂ Fe ₂ P ₂ Pd ₁
M _r [g mol ⁻¹]	530.66	777.63
shape	plate	block
color	orange	orange
crystal system	monoclinic	monoclinic
space group	P 2 ₁	P 2 ₁
crystal size [mm ³]	0.11 · 0.20 · 0.24	0.15 · 0.18 · 0.21
<i>a</i> [Å]	8.4986(1)	7.9017(1)
<i>b</i> [Å]	23.7259(3)	11.1250(1)
<i>c</i> [Å]	10.8182(1)	18.4013(2)
α [°]	90	90
β [°]	100.8041(6)	102.6517(8)
γ [°]	90	90
<i>V</i> [Å ³]	2142.68(4)	1578.32(3)
<i>Z</i>	4	2
<i>F</i> (000)	1080	792
θ range for data collection [°]	1.717-30.034	1.134-30.026
ρ_{calcd} [g cm ⁻³]	1.645	1.636
absorption coeff. μ [mm ⁻¹]	1.652	1.763
measured reflections	24770	13303
independent reflections	12503 (merging $r = 0.049$)	8293 (merging $r = 0.034$)
used reflections ^[b]	10475	7544
parameters refined	489	353
$R^{[c]}$	0.0268	0.0296
$R_w^{[d]}$	0.0472	0.0387
goodness of fit	0.9833	0.9913

[a] All data were collected using Mo K_α ($\lambda = 0.71073$ Å) at 173 K. [b] Observation criterion: $I > 3\sigma(I)$. [c] $R = \sum ||F_o| - |F_c|| / \sum |F_o|$. [d] $R_w = \{\sum [w(F_o - F_c)^2] / \sum [w(F_o)^2]\}^{1/2}$.

	53	54
formula	C ₃₈ H ₅₈ Cl ₂ Fe ₂ P ₂ Pd ₁ Si ₂	C ₄₀ H _{51.50} B ₁ Cl ₂ F ₄ Fe ₂ P ₂ Rh ₁
M _r [g mol ⁻¹]	922.00	966.60
shape	plate	plate
color	red	orange
crystal system	triclinic	monoclinic
space group	P 1	P 1 2 ₁ 1
crystal size [mm ³]	0.08 · 0.16 · 0.18	0.09 · 0.17 · 0.50
<i>a</i> [Å]	9.2341(5)	10.1472(2)
<i>b</i> [Å]	13.4290(2)	20.6777(3)
<i>c</i> [Å]	18.0505(5)	19.7484(2)
α [°]	97.53	90
β [°]	90	101.5094(9)
γ [°]	110.11	90
<i>V</i> [Å ³]	2081.32(13)	4060.30(11)
<i>Z</i>	2	4
<i>F</i> (000)	952	1974
θ range for data collection [°]	1.139-27.432	1.052-27.866
ρ_{calcd} [g cm ⁻³]	1.471	1.581
absorption coeff. μ [mm ⁻¹]	1.404	1.365
measured reflections	18262	34937
independent reflections	18262 (merging <i>r</i> = 0.000)	19310 (merging <i>r</i> = 0.055)
used reflections ^[b]	10958	10723
parameters refined	848	938
<i>R</i> ^[c]	0.0471	0.0384
<i>R</i> _w ^[d]	0.0824	0.0878
goodness of fit	1.1063	1.0007

[a] All data were collected using Mo *K*_α ($\lambda = 0.71073$ Å) at 173 K. [b] Observation criterion: $I > 3\sigma(I)$. [c] $R = \sum ||F_0| - |F_C|| / \sum |F_0|$. [d] $R_w = \{\sum [w(F_0 - F_C)^2] / \sum [w(F_0)^2]\}^{1/2}$.

	55	56
formula	C ₃₈ H ₃₈ Cl ₁ Fe ₁ P ₂ Rh ₁	C ₂₈ H ₃₀ Cl ₂ Fe ₁ P ₂ Pd ₁
M _r [g mol ⁻¹]	750.87	661.65
shape	plate	plate
color	orange	red
crystal system	monoclinic	triclinic
space group	P 2 ₁	P 1
crystal size [mm ³]	0.02 · 0.16 · 0.27	0.14 · 0.20 · 0.22
<i>a</i> [Å]	12.5733(3)	10.0875(2)
<i>b</i> [Å]	10.9522(3)	10.4665(2)
<i>c</i> [Å]	13.2138(3)	13.1753(2)
α [°]	90	86.7786(10)
β [°]	95.7859(16)	84.1075(11)
γ [°]	90	80.2617(11)
<i>V</i> [Å ³]	1810.34(8)	1362.70(4)
<i>Z</i>	2	2
<i>F</i> (000)	768	668
θ range for data collection [°]	1.549-27.844	1.555-27.885
ρ_{calcd} [g cm ⁻³]	1.377	1.612
absorption coeff. μ [mm ⁻¹]	1.043	1.521
measured reflections	16599	12548
independent reflections	8592 (merging <i>r</i> = 0.057)	12547 (merging <i>r</i> = 0.000)
used reflections ^[b]	4722	10107
parameters refined	400	614
<i>R</i> ^[c]	0.0341	0.0357
<i>R</i> _w ^[d]	0.0786	0.0521
goodness of fit	0.8841	1.0726

[a] All data were collected using Mo *K*_α ($\lambda = 0.71073$ Å) at 173 K. [b] Observation criterion: $I > 3\sigma(I)$. [c] $R = \sum ||F_0| - |F_C|| / \sum |F_0|$. [d] $R_w = \{\sum [w(F_0 - F_C)^2] / \sum [w(F_0)^2]\}^{1/2}$.

	69	70
formula	C ₆₉ H ₅₆ B ₁ Cl ₂ F ₂₄ Fe ₁ Ir ₁ P ₂	C ₇₃ H ₆₅ B ₁ F ₂₄ Fe ₁ Ir ₁ P ₂
M _r [g mol ⁻¹]	1732.89	1719.10
shape	plate	plate
color	red	orange
crystal system	monoclinic	monoclinic
space group	C 2	C 2
crystal size [mm ³]	0.04 · 0.11 · 0.39	0.04 · 0.21 · 0.40
<i>a</i> [Å]	18.4962(13)	19.0162(9)
<i>b</i> [Å]	18.6257(14)	18.5566(9)
<i>c</i> [Å]	19.6713(15)	19.7120(7)
α [°]	90	90
β [°]	92.364(3)	93.7050(10)
γ [°]	90	90
<i>V</i> [Å ³]	6771.1(9)	6941.4(5)
<i>Z</i>	4	4
<i>F</i> (000)	3432	3428
Θ range for data collection [°]	1.841-37.656	2.071-26.401
ρ_{calcd} [g cm ⁻³]	1.700	1.645
absorption coeff. μ [mm ⁻¹]	2.412	2.278
measured reflections	159022	21656
independent reflections	35202 (merging <i>r</i> = 0.041)	12318 (merging <i>r</i> = 0.038)
used reflections ^[b]	29945	10266
parameters refined	956	1001
<i>R</i> ^[c]	0.0324	0.0366
<i>R</i> _w ^[d]	0.0410	0.0520
goodness of fit	1.1158	1.1134

[a] All data were collected using Mo *K*_α ($\lambda = 0.71073$ Å) at 173 K. [b] Observation criterion: $I > 3\sigma(I)$. [c] $R = \sum ||F_0| - |F_C|| / \sum |F_0|$. [d] $R_w = \{\sum [w(F_0 - F_C)^2] / \sum [w(F_0)^2]\}^{1/2}$.

	71	75
formula	C ₆₈ H ₆₆ B ₁ F ₂₄ Fe ₁ Ir ₁ P ₂	C ₆₁ H ₅₀ B ₁ F ₂₄ Fe ₁ Ir ₁ N ₁ P ₁
M _r [g mol ⁻¹]	1660.05	1542.88
shape	block	block
color	red	red
crystal system	orthorhombic	triclinic
space group	P 2 ₁ 2 ₁ 2 ₁	P 1
crystal size [mm ³]	0.08 · 0.15 · 0.34	0.10 · 0.10 · 0.10
<i>a</i> [Å]	14.2169(3)	12.52820(10)
<i>b</i> [Å]	19.4540(4)	12.7268(2)
<i>c</i> [Å]	24.2927(5)	19.5631(3)
α [°]	90	97.0960(8)
β [°]	90	103.5043(8)
γ [°]	90	94.9326(8)
<i>V</i> [Å ³]	6718.8(2)	2988.36(7)
<i>Z</i>	4	2
<i>F</i> (000)	3312	1524
θ range for data collection [°]	1.660-34.971	2.953-27.909
ρ_{calcd} [g cm ⁻³]	1.641	1.715
absorption coeff. μ [mm ⁻¹]	2.350	2.610
measured reflections	246150	27022
independent reflections	29300 (merging <i>r</i> = 0.029)	27021 (merging <i>r</i> = 0.000)
used reflections ^[b]	26362	19391
parameters refined	974	1785
<i>R</i> ^[c]	0.0185	0.0434
<i>R</i> _w ^[d]	0.0258	0.0709
goodness of fit	1.1369	1.1315

[a] All data were collected using Mo *K*_α ($\lambda = 0.71073$ Å) at 173 K. [b] Observation criterion: $I > 3\sigma(I)$. [c] $R = \sum ||F_0| - |F_C|| / \sum |F_0|$. [d] $R_w = \{\sum [w(F_0 - F_C)^2] / \sum [w(F_0)^2]\}^{1/2}$.

	123	124
formula	C ₁₂₉ H ₁₂₆ B ₂ Cl ₆ F ₄₈ Ir ₂ N ₂ O ₂ P ₂	C ₆₈ H ₆₂ B ₁ F ₂₄ Ir ₁ N ₁ O ₁ P ₁
M _r [g mol ⁻¹]	3329.06	1599.20
shape	block	plate
color	red	red
crystal system	monoclinic	monoclinic
space group	P 2 ₁	P 2 ₁
crystal size [mm ³]	0.09 · 0.17 · 0.26	0.06 · 0.24 · 0.34
<i>a</i> [Å]	12.9688(8)	19.2425(4)
<i>b</i> [Å]	39.628(2)	13.0002(3)
<i>c</i> [Å]	13.2726(8)	26.8992(5)
α [°]	90	90
β [°]	99.048(3)	91.2820(10)
γ [°]	90	90
<i>V</i> [Å ³]	6736.3(7)	6727.3(2)
<i>Z</i>	2	4
<i>F</i> (000)	3316	3192
Θ range for data collection [°]	1.554-33.914	3.232-31.507
ρ_{calcd} [g cm ⁻³]	1.641	1.579
absorption coeff. μ [mm ⁻¹]	2.234	2.118
measured reflections	187781	115778
independent reflections	53195 (merging $r = 0.029$)	43410 (merging $r = 0.030$)
used reflections ^[b]	46913	37513
parameters refined	1874	1802
$R^{[c]}$	0.0355	0.0404
$R_w^{[d]}$	0.0340	0.0460
goodness of fit	1.1016	1.1187

[a] All data were collected using Mo K_α ($\lambda = 0.71073$ Å) at 173 K. [b] Observation criterion: $I > 3\sigma(I)$. [c] $R = \sum ||F_0| - |F_C|| / \sum |F_0|$. [d] $R_w = \{\sum [w(F_0 - F_C)^2] / \sum [w(F_0)^2]\}^{1/2}$.

	125	126
formula	C ₆₄ H ₆₂ B ₁ F ₂₄ Ir ₁ N ₁ O ₁ P ₁	C ₆₉ H ₆₄ B ₁ F ₂₄ Ir ₁ N ₁ O ₁ P ₁
M _r [g mol ⁻¹]	1551.16	1613.23
shape	plate	plate
color	orange	red
crystal system	triclinic	triclinic
space group	P 1	P 1
crystal size [mm ³]	0.07 · 0.13 · 0.26	0.09 · 0.21 · 0.23
<i>a</i> [Å]	12.9614(8)	12.7767(3)
<i>b</i> [Å]	18.9983(11)	13.6956(3)
<i>c</i> [Å]	26.1691(14)	19.7389(4)
α [°]	94.425(3)	77.4150(10)
β [°]	95.517(3)	88.7350(10)
γ [°]	90.862(3)	88.3570(10)
<i>V</i> [Å ³]	6393.4(6)	3369.19(13)
<i>Z</i>	4	2
<i>F</i> (000)	3096	1612
θ range for data collection [°]	1.568-38.568	1.595-28.326
ρ_{calcd} [g cm ⁻³]	1.611	1.590
absorption coeff. μ [mm ⁻¹]	2.226	2.116
measured reflections	686797	110973
independent reflections	141167 (merging <i>r</i> = 0.053)	33288 (merging <i>r</i> = 0.031)
used reflections ^[b]	100015	29238
parameters refined	3350	1874
<i>R</i> ^[c]	0.0306	0.0229
<i>R</i> _w ^[d]	0.0516	0.0296
goodness of fit	1.1361	1.1234

[a] All data were collected using Mo *K*_α ($\lambda = 0.71073$ Å) at 173 K. [b] Observation criterion: $I > 3\sigma(I)$. [c] $R = \sum ||F_0| - |F_C|| / \sum |F_0|$. [d] $R_w = \{\sum [w(F_0 - F_C)^2] / \sum [w(F_0)^2]\}^{1/2}$.

5.2 List of Abbreviations

9-BBN	9-borabicyclo[3.3.1]nonane
Ac	acetyl
acac	acetylacetonate
aq.	aqueous
Ar	aryl
B3LYP	Becke, three-parameter, Lee-Yang-Parr exchange correlation functional
BA _{rF}	tetrakis[3,5-bis(trifluoromethyl)phenyl]borat
Bn	benzyl, phenylmethyl
br	broad
Bu	butyl
bnz	benzonitrile
<i>c</i>	concentration
cat	catalyst
cod	1,5-cyclooctadiene
conc.	concentration
conv.	conversion
COSY	Homonuclear Correlation Spectroscopy
Cp	cyclopentadienyl
Cy	cyclohexyl
d	doublet
δ	chemical shift (NMR)
dabco	1,4-diazabicyclo[2.2.2]octane
DBU	1,8-diazabicyclo[5.4.0]undec-7-ene
DCE	1,2-dichloroethane
DEPT	Distorsionless Enhancement by Polarisation Transfer
DFT	Density Functional Theory
DIBALH	di- <i>iso</i> -butylaluminium hydride
DMF	<i>N,N</i> -dimethyl formamide
dr	diastereoisomeric ratio
E	electrophile
EA	elemental analysis

<i>ee</i>	enantiomeric excess
EI	Electron-impact Ionization
Et	ethyl
equiv.	equivalent(s)
EWG	Electron Withdrawing Group
ESI-MS	Electron Spray Ionization Mass Spectrometry
FAB	Fast Electron Bombardment
GC	gas chromatography
h	hour(s)
HMBC	Heteronuclear Multiple Bond Correlation
HMQC	Heteronuclear Multiple Quantum Coherence
HOESY	Heteronuclear Overhauser Effect Spectroscopy
HPLC	High Performance Liquid Chromatography
Hz	hertz
<i>i</i>	<i>iso</i>
IR	Infrared Spectroscopy
<i>J</i>	coupling constant
LA	Lewis acid
LDA	lithium di- <i>iso</i> -propylamide
LG	leaving group
m	multiplet (NMR), medium (IR)
M	molarity, mol/L
Me	methyl
Men	menthyl
mL	mililiter
min	minutes
m.p.	melting point
MS	Mass Spectrometry
Ms	mesyl, methanesulfonyl
<i>m/z</i>	mass-to-charge ratio
nbd	norbornadiene
n.d.	not determined
NBS	<i>N</i> -bromo-succinimide
NMR	Nuclear Magnetic Resonance

NOESY	Nuclear Overhauser Enhancement Spectroscopy
Nu	nucleophile
O	oxidant
<i>o</i> Tol	<i>ortho</i> -tolyl
Ox	oxazoline
Ph	phenyl
PHIP	<i>para</i> -Hydrogen Induced Polarization
PHOX	phosphino-oxazoline
PGSE	Pulse Gradient Spin-Echo
ppm	parts per million
Pr	propyl
Py	pyridine
q	quartet
quant.	quantitative
quin	quintet
rac.	racemic
Red-Al	sodium bis(2-methoxyethoxy)aluminium hydride
R_f	retention factor
rt	room temperature
S	solvent
s	singlet (NMR), strong (IR)
sat.	saturated
s/c	substrate to catalyst ratio
<i>sec</i>	secondary
sep	septet
S_N1	unimolecular nucleophilic substitution
S_N2	bimolecular nucleophilic substitution
SPO	secondary phosphine oxide(s)
t	triplet
TBAF	tetrabutylammonium fluoride
TBD	1,5,7-triazabicyclo[4.4.0]dec-5-ene
TBME	<i>tert</i> -butyl methyl ether
<i>t</i> Bu	<i>tert</i> -butyl, 2-methyl-2-propyl
TCT	2,4,6-trichloro[1,3,5]triazine

<i>tert</i>	tertiary
THF	tetrahydrofuran
TLC	Thin Layer Chromatography
TFA	trifluoroacetate
TMEDA	<i>N,N,N',N'</i> -tetramethylethylenediamine
TMP	2,2,6,6-tetramethylpiperidide
TMS	tetramethylsilyl
TOF	Turn Over Frequenzy
Tol	toluene
t_R	retention time
Ts	tosyl, 4-toluenesulfonyl
VSEPR	Valence Shell Electron Pair Repulsion
w	weak

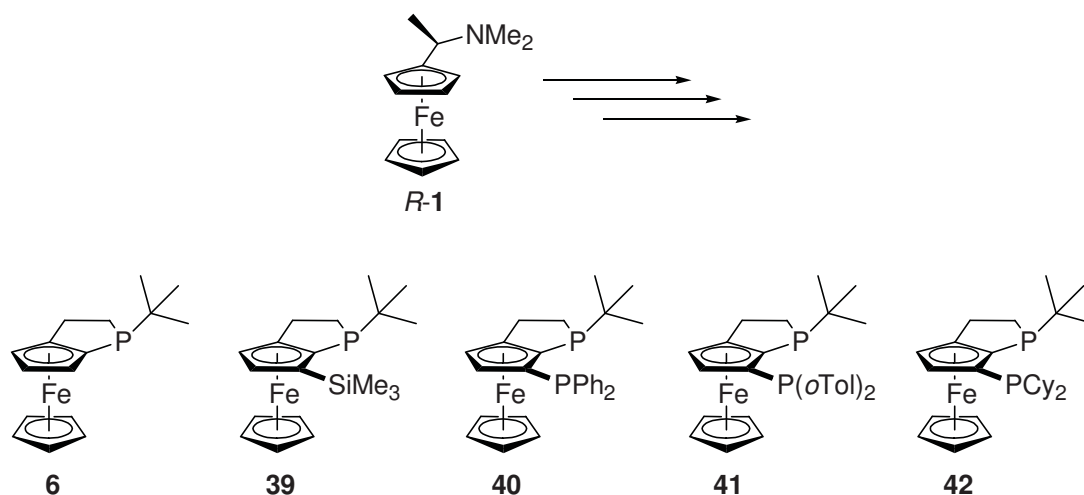
5.3 References

- [1] A. Altomare, G. Cascarno, C. Giacovazzo, A. Guagliardi, *J. Appl. Crystallogr.* **1993**, 26, 343.
- [2] D. Watkin, R. Cooper, C. K. Prout, *Z. Kristallogr.* **2002**, 217, 429.

Chapter 6

Summary

A stereoselective synthesis of P-chiral ferrocenephospholanes (**6**, **43**, **40**, **41**, **42**) was developed starting from *Ugi*'s amine (**1**) (Scheme 6.1). Diastereoselective *ortho*-lithiation and a base-induced stereoconvergent intramolecular hydrophosphination were the key steps in the synthetic pathway.



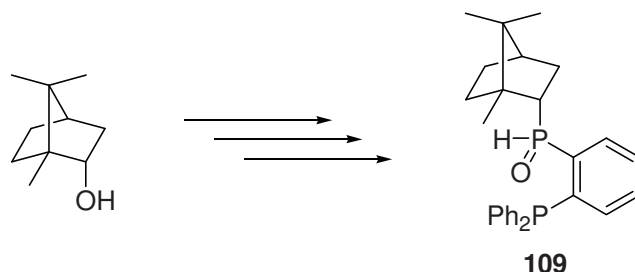
Scheme 6.1. Ferrocenephospholanes from *Ugi*'s amine.

The phosphines obtained were tested in the transition-metal catalyzed asymmetric hydrogenation of different substrate classes such as dehydroamino acid derivatives, unsaturated esters and ketones. The results showed that these ligands cannot compete with the established systems in terms of activity and selectivity.

A closer look at the coordination behaviour of ligand **40** implied that chelation leads to a strained molecule. The complexes of **40** with $[\text{Rh}(\text{nbd})\text{Cl}]_2$, $[\text{Rh}(\text{cod})\text{Cl}]_2$ and $[\text{Ir}(\text{cod})\text{Cl}]_2$ showed a dynamic behaviour in solution. Competition experiments resulted in metal-exchange revealing labile complexes. The resulting complexes were dependent on the solvent used and the diene ligand of the corresponding metal source.

Hydrogenation experiments showed for the activation of the precatalyst a dramatic dependence on the diene ligand present in the metal complex. Whereas $[\text{Rh}(\mathbf{40})(\text{nbd})\text{Cl}]$ was easily converted into the active catalyst, the counterpart with 1,5-cyclooctadiene was basically inert towards dihydrogen.

With terpenes as starting material P-chiral secondary phosphine oxides have been prepared. The borneol-derived bidentate ligand **109** (Scheme 6.2) was tested in the rhodium-catalyzed asymmetric hydrogenation.



Scheme 6.2. Synthesis of a phosphine-SPO-ligand.

The enantioselectivities obtained were up to 90% *ee* (TOF = 12000 h⁻¹) with dimethyl itaconate and up to 93% *ee* (TOF = 2700 h⁻¹) with methyl acetamidoacrylate.

A hydroxyethyl-substituted bisphosphine ligand (**118**) was synthesized and the rhodium complex shown to be of low reactivity in the hydrogenation of methyl acetamidoacrylate although an enantiomeric excess of 89% was obtained.

Menthol derived P-chiral phosphino-oxazoline-iridium complexes (**121-128**) (Figure 6.1) were prepared and applied in the asymmetric hydrogenation.

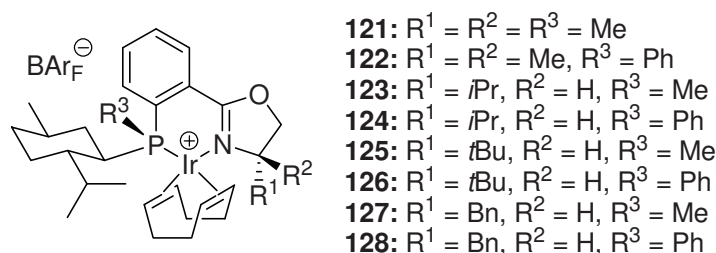


Figure 6.1. Menthyl derived P-chiral phosphino-oxazoline-iridium complexes.

The catalysts were generally very active but in most cases the enantioselectivities obtained were lower than with previously reported PHOX-systems. In the reduction of *E*-2-methylcinnamate (**74**) the best complex (**125**), giving 91% *ee*, was comparable with published phosphino-oxazoline-iridium catalysts. The terminal olefin 2-(4-methoxyphenyl)-1-butene (**134**) was hydrogenated with an enantiomeric excess of 87% which represents the highest selectivity achieved with PHOX-catalysts for this substrate.

Curriculum Vitae

Björn Gschwend

Date of Birth: 7 January 1980
Place of Birth: Basel, Switzerland
Nationality: Swiss
Hometown: Altstätten SG

Education

University

10/2005 – 9/2009 PhD work “P-Chiral Phosphorus Ligands: Synthesis and Application in Asymmetric Hydrogenation” under the supervision of Prof. Andreas Pfaltz at the University of Basel, Switzerland
9/2004 – 2/2005 Diploma thesis “Approaches to a Heteroleptic Ruthenium Metallodendrimer” under the supervision of Prof. Edwin C. Constable and Prof. Catherine E. Housecroft at the University of Basel, Switzerland
9/2004 Diplom
9/2002 2. Vordiplom
9/2001 1. Vordiplom
9/2000 – 2/2005 Studies in Chemistry at the University of Basel, Switzerland

School

8/1996 – 12/1999 Matura, Gymnasium Typus C, MuttENZ BL, Switzerland

Work Experience

10/2006 – 7/2008 Laboratory Teaching Assistant, Department of Chemistry, University of Basel, supervision of chemistry students in basic and advanced organic chemistry
5/2005 – 9/2005 Internship in the Section of Catalysis Research at Solvias AG, Basel, Switzerland

Miscellaneous

9/2005 – 9/2009 Secretary of the Swiss Young Chemists Association
2/2000 – 6/2000 Military Service

During my education at the University of Basel I attended lectures given by:

E. C. Constable, B. Giese, H. J. Güntherodt, P. C. Hauser, C. E. Housecroft, H. Huber, H. C. ImHof, M. Jungen, T. Kaden, J. P. Maier, W. P. Meier, M. Oehme, A. Pfaltz, C. Schönenberger, U. Séquin, H. Sigel, P. Strazewski, A. Vedani, H. Wennemers, H.-J. Wirz, W.-D. Woggon, A. Zuberbühler.

Eidesstattliche Erklärung

Ich erkläre, dass ich die Dissertation „P-Chiral Phosphorus Ligands: Synthesis and Application in Asymmetric Hydrogenation“ nur mit der darin angegebenen Hilfe verfasst und bei keiner anderen Universität und keiner anderen Fakultät der Universität Basel eingereicht habe.

Basel, 26.08.2009

Björn Gschwend

